AD-A150 682 ANALYSIS OF ATMOSPHERIC INTERFEROMETER DATA(U) 1/3
OPTIMETRICS INC LAS CRUCES NM J A DOWLING ET AL.
JUL 84 OMI-102 AFGL-TR-84-0177 F19628-83-C-0040

UNCLASSIFIED F/G 20/14 NL

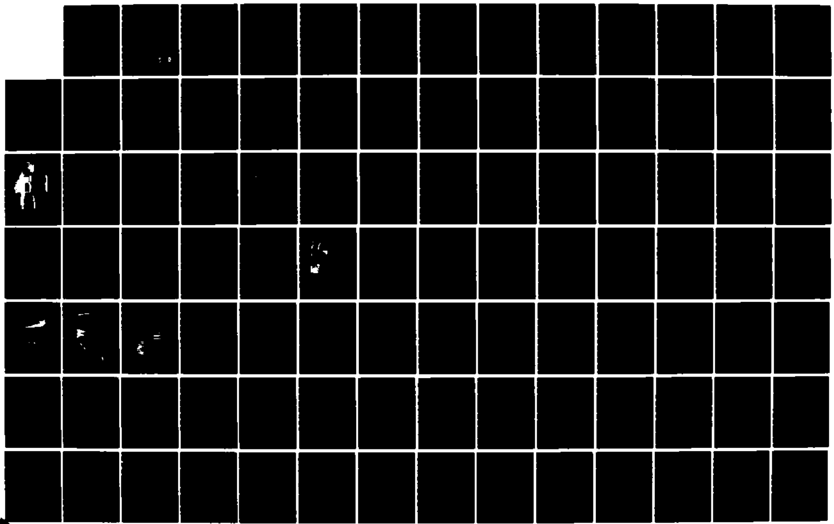

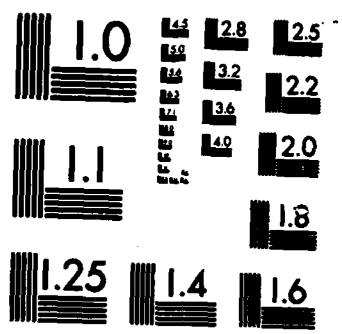

MICROCOPY RESOLUTION TEST CHART
NATIONAL BUREAU OF STANDARDS-1963-A

AFGL-TR-84-0177

AD-A150 682

ANALYSIS OF ATMOSPHERIC INTERFEROMETER DATA

James A. Dowling
William O. Gallery
Sean G. O'Brien

OptiMetrics, Inc.
106 E. Idaho, Suite G
Las Cruces, New Mexico 88001

Final Report
January 1983 - January 1984

July 1984

Approved for public release; distribution unlimited

AIR FORCE GEOPHYSICS LABORATORY
AIR FORCE SYSTEMS COMMAND
UNITED STATES AIR FORCE
HANSCOM AFB, MASSACHUSETTS 01731

"This technical report has been reviewed and is approved for publication"

(Signature)
LEONARD W. ABREU
Contract Manager

(Signature)
BERTRAM D. SCHURIN
Branch Chief

FOR THE COMMANDER

(Signature)
JOHN S. GARING
Division Director

This report has been reviewed by the ESD Public Affairs Office (PA) and is releasable to the National Technical Information Service (NTIS)

Qualified requestors may obtain additional copies from the Defense Technical Information Center. All others should apply to the National Technical Information Service.

If your address has changed, or if you wish to be removed from the mailing list, or if the addressee is no longer employed by your organization, please notify AFGL/DAA, Hanscom AFB, MA 01731. This will assist us in maintaining a current mailing list.

Unclassified
SECURITY CLASSIFICATION OF THIS PAGE

REPORT DOCUMENTATION PAGE

1a. REPORT SECURITY CLASSIFICATION: Unclassified

1b. RESTRICTIVE MARKINGS:

2a. SECURITY CLASSIFICATION AUTHORITY:

2b. DECLASSIFICATION/DOWNGRADING SCHEDULE:

3. DISTRIBUTION/AVAILABILITY OF REPORT: Approved for public release; distribution unlimited

4. PERFORMING ORGANIZATION REPORT NUMBER(S): OMI-102

5. MONITORING ORGANIZATION REPORT NUMBER(S): AFGL-TR-84-0177

6a. NAME OF PERFORMING ORGANIZATION: OptiMetrics, Inc.

6b. OFFICE SYMBOL (If applicable):

7a. NAME OF MONITORING ORGANIZATION:

6c. ADDRESS (City, State and ZIP Code): 106 E. Idaho, Suite G, Las Cruces, New Mexico 88001

7b. ADDRESS (City, State and ZIP Code):

8a. NAME OF FUNDING/SPONSORING ORGANIZATION: Air Force Geophysics Laboratory

8b. OFFICE SYMBOL (If applicable): OPI

9. PROCUREMENT INSTRUMENT IDENTIFICATION NUMBER: F19628-83-C-0040

8c. ADDRESS (City, State and ZIP Code): Hanscom AFB, Massachusetts 01731, Monitor/Leonard W. Abreu

10. SOURCE OF FUNDING NOS.

PROGRAM ELEMENT NO.	PROJECT NO.	TASK NO.	WORK UNIT NO.
62101F	7670	09	AR

11. TITLE (Include Security Classification): Analysis of Atmospheric Interferometer Data

12. PERSONAL AUTHOR(S): Dowling, James A., Gallery, William O., and O'Brien, Sean G.

13a. TYPE OF REPORT	13b. TIME COVERED	14. DATE OF REPORT (Yr., Mo., Day)	15. PAGE COUNT
Final	FROM Jan 83 TO Jan 84	1984 July	212

16. SUPPLEMENTARY NOTATION:

17. COSATI CODES

FIELD	GROUP	SUB. GR.

18. SUBJECT TERMS (Continue on reverse if necessary and identify by block number): Atmospheric transmission, Fourier transform spectrometer, Water vapor continuum absorption infrared transmission

19. ABSTRACT (Continue on reverse if necessary and identify by block number)

In this study of atmospheric

A study has been performed in which several examples of laser-transmissometer-calibrated, high-resolution Fourier transform spectrometer (FTS) measurements ~~have been~~ are compared with corresponding spectra generated using the FASCOD1C computer model. ~~The~~ experimental data were collected at three coastal sites and one inland site. ~~The~~ measurement path-lengths varied between 4.07 and 6.4 km. Water vapor partial pressures varied between 2.0 and 20.5 torr, partial pressure of water vapor.

Of particular interest in this study is the use of the experimental data in comparison~~s~~ to the water vapor continuum absorption infrared model contained in the FASCOD1C computer model. ~~It was found that~~ the data were found to agree with FASCODE predictions for the H_2O continuum absorption to within the range of uncertainty of the experimental data. The N_2 continuum absorption calculated using FASCOD1C appears to be smaller than that observed and this observation is

20. DISTRIBUTION/AVAILABILITY OF ABSTRACT: UNCLASSIFIED/UNLIMITED ☐ SAME AS RPT. ☐ DTIC USERS ☐

21. ABSTRACT SECURITY CLASSIFICATION: UNCLASSIFIED

22a. NAME OF RESPONSIBLE INDIVIDUAL:

22b. TELEPHONE NUMBER (Include Area Code):

22c. OFFICE SYMBOL:

DD FORM 1473, 83 APR EDITION OF 1 JAN 73 IS OBSOLETE.

Unclassified
SECURITY CLASSIFICATION OF THIS PAGE

thought to be related to an unmodeled temperature dependence in the N_2 continuum absorption.

The experimental high-resolution spectra were compared with calculated continuum absorption by selecting 49 discreet frequencies in the 1900 - 3200/cm^{-1} region which were minimally influenced by discreet line absorption. Corrections for local line and N_2 and CO_2 continuum absorptions were applied to the experimental data at these 49 frequencies. The data were then compared with H_2O continuum absorption coefficients calculated using the FASCOD1C model and the 1982 version of the AFGL atmospheric absorption line compilation.

Detailed high-resolutuion comparisons of the experimental data to FASCODE - generated spectra show excellent agreement in nearly all features throughout the 1900 - 3200/cm^{-1} spectral region. A notable exception occurs with several weak H_2O vapor absorption lines occurring between 2390/cm^{-1} and 2490 cm^{-1}. Recommended line strength values for these several lines have been derived from the experimental data and are provided.

Recommendations for further analysis of the data base utilized in the present study and for additional measurements are discussed.

ACKNOWLEDGEMENTS

A great many individuals contributed to the generation of the data base which is analyzed in the present study. One of the authors (James A. Dowling) was associated with and primarily responsible for the design and deployment of the NRL IMORL facility during the several years that the data base treated herein was generated. Accordingly the following acknowledgements are made.

Many individuals at NRL contributed to this work, especially: T. Cosden - IMORL mechanical design, R. Horton - IMORL optical design, experimental procedures, and data collection and analysis, R. Harris - electronic design, S. Hanley - data collection and analysis, K. Haught - data collection and analysis, D. Garcia - data collection and analysis, P. Livingston - programmatical representation and direction, M. Woytko, C. Gott, J. Cox, W. DeMent, and M. Cochran - IMORL system construction and operation. R. Patten was instrumental in making the NRL IMORL data base available for the present analysis. The IMORL optical system was manufactured by the Muffoletto Optical Co., Baltimore, MD and the FTS system was manufactured by the MIDAC Corporation, Newport Beach, CA.

The work reported herein was sponsored by several DoD agencies. The principals at each of these offices who were instrumental in making this work possible were: NAVSEA PMS-405 - D. Finkleman and M. Hughes, NOSC - Juergen Richter, ASL - G. Hoidale, AFGL - S. Clough, F. Kneizys, and L. Abreu.

The careful and comprehensive work performed in the preparation of the text and numerous figures in this report by Deborah Christmas and Valerie Torres is greatly appreciated.

CONTENTS

LIST OF ILLUSTRATIONS

LIST OF TABLES

1
BACKGROUND AND INTRODUCTION

This report describes the analysis of a collection of high-resolution atmospheric transmittance spectra measured during several field experiments performed by the Naval Research Laboratory (NRL) between 1976 and 1979. The data analyzed in the present study consists of 52 individual high-resolution (0.0625 cm^{-1}) spectra for which an absolute-transmission calibration was obtained by nearly-concurrent measurements of deuterium-fluoride (DF) laser transmittance over the same atmospheric path.

The four experiments which yielded the data base analyzed in this study were conducted at three coastal and one inland locations using the NRL Infrared Mobile Optical Radiation Laboratory (IMORL). The IMORL system was an outgrowth of earlier NRL measurement systems used for studies of atmospheric turbulence effects on laser propagation. The system is briefly described in Section 2.

The first NRL experiment in which laser-extinction-calibrated Fourier-transform spectrometer (FTS) data were collected was performed at the Patuxent River Naval Air Station (PRNAS), Maryland in the fall of 1976 [1]. This experiment was followed by a similar, extended measurement program at the Cape Canaveral Air Force Station (CCAFS), Florida during the late-winter and spring of 1977 [2, 3]. Later experiments were performed at the White Sands Missile Range (WSMR), New Mexico [4], and at San Nicolas Island (SNI), California in the spring of 1979 [5].

A principal objective behind the combined use of high-resolution FTS measurements with high-accuracy transmittance values obtained with the IMORL laser transmissometer system

was a measurement of the weak but important absorption in the 3-5 μm atmospheric window contributed by the "so-called" water vapor continuum absorption. Earlier NRL long-path transmittance measurements had shown that the uncertainties associated with the understanding of this continuum absorption represented a major limitation in the ability to correctly predict molecular absorption coefficients for DF laser atmospheric propagation. The high-resolution FTS data provide a direct measure of atmospheric transmittance at spectral locations in the 3-5 μm region where contributions to the absorption coefficient due to strong individual atmospheric absorption lines are minimal or negligible. At these frequencies the residual molecular absorption is due to the water vapor continuum above or the combination of water vapor continuum, the N_2 continuum and the ν_3 CO_2 band edge continuum.

Previous analysis and model comparisons have been performed using the large data base of laser transmittance values measured during the several NRL field experiments [1-5]. However, only preliminary comparisons of the NRL high-resolution FTS data to line-by-line high resolution calculations were made [6-7].

The approach used in this study makes use of the high resolution NRL FTS data by comparing measured extinction coefficients, after correction for calculated contributions due to local lines, and due to N_2 and CO_2 continua, with calculated water vapor continuum absorption coefficients obtained with the FASCOD1C model [8]. The 1982 AFGL atmospheric absorption line parameters compilation [9] was used together with FASCOD1C for the calculation of local line contributions.

This report is divided into 4 sections, the first being this introduction. In Section 2 the NRL Data base is described. The IMORL apparatus is briefly described in subsection 2.1 and the field measurement locations and meteorological conditions are described in subsection 2.2.

Data analysis, procedures and results are described in Section 3. Subsection 3.1 describes the water vapor continuum analysis and in subsection 3.2 the limited analysis performed comparing individual measured and calculated line absorptions is presented.

Section 4 presents a summary of the conclusions which can be drawn from the analysis and presents a list of recommendations based on the findings in this study.

2
THE NRL HIGH-RESOLUTION ATMOSPHERIC TRANSMISSION DATA BASE

2.1 EXPERIMENTAL APPARATUS

The Infrared Mobile Optical Radiation Laboratory (IMORL) was developed at NRL as a field laboratory for precision atmospheric propagation measurements. Detailed descriptions of the electro-optical instrumentation contained in this facility are presented in References 10 and 11. The essential features of this system are briefly described below to provide the reader with an orientation regarding the high-resolution FTS data base analyzed in this report.

The IMORL system was used extensively to collect laser-calibrated high-resolution atmospheric transmission spectra. The system included several infrared laser and blackbody sources, large, stable telescope optics, a Fourier transform spectrometer (FTS) system, and various support equipment, all of which were transported in and operated from several large semi-trailers. The usual measurement configuration consisted of an optical transmitter trailer housing HeNe, Nd-YAG, DF, CO, and CO_2 single-line, cw laser sources, relay optics, and a large, stably-mounted and precisely-pointed 91 cm aperture, f/35 Cassegrainian collimating telescope. The small cw, combustion-driven DF laser used for much of the laser extinction work required a large (755 l/s) vacuum system for operation. This pump was housed in a separate trailer; a 20 cm diameter vacuum line was installed between the transmitter and vacuum pump trailers once the two trailers were properly located at a measurement site. Two additional trailers contained office space, meteorological signal processing and recording electronics, and bottled

gases and other consumable supplies used during the course of an experiment.

The FTS system and apparatus used for laser extinction measurements were housed in a receiver trailer containing a 120 cm aperture, f/5 newtonian telescope. The large receiver telescope aperture insured that the entire laser beam used during long path extinction measurements could be collected, thereby providing reliable absolute transmission calibrations for the FTS measurements. High resolution transmission spectra were taken by substituting a 1300 K blackbody source for the laser source in the transmitter optical system and adjusting the receiver optical system so as to couple the FTS system to the 120 cm collecting telescope. Repeated calibrations and extensive experience with the measurement system in field experiments demonstrated that absolute transmission could be reliably measured for long atmospheric paths with an uncertainty less than $\pm 3\%$.

Figure 1 is a photograph of the transmitter station taken during the experiment at CCAFS. From left to right in the figure can be seen an NRL aerosol-micrometeorological measurement van, the IMORL vacuum pump trailer, optical transmitter trailer (the 91 cm aperture telescope mirror and telescope frame may be seen through the open doors), and the office trailer.

Figure 2 is a schematic depicting the experimental arrangement used for laser extinction measurements. The output beam from any of the several laser sources used was first collimated by auxiliary optics to a diameter of approximately 18 mm. The beam was then focused via the off-axis parabolic mirror shown in the upper left of Figure 2 and then diverged to fill the 91 cm transmitter telescope aperture. A 37 Hz, 50% duty cycle chopper modulated the beam near the focus formed by the off-axis parabola. The

FIGURE 1. NRL IMORL TRANSMITTEI STATION DURING THE CCAFS EXPERIMENT.

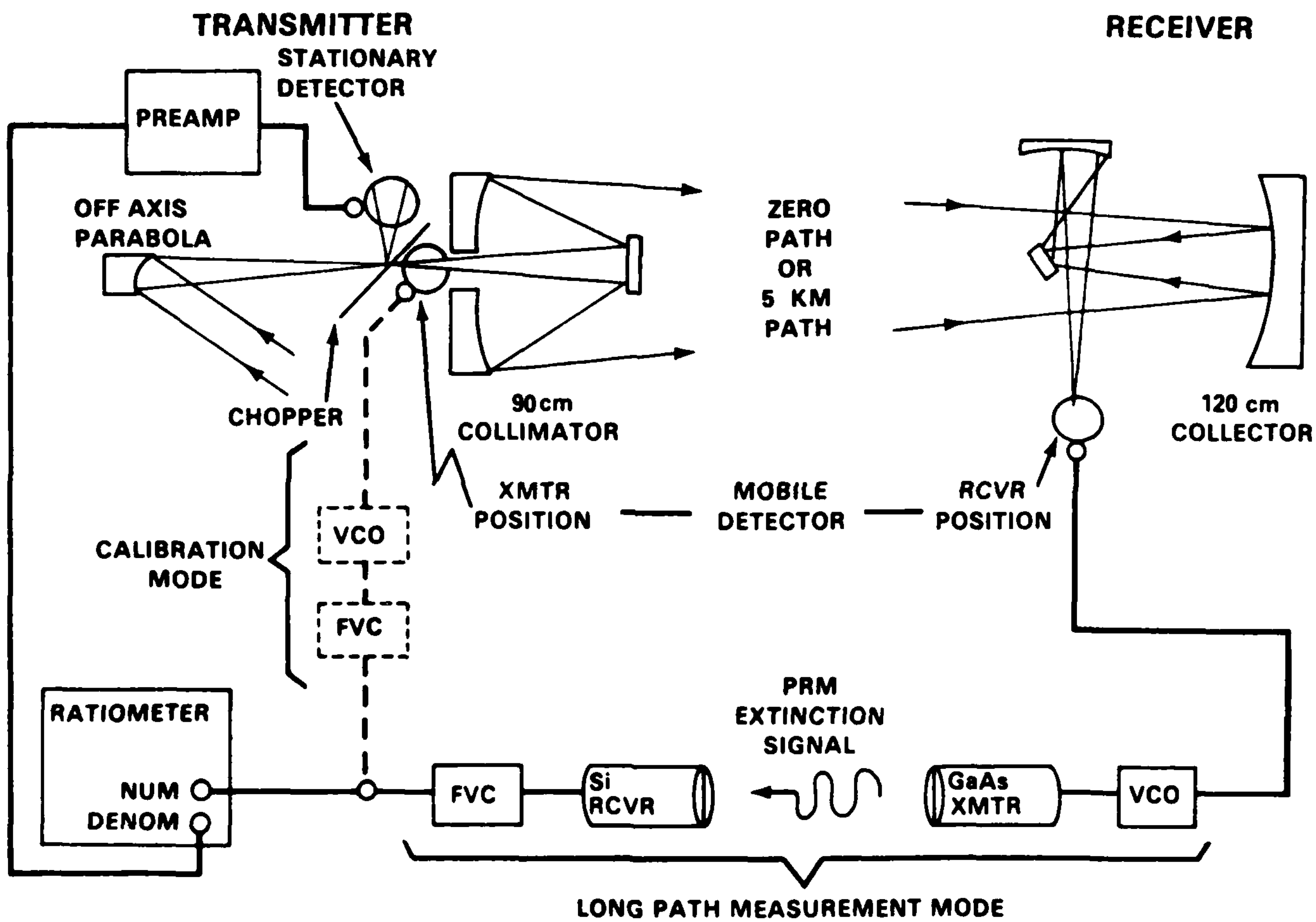

FIGURE 2. NRL IMORL LASER EXTINCTION MEASUREMENT SCHEMATIC.

beam was alternately transmitted through the telescope and reflected onto the stationary detector as shown. The mobile detector shown in Figure 2 was placed in the "XMTR" position for calibration measurements in which the relative response of the two detectors was measured. The mobile detector was then placed near the focus of the 120 cm aperture receiver telescope for a) calibrations of the large telescope optical efficiency or b) long path extinction measurements. The calibration measurements were carried out with the transmitter and receiver trailers immediately opposite one another, i.e., for zero atmospheric path. When the trailers were separated for long path measurements the two types of calibration data were then used to determine absolute atmospheric transmittance for the several laser lines studied. As shown in Figure 2, the signal produced by the mobile detector in the receiver trailer at one end of the measurement path was relayed to the transmitter by means of a pulse-rate-modulated (PRM) GaAs-laser-based data link. This signal, proportional to laser power at the receiver, was connected to the numerator input of a special purpose analog ratiometer, [11]. The stationary detector signal, proportional to the transmitted laser power was connected to the denominator input of the ratiometer. Thus, a real time measure of transmittance for the laser line being studied was available at the transmitter site. The ratiometer reading was corrected for the relative response of the two detectors for that laser line (monitored daily) and the efficiency of the large optical elements beyond the chopper in order to obtain absolute transmission readings. As shown in Figure 2, the voltage-controlled oscillator (VCO) and frequency-to-voltage converter (FVC) used with the GaAs data link were also connected in the numerator circuit of the ratiometer when the mobile detector was used in the "XMTR"

position, so that their combined transfer function was normalized out of the final extinction ratio.

Figure 3 is a schematic diagram showing the configuration of the transmitter and receiver optical systems used for FTS measurements.

Local meteorological measurements were usually performed at each end of the measurement path. Absolute humidity, air temperature and pressure, and wind conditions were monitored in order to document local conditions during a series of measurements, to provide assurance that uniform environmental conditions existed along the measurement path, and that there conditions remained constant during a complete measurement cycle. The period required to make both laser extinction and FTS measurements, in turn, was typically about one hour. Measurements using an aerosol spectrometer system in the NRL aerosol van were performed during some of the measurements analyzed in this report. Infrared aerosol extinction estimates based on Mie scattering calculations, utilizing the measured particle distributions, have shown good agreement with results derived from infrared extinction measurements at Nd-YAG and DF laser wavelengths. This agreement was obtained during earlier experiments [12] conducted at an inland location, removed from the local effects of surf, etc., which existed during three of the four experiments addressed in this report. However, for the measurements discussed in this report, poor agreement between aerosol-analyzer-derived extinction coefficients and those determined from long-path optical measurements was generally observed.

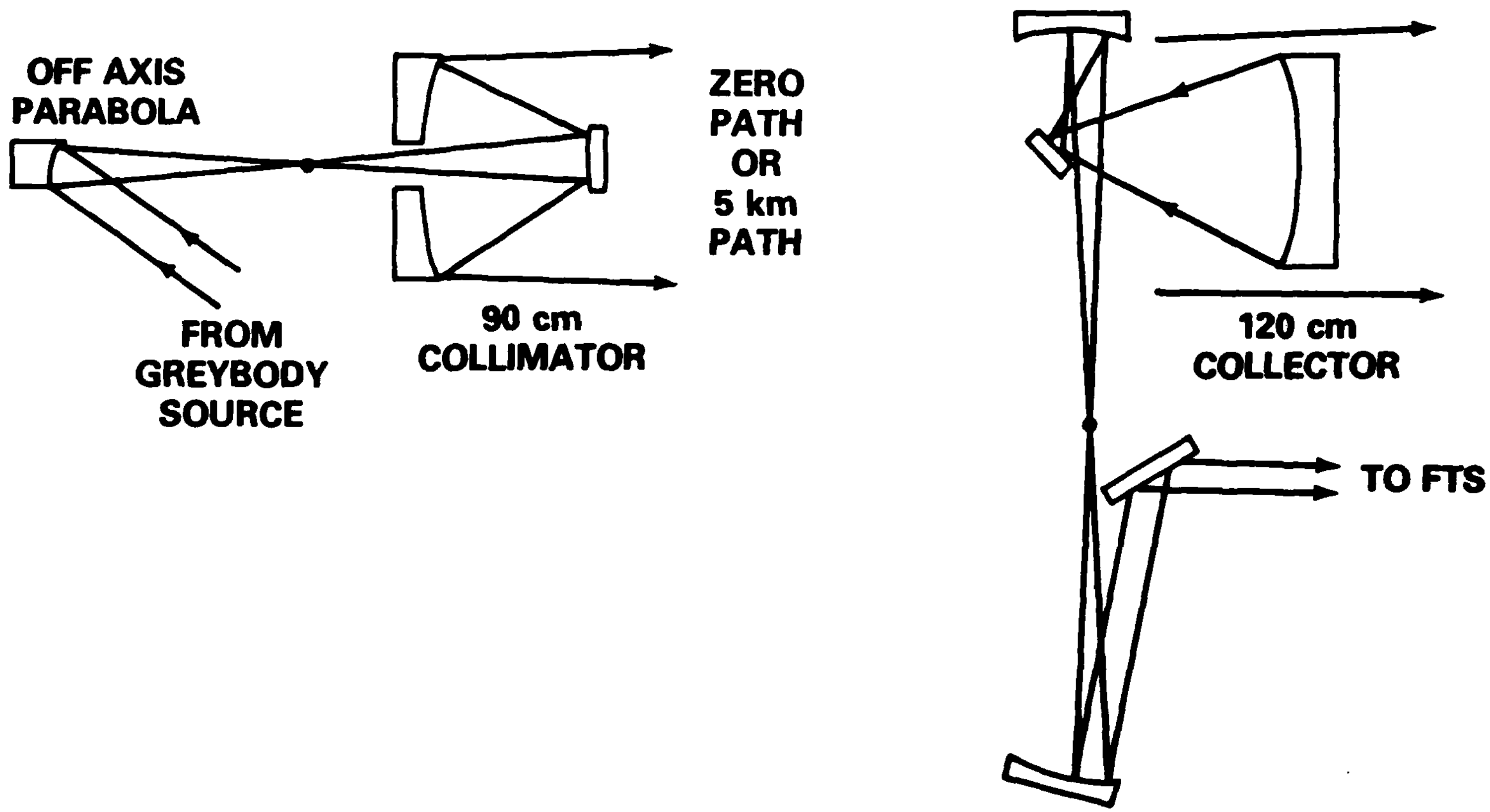

FIGURE 3. OPTICAL SCHEMATIC DIAGRAM FOR FTS MEASUREMENTS.

2.2 FIELD MEASUREMENT LOCATIONS AND METEOROLOGICAL CONDITIONS

2.2.1 PATUXENT RIVER NAVAL AIR STATION

The 5.12 km overwater path used for the PRNAS measurements is shown in Figure 4. The IMORL transmitter station was located at the south end of the PRNAS at location A in the figure. The receiver station was placed at location B in the figure which is a small radar installation used to support operations at the PRNAS.

All of the PRNAS spectra analyzed in this report were measured during mid-November 1976 except for the one designated PR024 which was measured on 24 September. The meteorological conditions occurring on September 24 included moderate values of air temperature and absolute humidity of 18.3^{o}C and 12.0 torr water vapor partial pressure (ppH_2O), respectively. The remainder of the spectra were collected between 8 and 19 November 1976, during conditions of relatively low air temperatures (-1.7 to 8.5^{o}C) except for 19 November when the air temperature was 17.5^{o}C. The absolute humidity variations encountered during November were confined to relatively low values between 2.5 and 3.0 torr ppH_2O.

Table 1 presents summary of the meteorological conditions occurring during the PRNAS measurements. Also included in Table 1 is information relating to measured and/or derived aerosol extinction values at 0.5 μm and 3.8 μm. For the PRNAS data, the aerosol extinction coefficients at 0.55 μm were obtained from visibility measurements performed for times close to the laser extinction measurement times. The corresponding values for 3.8 μm were obtained from the 0.55 μm values using the wavelength scaling procedure described in subsection 3.1.1.2. The four right-most columns

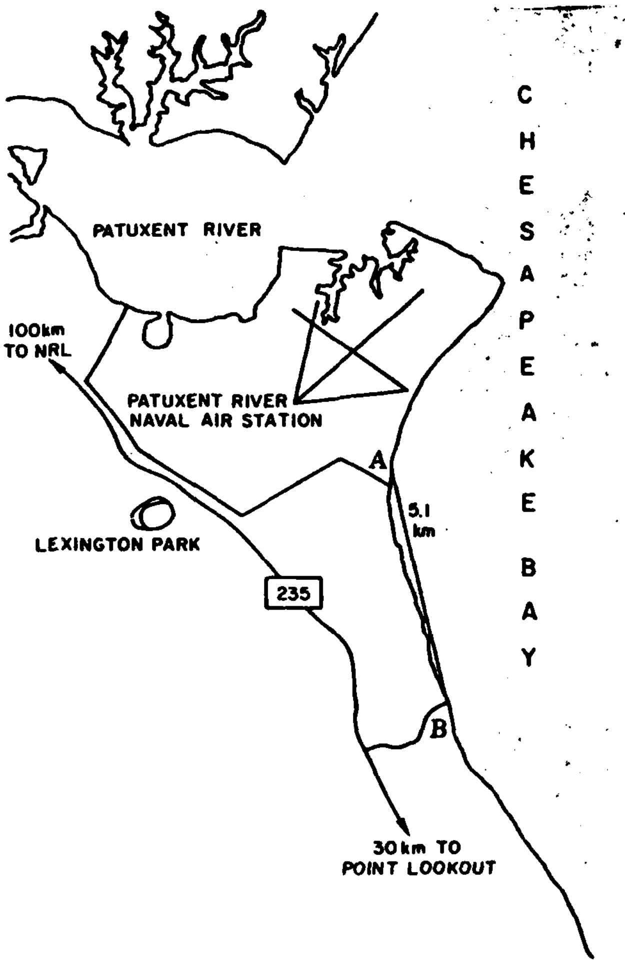

FIGURE 4. PRNAS ATMOSPHERIC TRANSMISSION TEST SITE.

TABLE 1. SUMMARY OF METEOROLOGICAL CONDITIONS AND LASER NORMALIZATION PARAMETERS FOR PRNAS SPECTRA.

Date	Local Time		Spectrum Number	AT† (°C)	PPH_2O† (Torr)	RH (%)	WD† (°)	WS† (m/s)	Visibility† (km)	σ_{AER}		H_2O Continuum Tabulation	H.R. Digital File	Absolute Normalization	
	FTS	Laser								0.55μm (km^{-1})	3.8μm (km^{-1})			Correction Factor	Fitting Error (±)
9-24-76	1445	1542	PR24	18.3	12.0	67	40	1.03	12.97	0.127	.1071	Yes	No	1.0024	0.040
11-08-76	1540	1626	PR37	0	2.5	69	290	5.15	12.97	0.127	.1092	Yes	No	1.0108	0.033
	1800	1626	PR39	-1.7	2.5	78	300	4.63	12.97	0.127	.1591	Yes	No	1.0087	0.036
11-09-76	1115	1633	PR40	5.2	2.0	47	200	4.12	12.97	0.127	.0895	Yes	No	1.0105	0.0239
	1700	1633	PR42	4.6	2.4	55	230	4.12	12.97	0.127	.0950	Yes	No	0.9971	0.0264
11-11-76	1619	1249	PR49	8.5	3.0	66	20	3.09	12.97	0.127	.1061	Yes	No	1.0086	0.0229
11-17-76	1615	1630	PR50	6.8	3.0	56	[illegible]	4.63	12.97	0.127	.0960	Yes	No	1.0023	0.0478
11-18-76	1630	1535	PR54	3.9	2.8	72	240	1.54	12.97	0.127	.1224	Yes	No	1.0069	0.0291
11-19-76	1320	1515	PR55	17.5	2.5	40	260	3.60	12.97	0.127	.0886	Yes	No	0.9956	0.0238
	1335	1515	PR56	17.5	2.5	40	260	3.60	12.97	0.127	.0886	Yes	No	0.9924	0.0379

†Meteorological data records were obtained for these quantities from the Naval Ocean Command (NAVOCOM) weather station at PRNAS. In cases where both NRL and NAVOCOM data were available and differed, the average value of the two data items was used.

of Table 1 contain information relating to the availability of previously unpublished tabulations of values for local transmission maxima in the 2400 - 3200 cm^{-1} region for the spectra, the availability of a high resolution digital tape file for the spectrum, and absolute-transmission-normalization correction factors and fitting errors derived as part of the present study. The latter two quantities are discussed in Section 3.

2.2.2 CAPE CANAVERAL AIR FORCE STATION

The location of the 5.08 km path used for the CCAFS measurements described in this report is shown in Figure 5. The optical transmitter station was located at the shore end of Camera Rd. "A" and the receiver station was located at the shore end of South Patrol Rd. as shown in the figure.

One of the principal advantages of the CCAFS site for laser propagation and high-resolution transmission studies during the late-winter and spring seasons is the wide variation in absolute humidity which can be expected to occur at that location. Since water vapor in its two most abundant isotopic forms (H_2O and HDO) is a principal molecular absorber at DF, CO and CO_2 laser wavelengths, validation of molecular absorption models is greatly facilitated by experimental data collected under such widely ranging conditions, particularly when associated meteorological changes in aerosol composition and concentration and air temperature are relatively small by comparison. The variation of meteorological conditions encountered during the NRL 1977 CCAFS experiment proved to be quite useful in meeting the experimental objectives; a range of absolute humidity between a moderately low value of 6 torr ppH_2O to over 20 torr ppH_2O was observed. The wind conditions encountered during the

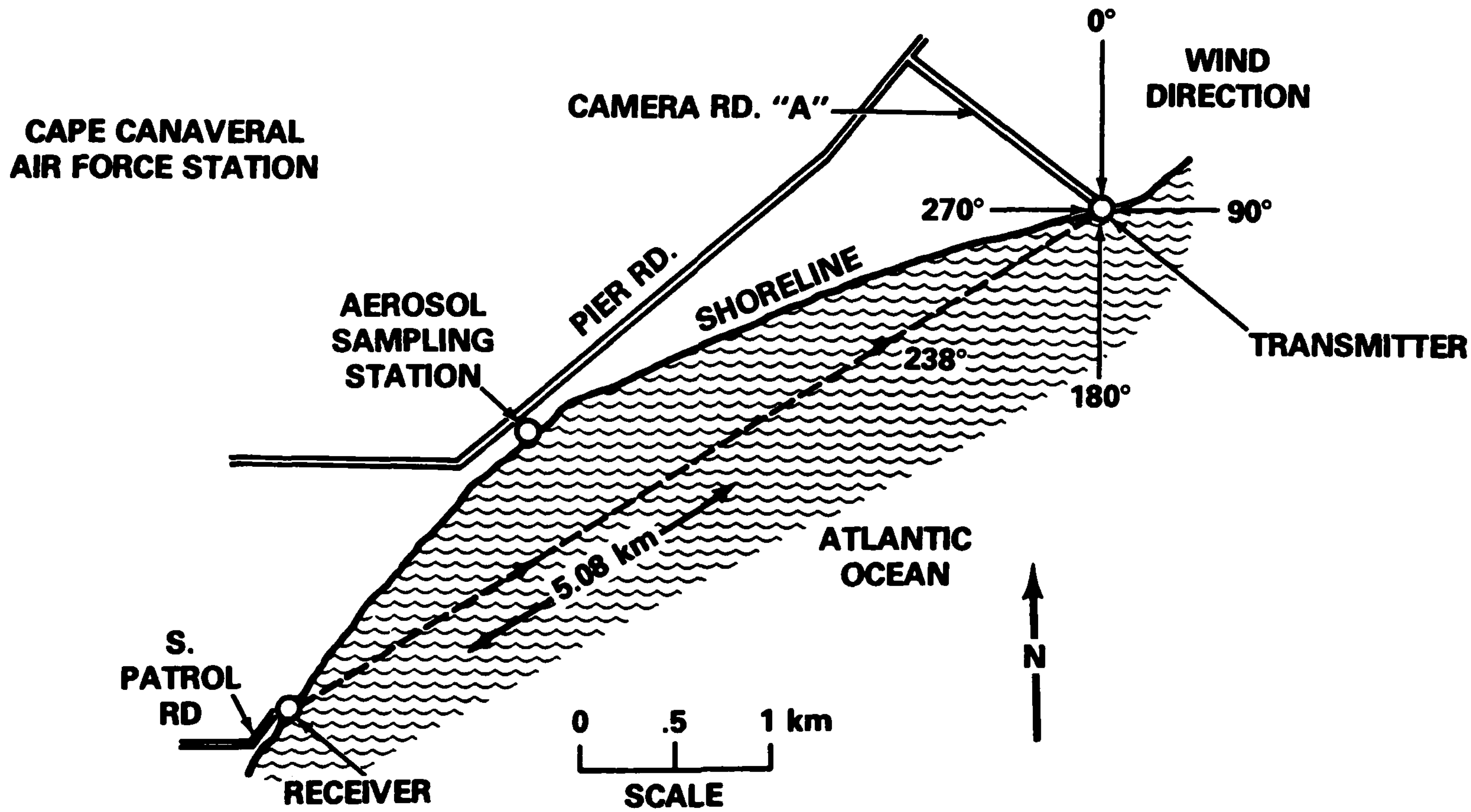

FIGURE 5. CCAFS ATMOSPHERIC TRANSMISSION TEST SITE.

experiment included winds originating from both overwater and overland directions, giving rise to both maritime-like and predominately continental atmospheric aerosol compositions, and a range of visibilities between 10 and 50 km. Table 2 contains a summary of the meteorological conditions encountered during the experiment. The maximum and minimum values observed for several relevant meteorological parameters are listed in part 1 of the table while part 2 contains a daily summary including the nature of the wind conditions (absolute wind direction, direction relative to the optical propagation path, and wind speed) along with the absolute humidity, air temperature, visibility, and insolation recorded during each of the transmission measurements periods. Apparent aerosol extinction (AAE) values (measured extinction minus calculated molecular absorption) for the four laser wavelength regions studied are also included in section 2 of the table.

The symbol "~" used in several places in Table 2 is intended to indicate average or approximate values for the corresponding entry as a result of: a) forming averages based on visual inspection of the appropriate individual values, or b) estimating a typical average value for a parameter which changed in a systematic manner during the course of an experiment period; e.g., insolation typically varied from about 1.2 w/cm^2 around 1300 hours to about 0.80 w/cm^2 near 1500 hours, therefore an entry of 1.00 w/cm^2 is used as an average value.

Some general observations can be made upon examination of Table 2. During the first of the three periods when long-path transmission measurements were performed (March 2 through 15, 1977) three distinct frontal passage situations were encountered, occurring on 2, 8 and 14 March. The frontal passages were typified by overland wind directions,

TABLE 2. SUMMARY OF METEOROLOGICAL CONDITIONS OCCURRING DURING 1977 CCAFS EXPERIMENT.

1. Maximum and Minimum Values

	ppH_2O (torr)	AT (^oC)	BP (mb)	SR (w/cm^2)	WS (m/s)	VIS (km)
MAXIMUM	20.9	30	1022	2.2	8.0	50
MINIMUM	5.5	18	1012	0.4	0.0	10

ppH_2O = partial pressure of water vapor

AT = air temperature

BP = barometric pressure

SR = solar radiation

WS = wind speed

VIS = visibility (visual range)

TABLE 2. CONTINUED.

2. Daily Record of Wind Character, Meteorological Parameters and Apparent Aerosol Extinction (AAE) Values

Date	Wind Direction (DEG)	OL/OW†	Angle Relative To Optical Path (DEG)*	Wind Speed (m/s)	Visibility (km)	ppH_2O (torr)	AT (°C)	Insolation (w/cm²)	AAE HeNe (km^{-1})	AAE Nd-YAG (km^{-1})	AAE DF (km^{-1})	AAE CO_2 (km^{-1})
3-2-77	30	OL	~30	4.0	33	5.5	18.0	~1.10	.065			.011
3-3-77	100	OW	~40	3.7	18	13.4	18.6	~ .94			.140	
3-7-77	245	OL	~//	0.1	11	17.0	27.3	~2.20	.091		.060	
3-8-77	27	OL	~30	3.3	20	10.0	19.8	~ .85	.104		.070	.005
3-9-77	67	OW	~//	3.3	12	11.0	19.5	~ .65	.134		.080	.020
3-10-77	70	OW	~//	2.3	8	14.5	20.0	~ .24	.347			.030
3-11-77	115	OW	~45	0.1	14	16.0	22.0	~ .90	.214		.120	-.015
3-12-77	145	OW	~⊥	2.0	16	17.0	22.0	~ .90	.140		.085	
3-14-77	40	OL	~20	2.5	23	7.0	24.2	~1.00	.099		.050	.050
3-15-77	310	OL	~⊥	1.8	30	11.0	22.8	~ .95	.103		.030	.015
3-31-77	150	OW	~⊥	4.5	24	18.2	25.0	~ .86			.055	
4-1-77	130	OW	~70	4.0	14	18.4	24.1	~1.00	.196		.040	-.030
4-2-77	137	OW	~80	5.0	~30	18.7	25.0	~1.00	.115	.083	.030	-.055
4-4-77	157	OW	~⊥	8.7	20	18.3	24.2	~ .90	.160	.148	.080	-.030
4-5-77	270	OL	~30	6.3	48	9.8	24.9	~ .45	.063	.050	.020	.007
5-16-77	100	OW	~40	5.5	24	15.0	25.0	~1.08	.117	.049		-.020
5-17-77	62	OW	~//	6.1	14	15.3	26.0	~1.03	.138	.038		-.020
5-20-77	78	OW	~20	3.3	25	14.7	26.2	~1.03	.101	.049	.080	
5-21-77	~85	OW	~30	5.0	16	16.4	26.3	~1.10	.164	.062	.040	
5-23-77	~90	OW	~30	~3.0	46	18.2	25.8	~1.20	.048	.055	.030	-.055
5-24-77	115	OW	~60	~4.9	33	20.8	26.5	1.30	.057	.056	.045	-.055
5-25-77	220	OW	~20	2.9	22	20.4	28.6	~ .66	.100	.068	.040	-.065

Date/Time	AAE HeNe (km^{-1})	AAE Nd-YAG (km^{-1})
3-14-77		
1006	.099	
1603	.099	
4-2-77		
1151	.127	.074
1237	.126	.080
1315	.116	.075
1422	.110	.077
1503	.104	.087
1545		.089
4-4-77		
1053	.127	.105
1133	.113	.107
1209		.106
1452	.172	.160
1533	.183	.171
1617	.207	.195

† OL = overland; OW = overwater

* ~ = approximately or variable with average value indicated; // = parallel; ⊥ = perpendicular

relatively low values of absolute humidity and high visibilities. (Refer to Figure 5 for wind direction information). The four days occurring during the middle portion of this period (March 9 through 12, prior to a cold front passage on 14 March) exhibited a weather pattern marked by winds moving from NE to SE, along with increasing absolute humidity and decreasing visibility. It is interesting to note that the air temperature decreases lag the onset of frontal passages by as much as one day; note the drop in air temperature on 8 March and the less dramatic drop on 15 March after several days of systematically increasing temperatures.

The second and third long-path measurement periods (31 March through 5 April and 16 May through 25 May, respectively) presented more static weather situations with predominately overwater wind conditions except for 5 April when another frontal passage occurred. During the second period generally high water vapor conditions (18 torr ppH_2O), high air temperatures (24^oC) and moderate visibilities (14 to 30 km) accompanied the steady and moderate (~5 m/s) overwater winds which were primarily perpendicular to the optical path (see Figure 5). Measurements performed during this period should be quite representative of overwater propagation conditions since the conditions along the propagation path would be expected to be more nearly uniform with a wind direction near-normal to the optical path. The third experimental period between 16 and 25 May inclusive exhibited exclusively overwater wind conditions with intermediate to high values of absolute humidity, increasing air temperatures and moderate to high visibilities. On all days during the third measurement period, with the exception of 17 May, wind directions were nearly perpendicular to the optical path and varied between

ENE and SSW. These general observations are useful when interpreting the transmission measurements analyzed in this report.

Table 3 contains the information pertinent to the CCAFS spectra analogous to that presented in Table 1 for the PRNAS data.

2.2.3 SAN NICOLAS ISLAND

The 4.07 km overwater path used in the SNI measurements is shown in Figure 6. The NRL IMORL transmitter station was located at site A and the receiver was located at site C in the figure. The path is located along the northern shoreline of SNI.

The meteorological conditions occurring during the SNI experimental period were quite constant when compared with the PRNAS and especially the CCAFS data. A small variation of less than 1 torr in absolute humidity (8.1 to 8.9 torr ppH_2O) and of slightly more than one degree Celsius in air temperature (10.1 to 11.7^oC) characterize the atmospheric conditions occurring during the times that laser transmission and FTS measurements were made. In general, moderately high windspeeds between 5.7 and 11.5 m/s, accompanied by moderate visibilities, occurred during the measurement period. The moderately high windspeeds and the proximity of shoals upwind of the propagation path are viewed as contributing to the generation of proportionately larger aerosol extinction coefficients in the 3-5 μm region than in the case of the CCAFS or PRNAS data. The relatively isolated location of SNI in the open ocean is expected to result in the presence of a more maritime-like aerosol with a proportionately larger number of larger particles, resulting from condensation on wave-generated salt-particle nuclei. In these cases aerosol extinction coefficients are expected to

TABLE 3. SUMMARY OF METEOROLOGICAL CONDITIONS AND LASER NORMALIZATION PARAMETERS FOR THE CCAFS SPECTRA.

Date	Local Time		Spectrum Number	AT (°C)	PPH_2O (Torr)	D.P. (°C)	RH (%)	WD (°)	WS (m/s)	Visibility (km)	σ_{AER}		H_2O Continuum Tabulation	H.R. Digital File	Absolute Normalization	
	FTS	Laser									0.55μm (km^{-1})	3.8μm (km^{-1})			Correction Factor	Fitting Error (±)
3-03-77	1250	1445	CC083	17.8	13.2	15.8	82	107	3.5	18		.1321	Yes			
3-31-77	1215	1416	CC119	26.0	16.8	20.6	76	152	4.5	24		.057	Yes	Yes	1.005	0.0083
	1245	1416	CC120	25.6	18.0	20.6	76	152	4.5	24		.057	Yes	Yes	1.0010	0.0122
4-01-77	1310	1225	S0121	24.0	17.7	20.3	79	115	3.0	14	.196	.1721	Yes	Yes	0.9999	0.0 49
5-20-77	1350	1511	CC144	26.7	14.7	17.2	66	80	3.2	25	.101	.055	Yes	Yes	0.994	0.0140
	1415	1511	CC145	26.7	14.8	17.2	66	80	3.2	25	.101	.055	Yes	Yes	0.9913	0.0145
5-21-77	1245	1152	CC147	26.3	16.3	18.8	64	91	4.9	16	.164	.088	Yes	Yes	1.0078	0.0344
	1300	1347	CC148	26.5	16.5	18.8	63	90	4.8	15	.164	.094	Yes	Yes	1.0074	0.0363
5-23-77	1310	1226	CC153	26.8	17.5	20.4	73	112	2.0	37	.048	.036	No	Yes	1.0173	0.0158
	1330	1450	CC154	26.6	17.4	20.7	72	78	4.8	55	.048	.022	No	Yes	1.0108	0.0201
5-24-77	1145		CC157	26.9	20.3	22.6	76	130	3.2	29	.057	.063	No	Yes	1.0041	0.0210
	1210	1349	CC158	26.8	20.0	22.6	78	110	5.1	33	.057	.069	No	Yes	1.0058	0.0224
	1535	1349	CC159	26.7	21.6	22.6	78	110	5.1	33	.057	.069	No	Yes	0.9986	0.0124
5-25-77	0955	1125	S0160	29.5	20.0	22.2	64	145	3.3	29	.100	.047	No	Yes	1.0004	0.0035
	1155	1125	S0161	30.0	20.5	22.6	64	145	3.3	29	.100	.047	No	Yes	0.9981	0.0025

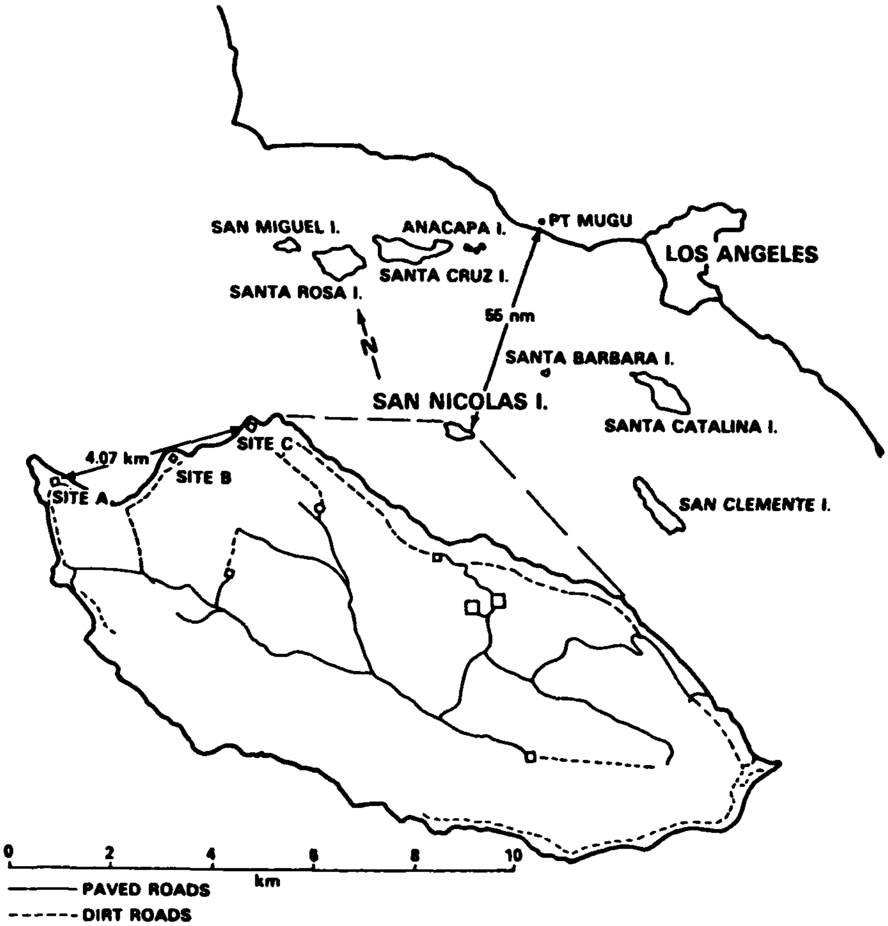

FIGURE 6. SNI ATMOSPHERIC TRANSMISSION TEST SITE.

be more nearly comparable for visible and infrared wavelengths than in the case of a continental aerosol where the particulate size distribution contains relatively fewer large particles.

Table 4 contains a summary of the information pertaining to the SNI spectra that was presented earlier for the PRNAS and CCAFS data in Tables 1 and 2.

2.2.4 WHITE SANDS MISSILE RANGE

The measurement sites used for the WSMR/ASL experiment are shown in Figure 7. The IMORL transmitter station was located on an elevated berm approximately 5 m above the desert floor near WSMR Arky site. The receiver station was located on a berm used for photographic data collection at the WSMR PAT site and was approximately 8 m above the desert floor. The propagation path of 6.4 km extended in a nearly north-south direction as shown in Figure 7.

The meteorological conditions occurring during the WSMR experiment are characterized by moderate temperatures (15.6 to 21.7°C), low absolute humidities ranging between 2.0 and 4.5 torr ppH_2O and very high visibilities, varying between 46 and 168 km.

A summary of the meteorological conditions and normalization parameters describing the WSMR FTS data is presented in Table 5.

TABLE 4. SUMMARY OF METEOROLOGICAL CONDITIONS AND LASER NORMALIZATION PARAMETERS FOR SNI SPECTRA.

Date	Local Time		Spectrum Number	AT (°C)	PPH_2O (Torr)	RH (%)	WD (°)	WS (m/s)	Visibility† (km)	σ_{AER}		H_2O Continuum Tabulation	H.R. Digital File	Absolute Normalization	
	FTS	Laser								0.55μm (km^{-1})	3.8μm (km^{-1})			Correction Factor	Fitting Error (±)
5-01-79	1031	1004	SNI01	10.9	8.8	91	249	6.75	48	.054	.030	No	Yes	1.0	.0225
	1107	1004	SNI02	10.9	8.6	91	249	6.75	48	.054	.030	No	Yes	1.0	.0244
	1611	1344	SNI04	11.2	8.3	84	269	11.3	33	.092	.051	No	Yes	1.0	.0132
	1725	1853	SNI05	11.1	8.2	76	260	11.5	33	.214	.053	No	Yes	1.0	.0150
5-02-79	0937	0846	SNI06	10.4	8.4	82	275	11.4		.333	.227	No	Yes	1.0	.0139
	1604	1504	SNI09	10.8	8.8	82	258	8.9	29	.209	.136	No	Yes	1.0	.0181
	1900	1826	SNI10	10.6	8.9	80	259	7.6	24	.383	.274	No	Yes	1.0	.0164
5-03-79	0900	0828	SNI11	10.1	8.9	88	271	5.7	24	.306	.202	No	Yes	1.0	.0300
	1910	1833	SNI12	10.5	8.2	80	265	6.6	35	.128	.073	No	Yes	1.0	.0491
5-07-79	1439	1516	SNI14	11.7	8.9	80	255	10.9	36	.154	.110	No	Yes	1.0	.0266
	1950	1831	SNI16	11.3	8.8	82	256	11.4	20	.192	.136	No	Yes	1.0	.0392
5-08-79	1015	0938	SNI17	11.1	8.1	76	277	10.9	47	.101	.065	No	Yes	1.0	.0318
5-09-79	2020	1914	SNI24	10.8	8.1	81	275	10.5	21	.394	.266	No	Yes	1.0	.0109

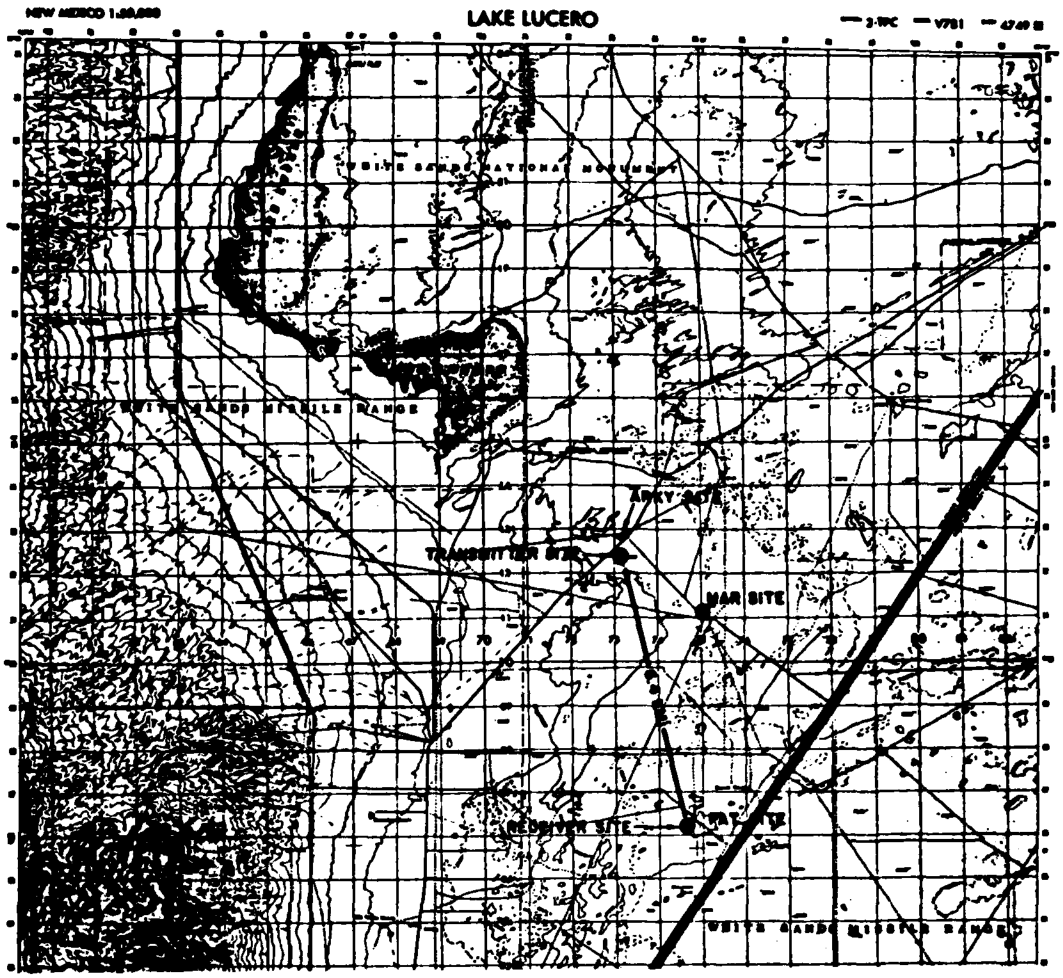

FIGURE 7. WSMR ATMOSPHERIC TRANSMISSION TEST SITE.

TABLE 5. SUMMARY OF METEOROLOGICAL CONDITIONS AND LASER NORMALIZATION PARAMETERS FOR WSMR SPECTRA.

Date	Local Time		Spectrum Number	AT† (°C)	PPH_2O† (Torr)	RH (%)	WD† (°)	WS† (m/s)	Visibility† (km)	σ_{AER}		H_2O Continuum Tabulation	H.R. Digital File	Absolute Normalization	
	FTS	Laser								0.55μm (km^{-1})	3.8μm (km^{-1})			Correction Factor	Fitting Error (±)
3-14-79	1538	1630	ASL 04RN	17.8††	4.5††	34	140††	8.5††	100	.039	.003	No	Yes	1.0	.0225
	1741	1630	06	17.8††	4.5††	34	140††	8.5††	100	.039	.003	No	Yes	1.0	.0159
3-16-79	1606	1705	13	21.7	3.5	27	190	6.9	168	.023	.001	No	Yes	1.0	.0336
	1623	1705	14	21.7	3.5	27	190	6.9	168	.023	.001	No	Yes	1.0	.0280
	1757	1705	15	21.7	3.5	27	190	6.9	168	.023	.001	No	Yes	1.0	.0197
3-17-79	1551	1652	17	19.4	2.0	21	230	7.9	46	.086	.008	No	Yes	1.0	.0190
	1615	1652	18	19.4	2.0	21	230	7.9	46	.086	.008	No	Yes	1.0	.0143
	1740	1652	19	19.4	2.0	21	230	7.9	46	.086	.008	No	Yes	1.0	.0147
	1751	1652	20	19.4	2.0	21	240	7.9	46	.086	.008	No	Yes	1.0	.0155
3-18-79	1623	1700	22	15.6	3.1	27	200	2.0	151	.025	.003	No	Yes	1.0	.0280
	1737	1700	23	15.6	3.1	27	200	2.0	151	.025	.003	No	Yes	1.0	.0418

†Data at Arky Site not available; values used were interpolated between measurements taken at WSMR Desert Site and Holloman Air Force Base.

††Directly measured at Arky Site.

3
DATA ANALYSIS

3.1 WATER VAPOR CONTINUUM ABSORPTION ANALYSIS

3.1.1 EVALUATION OF ABSOLUTE-TRANSMISSION NORMALIZATION UNCERTAINTIES

The procedures used in deriving absolute transmission calibrations for the NRL FTS spectra involved the initial generation of a relative transmission spectrum, followed by absolute-transmission normalization of this spectrum using the measured absolute transmittance values obtained from a set of DF laser transmittance measurements.

By ratioing the long-path spectra to local source spectra, the source, beamsplitter, and detector spectral response functions were removed from the resulting spectra. The ratioed spectra were then converted from relative to absolute transmission by determining the scale factor needed to convert the relative transmission value of a spectrum at a particular laser frequency to the absolute transmission value obtained by means of an independent, long-path laser extinction measurement.

Detailed numerical examples showing the application of these procedures to the normalization of the WSMR and SNI data are provided in References 4 and 5, respectively. During the course of the detailed procedures used in the normalization of the WSMR and SNI spectra, the selection of a subset of the several available DF laser transmittance measurements was made to exclude measurements for laser lines located in close proximity to strong atmospheric absorption lines. The uncertainty associated with using a measured transmittance value for such a line to normalize an FTS spectrum was found to be substantially larger (several percent uncertainty) than that associated with the use of a

line well isolated from the effects of strong local lines. Consequently, a re-evaluation of the atmospheric-transmission-normalization of the PRNAS and CCAFS spectra was performed, excluding such lines in question (e.g. the P2-10 DF laser line). The results of this re-normalization are shown under the heading "absolute normalization correction factor" in Tables 1, 2, 4, and 5. As can be seen in the tables, the absolute-transmission correction factors thus obtained differ from unity by $\pm 1\%$ and are consequently not significant within the overall experimental uncertainty in the measured data. These correction factors do not apply to the WSMR and SNI data which were originally normalized using the selected subset of laser line measurements. The right-most columns in Tables 1, 2, 4, and 5 list the RMS deviations of the differences between measured individual laser transmittance values and the absolute transmittance value of a resultant normalized FTS spectrum at the frequency of that laser line (actually the transmittance values at the two spectrum sample locations that bracket the position of the laser line frequency). These RMS deviations (labeled fitting errors in the tables) provide a measure of the overall quality of fit or normalization uncertainty, as well as an indirect measure of spectral signal to noise ratio. For the best examples (several CCAFS spectra) these quantities are $< \pm 1\%$ in absolute transmittance. The "worst case" examples are seen be $\sim \pm 5\%$ in absolute transmittance. It is felt that the strength of atmospheric turbulence along the measurement path occurring during both the laser and FTS transmittance measurements is a primary factor in determining the magnitude of the fitting errors listed in the tables. The smaller numerical values correspond to data of higher quality and greater reliability.

3.1.2 CORRECTIONS TO THE EXPERIMENTAL DATA

In the 3-5 μm window considered here, three phenomena play major roles in the reduction of atmospheric transmission data, namely aerosol extinction, molecular absorption lines, and molecular continuum absorption. Multiple-scattering effects due to aerosols are not significant in the data examined below, since the aerosol extinction coefficients are typically small ($< 0.2\ km^{-1}$). Modification of apparent transmission by thermal emission is also neglected in the following analysis since the laser source used in the measurements was modulated at the source location. Unmodulated emission from the intervening path was therefore not detected in the laser extinction measurements. Independent FTS measurements of the optical path emission (using the same configuration as used during laser and FTS transmission measurements, only with the blackbody source not operating) showed that path emission in the 3-5 μm region was negligible compared with the blackbody source signal.

The comparisons of measured FTS data with water continuum absorption calculations performed using the FASCODE model which are presented below are based on a correction of the measured data for local absorption line, CO_2 and N_2 continuum, and aerosol scattering effects. The optical depth at selected frequencies arising from the first two types of corrections was calculated and subtracted from the optical depths obtained from the measured data. Aerosol scattering contributions to the optical depths obtained from the transmission data are not readily discernible. In most cases (for data other than selected CCAFS spectra) reliable, independent aerosol extinction values are not available, consequently no well-defined distinction between water continuum absorption and aerosol scattering contributions to the measured optical depth can be made. In these cases the

"shape" of the water vapor continuum absorption coefficient can be examined by comparisons with comparable values calculated using the FASCODE model. This approach relies upon the assumption that the aerosol contribution to the measured optical depth can be obtained from the difference between the measured optical depth, corrected for local line and N_2 and CO_2 continua contributions, and the calculated optical depth due to water vapor continuum absorption obtained using FASCODE. That is, the magnitude of the calculated water vapor continuum absorption is assumed to be correct at some frequency and the difference between it and the measured optical depth (appropriately corrected for molecular absorption) is the aerosol extinction component at that frequency. This aerosol component, with appropriate scaling in wavelength, can then be subtracted from the measured data throughout the 1900 - 3100 cm^{-1} region and any systematic differences between the measured optical depth and that calculated using FASCODE can be determined.

Detailed information describing the calculated local line and N_2 and CO_2 continuum corrections and the corrections for aerosol extinction applied to the measured data is presented in the following two subsections.

3.1.2.1 Corrections for Local Line and for CO_2 and N_2 Continuum Contributions

The water vapor continuum is best observed at wavenumbers where molecular line contributions to total absorption are minimized. A set of 49 such wavenumbers in the 3-5 μm band was chosen for this study. Nevertheless, the effects of wings of molecular lines local to the selected wavenumbers is frequently strong and must be evaluated.

The local line absorption at a frequency ν_o is defined as the absorption due to all the lines whose centers are

within some distance $\Delta\nu$ from ν_o. The difference between the measured and the local line absorptions is the "continuum". The magnitude of the continuum depends upon the interval $\Delta\nu$. For the calculations performed in this study $\Delta\nu = 25\ cm^{-1}$ around the line frequency ν_o. The local line contributions were computed with the aid of FASCOD1C, in a mode where continuum effects were excluded. The results of this computation were considered reasonably accurate, since much theoretical and experimental work has been made in the description of line shapes and strengths in this wavenumber region.

The local line contributions were calculated using the computer program FASCOD1C [8] and the 1982 version of the AFGL Atmospheric Line Parameters Compilation [9]. This program uses a Voigt line shape for all molecules except CO_2 for which an exponential-tailed line shape described in [13] is used. These calculations are concerned with the regions between lines and away from line centers. In these regions the Voigt line shape is essentially the Lorentz line shape.

A final phenomenon treated in this work is the molecular continuum absorption due to N_2 and CO_2. These continua are especially prominent in the 2200-2500 cm^{-1} wavenumber region, as is the ν_3 CO_2 band. In recognition of the strong absorption band and continuum, no sampling points were situated in the 2223 - 2400 cm^{-1} wavenumber interval. The N_2 and CO_2 continuum models of FASCOD1C were utilized to estimate continuum absorption at sampling points in the vicinity of the ν_3 band.

The absorption coefficient due to the water vapor continuum α_{wc} is simply the observed total extinction coefficient ε minus the individual coefficients due to other effects:

$$\alpha_{wc} = \varepsilon - (\alpha_{LL} + \alpha_{CON} - \sigma_{AER}), \qquad (1)$$

where α_{LL} is the absorption coefficient due to local lines, σ_{AER} is the aerosol extinction coefficient at 3.8 μm, and α_{CON} is the N_2 and CO_2 continuum absorption coefficient (all dimensions are in km^{-1}).

For this analysis, 49 wavenumbers were chosen for which the absorption is a local minimum; these wavenumbers are listed in Table 6. There are 16 points between 1930 and 2224 cm^{-1}, and 33 points between 2400 and 3059 cm^{-1}, spaced approximately every 20 cm^{-1}. Figure 8 shows the location of these points on a plot of the measured spectrum ASL06RN. Figure 9 shows the 2 cm^{-1} wide region around each point and includes both the measured spectrum ASL06RN plus calculations of only the local line contribution for 2.5, 5.0, 10.0, and 20.0 torr of water vapor. These plots demonstrate that the chosen points are points of locally minimum absorption and also minimum local line contributions. The measured spectrum shows that there are no significant lines at the chosen wavenumbers which are missing from the AFGL line tape.

It should be noted that the resolution of the measured transmittances is limited by the instrument function. Since the measured spectra are unapodized, the instrument function has the form sin ν/ν with a half width at half height of about 0.019 cm^{-1} (and a full width at the base of 0.0625 cm^{-1}). The halfwidths (half width at half height) of the absorption lines in this region are about 0.1 cm^{-1} on the average but for some water lines they are as small as 0.01 cm^{-1}. The effect of the instrument function width is to degrade the spectrum around the center of lines, increasing the measured width of the lines and decreasing the measured absorption at the line center. Therefore it is not strictly proper to plot the logarithm of the measured transmittances on an optical depth scale, as in Figure 9. How-

TABLE 6. SELECTED FREQUENCIES FOR MINIMUM LOCAL LINE CONTRIBUTIONS.

	ν (cm^{-1})		ν (cm^{-1})
1.	1930.30	26.	2599.84
2.	1952.50	27.	2618.64
3.	1974.10	28.	2640.58
4.	1979.60	29.	2661.55
5.	2004.65	30.	2679.51
6.	2031.25	31.	2700.72
7.	2056.05	32.	2719.28
8.	2084.35	33.	2740.74
9.	2102.15	34.	2760.69
10.	2130.50	35.	2778.95
11.	2150.05	36.	2800.10
12.	2159.05	37.	2820.11
13.	2166.80	38.	2839.40
14.	2177.60	39.	2860.19
15.	2190.95	40.	2880.80
16.	2223.68	41.	2899.72
17.	2400.00	42.	2920.40
18.	2420.42	43.	2941.37
19.	2440.85	44.	2959.87
20.	2480.33	45.	2979.52
21.	2501.00	46.	3000.55
22.	2520.65	47.	3020.26
23.	2540.83	48.	3040.45
24.	2560.42	49.	3058.71
25.	2580.37		

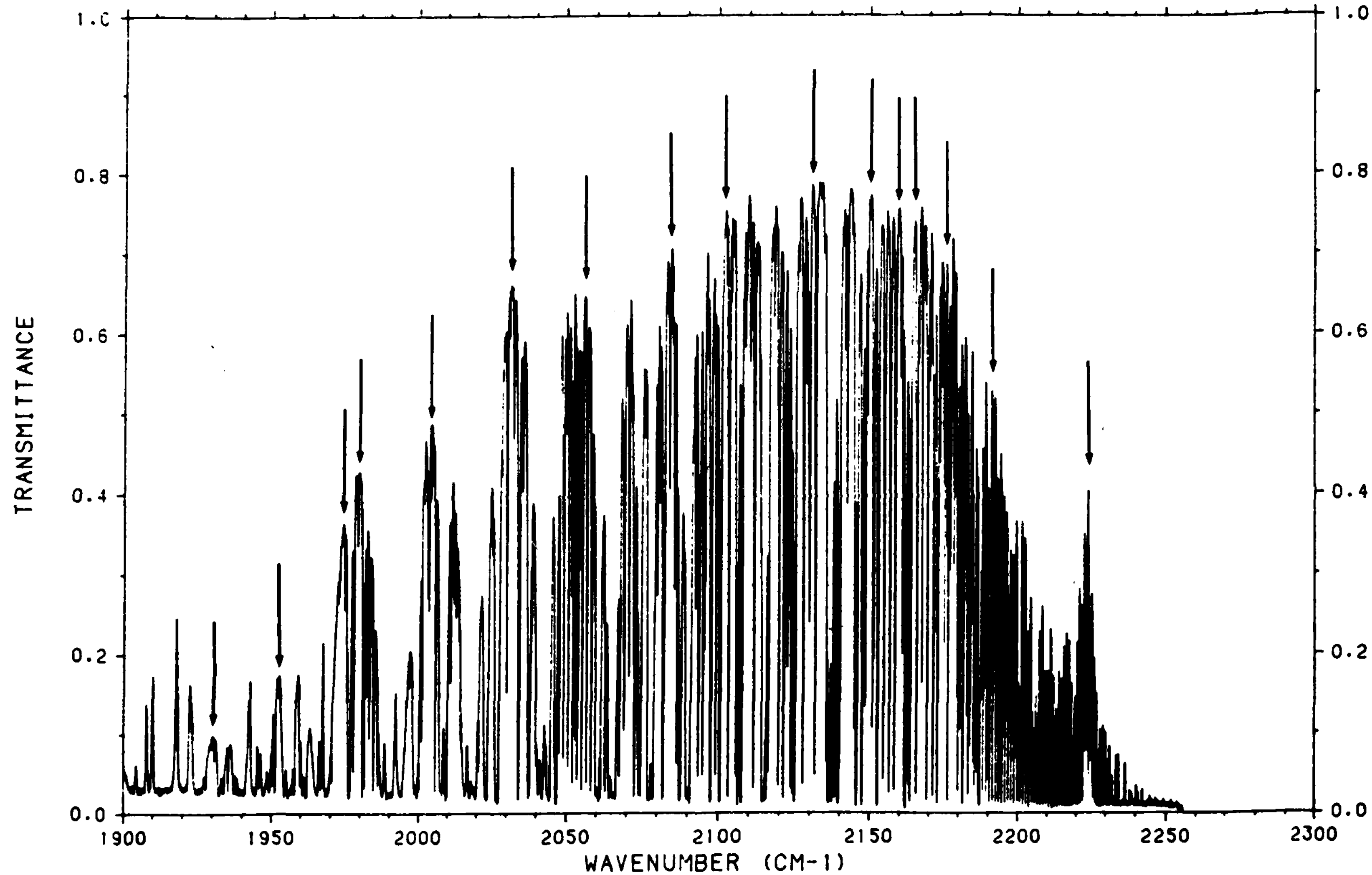

FIGURE 8. MEASURED SPECTRUM ASL06RN WITH ARROWS SHOWING THE LOCATION OF SELECTED WAVENUMBERS IN TABLE 5. (a): 1900 cm^{-1} to 2300 cm^{-1}

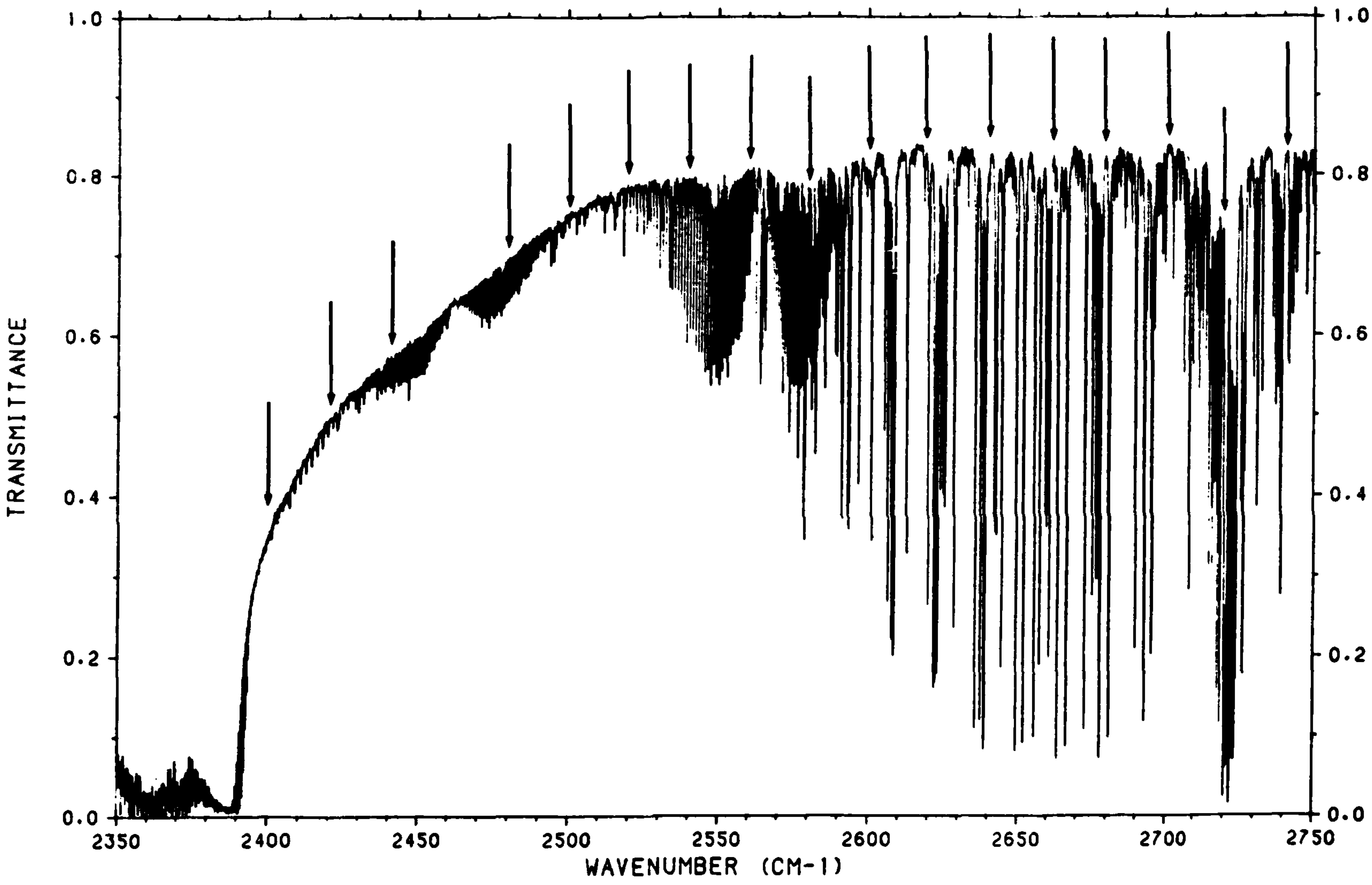

FIGURE 8. CONTINUED, (b): 2350 cm^{-1} to 2750 cm^{-1}.

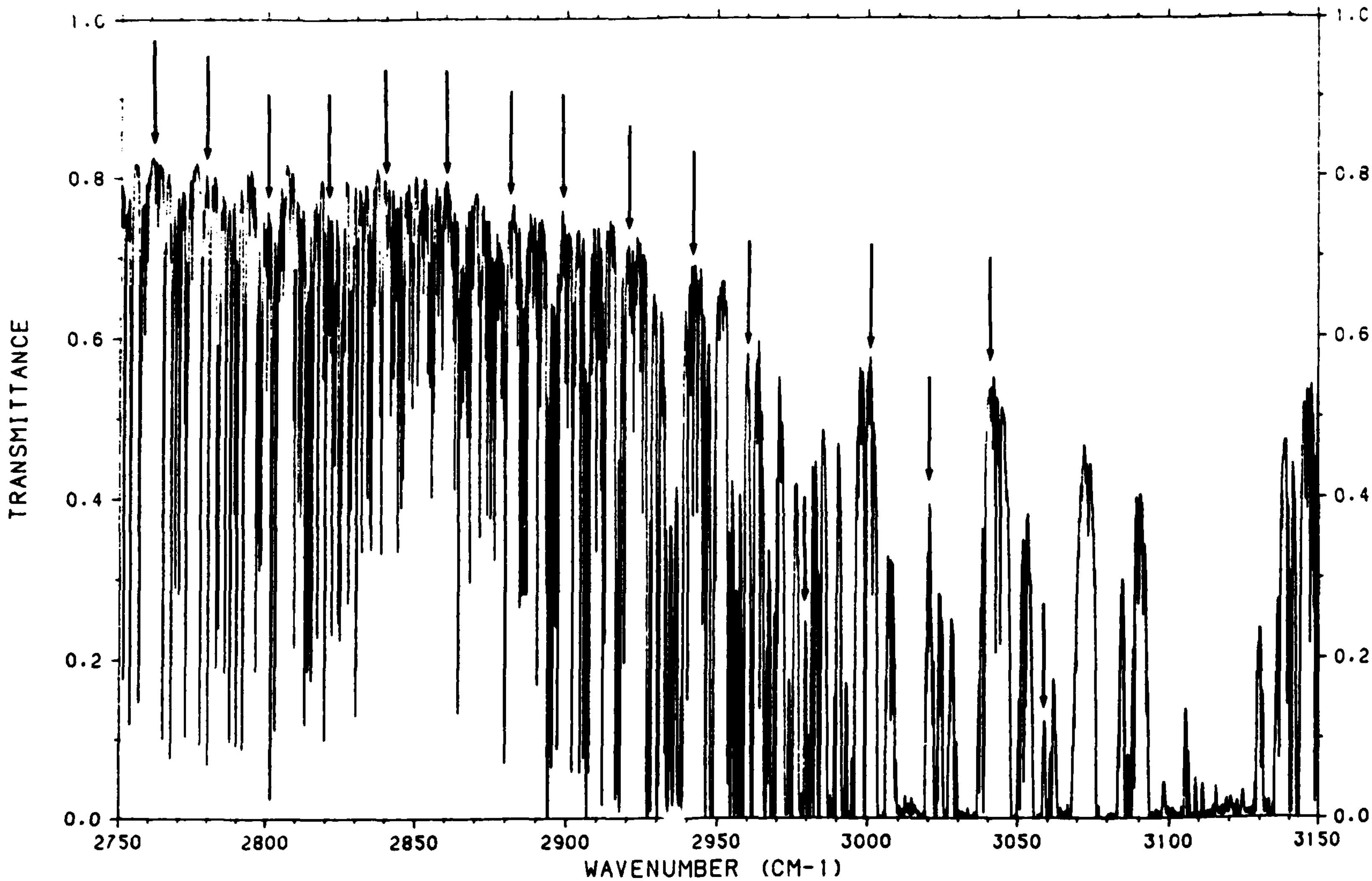

FIGURE 8. CONTINUED, (c): 2750 cm^{-1} to 3150 cm^{-1}.

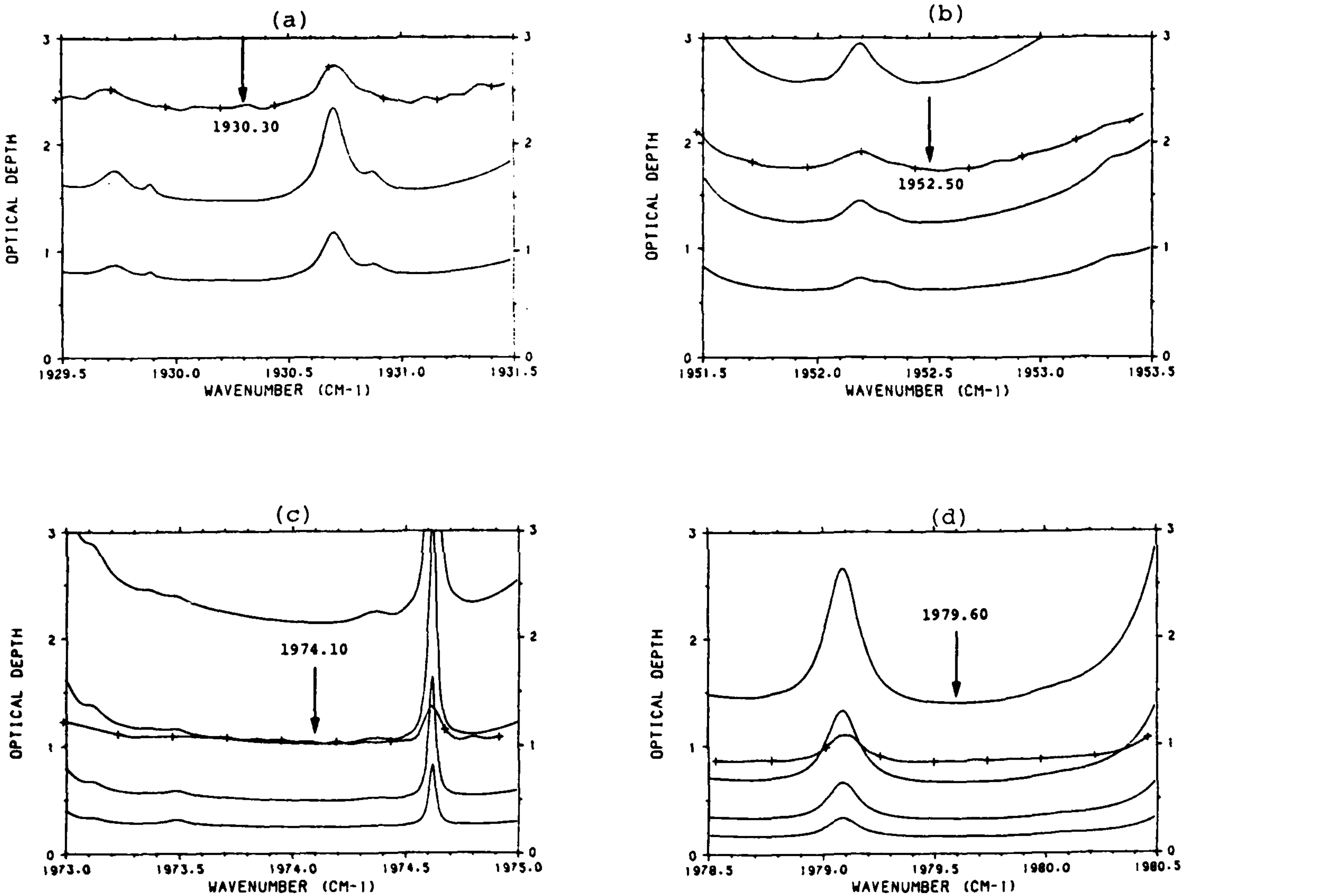

FIGURE 9. CALCULATED LOCAL LINE CONTRIBUTIONS TO THE OPTICAL DEPTH AROUND THE POINTS LISTED IN TABLE 5 FOR THE FOLLOWING CONDITIONS: P = 886 mb, T = 20°C, ppH_2O = 2.5, 15.0, 10.1, and 20 TORR, L = 6.4 km, PLUS MEASURED SPECTRUM ASL06RN (SYMBOLS). (a): 1930.30 cm^{-1}, (b): 1952.50 cm^{-1}, (c): 1974.10 cm^{-1}, (d): 1979.60 cm^{-1}.

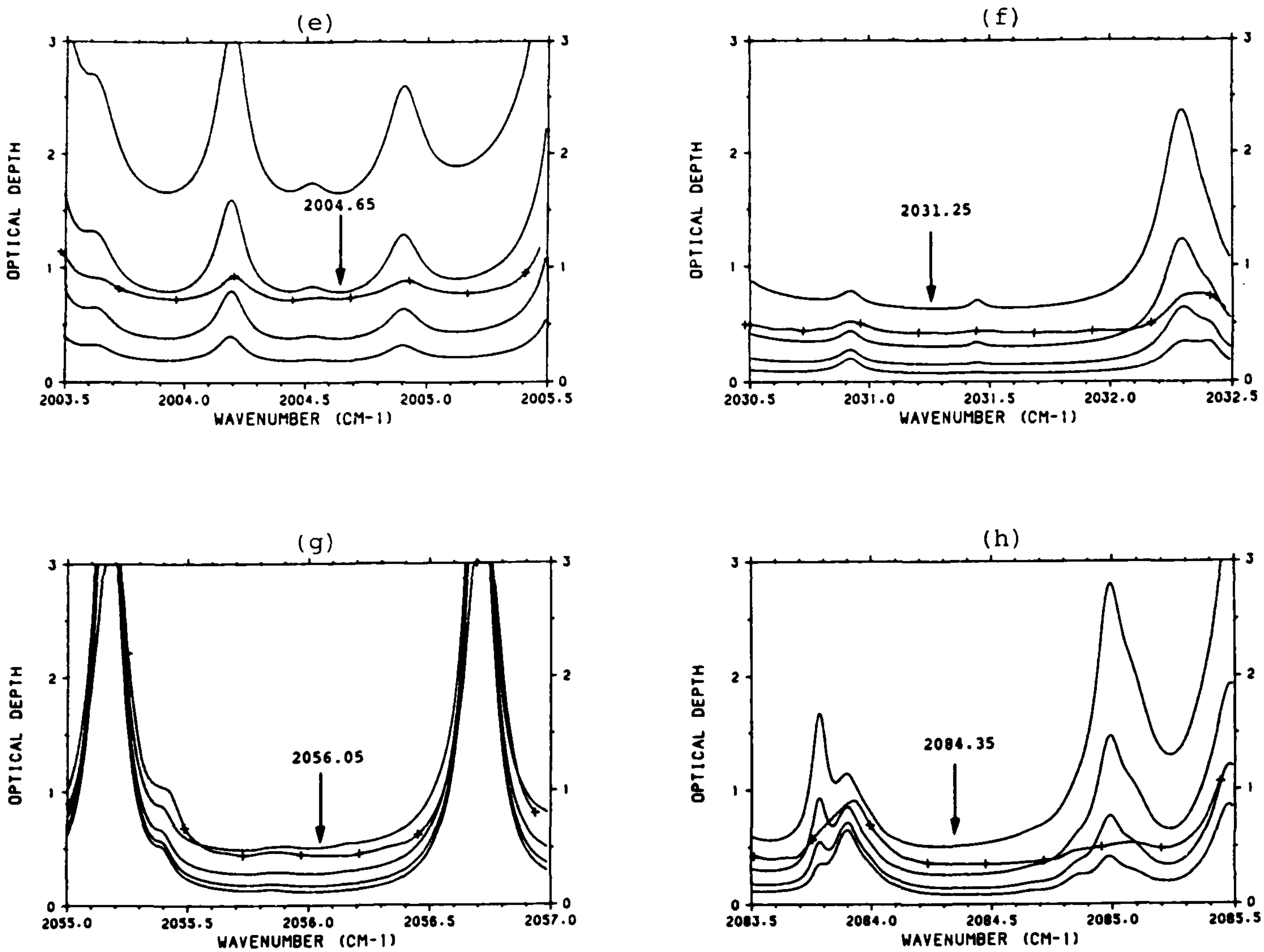

FIGURE 9. CONTINUED, (e): 2004.65 cm^{-1}, (f): 2031.25 cm^{-1}, (g): 2056.05 cm^{-1}, (h): 2084.35 cm^{-1}.

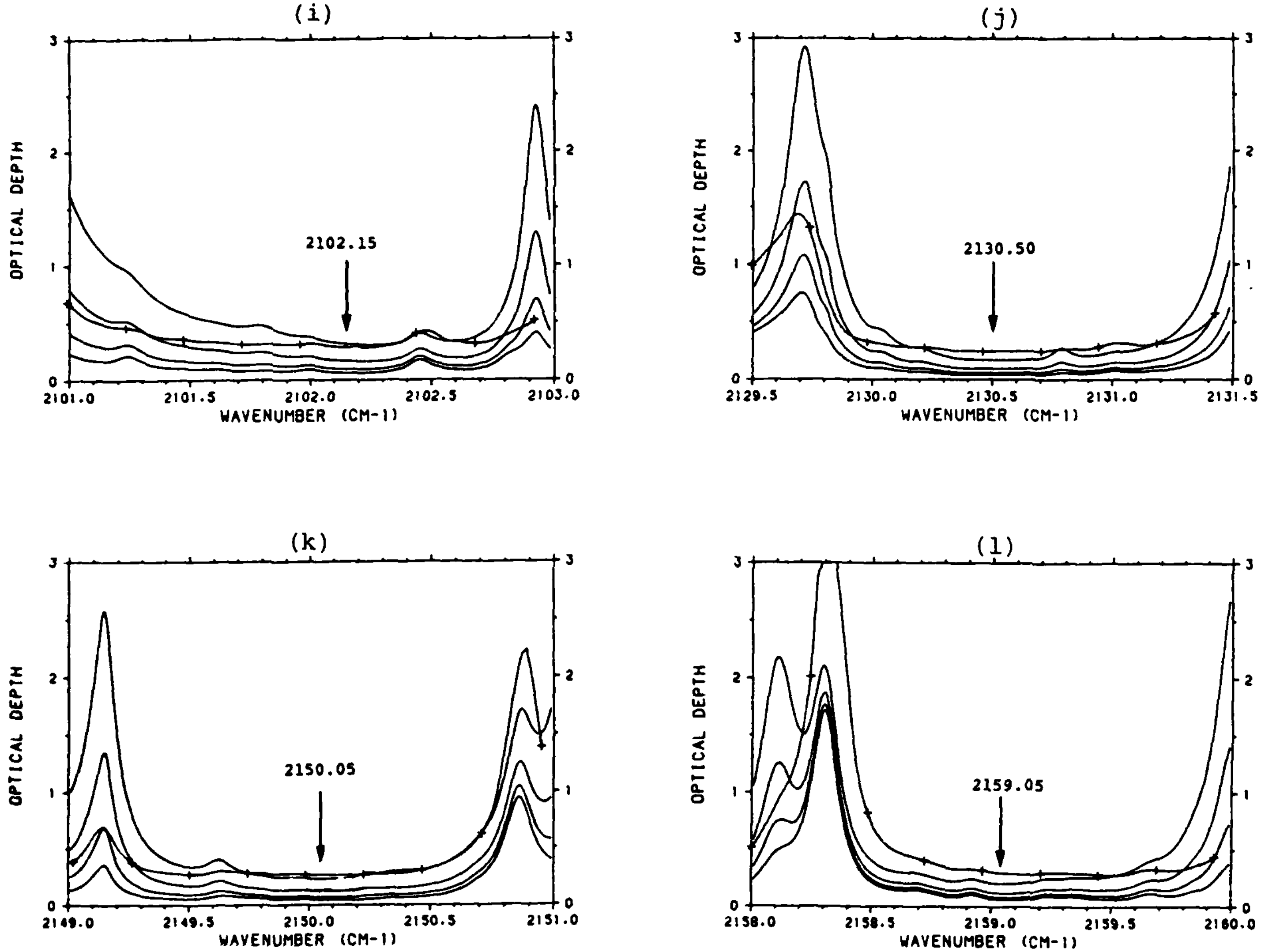

FIGURE 9. CONTINUED, (i): 2102.15 cm^{-1}, (j): 2130.50 cm^{-1}, (k): 2150.05 cm^{-1}, (l): 2159.05 cm^{-1}.

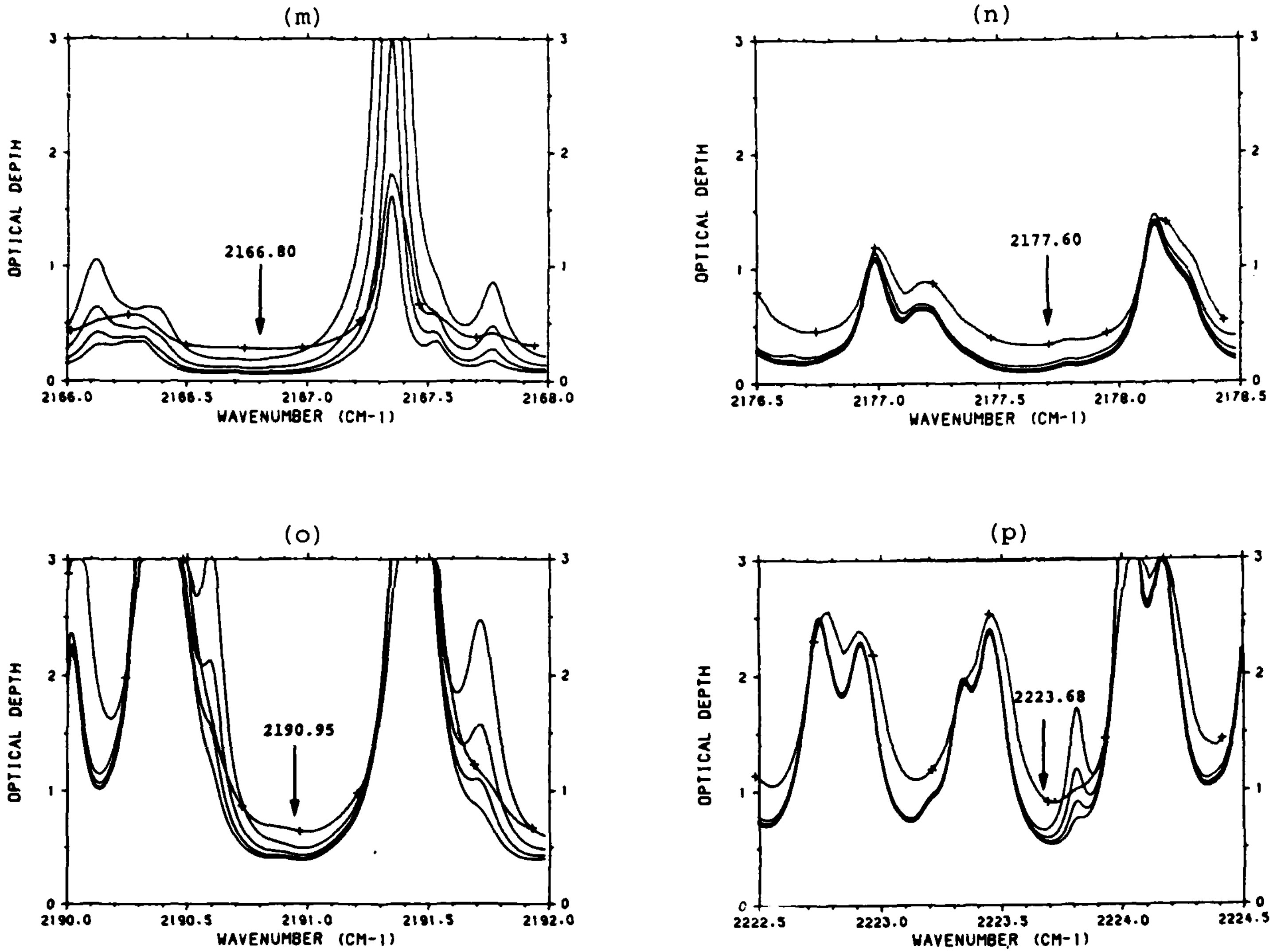

FIGURE 9. CONTINUED, (m): 2166.80 cm^{-1}, (n): 2177.60 cm^{-1}, (o): 2190.95 cm^{-1}, (p): 2223.68 cm^{-1}.

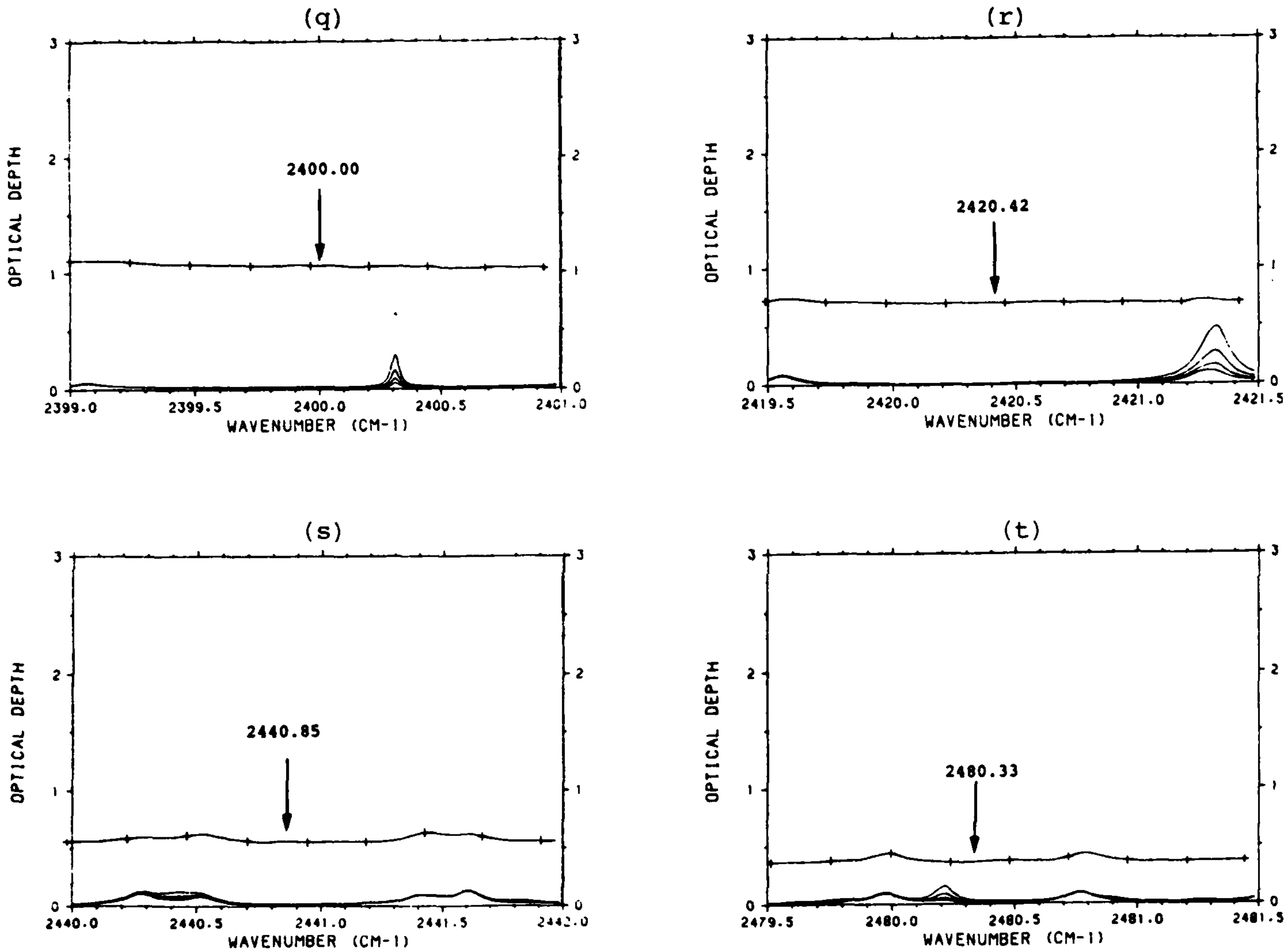

FIGURE 9. CONTINUED, (q): 2400.00 cm^{-1}, (r): 2420.42 cm^{-1}, (s): 2440.85 cm^{-1}, (t): 2480.33 cm^{-1}.

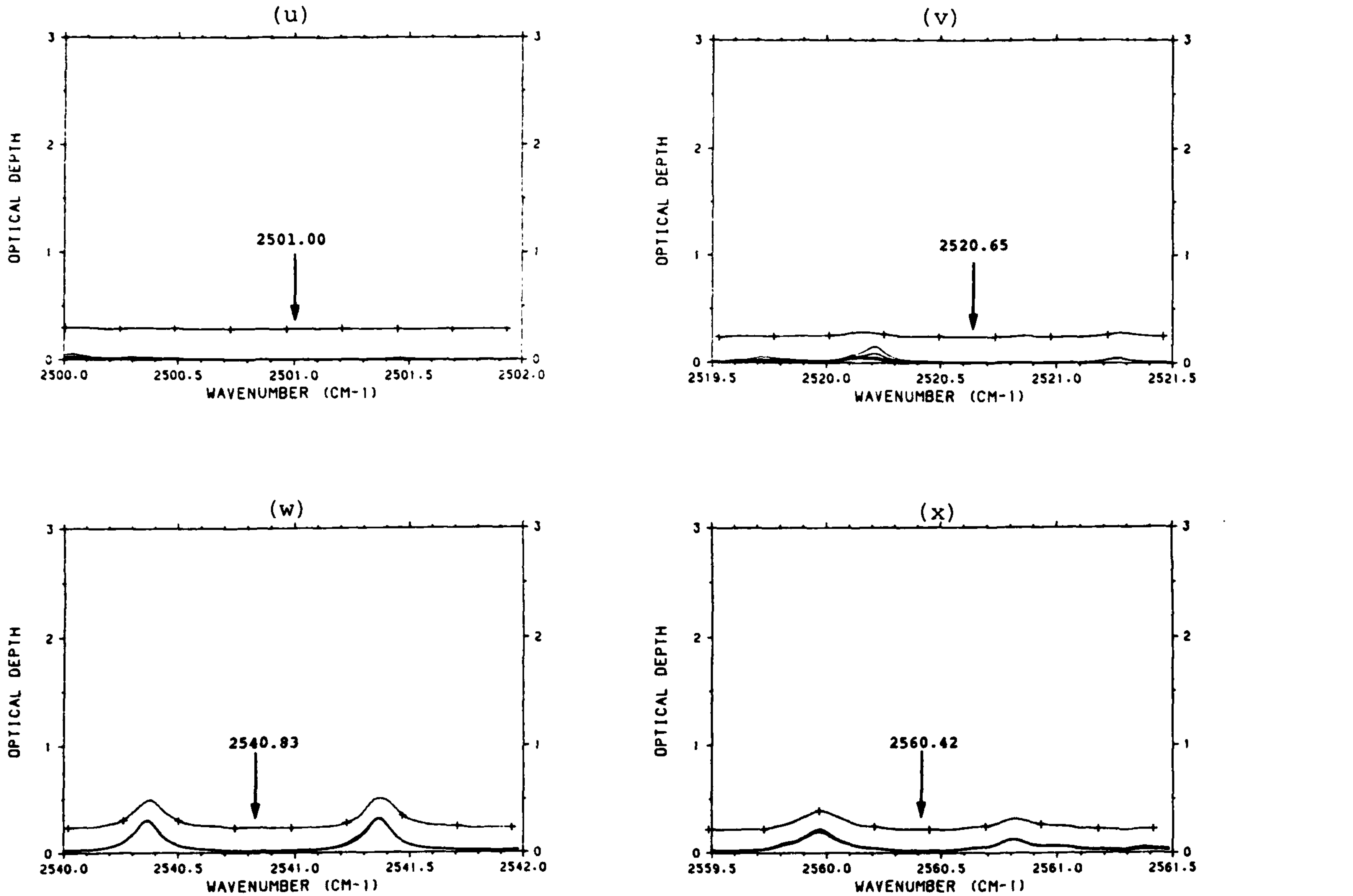

FIGURE 9. CONTINUED, (u): 2501.00 cm^{-1}, (v): 2520.65 cm^{-1}, (w): 2540.83 cm^{-1}, (x): 2560.42 cm^{-1}.

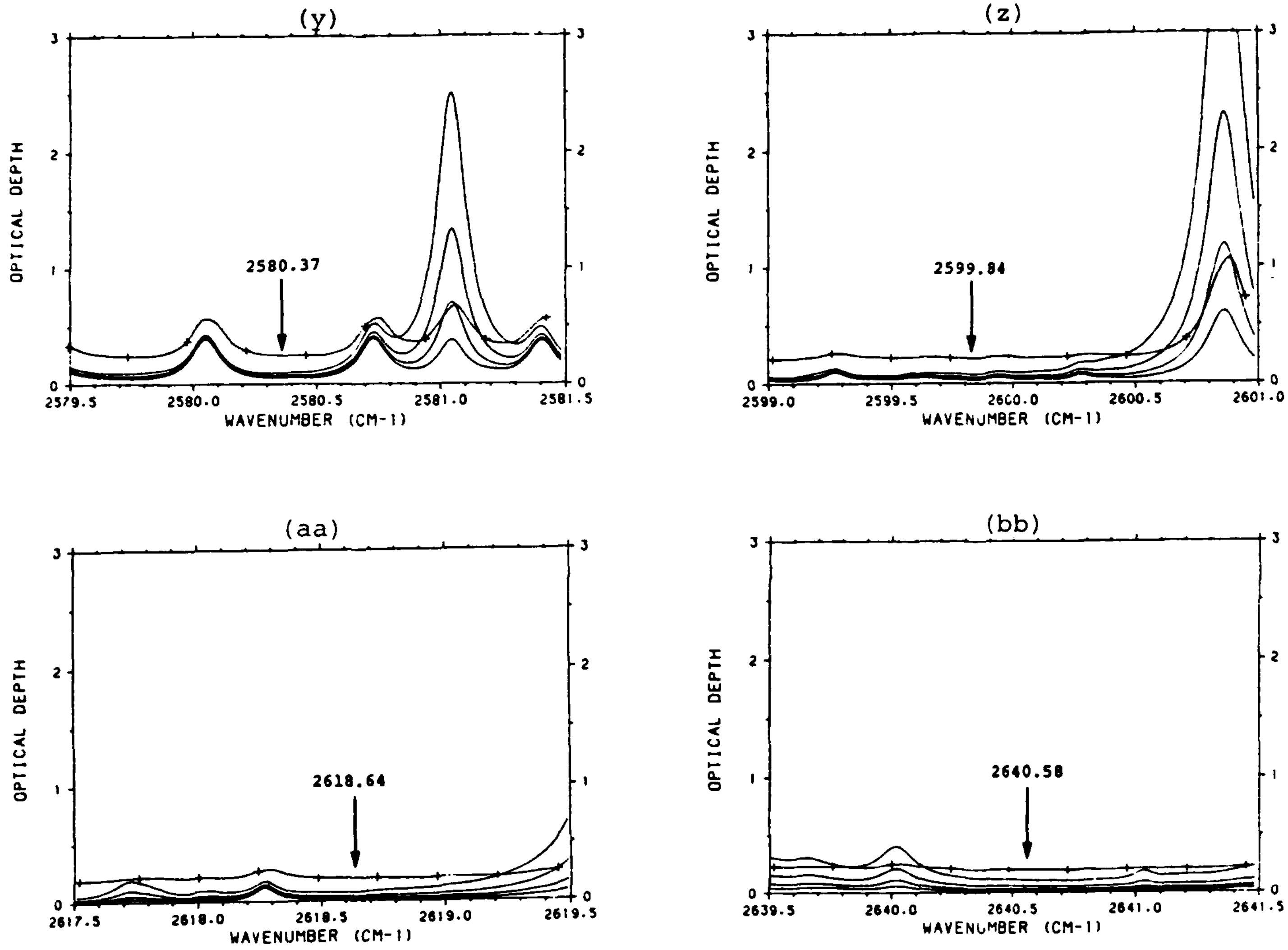

FIGURE 9. CONTINUED, (y): 2580.37 cm^{-1}, (z): 2599.84 cm^{-1}, (aa): 2618.64 cm^{-1}, (bb): 2640.58 cm^{-1}.

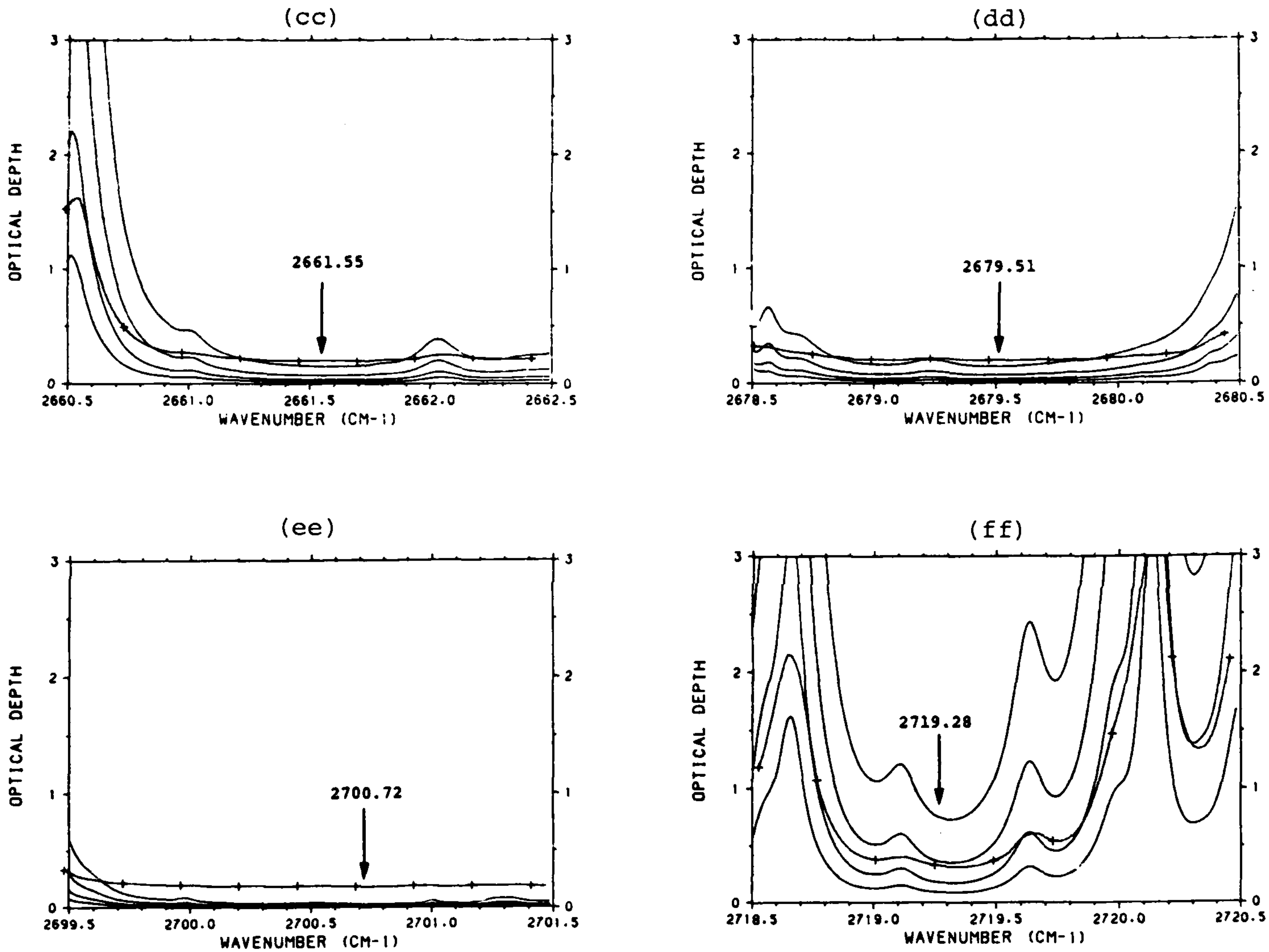

FIGURE 9. CONTINUED, (cc): 2661.55 cm^{-1}, (dd): 2679.51 cm^{-1}, (ee): 2700.72 cm^{-1}, (ff): 2719.28 cm^{-1}.

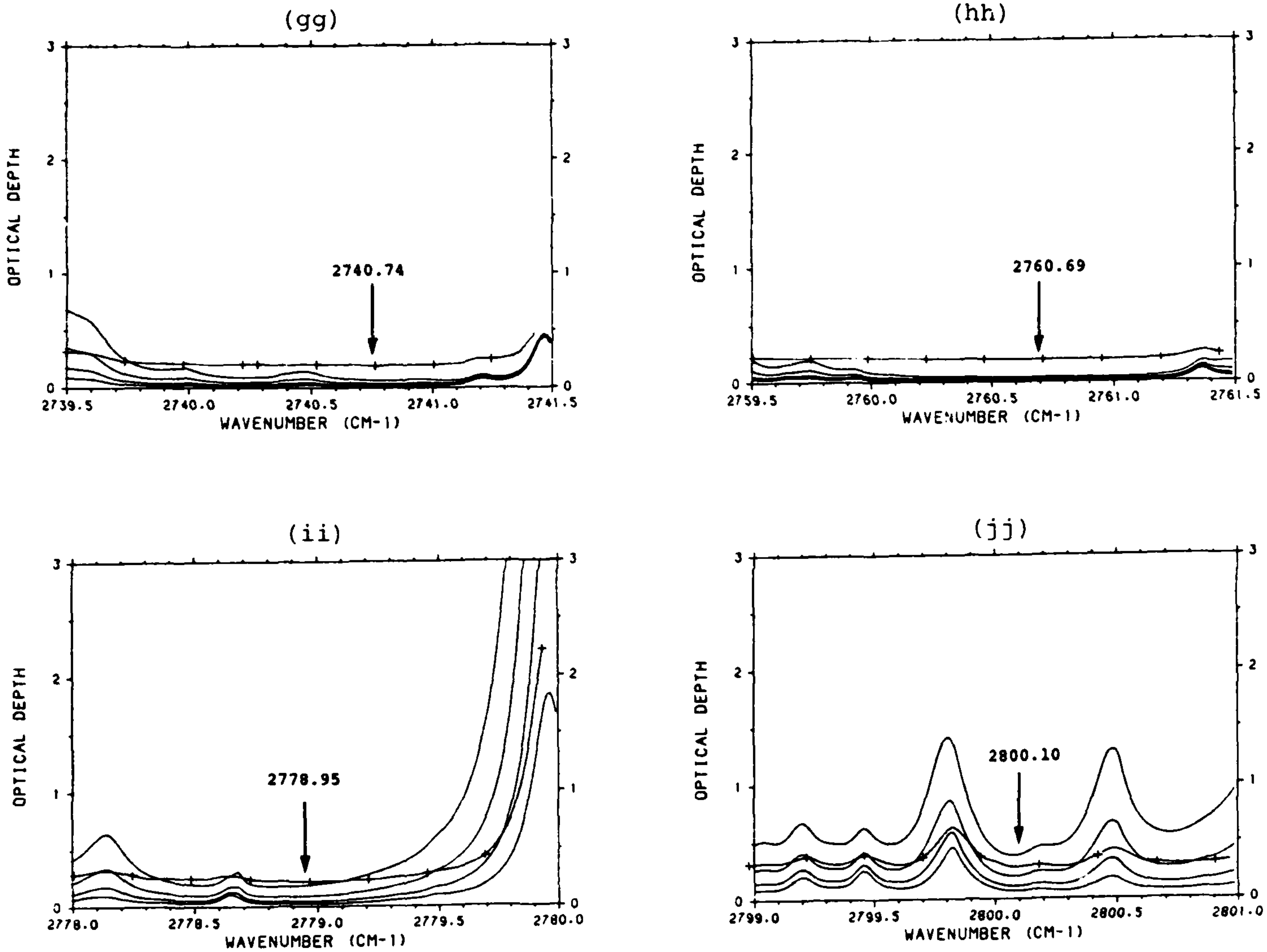

FIGURE 9. CONTINUED, (gg): 2740.74 cm^{-1}, (hh): 2760.69 cm^{-1}, (ii): 2778.95 cm^{-1}, (jj): 2800.10 cm^{-1}.

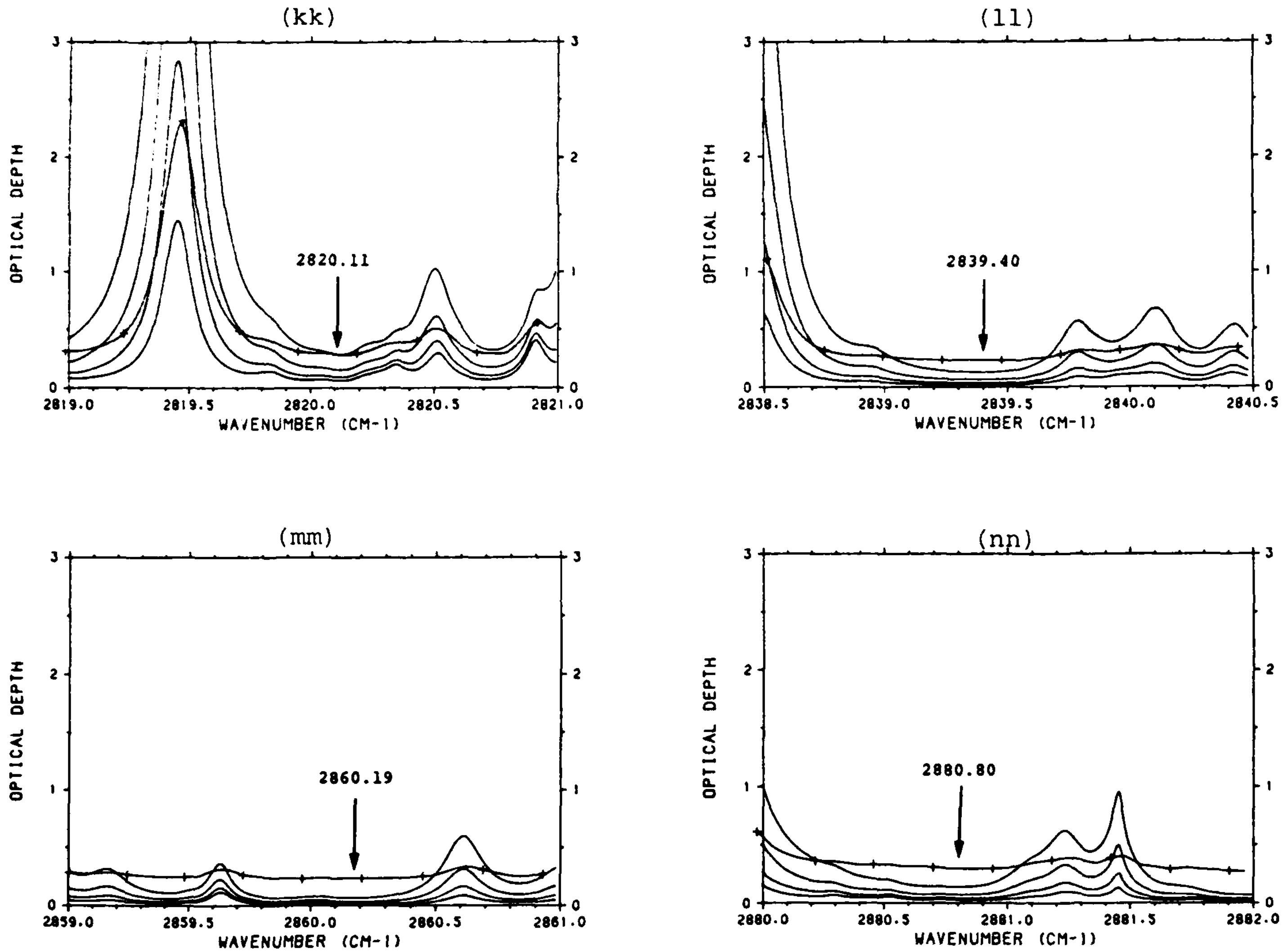

FIGURE 9. CONTINUED, (kk): 2820.11 cm^{-1}, (11): 2839.40 cm^{-1}, (mm): 2860.19 cm^{-1}, (nn): 2880.80 cm^{-1}.

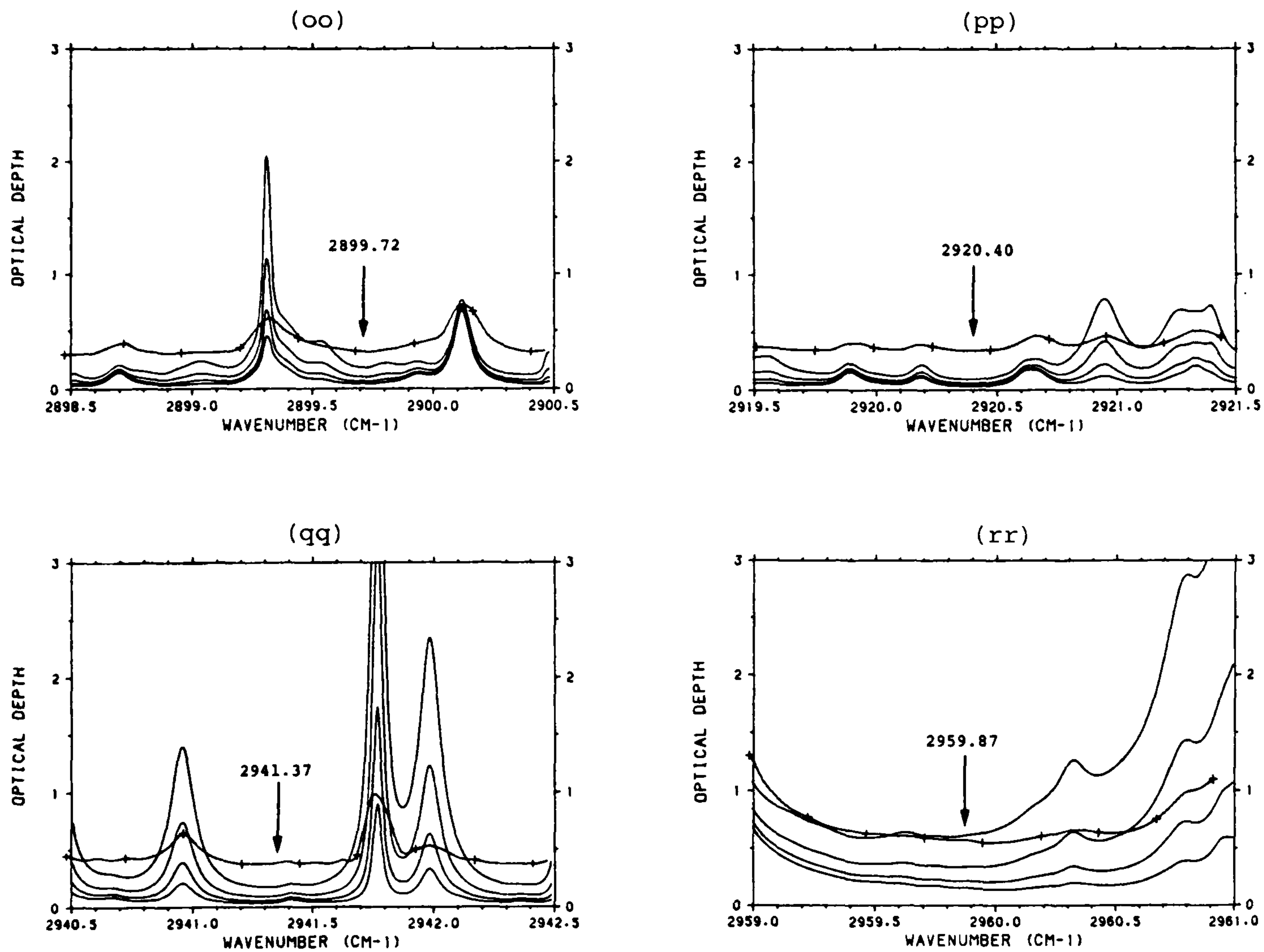

FIGURE 9. CONTINUED, (oo): 2899.72 cm^{-1}, (pp): 2920.40 cm^{-1}, (qq): 2941.37 cm^{-1}, (rr): 2959.87 cm^{-1}.

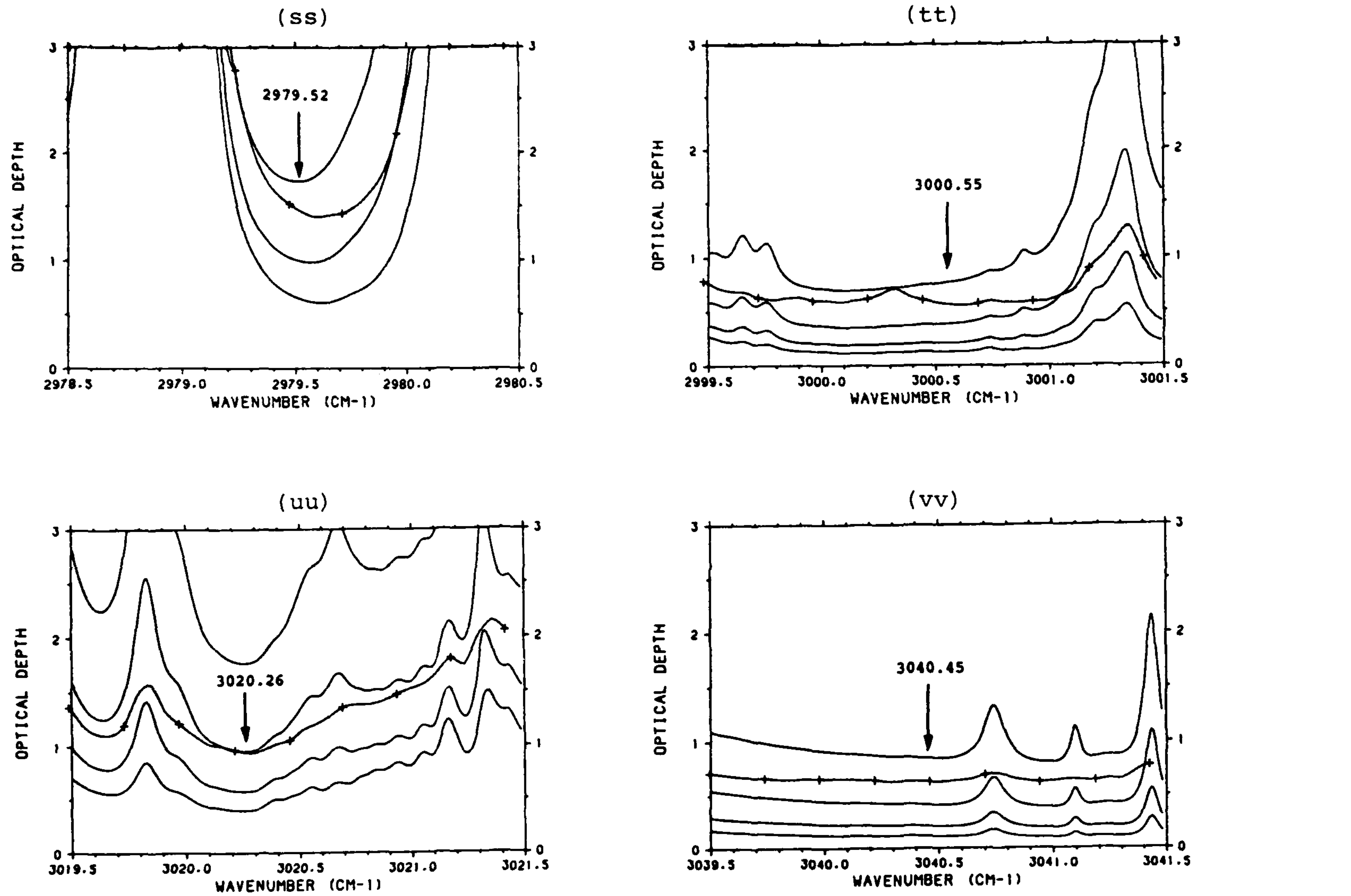

FIGURE 9. CONTINUED, (ss): 2979.52 cm^{-1}, (tt): 3000.55 cm^{-1}, (uu): 3020.26 cm^{-1}, (vv): 3040.45 cm^{-1}.

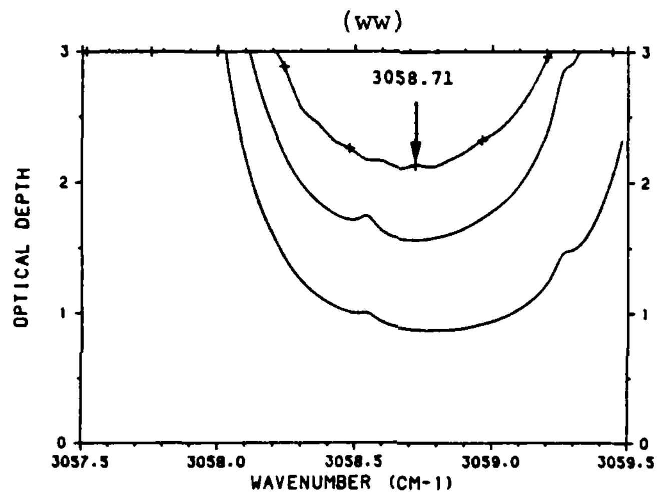

FIGURE 9. CONTINUED, (ww): 3058.71 cm^{-1}.

ever, we are concerned here with the regions between absorption lines where the effect of the instrument function is negligible.

Table 7 lists the meteorological conditions corresponding to the measured spectra used in this study. For each of these spectra, the measured optical depth (= -ln T) was corrected for aerosol, local line, and N_2 and CO_2 continuum contributions. The differences are then the measured continuum values. Table 8 lists 19 sets of conditions for the local line and N_2 and CO_2 continuum calculations along with the measured spectra associated with each calculation. Table 9 gives the volume mixing ratios used to calculate the path-integrated amounts for the gases other than water vapor. A single local line calculation was used for spectra with similar water vapor partial pressures. No aerosol extinction was included in the calculation. The local line contributions were calculated at approximately every 0.05 cm^{-1} which, in general, did not match exactly the wavenumbers in Table 6. For each wavenumber in Table 6, the nearest three calculated points were averaged. Similarly, the measured spectra are tabulated at intervals of about 0.06 cm^{-1}. For all but the Cape Canaveral spectra, the three measured points nearest to the wavenumbers in Table 6 were used; for the Cape Canaveral spectra, only the nearest point was used. The results of the calculated values for the local line, and N_2 and CO_2 continuum contributions for each of the frequencies listed in Table 6 and for each of the 19 cases listed in Table 8 are tabulated in appendices B and C, respectively.

3.1.2.2 <u>Corrections for Aerosol Scattering</u>

Attenuation due to aerosol extinction is not a well-defined quantity in the available data, for various reasons.

TABLE 7. METEOROLOGICAL CONDITIONS FOR EACH SPECTRUM.

SPECTRUM	T (^{o}C)	PPH_2O (torr)	U (gm/cm^2)	P (mb)	VIS (km)
Patuxent River L = 5.12 km					
PR024	18.7	11.4	6.14	NA	13†
PR037	0	2.8	1.32	NA	13
PR039	-1.7	2.8	1.32	NA	13
PR040	6.5	2.8	1.06	NA	13
PR042	5.4	2.8	1.28	NA	13
PR049	7.9	4.3	1.73	NA	13
PR050	7.0	4.7	1.58	NA	13
PR054	3.9	3.3	1.48	NA	13
PR055	17.3	2.5	1.27	NA	13
PR056	17.3	2.5	1.27	NA	13
Cape Canaveral L = 5.08 km					
CC083	17.8	13.2	6.66	1021	20
CC119	25.0	18.0	8.24	1022	20
CC120	25.6	18.0	8.84	1021	20
CC121	24.0	17.7	8.74	1019	20
CC144	26.2	14.7	7.19	1019	20
CC145	26.2	14.7	7.19	1019	25
CC147	26.3	16.3	8.00	1020	14
CC148	26.3	16.3	8.09	1020	15
CC153	25.6	18.0	8.56	1015	50
CC154	26.0	18.3	8.52	1015	55
CC157	26.9	20.3	9.93	1017	30
CC158	26.8	20.0	9.79	1017	30
CC159	26.7	21.0	10.28	1016	35
CC160	29.5	20.0	9.70	1015	22
CC161	30.0	20.5	9.92	1015	24

†Data obtained from the Naval Ocean Command Weather Station at PRNAS

TABLE 7. (CONTINUED).

SPECTRUM	T (°C)	PPH_2O (torr)	U (gm/cm^2)	P (mb)	VIS (km)
White Sands Missile Range	L = 6.4 km				
ASL04	17.8	4.5	2.86	886	100
ASL06	17.8	4.5	2.86	886	100
ASL13	21.7	3.5	2.19	878	168
ASL14	21.7	3.5	2.19	878	168
ASL15	21.7	3.5	2.19	878	168
ASL17	19.4	2.0	1.26	878	46
ASL18	19.4	2.0	1.26	878	46
ASL19	19.4	2.0	1.26	878	46
ASL20	19.4	2.0	1.26	878	46
ASL21	15.6	3.1	1.98	879	151
ASL23	15.6	3.1	1.98	879	151
San Nicholas Island	L = 4.07 km				
SNI01	10.9	8.8	3.64	1013	48
SNI02	10.9	8.6	3.56	1013	48
SNI04	11.2	8.3	3.43	1013	33
SNI05	11.1	8.2	3.39	1013	33
SNI06	10.4	8.4	3.48	1013	NA
SNI09	10.8	8.8	3.64	1013	29
SNI10	10.6	8.9	3.69	1013	24
SNI11	10.1	8.9	3.69	1013	24
SNI12	10.5	8.2	3.39	1013	35
SNI14	11.7	8.9	3.67	1013	36
SNI16	11.3	8.8	3.64	1013	20
SNI17	11.1	8.1	3.35	1013	20
SNI24	10.8	8.1	3.35	1013	NA

TABLE 8. PARAMETERS FOR LOCAL LINE CALCULATIONS.

FASCODE CASE					CORRESPONDING MEASUREMENT
	P (mb)	T (c)	Water Vapor (torr)	Path (km)	
1	886	17.8	4.5	6.4	ASL04, ASL06
2	878	21.7	3.5	6.4	ASL13, ASL14, ASL15
3	879	19.4	2.0	6.4	ASL17, ASL18, ASL19, ASL20
4	879	15.6	3.1	6.4	ASL21, ASL23
5	1013.25	11.0	8.0	4.07	SNI04, SNI05, SNI12, SNI17, SNI24
6	1013.25	11.0	8.5	4.07	SNI02, SNI06
7	1013.25	11.0	9.0	4.07	SNI01, SNI09, SNI10, SNI11, SNI13, SNI14, SNI16, SNI25, SNI26
8	1013.25	18.9	13.5	5.1	CC83
9	1013.25	26.0	14.75	5.1	CC144, CC145
10	1013.25	26.3	16.4	5.1	CC147, CC148
11	1013.25	26.7	17.4	5.1	CC153, CC154
12	1013.25	25.0	18.0	5.1	CC119, CC120, CC121
13	1013.25	26.8	20.0	5.1	CC157, CC158, CC160
14	1013.25	28.4	20.5	5.1	CC159, CC161
15	1013.25	0.0	2.8	5.12	PRO37, PRO39
16	1013.25	5.0	3.0	5.12	PRO40, PRO42, PRO54
17	1013.25	7.5	4.5	5.12	PRO49, PRO50
18	1013.25	17.3	5.5	5.12	PRO55, PRO56
19	1013.25	19.7	11.4	5.12	PRO24

TABLE 9. MIXING RATIOS FOR GASES OTHER THAN WATER VAPOR.

MOLECULE	MIXING RATIO (ppmv)
CO_2	330.
O_3	0.04
N_2O	0.27
CO	0.19
CH_4	1.15
O_2	2.095×10^5
N_2	7.805×10^5

Aerosol size distribution data obtained at the SNI site, for example, were probably dominated by surf-generated aerosols for most observed wind directions [5]. Under wind conditions where the aerosol sampling instrumentation at SNI was subjected to strong local surf effects and the majority of the 4.07 km over-water transmission path was not, the optical depth along the transmission path can be grossly overestimated. Sample calculations (which assume a particle size distribution homogeneous over the transmission path) confirm this point, yielding optical depths (due solely to aerosol extinction) which frequently exceed the observed optical depth. The aerosol extinction coefficient for the SNI data was therefore estimated using the Navy Aerosol Model [14]. This empirically-based model considers such factors as relative humidity, wind speed, visibility at 0.55 μm, and airmass type in the specification of an aerosol extinction coefficient at a particular wavelength. The SNI meteorological data (see Table 3) specify all necessary parameters, with the exception of airmass type.

Airmass type (open oceanic, coastal, continental) happens to correlate very well with the level of atmospheric radon (which is produced by the decay of radium in crustal rock formations). Reference 14 gives an expression for an integer parameter P (which varies between 1 and 10) descriptive of the airmass type:

$$P = \mathrm{INT}\,(Rn/4) + 1 \qquad (2)$$

where INT ( ) is a function which truncates its argument to the next lowest integer and Rn is the decay rate activity of atmospheric radon (expressed in picocuries per cubic meter). An oceanic airmass typically has P = 1 and a continental airmass usually has P = 10. Atmospheric radon measurements

were taken concurrently with the transmission spectra, [15,16], thus completing the essential input for the aerosol model. As expected, the aerosol extinction predicted by the model was frequently quite lower than that inferred from surf-influenced particle measurements for the SNI data.

For the other three experimental sites PRNAS, CCAFS, and WSMR, extinction coefficients in the 3-5 μm region were estimated by scaling values obtained in the photopic region from available visibility data, except for selected CCAFS data where Nd-YAG laser transmittance measurements were available.

The aerosol extinction coefficient for visible wavelengths is related to the visual range V by Koschmeider's formula:

$$\sigma_{0.55} = 3.912/V. \tag{3}$$

Incorporating a small correction for molecular scattering, the relationship becomes:

$$\sigma_{0.55} = 3.912/V - .0123. \tag{4}$$

For any given aerosol of known size distribution and composition, the relationship between extinction coefficients at various wavelengths remains constant. Therefore, we can perform the simple scaling:

$$\sigma_{AER}(\lambda,V) = \frac{\left(\frac{3.912}{V} - .0123\right)\sigma_{AER}(\lambda,\ V_o)}{\sigma_{AER}\ (0.55\,\mu m,\ V_o)} \tag{5}$$

Reference 17 provides the necessary parameters to apply this scaling formula for the aerosol types defined by Shettle and Fenn. This formula does not represent what actually happens in the atmosphere when the visibility changes. While the formula implies only a change in the aerosol number density, usually there is also a change in both the composition of the aerosol and the particle size distribution. This is because the change in visibility is often accompanied by a change in the relative humidity.

Attempts were made to minimize the impact of the uncertainties in the value of the aerosol extinction component to the total optical depth by excluding (where possible) those spectra obtained under conditions where the visual range was less than 20 km.

Attempts to estimate the aerosol extinction component of the total optical depth utilizing concurrent aerosol spectrometer measurements (CCAFS and SNI data) and/or concurrent visibility data (all data sets) did not yield consistent values for the observed water continuum absorption coefficients, when aerosol optical depths were subtracted from the measured total optical depth. Therefore, an alternate approach was used in the evaluation of the aerosol component in the experimental data. This latter approach assumes that magnitude of the calculated water continuum absorption coefficient is correct at a certain frequency and that the aerosol contribution can be estimated from the difference between the measured extinction and the calculated water continuum absorption coefficient at that frequency.

A cursory study of the FASCOD1C-computed local line and continuum contributions indicates that these factors make a minimum contribution to the total extinction at the 2700.720 cm^{-1} sample point. Under the assumption that the

local line and continuum results at this sample point are correct, one may subtract the computed results from the observed optical depth $\tau_{OBS}(\nu_o)$ at 2700.720 cm^{-1} to get an aerosol extinction coefficient:

$$\sigma_{AER}(\nu_o) = [\tau_{OBS}(\nu_o) - [\tau_{LL}(\nu_o) + \tau_{CONT}(\nu_o)]]/L_{PATH} \quad (6)$$

where ν_o = 2700.72 cm^{-1}, and L_{PATH} = total path length.

Equation 6 establishes the aerosol extinction coefficient at a particular wavenumber. The relatively large wavenumber range covered by the sampling points in this study makes the assumption of a wavenumber-invariant aerosol extinction coefficient somewhat tenuous. Examination of Figure 10 (which is a plot of maritime aerosol extinction as a function of wavelength presented in Figure 17 from Reference 17) indicates three things of interest here:

(a) the aerosol extinction curve is relatively free of kinks or strong curvature in the 3-5 μm interval

(b) the linearity of the curve in the 3-5 μm interval on the log-log plot means that fits of the form $\sigma(\nu)=C\nu^{-n}$ or $\sigma(\lambda)=C\lambda^{+n}$ can be made ($n<o$)

(c) the slope of the curve on the log-log plot does not appear to be strongly dependent upon relative humidity in the 50% - 95% range.

A straight line was fit to the 70% RH curve of Figure 10 and extended to the left and right boundaries of the plot frame. The (x, y) values at the two intersections give the value of n:

$$n = \frac{\ln y_2 - \ln y_1}{\ln x_2 - \ln x_1} = -0.968 \quad (7)$$

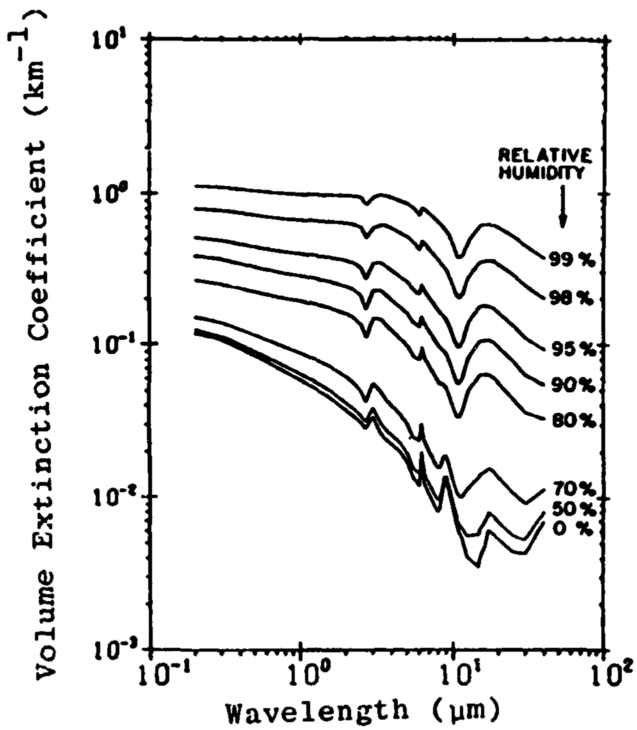

FIGURE 10. VOLUME EXTINCTION AS A FUNCTION OF RELATIVE HUMIDITY FOR A MARITIME AEROSOL WHOSE TOTAL NUMBER DENSITY IS FIXED AT 4,000 cm^{-3} [17].

thus, for the wavenumber (ν) domain, one obtains

$$\sigma_{AER}(\nu) = C\nu^{+0.968}, \tag{8}$$

where

$$C = \sigma_{AER}(\nu_o)\nu_o^{-0.968} \tag{9}$$

The value of C is the quantity determined for each observed spectrum, using the value for $\sigma_{AER}(\nu_o)$ given by Equation 6.

Plots showing the results of this fitting process for all of the spectra studied are contained in the following section. The relative results (how well the forms of the "observed" and theoretical H_2O continuum curves overlap) appear to be quite acceptable. The absolute fit of the continuum is only approximate, since the aerosol extinction uncertainties are poorly known.

A subset of the CCAFS spectra is amenable to further analysis regarding the magnitude of the water vapor continuum absorption coefficient at the 2700.720 cm^{-1} point. For certain of the CCAFS spectra, measured Nd-YAG laser transmittances at 1.06 μm are available [2,3]. Table 10 provides a listing of the Nd-YAG transmittance measurement times and extinction coefficients together with the identifications and measurement times for the FTS spectra and the times of the DF laser transmittance measurements used for normalization of the FTS spectra.

Using the curves shown in Figure 10, the ratio of the aerosol scattering coefficient at 3.7027 μm, (2700.720 cm^{-1}), to that at 1.06 μm can be estimated for various values of relative humidity. Figure 11 shows the dependence of the $\sigma_{3.7}/\sigma_{1.06}$ ratio upon relative humidity which was derived from the curves shown in Figure 10. Using the mea-

TABLE 10. MEASURED AEROSOL EXTINCTION COEFFICIENTS AT 0.63 μm AND 1.06 μm CORRESPONDING TO SELECTED CCAFS SPECTRA.

FTS SPECTRUM NUMBER	DATE/TIME	LASER EXTINCTION MEASUREMENT VALUE (km^{-1})/TIME			VISIBILITY VALUE (km)/TIME
		DF (3.6-4.0 μm)	HeNe (0.63 μm)	Nd-YAG (1.06 μm)	
CC083	3-03-77/1250	1445	--	--	18 @
CC119	3-31-77/1215	1420	.121 @ 1511		24 @ 1404
CC120	1245				
CC121	4-01-77/1310	1407	.196 @ 1438	--	
CC144	5-20-77/1350	1511	.101 @ 1438	.049 @ 1440	25 @ 1440
CC145	1415			.045 @ 1536	
CC147	5-21-77/1245	1156	.164 @ 1130	.062 @ 1133	15 @ 1329
CC148	1300	1347	.160 @ 1207	.066 @ 1208	
			.167 @ 1329	.067 @ 1331	
			.173 @ 1359	.082 @ 1401	
CC153	5-23-77/1310	1215	.029 @ 1236	.041 @ 1139	37 @ 1310
CC154	1330			.046 @ 1239	
				.056 @ 1433	
				.057 @ 1435	
			.041 @ 1558	.054 @ 1604	
CC157	5-24-77/1145	1349	.056 @ 1328	.049 @ 1113	29 @ 1133
CC158	1210		.075 @ 1328	.052 @ 1331	
CC159	1535		.056 @ 1409	.049 @ 1412	
			.058 @ 1503	.057 @ 1504	33 @ 1504
CC160	5-25-77/0955	1127	.119 @ 0847	.085 @ 0848	14 @ 0930
CC161	1155		.080 @ 0930	.051 @ 0932	
			.076 @ 1006	.054 @ 1010	29 @ 1130

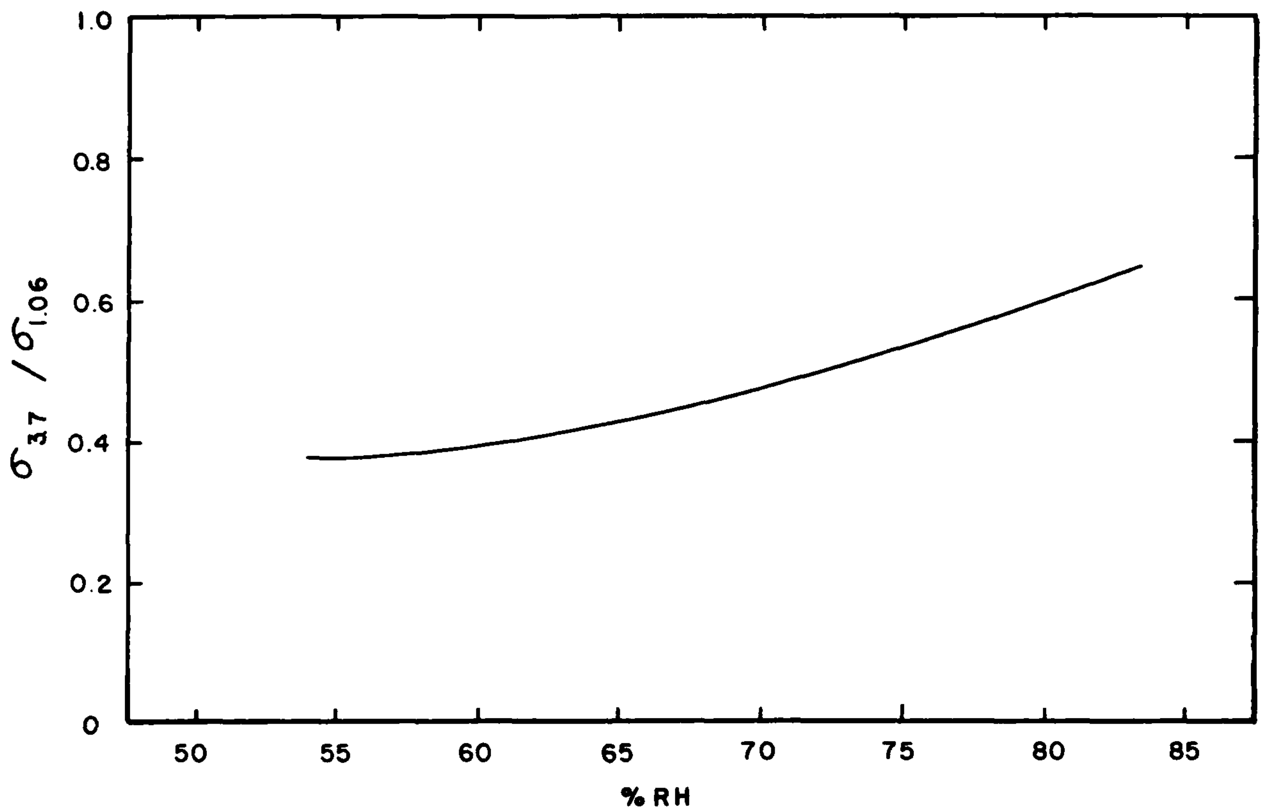

FIGURE 11. RATIO OF $\sigma_{3.7}/\sigma_{1.06}$ FOR MARITIME AEROSOL FOR VARIOUS VALUES OF R.H. DERIVED FROM REFERENCE 17.

sured values of $\sigma_{1.06}$ given in Table 10 and the scaling factor shown in Figure 11, aerosol contributions independent of the measured FTS extinction were obtained for the several CCAFS spectra listed in Table 10.

When these values of σ_{AER} at 2700.720 cm^{-1} are substituted into equation 1 independent values for α_{WC} can be obtained. Plots showing comparisons of the appropriately corrected measured data for the several CCAFS spectra listed in Table 10 to FASCODE water vapor continuum absorption calculations are shown in and discussed in Figure 16, subsection 3.1.4.

3.1.3 GENERATION OF WATER VAPOR ABSORPTION COEFFICIENTS FROM FASCOD1C

As configured in its public distribution form, the FASCOD1C code package does not permit direct access to individual H_2O, N_2, or CO_2 continua. That portion of the code responsible for generation of continuum absorption coefficients was extracted and configured to run as a "stand alone" program on a micro-computer. This continuum generation program accepts the following parameters as input: total air pressure, air temperature, column number densities of H_2O, CO_2, O_3, N_2O, CO, CH_4, O_2, and N_2, and the array of wavenumber values at which absorption is to be computed. The output is the optical depth due to water vapor continuum alone or the sum of all continua ($H_2O + N_2 + CO_2$).

The FASCOD1C local line and continuum computations were carried out for standard conditions which closely approximate those for which the observed transmission spectra were taken. Table 8 indicates the mapping between these standard conditions and specific atmospheric spectra.

[illegible] 4.06 given in Table 10 and the scaling [illegible]own in Figure 11, aerosol contributions independent of the measured FTS extinction were obtained for the several CCAFS spectra listed in Table 10.

When these values of σ_{AER} at 2700.720 cm^{-1} are substituted into equation 1 independent values for α_{WC} can be obtained. Plots showing comparisons of the appropriately corrected measured data for the several CCAFS spectra listed in Table 10 to FASCODE water vapor continuum absorption calculations are shown in and discussed in Figure 16, subsection 3.1.4.

3.1.3 GENERATION OF WATER VAPOR ABSORPTION COEFFICIENTS FROM FASCOD1C

As configured in its public distribution form, the FASCOD1C code package does not permit direct access to individual H_2O, N_2, or CO_2 continua. That portion of the code responsible for generation of continuum absorption coefficients was extracted and configured to run as a "stand alone" program on a micro-computer. This continuum generation program accepts the following parameters as input: total air pressure, air temperature, column number densities of H_2O, CO_2, O_3, N_2O, CO, CH_4, O_2, and N_2, and the array of wavenumber values at which absorption is to be computed. The output is the optical depth due to water vapor continuum alone or the sum of all continua ($H_2O + N_2 + CO_2$).

The FASCOD1C local line and continuum computations were carried out for standard conditions which closely approximate those for which the observed transmission spectra were taken. Table 8 indicates the mapping between these standard conditions and specific atmospheric spectra.

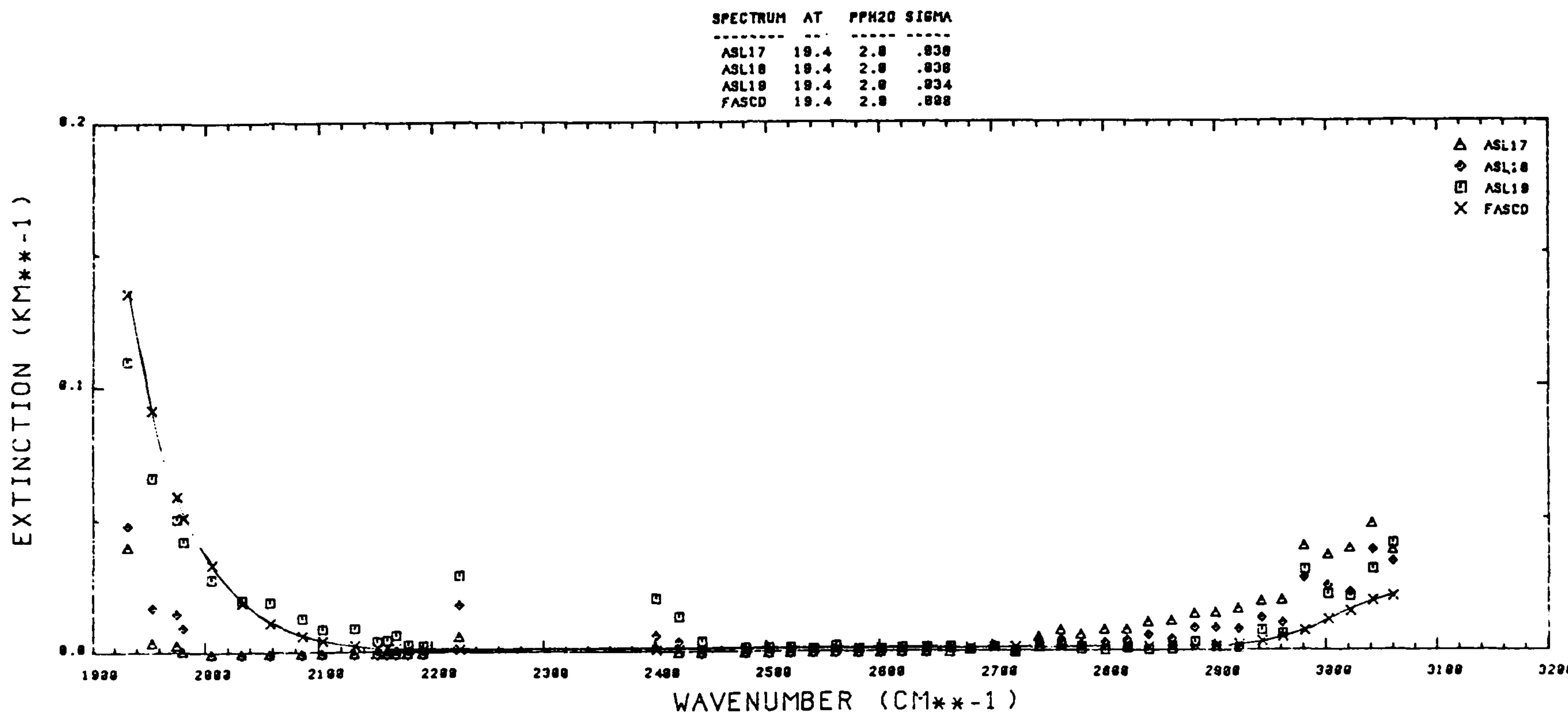

FIGURE 12a. COMPARISON OF CORRECTED SPECTRAL DATA TO FASCODE WATER CONTINUUM ABSORPTION CALCULATIONS ASL17, ASL18, AND ASL19 COMPARED WITH FASCODE CASE 3.

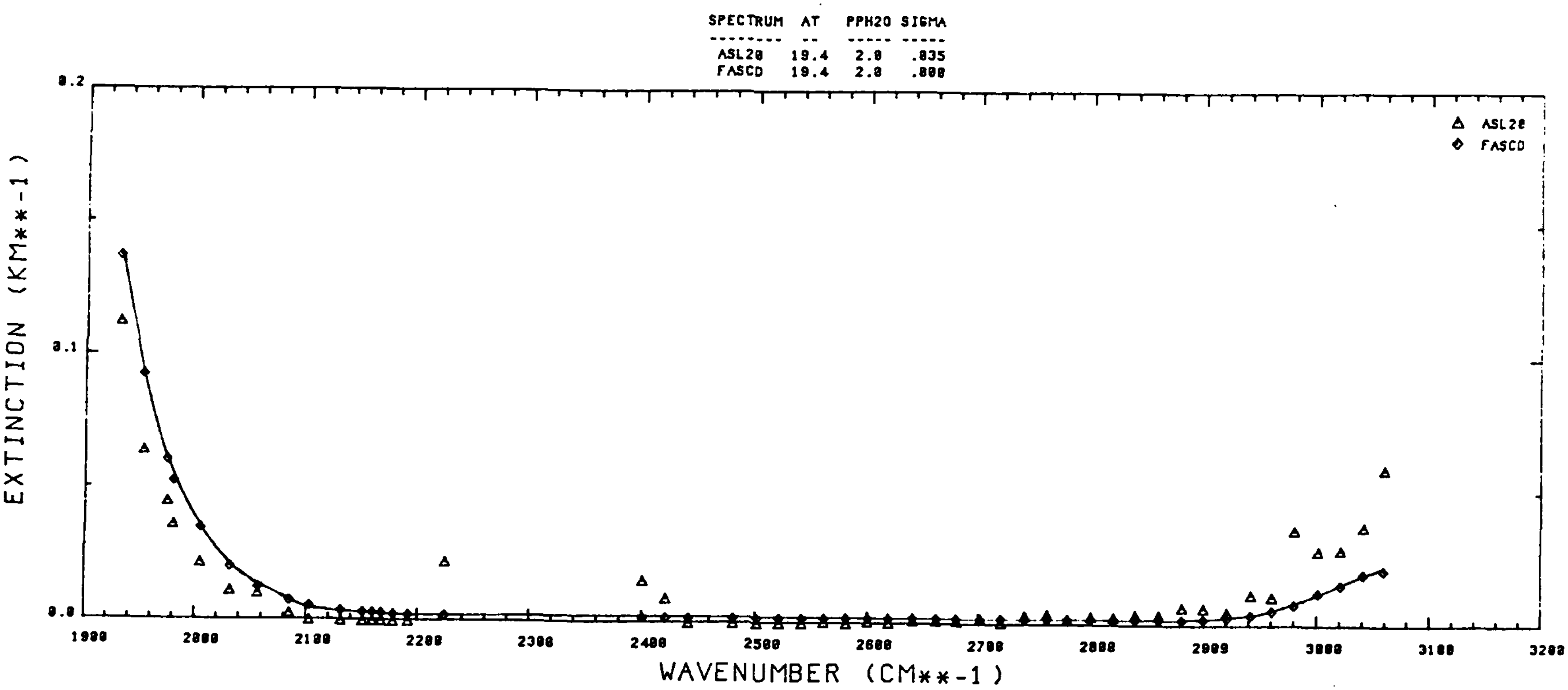

FIGURE 12b. COMPARISON OF CORRECTED SPECTRAL DATA TO FASCODE WATER CONTINUUM ABSORPTION CALCULATIONS ASL20 COMPARED WITH FASCODE CASE 3.

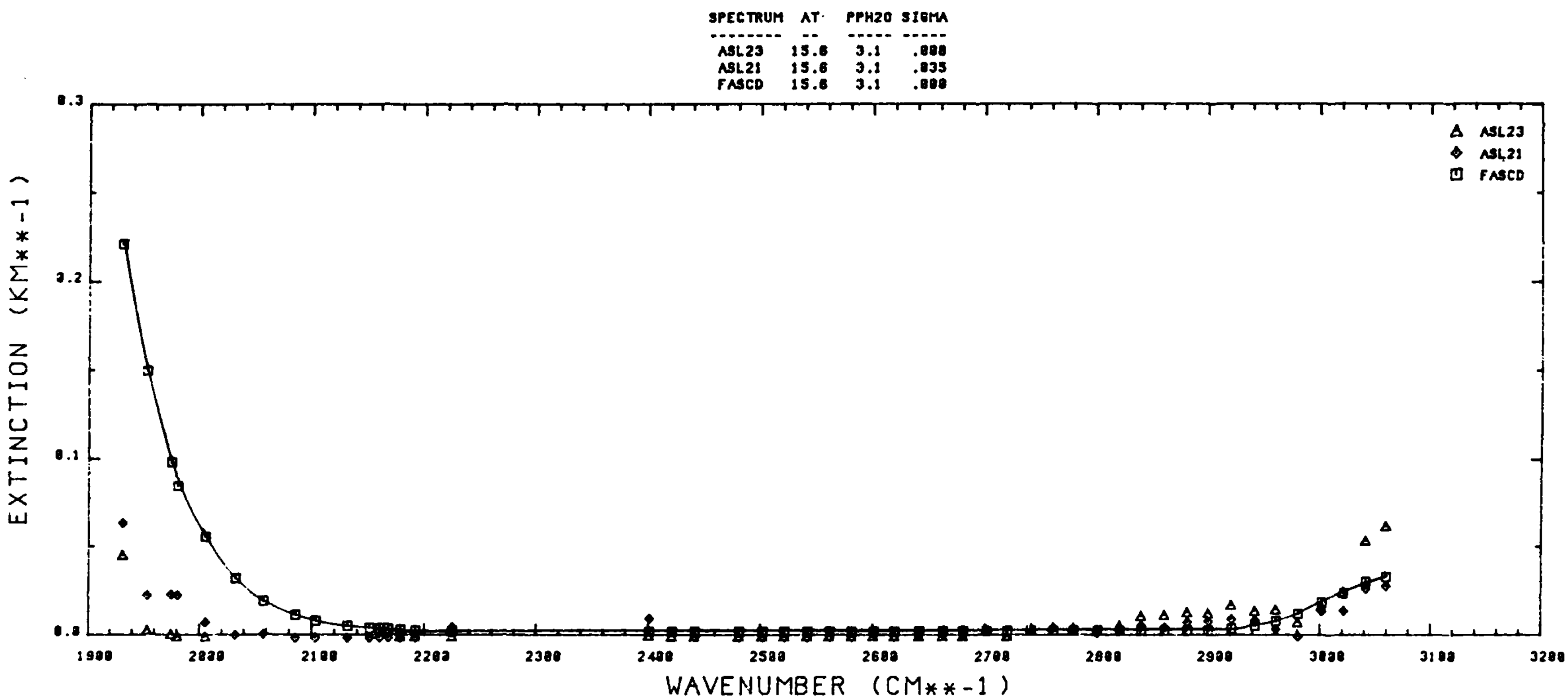

FIGURE 12c. COMPARISON OF CORRECTED SPECTRAL DATA TO FASCODE WATER CONTINUUM ABSORPTION CALCULATIONS ASL23 AND ASL21 COMPARED WITH FASCODE CASE 4.

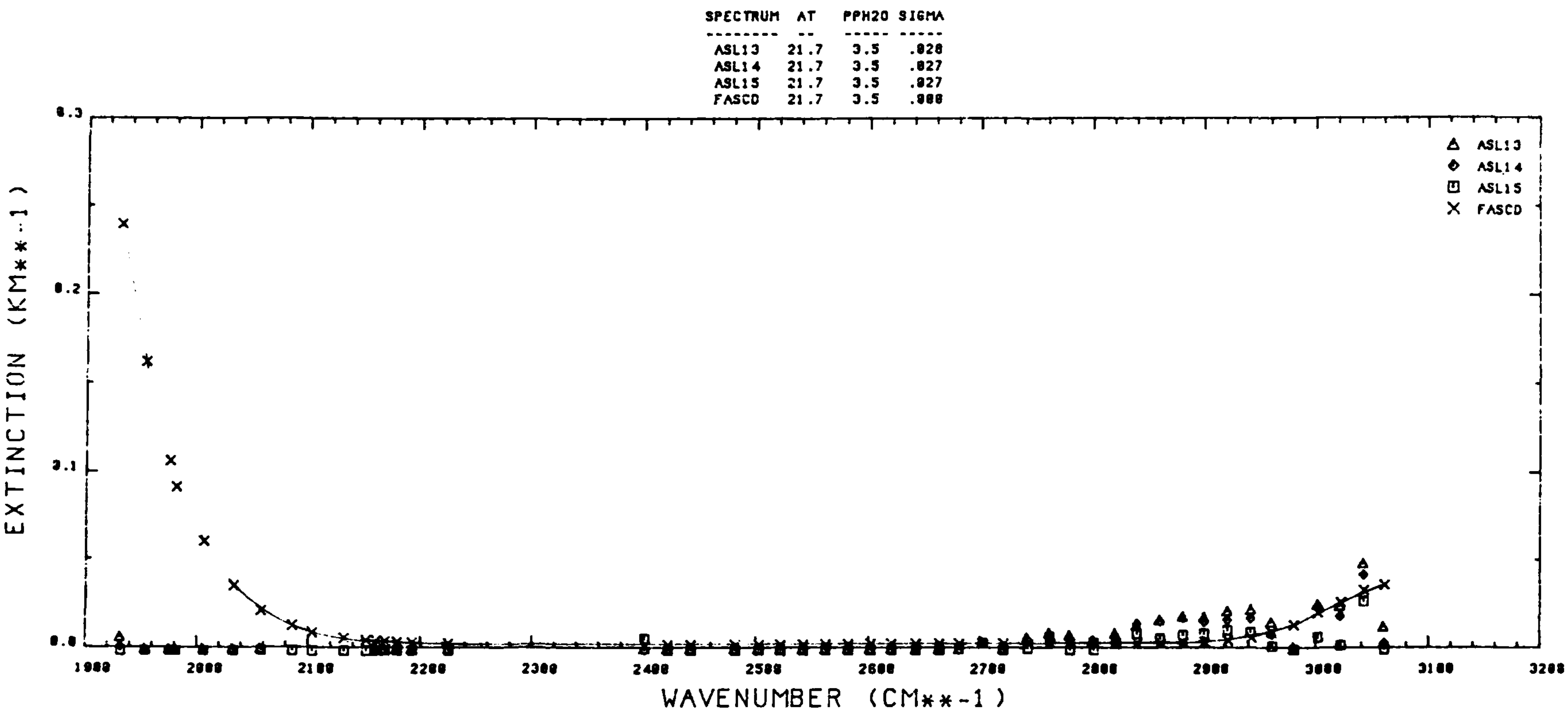

FIGURE 12d. COMPARISON OF CORRECTED SPECTRAL DATA TO FASCODE WATER CONTINUUM ABSORPTION CALCULATIONS ASL13, ASL14, and ASL15 COMPARED WITH FASCODE CASE 3.

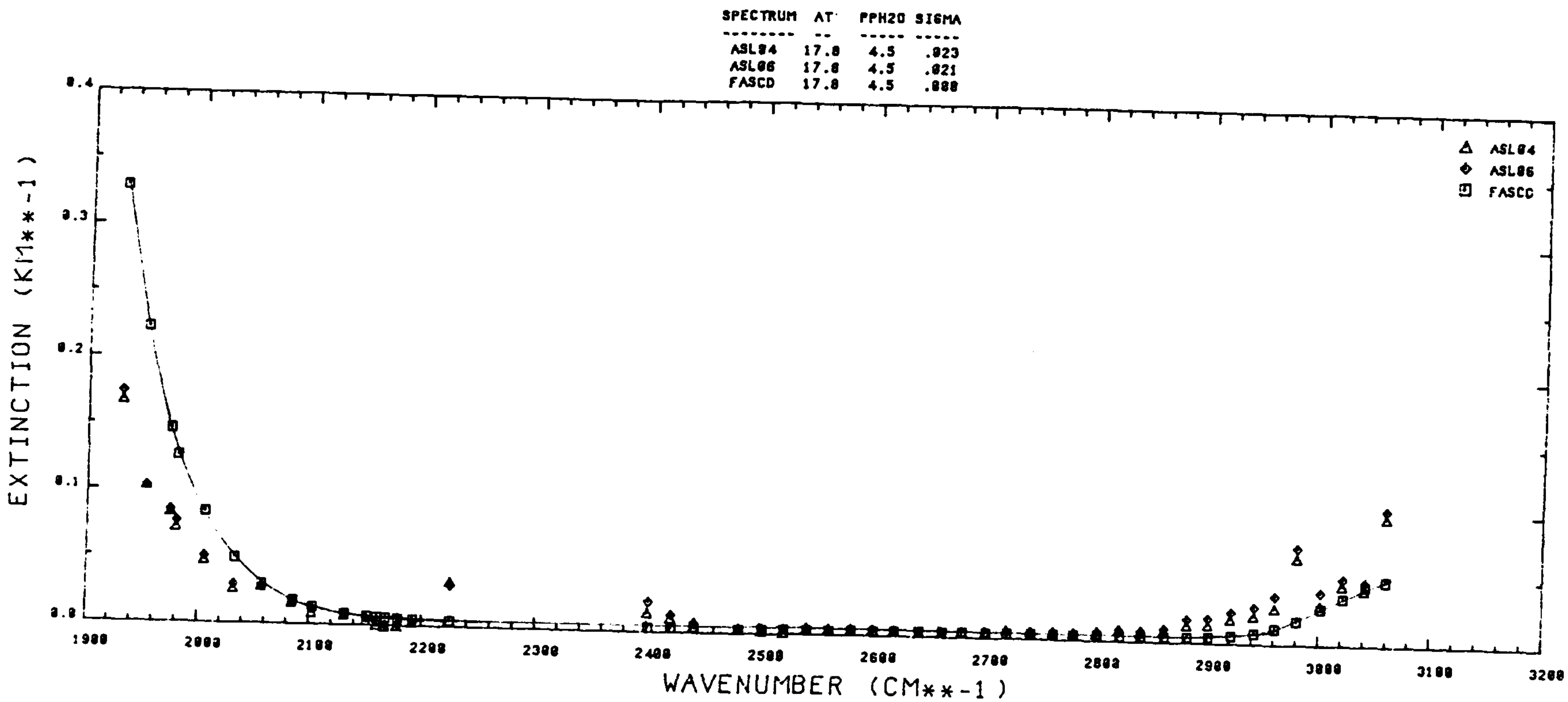

FIGURE 12e. COMPARISON OF CORRECTED SPECTRAL DATA TO FASCODE WATER CONTINUUM ABSORPTION CALCULATIONS ASL04 and ASL06 COMPARED WITH FASCODE CASE 1.

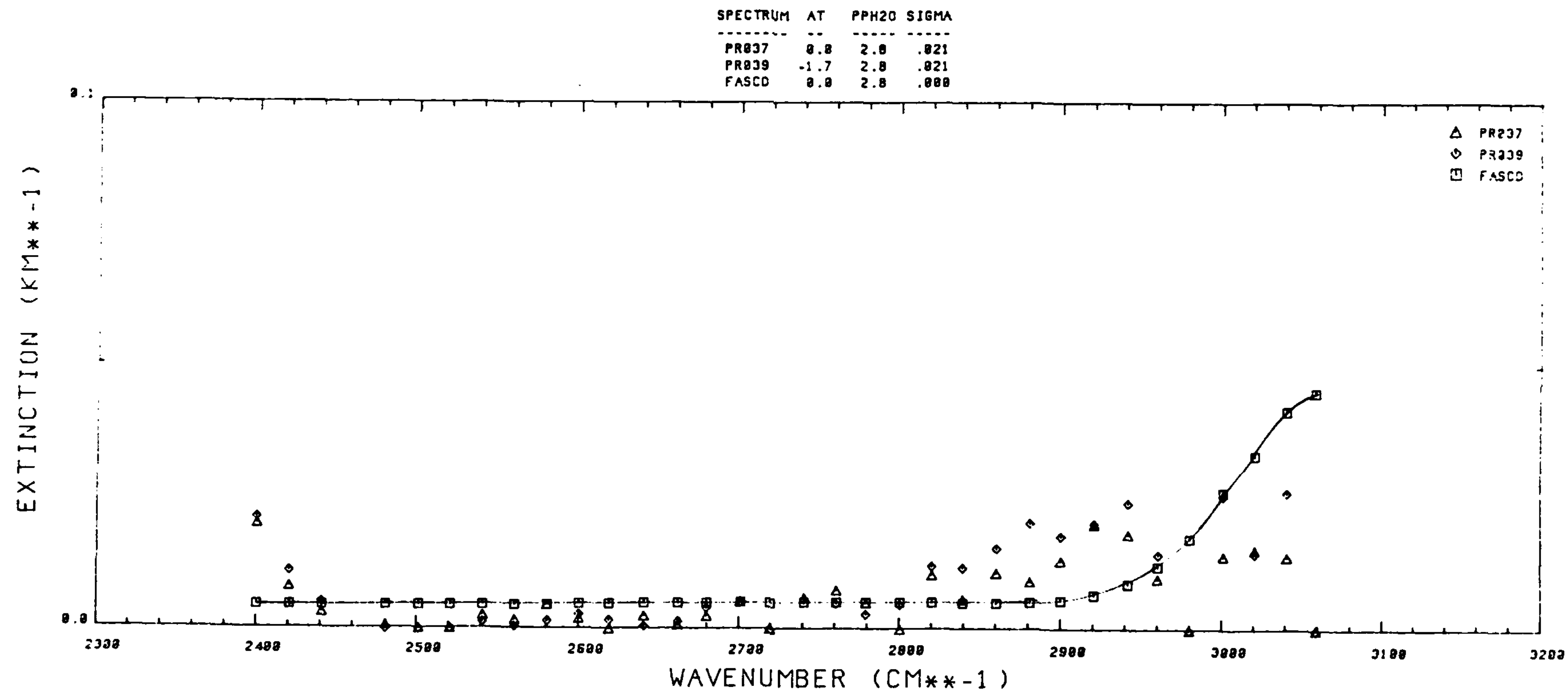

FIGURE 13a. COMPARISON OF CORRECTED PRNAS SPECTRAL DATA TO FASCODE WATER CONTINUUM ABSORPTION CALCULATIONS PRO37 and PRO39 COMPARED WITH FASCODE CASE 15.

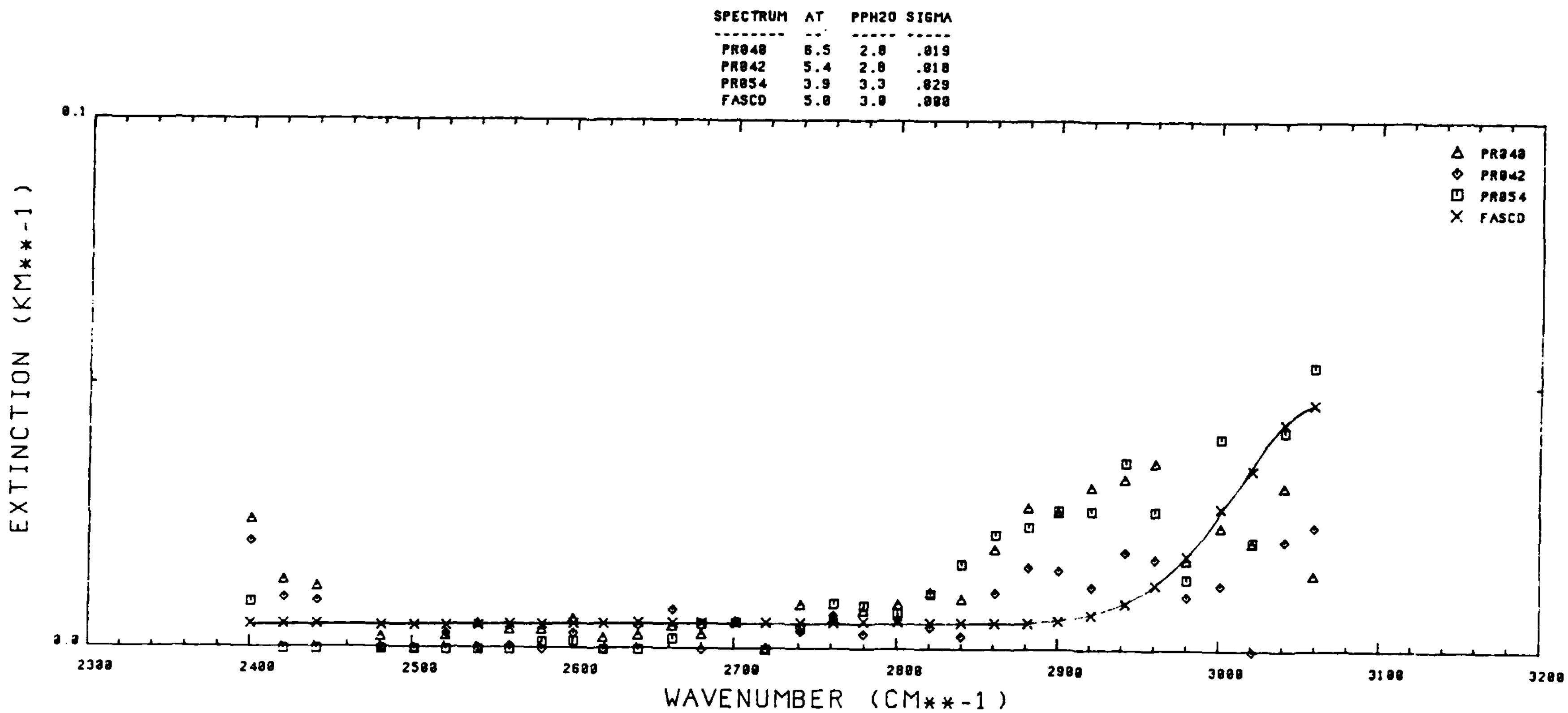

FIGURE 13b. COMPARISON OF CORRECTED PRNAS SPECTRAL DATA TO FASCODE WATER CONTINUUM ABSORPTION CALCULATIONS PRO40, PRO42, AND PRO54 COMPARED WITH FASCODE CASE 16.

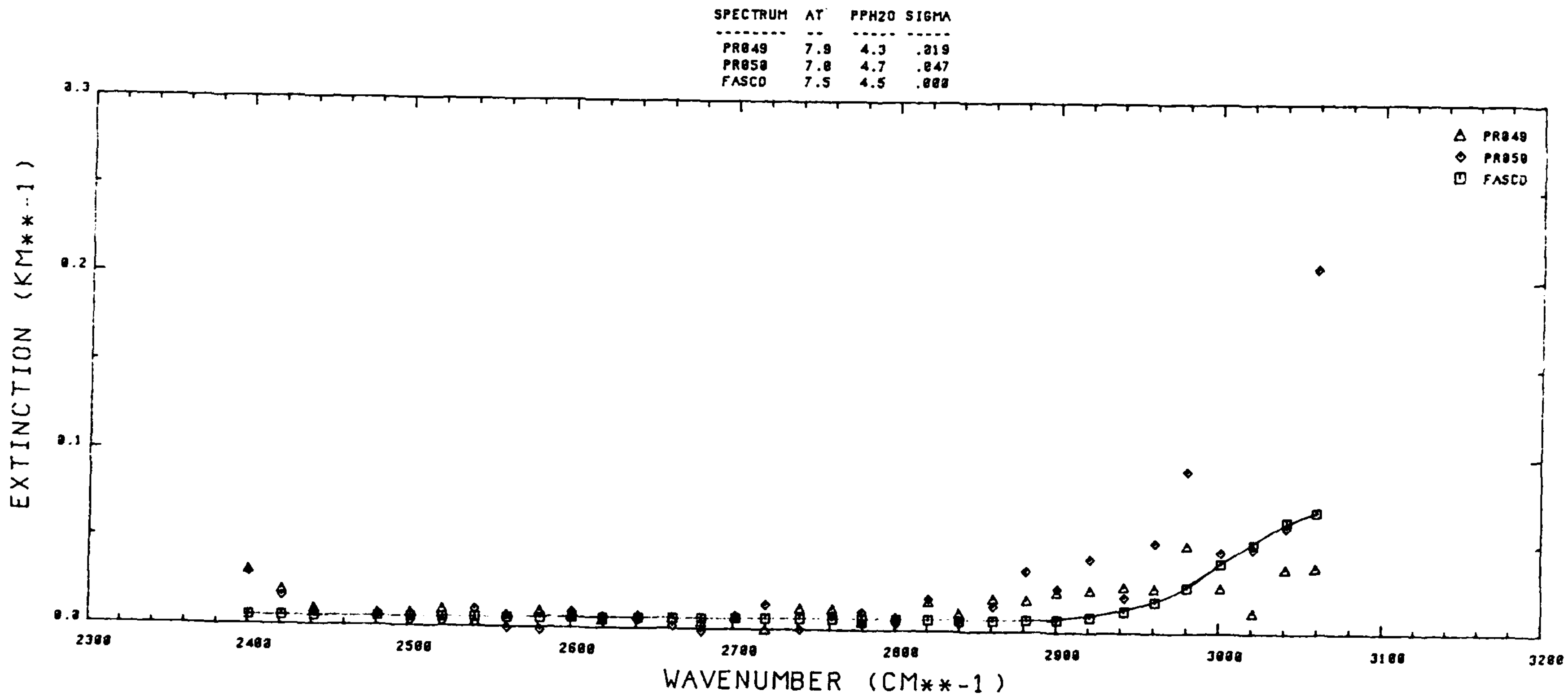

FIGURE 13c. COMPARISON OF CORRECTED PRNAS SPECTRAL DATA TO FASCODE WATER CONTINUUM ABSORPTION CALCULATIONS PRO49 AND PRO50 COMPARED WITH FASCODE CASE 18.

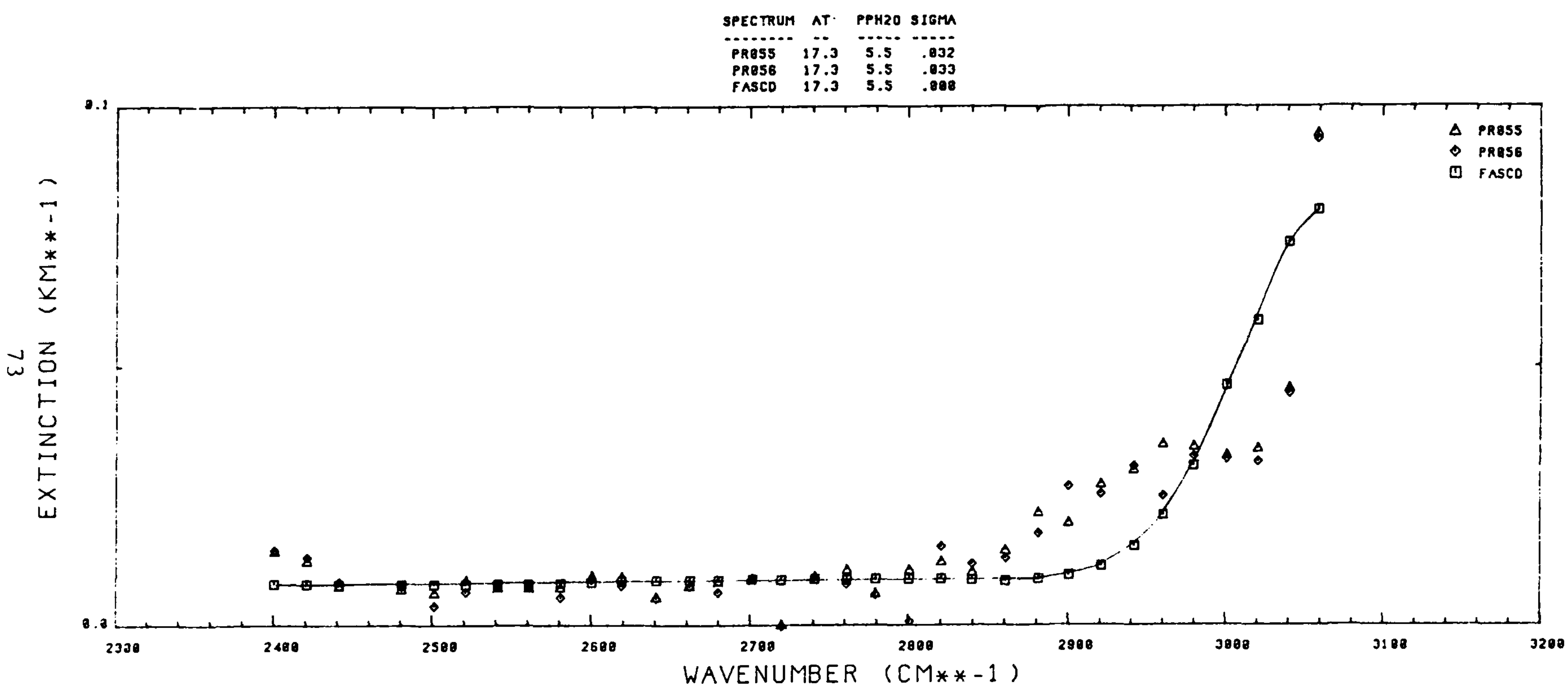

FIGURE 13d. COMPARISON OF CORRECTED PRNAS SPECTRAL DATA TO FASCODE WATER CONTINUUM ABSORPTION CALCULATIONS PRO55 AND PRO56 COMPARED WITH FASCODE CASE 18.

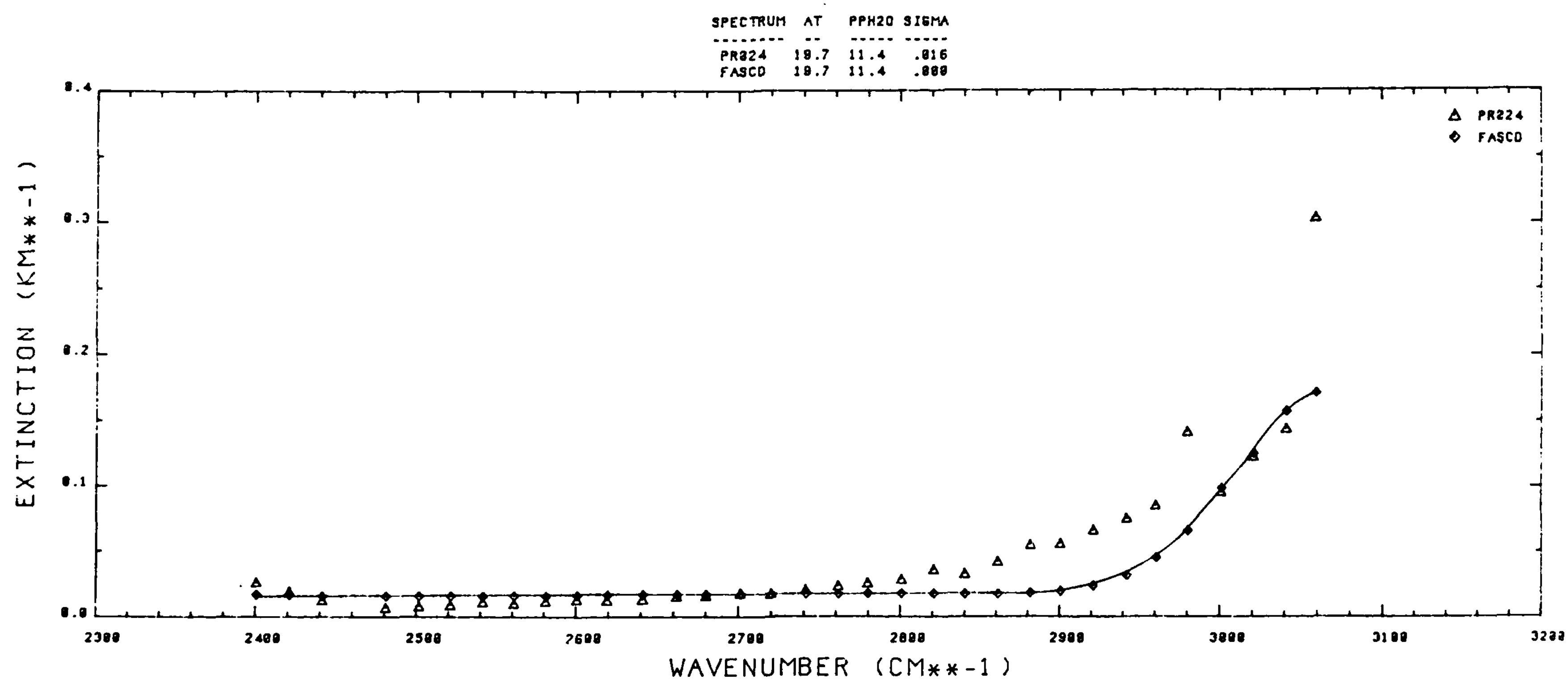

FIGURE 13e. COMPARISON OF CORRECTED PRNAS SPECTRAL DATA TO FASCODE WATER CONTINUUM ABSORPTION CALCULATIONS PRO24 COMPARED WITH FASCODE CASE 19.

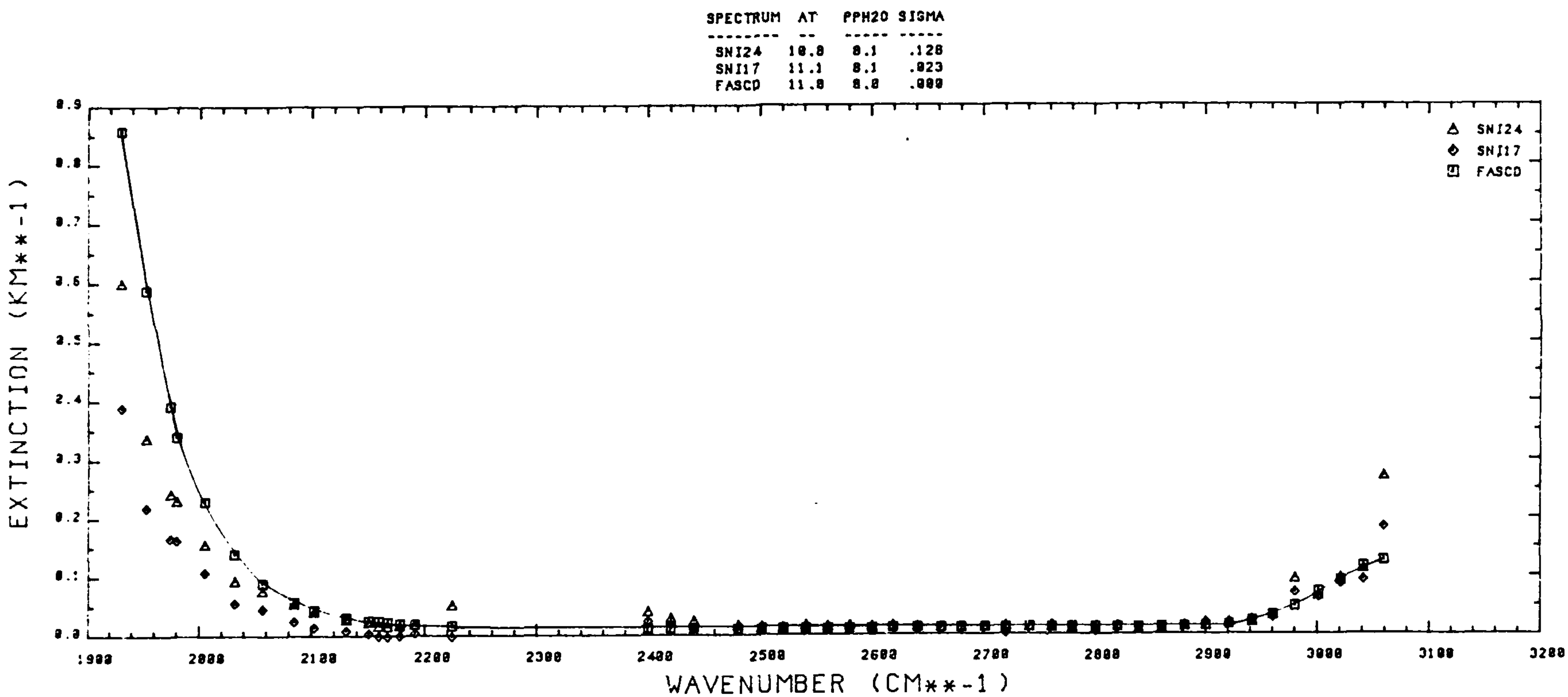

FIGURE 14a. COMPARISON OF CORRECTED SNI SPECTRAL DATA TO FASCODE WATER CONTINUUM ABSORPTION CALCULATIONS SNI24 AND SNI17 COMPARED WITH FASCODE CASE 5.

AD-A150 682 ANALYSIS OF ATMOSPHERIC INTERFEROMETER DATA(U) 2/3
OPTIMETRICS INC LAS CRUCES NM J A DOWLING ET AL.
JUL 84 OMI-102 AFGL-TR-84-0177 F19628-83-C-0040

UNCLASSIFIED F/G 20/14 NL

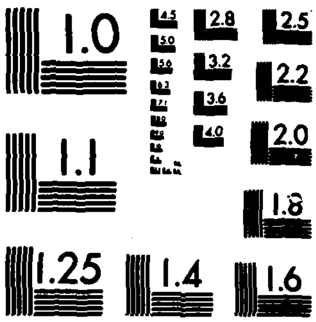

MICROCOPY RESOLUTION TEST CHART
NATIONAL BUREAU OF STANDARDS-1963-A

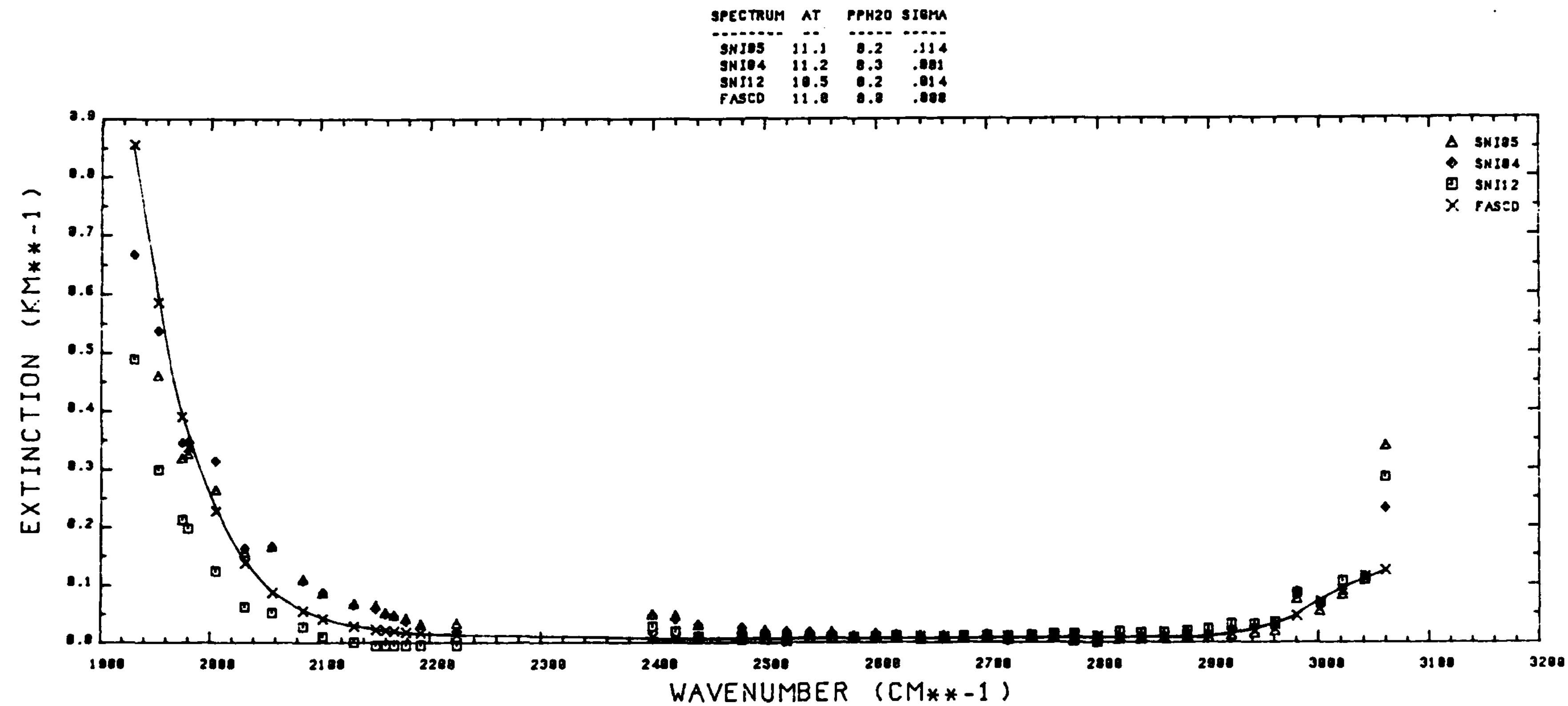

FIGURE 14b. COMPARISON OF CORRECTED SNI SPECTRAL DATA TO FASCODE WATER CONTINUUM ABSORPTION CALCULATIONS SNI05, SNI04, AND SNI12 COMPARED WITH FASCODE CASE 5.

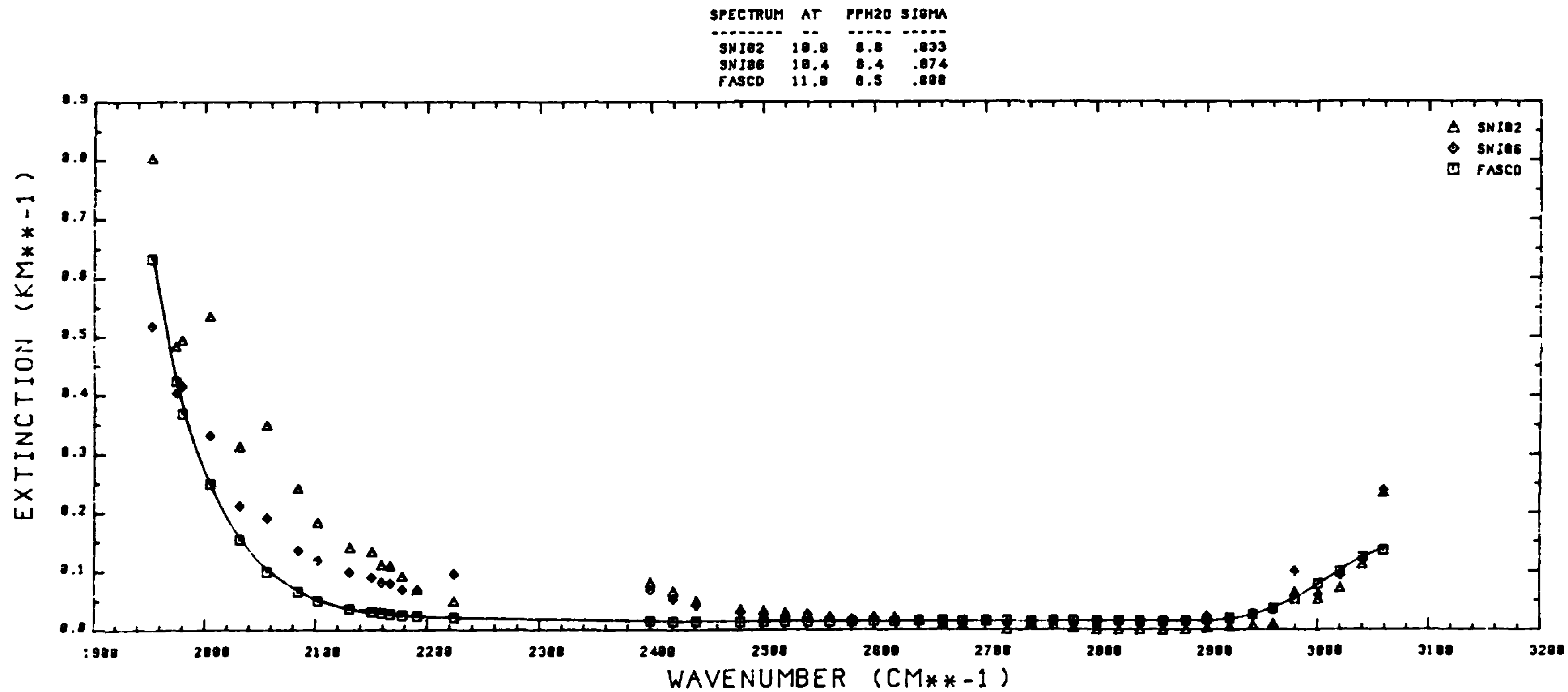

FIGURE 14c. COMPARISON OF CORRECTED SNI SPECTRAL DATA TO FASCODE WATER CONTINUUM ABSORPTION CALCULATIONS SNI02 AND SNI03 COMPARED WITH FASCODE CASE 6.

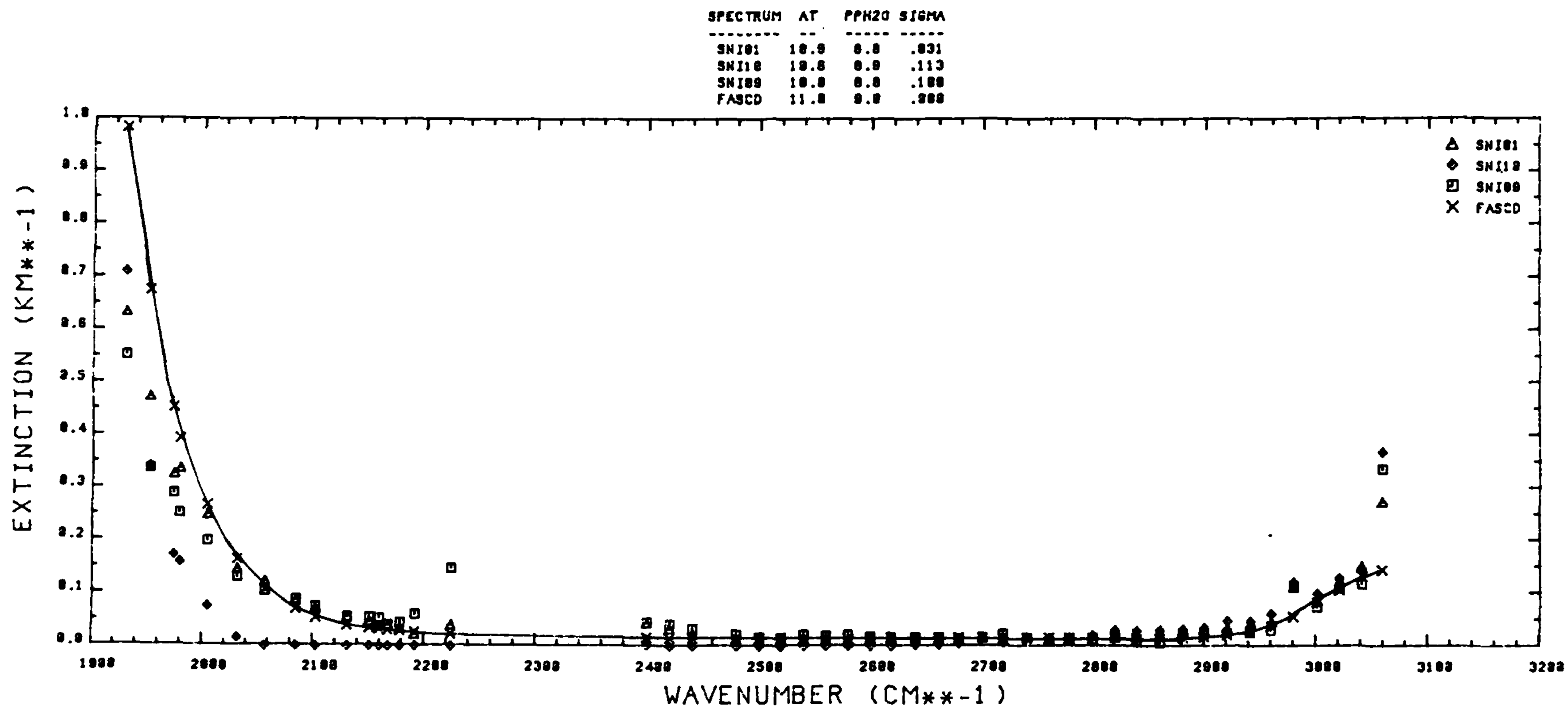

FIGURE 14d. COMPARISON OF CORRECTED SNI SPECTRAL DATA TO FASCODE WATER CONTINUUM ABSORPTION CALCULATIONS SNI01, AND SNI10, AND SNI09 COMPARED WITH FASCODE CASE 7.

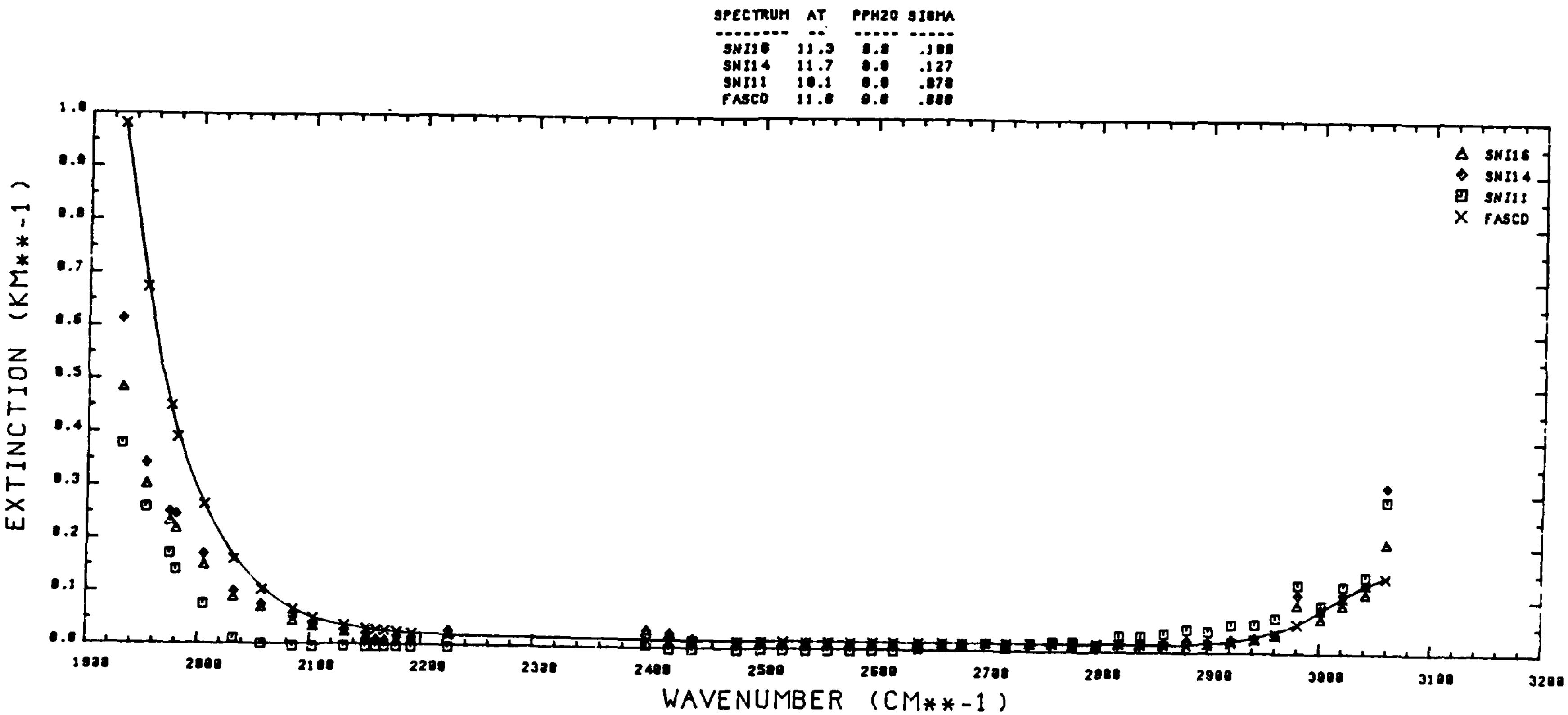

FIGURE 14e. COMPARISON OF CORRECTED SNI SPECTRAL DATA TO FASCODE WATER CONTINUUM ABSORPTION CALCULATIONS SNI16, SNI14, AND SNI11 COMPARED WITH FASCODE CASE 7.

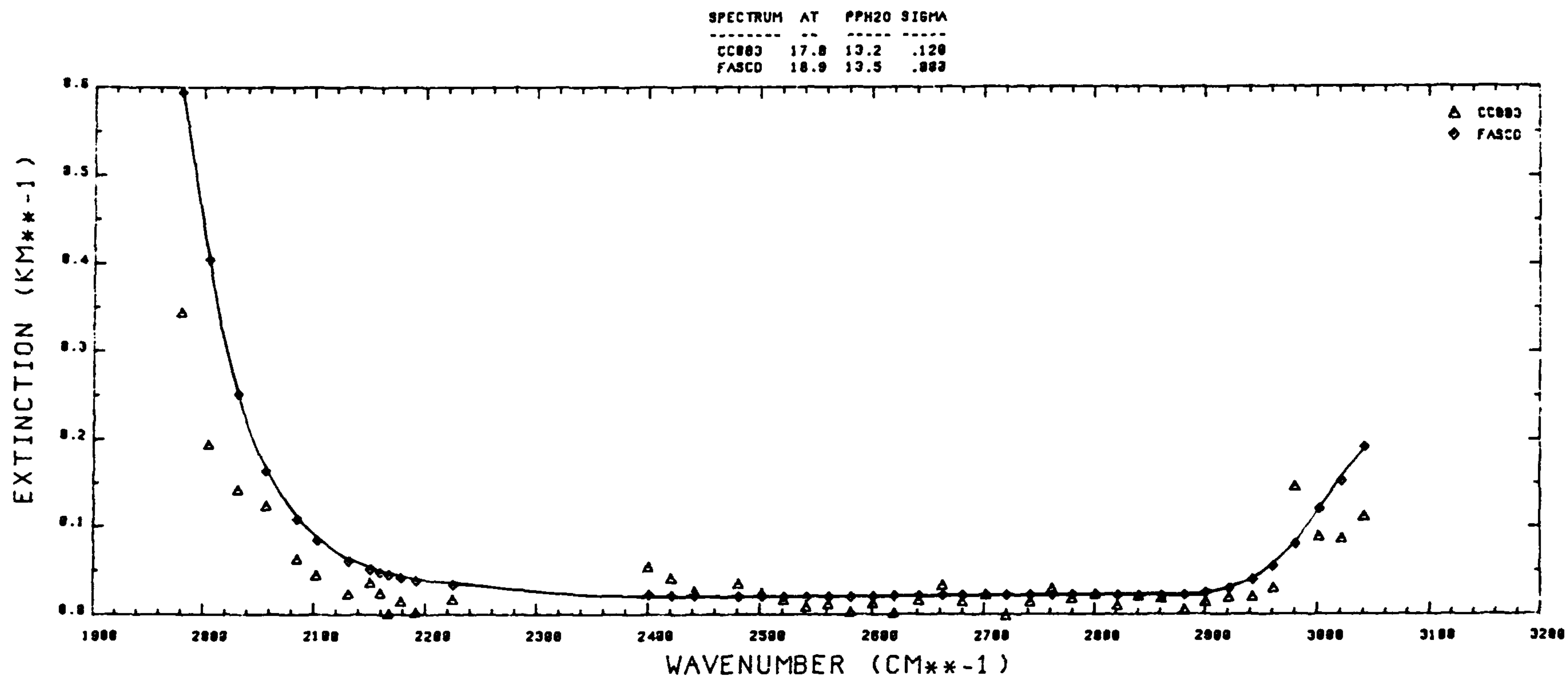

FIGURE 15a. COMPARISON OF CORRECTED CCAFS SPECTRAL DATA TO FASCODE WATER CONTINUUM ABSORPTION CALCULATIONS CC083 COMPARED WITH FASCODE CASE 8.

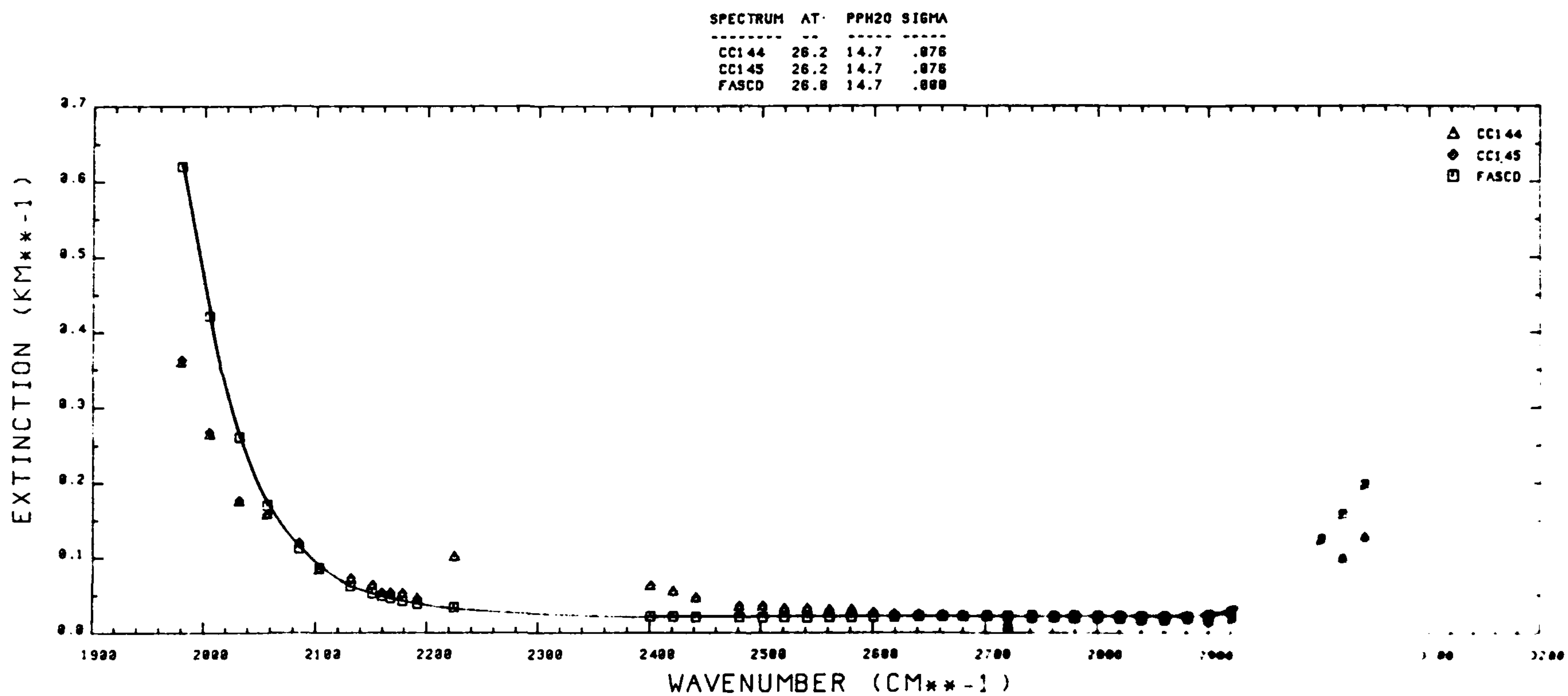

FIGURE 15b. COMPARISON OF CORRECTED CCAFS SPECTRAL DATA TO FAS[illegible] WATER CONTINUUM ABSORPTION CALCULATIONS CC144 AND CC14[illegible] WITH FASCODE CASE 9.

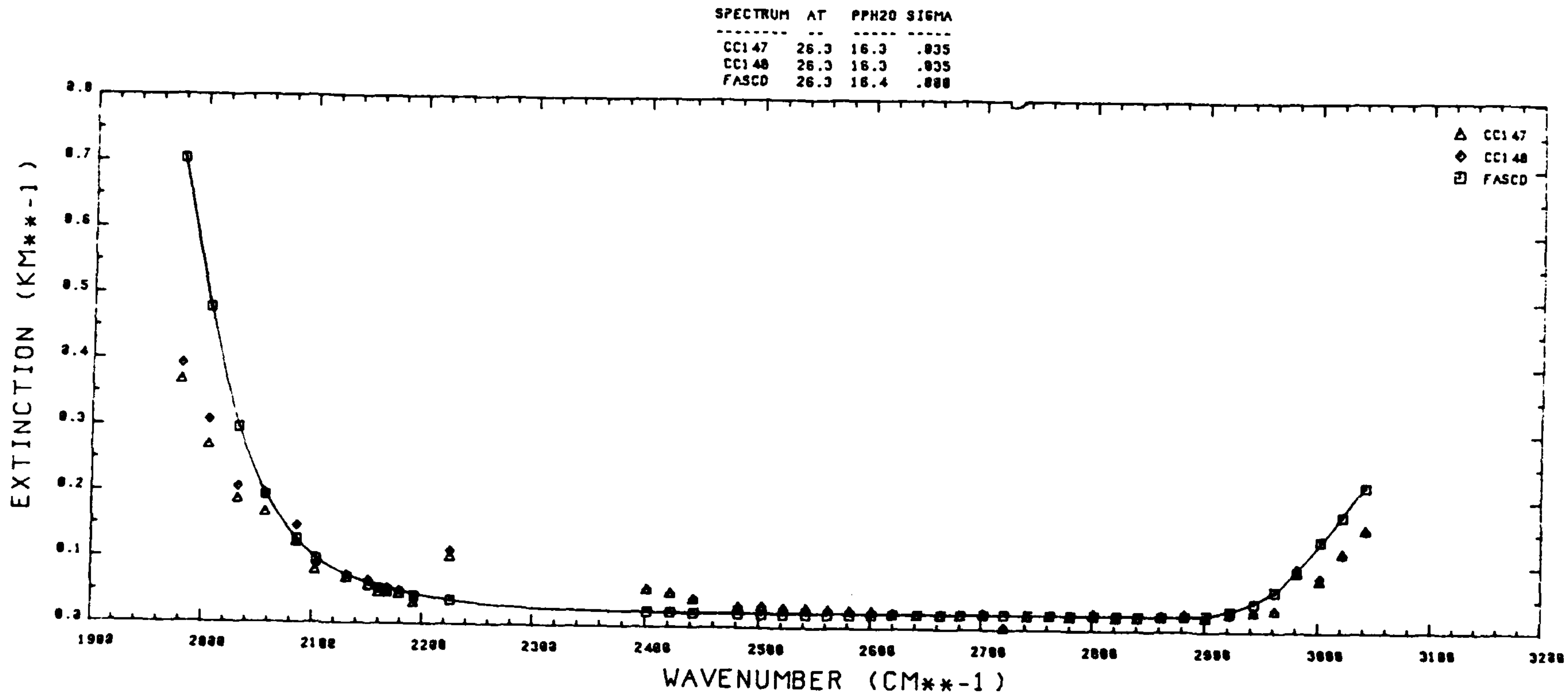

FIGURE 15c. COMPARISON OF CORRECTED CCAFS SPECTRAL DATA TO FASCODE WATER CONTINUUM ABSORPTION CALCULATIONS CC147 AND CC148 COMPARED WITH FASCODE CASE 10.

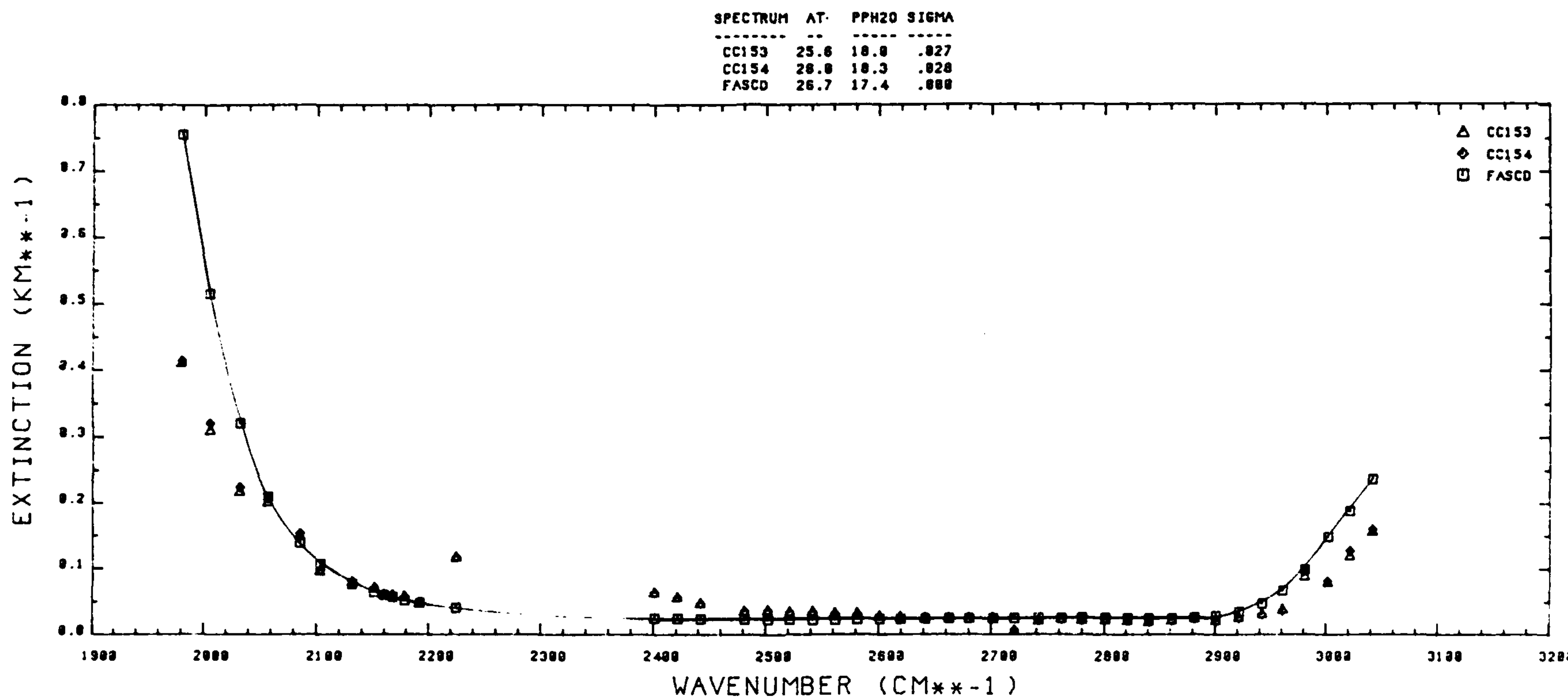

FIGURE 15d. COMPARISON OF CORRECTED CCAFS SPECTRAL DATA TO FASCODE WATER CONTINUUM ABSORPTION CALCULATIONS CC153 AND CC154 COMPARED WITH FASCODE CASE 11.

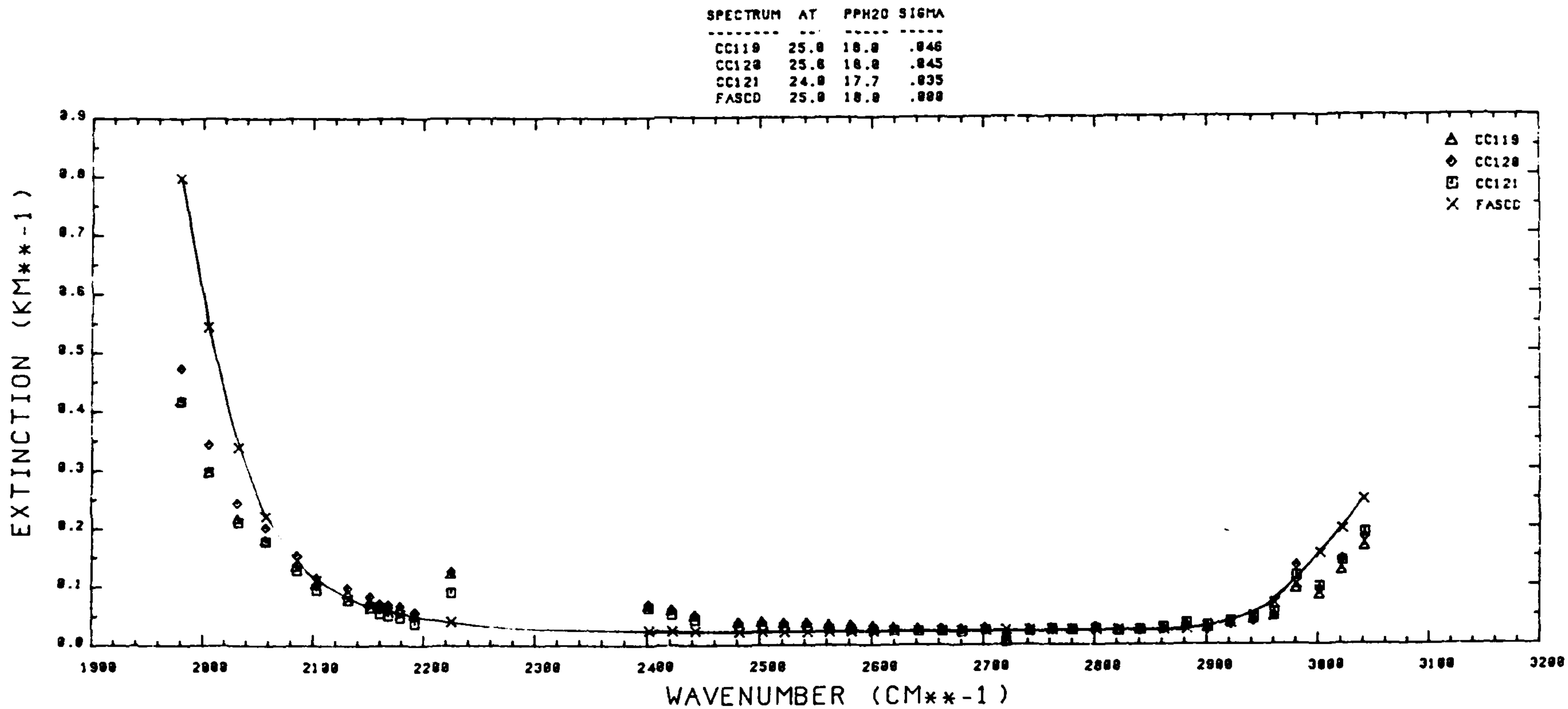

FIGURE 15e. COMPARISON OF CORRECTED CCAFS SPECTRAL DATA TO FASCODE WATER CONTINUUM ABSORPTION CALCULATIONS CC119, CCL20, AND CC121 COMPARED WITH FASCODE CASE 12.

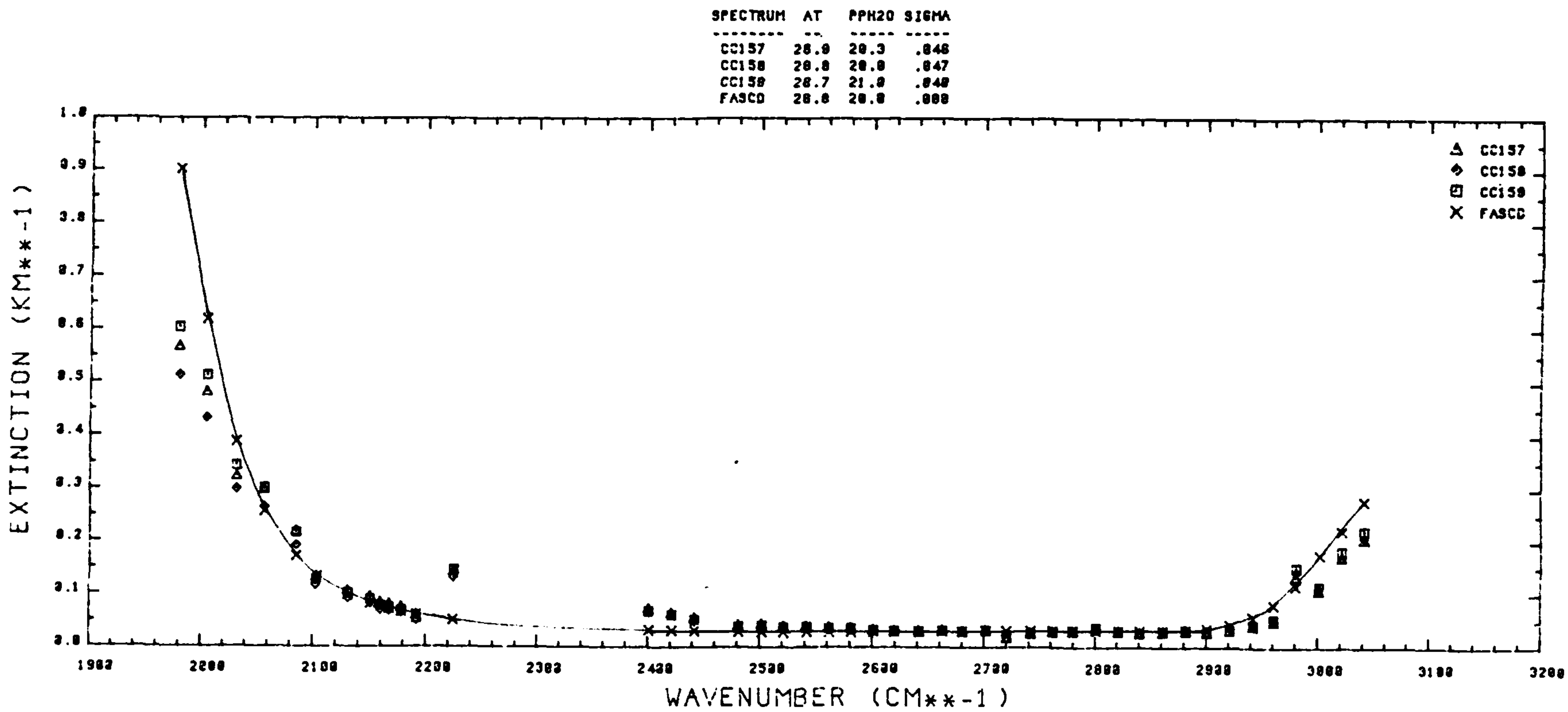

FIGURE 15f. COMPARISON OF CORRECTED CCAFS SPECTRAL DATA TO FASCODE WATER CONTINUUM ABSORPTION CALCULATIONS CC157, CC158, AND CC159 COMPARED WITH FASCODE CASE 14.

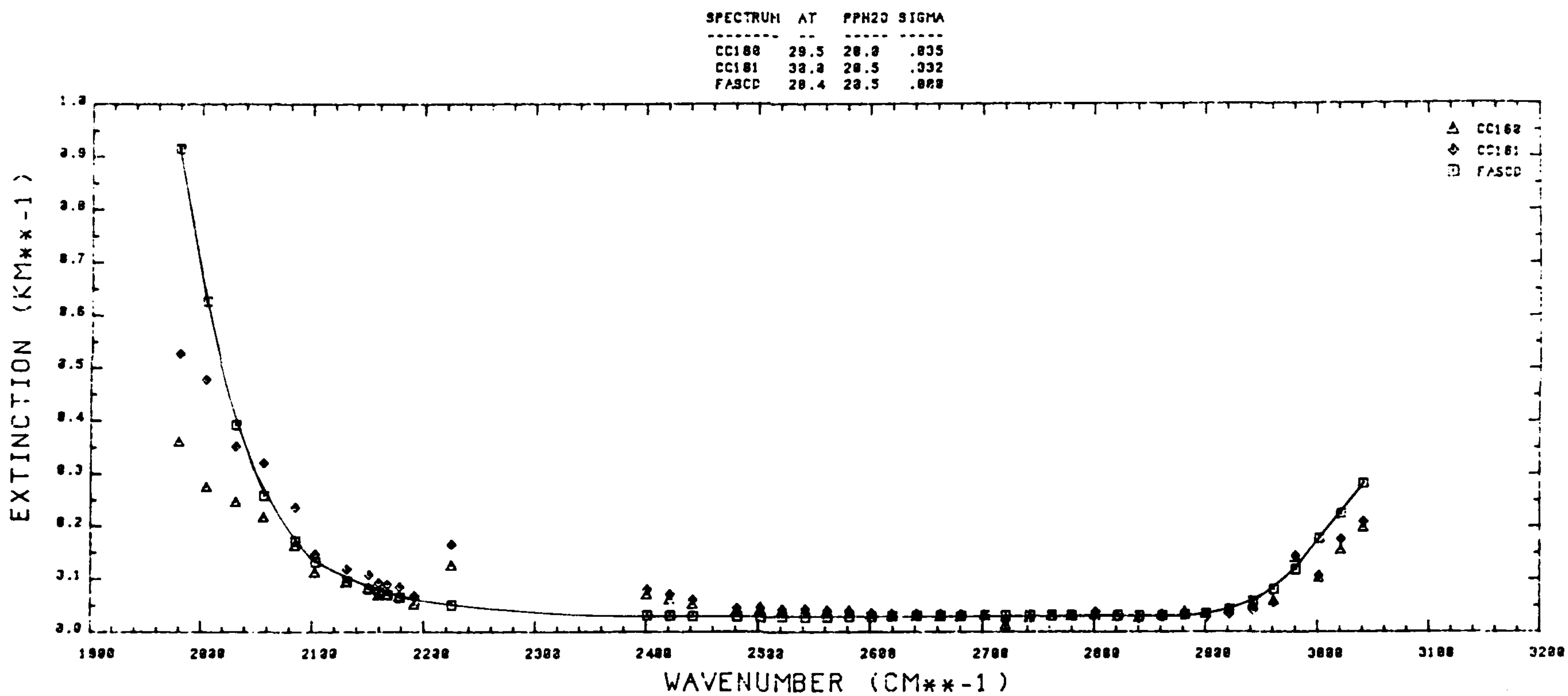

FIGURE 15g. COMPARISON OF CORRECTED CCAFS SPECTRAL DATA TO FASCODE WATER CONTINUUM ABSORPTION CALCULATIONS CC160, AND CC161 COMPARED WITH FASCODE CASE 14.

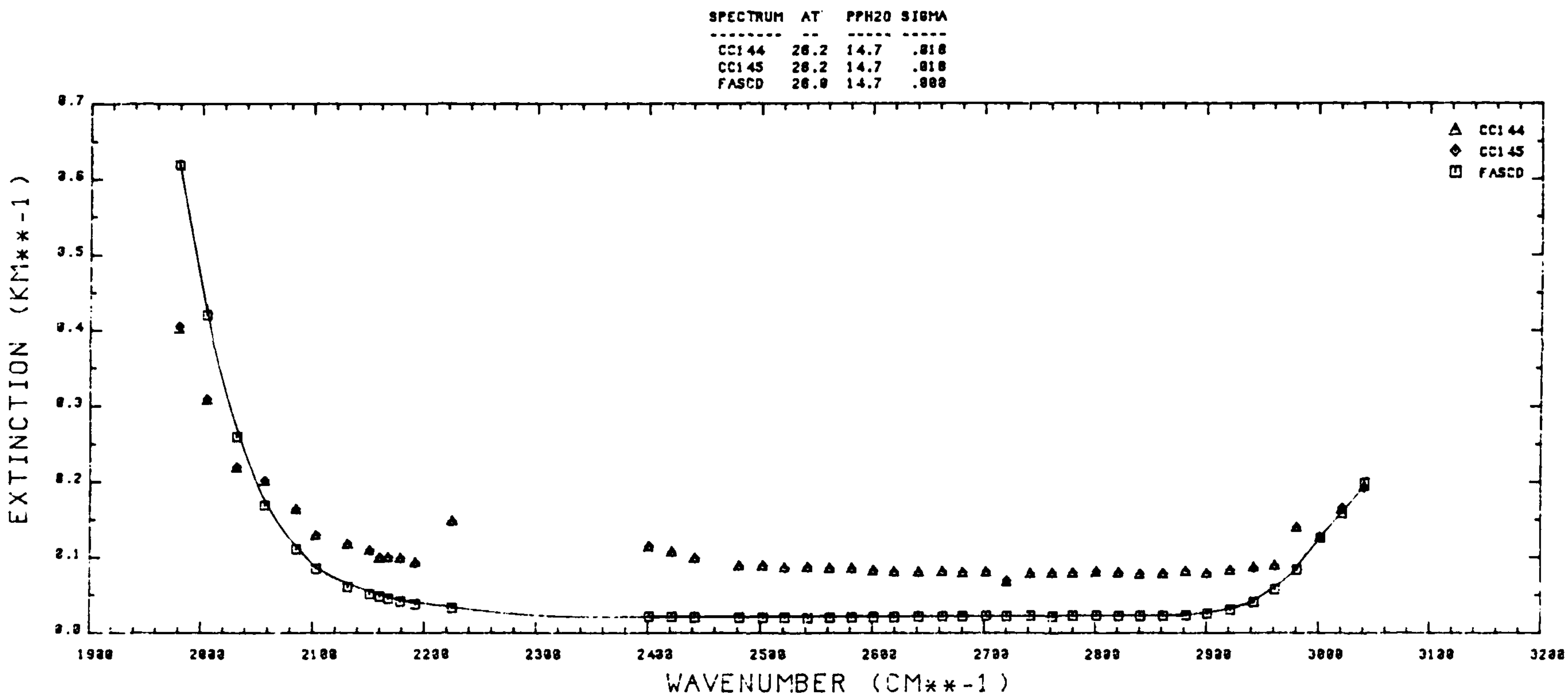

FIGURE 16a. COMPARISON OF CORRECTED CCAFS SPECTRAL DATA TO FASCODE WATER CONTINUUM ABSORPTION CALCULATIONS(MEASUREMENT-DERIVED AEROSOL EXTINCTION CORRECTIONS INCLUDED)CC144 AND CC145 COMPARED WITH FASCODE CASE 9.

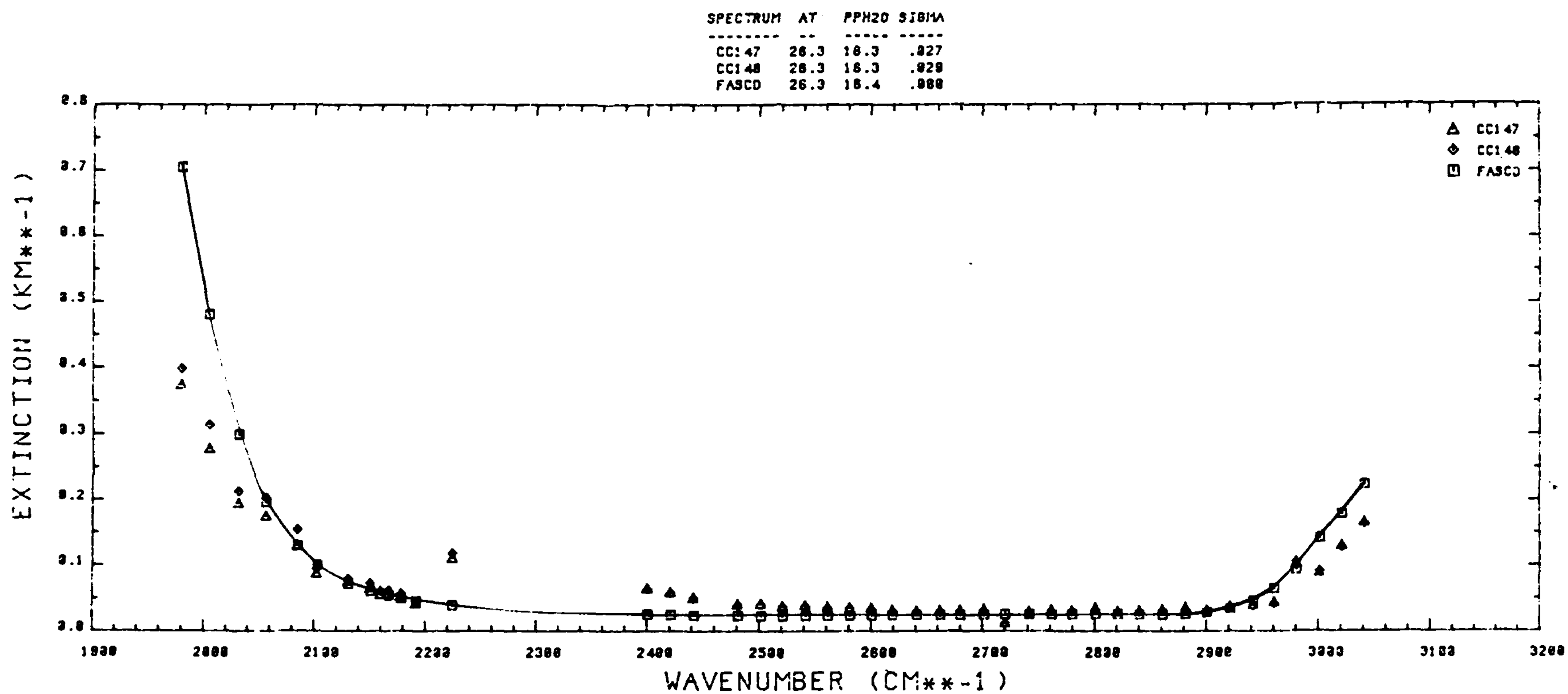

FIGURE 16b. COMPARISON OF CORRECTED CCAFS SPECTRAL DATA TO FASCODE WATER CONTINUUM ABSORPTION CALCULATIONS (MEASUREMENT-DERIVED AEROSOL EXTINCTION CORRECTIONS INCLUDED) CC147 AND CC148 COMPARED WITH CASE 10.

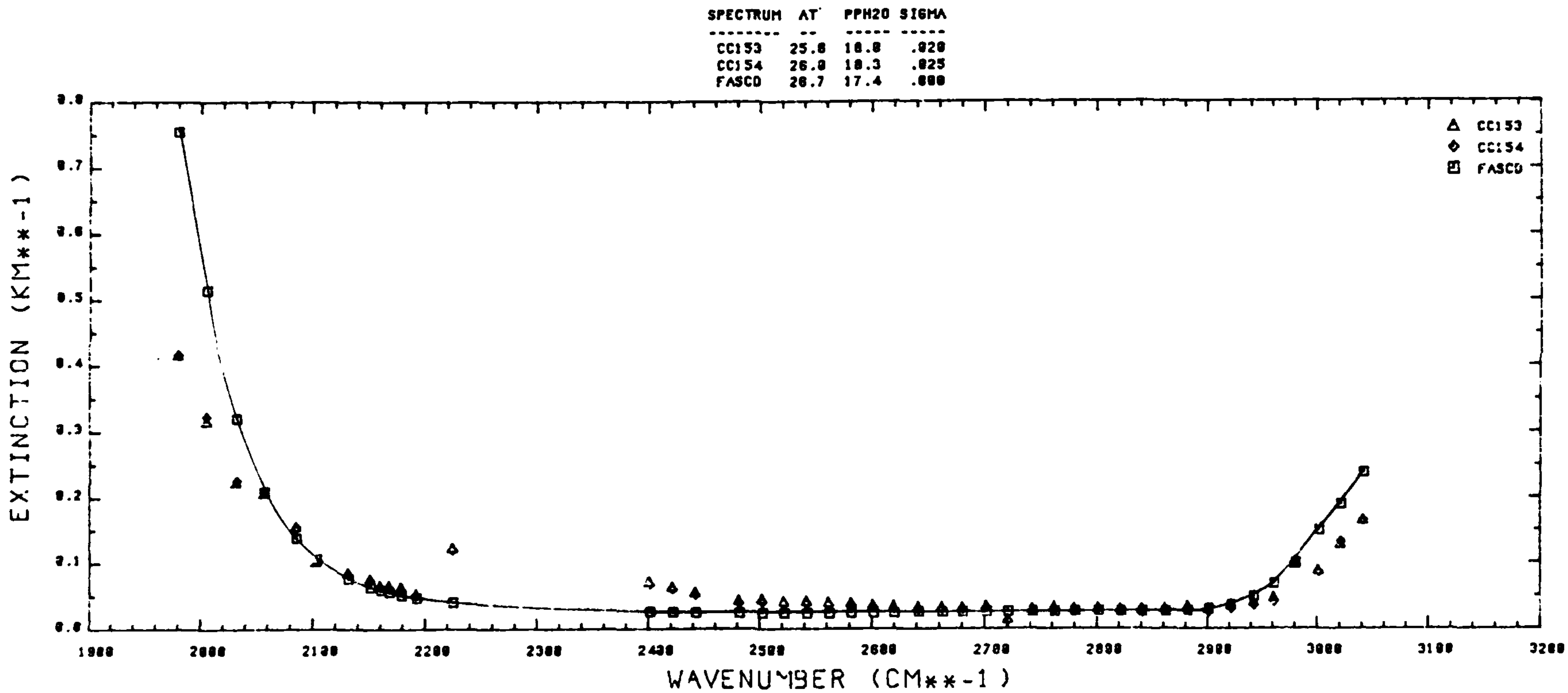

FIGURE 16c. COMPARISON OF CORRECTED CCAFS SPECTRAL DATA TO FASCODE WATER CONTINUUM ABSORPTION CALCULATIONS(MEASUREMENT-DERIVED AEROSOL EXTINCTION CORRECTIONS INCLUDED)CC153 AND CC154 COMPARED WITH FASCODE CASE 11.

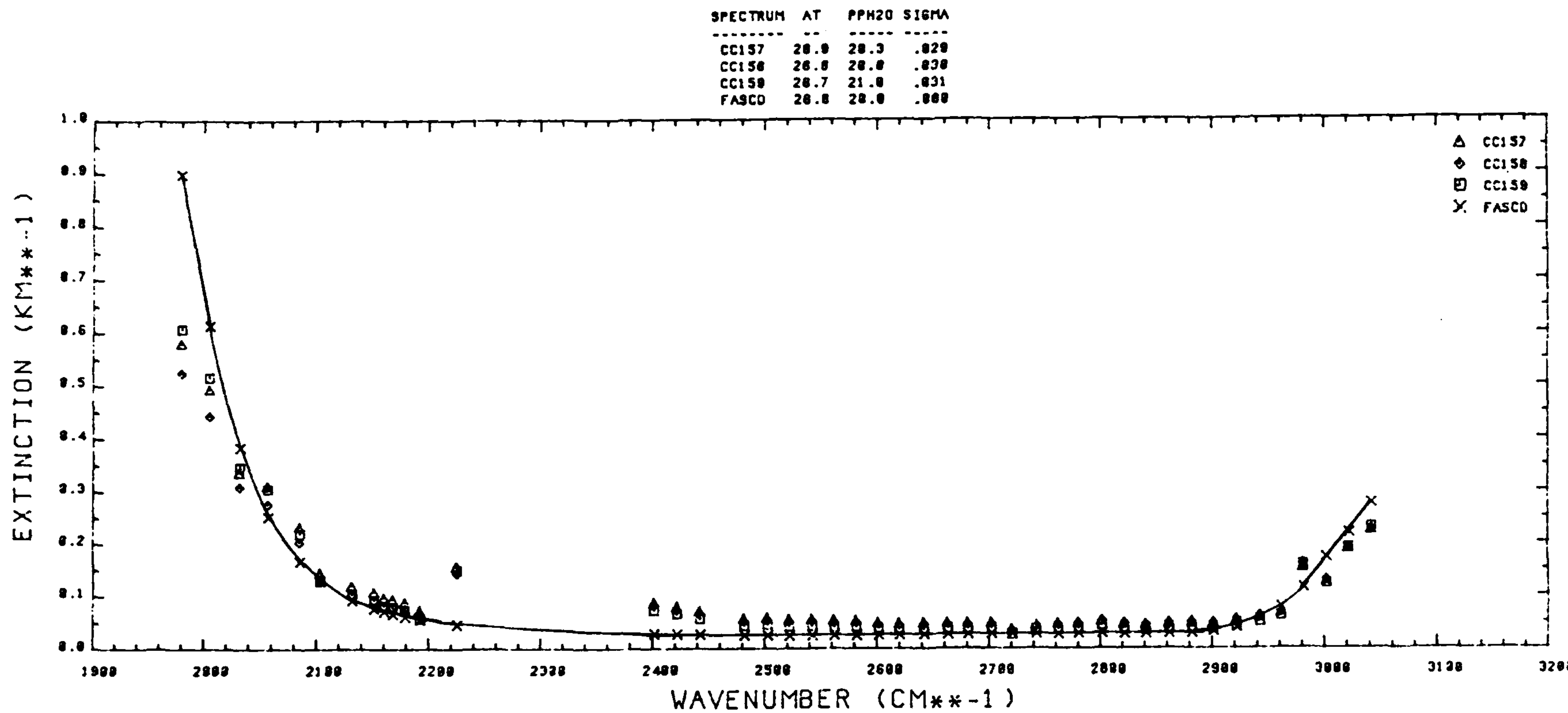

FIGURE 16d. COMPARISON OF CORRECTED CCAFS SPECTRAL DATA TO FASCODE WATER CONTINUUM ABSORPTION CALCULATIONS (MEASUREMENT-DERIVED AEROSOL EXTINCTION CORRECTIONS INCLUDED) CC157, CC158, AND CC159 COMPARED WITH FASCODE CASE 13.

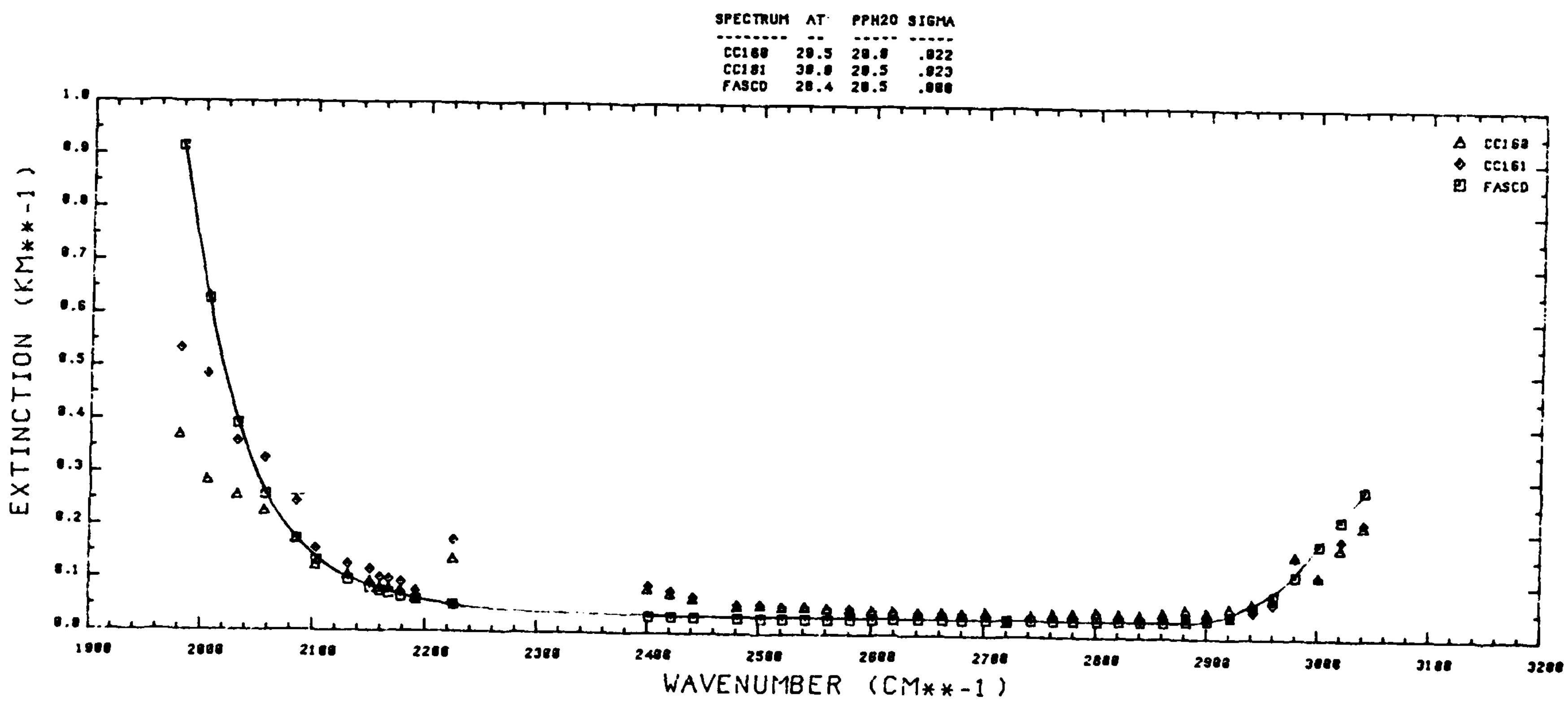

FIGURE 16e. COMPARISON OF CORRECTED CCAFS SPECTRAL DATA TO FASCODE WATER CONTINUUM ABSORPTION CALCULATIONS (MEASUREMENT-DERIVED AEROSOL EXTINCTION CORRECTIONS INCLUDED) CC160 AND CC161 COMPARED WITH FASCODE 14.

independent aerosol extinction components could be determined. In Figures 16 (a) through 16 (e) the data shown in Figures 15 (b) through 15 (g) (except 15 (e)), have been replotted, using the scaled Nd-YAG measurements to determine the aerosol extinction at 2700.270 cm^{-1}.

Tabular listings of the data shown in Figures 12 through 16 are contained in Appendix A. Included in these tabulations are the water vapor continuum absorption coefficient values calculated using the appropriate FASCODE case and the ratios and differences between each of the measured spectral values and the corresponding calculated values.

The DF laser line transmittance measurements typically used for absolute-transmittance normalization of the FTS spectra span the region between 2527.391 cm^{-1} (P2-12 line) and 2727.309 cm^{-1} (P2-4 line). This is the case for the ASL and SNI spectra. The PRNAS spectra were normalized using varied sets of DF laser transmittances as shown in Table 11. The CCAFS spectra shown in Figures 15 and 16 were normalized using six DF laser lines between the P2-12 line (2527.391 cm^{-1}) and the P1-6 line (2767.968 cm^{-1}).

Several observations can be made upon examination of the plots shown in Figures 12-16 and the corresponding tabulated data presented in Appendix A. Consistently, in all of the data sets, one sees that the experimental data point at 2223.68 cm^{-1} shows a considerably larger optical depth than does the FASCODE calculation. The converse is generally true for the data point located at 2719.28 cm^{-1}.

An examination of the local line optical depth calculations for these frequencies (shown in Figure 9) shows that they occur in troughs between strong absorption lines. In such situations small registration errors ($\lesssim$0.1 cm^{-1}) in the experimental wavenumber scale can cause substantial discre-

TABLE 11. DF LASER LINE FREQUENCIES USED FOR NORMALIZATION OF THE PRNAS FTS DATA.

SPECTRUM	RANGE OF DF LASER LINES			
	LOWEST WAVENUMBER		HIGHEST WAVENUMBER	
	LINE I.D.	WAVENUMBER (cm^{-1})	LINE I.D.	WAVENUMBER (cm^{-1})
PRO37	P2 - 12	2527.391	P2 - 7	2742.997
PRO40 PRO42 PRO54	P3 -10	2496.721	P1 - 6	2767.968
PRO49 PRO50				
PRO55 PRO56	P2 - 12	2527.391	P1 - 6	2767.968
PRO24	P2 - 12	2527.391	P2 - 7	2742.997

pancies in the calculated corrections for local line contributions. Further examination of the plots shown in Figure 9 shows that data points located at 2979.52 cm^{-1} and 3020.26 cm^{-1} also fall into this category. It is not surprising to see the experimental data points corresponding to the four above frequencies deviate from otherwise smooth curves in the plots shown in Figures 13-16.

Additional observations are consistently evident in all of the comparisons shown in Figures 12-16. These include (with respect to the calculated FASCODE results): a) consistently larger measured extinction values for the three frequencies 2400.00, 2420.42, and 2440.84 cm^{-1}, b) consistently lower measured extinction values for the data points between 1930.30 and 2190.95 cm^{-1}, and c) for those spectra collected during conditions of lower absolute humidity, (ASL and PRNAS) generally a larger measured extinction than the calculated values for $\nu > 2800$ cm^{-1}.

In comparing the plots with one another one should be mindful of the differences in the ordinate scales for the various plots. The ASL and PRNAS spectra were collected during conditions of low absolute humidity and the water continuum absorption coefficients are correspondingly low, with typical values ranging from 0.002 to 0.009 km^{-1} at 2700 cm^{-1}, except for spectrum PR024 where the value is 0.019 km^{-1}. Small uncertainties in the aerosol component of the total extinction tend to obscure the comparisons shown in Figures 12 and 13 for the ASL and PRNAS data. In general, the magnitude of the calculated water continuum absorption coefficient is comparable to or even smaller than the experimental uncertainty in the measured extinction coefficient corresponding to a $\pm 3\%$ transmittance measurement uncertainty. The relative uncertainty in extinction, $d\varepsilon/\varepsilon$,

is related to the relative uncertainty in transmittance dT/T by the relationship:

$$d\varepsilon/\varepsilon = -(1/\ln T)\ dT/T. \qquad (10)$$

When the extinction coefficient at 2700 cm^{-1}, ε, equals 0.002 km^{-1} (apart from aerosol contributions), the transmittance of a 5.1 km path is 99%. A $\pm 3\%$ value for dT/T translates into a 300% uncertainty in $d\varepsilon/\varepsilon$. The aerosol component required to produce agreement between the measured extinction coefficient and the calculated FASCODE water continuum absorption coefficient is typically 0.02 to 0.03 km^{-1} for the ASL and PRNAS spectra shown in Figures 12 and 13, and consequently overwhelms the small water vapor continuum absorption coefficients corresponding to these spectra. The relatively large amount of scatter in the data points between 2800 and 3060 cm^{-1} seen in the ASL spectra reflects the fact that the measured transmittances were very high, on the order of 80%. In this case $d\varepsilon/\varepsilon = 4.5 \times dT/T$ or $\pm 13.4\%$ for a value of $dT/T = \pm 3\%$. There is an indication, within the uncertainties identified above, that the experimental absorption coefficient values are usually larger than the calculated values in the region from 2800 cm^{-1} to 2980 cm^{-1} and frequently smaller than the calculated values for $\nu > 3000$ cm^{-1}. The latter behavior is apparent in the PRNAS spectra collected for absolute humidities, $\gtrsim$ 5.5 torr ppH_2O.

The SNI Spectra show generally good agreement with the FASCODE calculations in the spectral region between 2600 cm^{-1} and 3000 cm^{-1}. Due to the large variation in absorption coefficient between 1970 cm^{-1} and 2200 cm^{-1} the plots shown in Figures 14 (a) through 14 (e) are scaled such that the coefficient values between 2400 cm^{-1} and 2900 cm^{-1} are

difficult to discern. The tabular listings of the plotted values presented in appendix A are useful for obtaining quantitative comparisons in this spectral region.

A general feature of all of the SNI data except for the plots of spectra SNI02, SNI04, SNI05, and SNI06 is that the experimental data points between 1974.10 cm^{-1} and 2223.68 cm^{-1} lie below the calculated points as do the ASL spectral points in this region. The relatively large aerosol component and its associated uncertainty undoubtedly contribute to the inconsistencies seen in the SNI data.

In all of the comparisons of the SNI data shown in Figures 14 (a) through 14 (e) the data points between 2959.87 cm^{-1} and 3058.71 cm^{-1} exhibit larger extinction values than do the corresponding calculated points.

As previously discussed, the effects of uncertainties associated with the correction for local line contributions render the corrected values of the data points at 2979.52 cm^{-1} questionable.

The CCAFS data shown in Figures 15(a) through 15(g) show rather consistent behavior in that the experimental extinction values are smaller than the calculated values between 1930.30 cm^{-1} and 2102.15 cm^{-1} and again between 2880.80 cm^{-1} and 3058.71 cm^{-1}. In general, the CCAFS data points fall on smoother curves than do the data from the other three data sets. This is in part due to the fact that the higher molecular absorption coefficients seen in the CCAFS data are larger than the fundamental experimental uncertainties in the measurements. The several data points subject to errors in the local-line-absorption corrections are quite obvious when examining the plots of the CCAFS data. A good comparison of the "shape" of the FASCODE water continuum absorption coefficient with that determined by the

experimental data is presented in the several plots of the CCAFS data shown in Figures 15(a) through 15(g).

The use of Nd-YAG laser transmittance measurements as an independent means of assessing the aerosol extinction component in the 3-5 μm region was discussed in subsection 3.1.2.2. The CCAFS spectra for which Nd-YAG laser transmittance values are available are listed in Table 9 and include the spectra designated as CC144, -145, -147, -148, -153, -154, -157, -158, -159, -160, and -161. These spectra were re-plotted using infrared aerosol extinction coefficients at 2700.72 cm^{-1} derived from the measured Nd-YAG extinction coefficients listed in Table 10. The humidity and wavelength scaling discussed in subsection 3.1.2.2 and the modeled wavelength dependence given by Equations 8 and 9 were used. Figures 16(a) through 16(e) show the results of using this approach to determine an experimental water vapor continuum absorption coefficient.

The comparison shown in Figure 16(a) between experimental data points for spectra CC144 and CC145 and calculated values for FASCODE case 9 shows a significant difference between the measured and calculated values. Over the spectral range from 2501.00 cm^{-1} to 2958.87 cm^{-1} the experimental data points for the two CCAFS spectra are essentially superimposed on one another and are larger than the corresponding calculated points by an amount varying from 0.067 km^{-1} at 2501.00 cm^{-1} to 0.034 km^{-1} at 3959.87 cm^{-1} (see Appendix A for a tabulation of the difference values).

The several comparisons shown in Figures 16(b) through 16(e) show generally close agreement between the magnitudes of the measured data and calculated values over the 2599.84 cm^{-1} to 2941.37 cm^{-1} region. In light of the distinctly different appearance of the comparison shown in Figure 16(a), it is likely that the relatively large differences in

extinction values are due to an incorrect determination of the aerosol component of the total extinction. The time differences between the FTS and calibrating DF laser measurements are comparable for the CC144 and CC145 spectra to those for the several succeeding spectra and the measured aerosol extinction coefficient at 1.06 μm remained fairly constant during the FTS and DF laser measurement period. The discrepancy in evaluation of the aerosol component for the spectra shown in Figure 16(a) therefore cannot be readily explained on the basis of the above considerations.

The remaining data and comparisons shown in Figures 16(b) through 16(e) form a rather consistent data set. In all cases the measured values exceed the calculated values over the range between 2400.00 cm^{-1} and 2941.37 cm^{-1}. A crossover occurs between 2920 and 2940 cm^{-1} and the experimental data are lower than the calculated values for wavenumbers larger than 2940 cm^{-1}.

Looking at the comparisons in the longer wavelength region one sees good agreement in extinction magnitude for the data points between 2130.50 cm^{-1} and 2190.95 cm^{-1}. The measured extinction values are consistently smaller than the calculated values for wavenumbers smaller than 2130.50 cm^{-1}. The ratio of the measured extinction values to those calculated using FASCODE for all of the data shown in Figures 12 through 16 is tabulated in Appendix A. These ratios can be used to determine the size of the correction factor needed to produce exact agreement between the measured data and the FASCODE result, keeping in mind that the validity of the correction factor so derived rests on the validity of the aerosol extinction corrections described above.

For purposes of quantitatively determining a correction factor for the FASCODE water vapor continuum absorption coefficient, the spectral values plotted in Figures 16 (b)

through 16 (e) were divided into two groups, corresponding to different ranges of absolute humidity. Data for spectra CC147, -148, -153, and -154, corresponding to the absolute humidity range between 16.3 and 17.4 torr ppH_2O, were averaged together as were those for spectra CC157, -158, -159, -160, and -161 which correspond to the water vapor partial pressures of 20.0 and 20.5 torr. The average values of the ratio of the measured data to the calculated values, CC/FCD, for each of the two groupings are plotted as two separate curves versus wavenumber in Figures 17(a) and 17(b).

In Figure 17(a), the measured values are seen to be about 55% of the calculated values at 1980 cm^{-1}, rising to near unity around 2060 cm^{-1}. The data points corresponding to the higher absolute humidities define a lower-valued curve nearly parallel to that for the lower humidity data. The two curves show small variations with wavenumber around the value of unity in the region between 2060 cm^{-1} and 2140 cm^{-1}. The error bars, shown only on one curve for simplicity, represent the RMS deviated from the average value calculated for each set of spectra. The RMS values are comparable in magnitude for each of the two curves shown in Figure 17(a).

The shorter wavelength data shown in Figure 17(b) show a considerably larger value for the CC/FCD ratio of about 2.4 at 2400 cm^{-1}, dropping to a value of unity around 2925 cm^{-1} and then to a value of 0.55 at 3000 cm^{-1}. As in the case of the long wavelength region shown in Figure 17(a), the data for the two absolute humidity groupings define two nearly parallel curves, only with the higher humidity curve showing larger extinction values in this case.

The rapid increase of the value of the CC/FCD ratio for wavenumbers shorter than 2700 cm^{-1} seen in Figure 17(b) can probably be attributed to inaccuracies in the calculated corrections for CO_2 and N_2 continuum contributions to the total extinction. An examination of the calculated CO_2 and N_2 continuum contributions tabulated in Appendix C shows that the N_2 continuum contribution is important for wavenumbers between 2084.35 cm^{-1} and 2223.68 cm^{-1} on the long wavelength side of the ν_3 CO_2 band and for wavenumbers between 2400.00 cm^{-1} and 2740.74 on the short wavelength side. Superimposed on the N_2 continuum absorption coefficient is the CO_2 band-wing continuum, important for wavenumbers between 2400.00 cm^{-1} and about 2520 cm^{-1}.

Thus, the initial sharp rise of the CC/FCD curves in Figure 17 for wavenumbers below 2700 cm^{-1} likely can be attributed to an under-estimation of the N_2 continuum absorption in the FASCODE model. For wavenumbers below about 2520 cm^{-1} in Figure 17(b) the sum of the CO_2 and N_2 absorptions are underestimated. Since the N_2 continuum appears to be underestimated in the region between 2520 cm^{-1} and 2720 cm^{-1}, and no abrupt discontinuity in the curves shown in Figure 17(b) is evident around 2520 cm^{-1}, it is likely that the N_2 continuum underestimate is the major contributor to the large values of the CC/FCD ratio seen in Figure 17(b) between 2400 cm^{-1} and 2720 cm^{-1}. The slopes of the curves in Figure 17(b) level out around 2700 cm^{-1} (before turning down around 2800 cm^{-1}), at a value of about 1.25, indicating that the calculated FASCODE water vapor continuum absorption coefficient is about 77% of the average experimental values in this region.

For wavenumbers greater than about 2925 cm^{-1} the CC/FCD ratio is less than unity in Figure 17(b) indicating that the model predicts anomalously high water vapor absorption in this region.

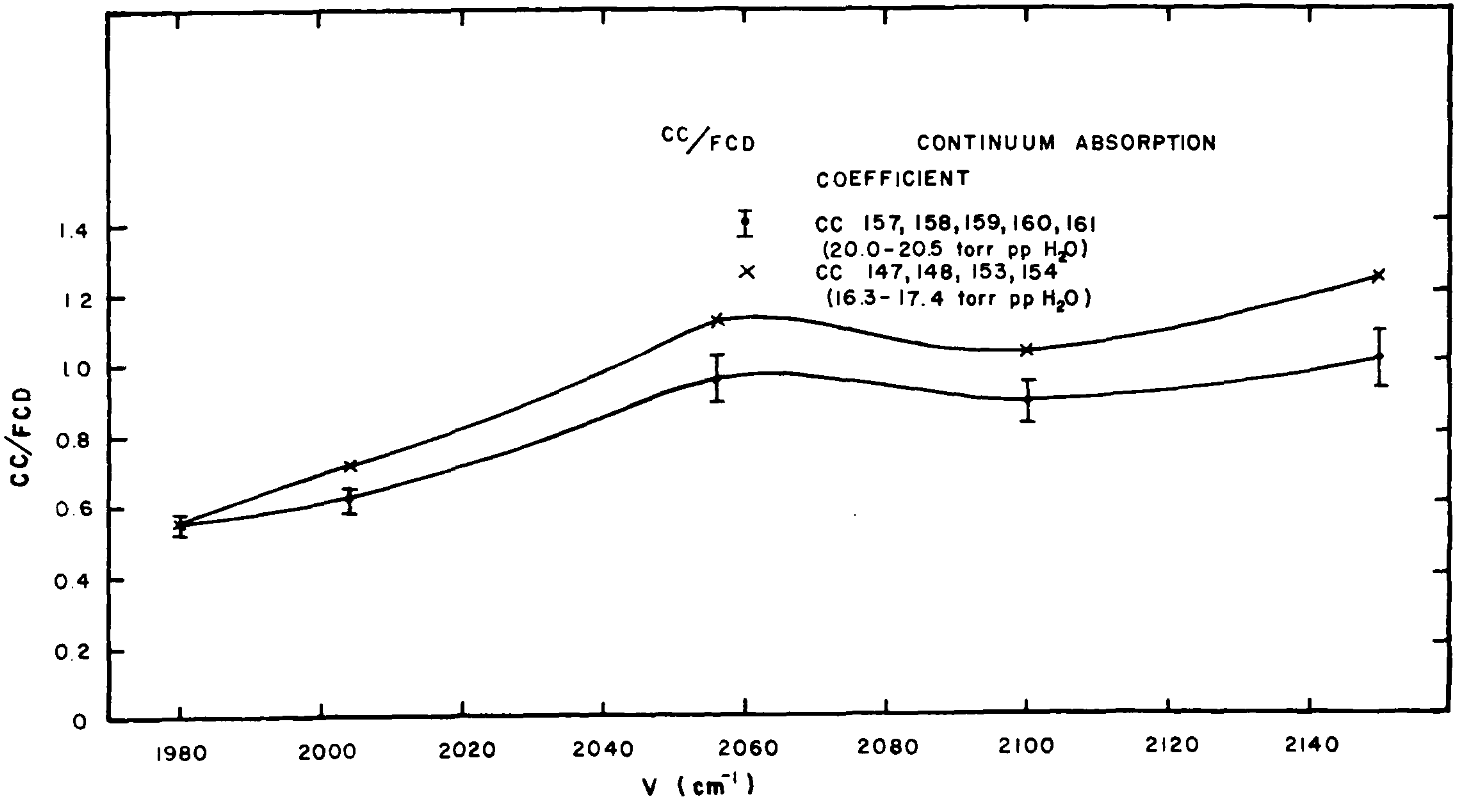

FIGURE 17a. RATIO OF MEASURED TO CALCULATED VALUES FOR WATER VAPOR CONTINUUM ABSORPTION COEFFICIENTS VERSUS WAVENUMBER, 1980 cm^{-1} to 2140 cm^{-1}.

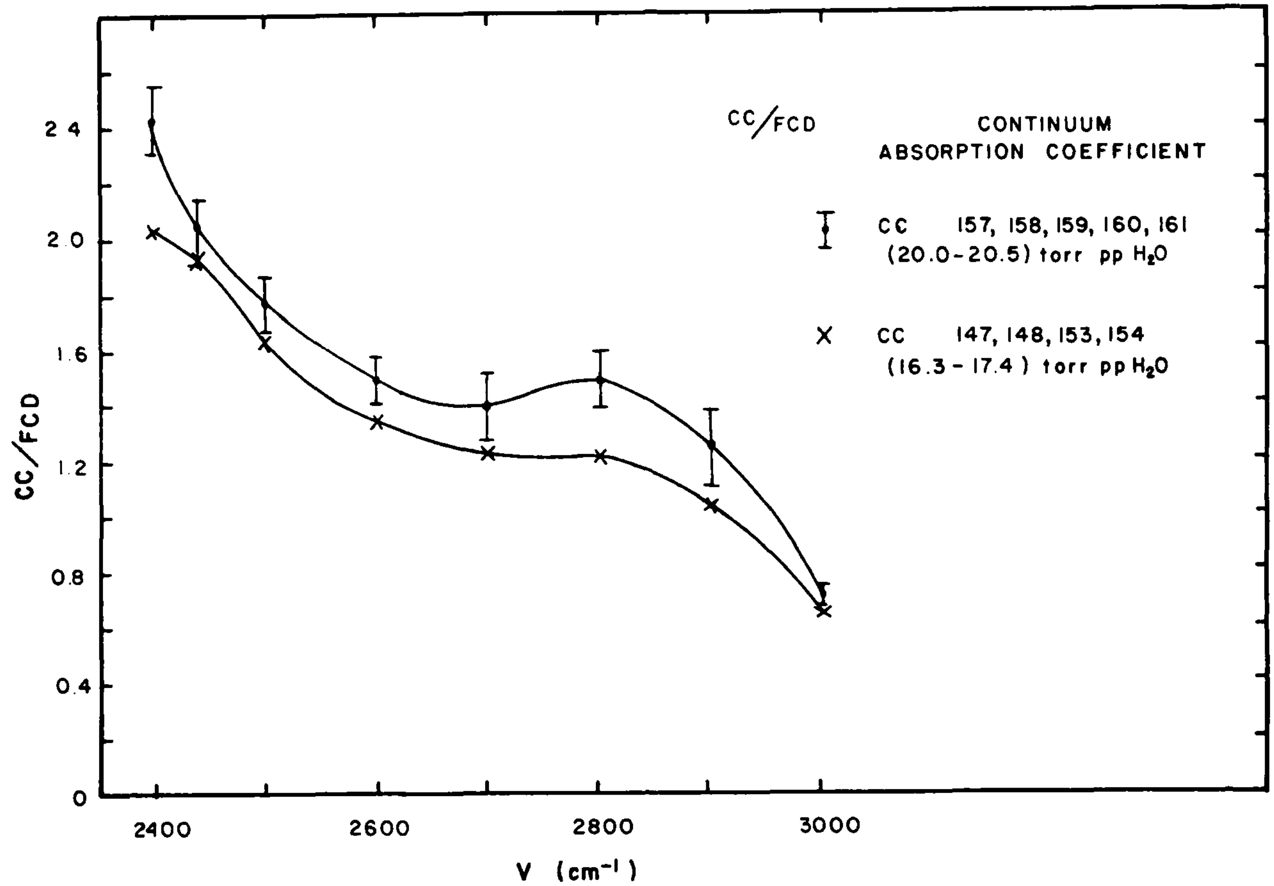

FIGURE 17b. RATIO OF MEASURED TO CALCULATED VALUES FOR WATER VAPOR CONTINUUM ABSORPTION COEFFICIENTS VERSUS WAVENUMBER, 2400 cm^{-1} to 3000 cm^{-1}.

It is interesting to note also that the positive slope in the region of the curves shown in Figure 17(a) between 2100 cm^{-1} and 2160 cm^{-1} is consistent with the observation made with respect to Figure 17(b) that the predicted N_2 continuum absorption coefficients are too large.

The comparisons shown in Figure 17(b) should not be interpreted as showing that the experimental water vapor continuum absorption coefficient is 2.4 times as large as the FASCODE-calculated result at 2400 cm^{-1}. The point has already been made that the calculated N_2 continuum absorption coefficient is too large and probably accounts for the discrepancies shown in Figure 17(b). The relative magnitudes of the calculated H_2O and $CO_2 + N_2$ continuum absorption coefficients can be determined by an examination of the results tabulated in Appendices A and C respectively. Since the magnitude of the $CO_2 + N_2$ continuum optical depths at 2400 cm^{-1} is some 25 to 28 times larger than the calculated H_2O continuum absorption coefficients at that frequency (0.7 to 0.9 versus 0.025 to 0.035), the apparently large deviation from unity shown in Figure 17(b) must be kept in this context. The large deviations represent only a 10 - 12% change in the magnitude of the calculated N_2 optical depth at 2400 cm^{-1}.

The error bars plotted in Figures 17(a) and 17(b) show the RMS deviations from the average values for the CC/FCD ratios plotted for each group of spectra.

The uncertainties in the measured data associated with the ratios shown in Figures 17(a) and 17(b) can be determined by combining the experimental uncertainties in the measured data together with the uncertainties associated with the calculated local line contributions and estimated aerosol extinction corrections.

The experimental uncertainty in the measured transmittance is accepted to be ±3% in most cases and in all of the cases shown in Figures 17(a) and 17(b). Typically the maximum average transmittance values in the spectral range shown in the figures is about 80%. Referring to Equation 10 we see that the resultant uncertainty in measured optical depth corresponding to a ±3% transmittance uncertainty is ±13.5%.

The calculated local line contributions to the total optical depth can be seen to range from low values of 0.3 to 0.4 of the FASCODE-calculated H_2O continuum absorption values to higher values which are 20 to 150 times as large as the H_2O continuum values, depending upon the particular wavenumber locations under consideration. Since the comparison plots shown in Figures 12-16 show generally smooth behavior as a function of wavenumber for a wide variation in local-line-correction values to the optical depth, (see Appendix B), it may be concluded that the magnitudes of the calculated corrections are generally quite good, except for the specific wavenumber previously noted. Assuming a conservative estimate of a ±20% uncertainty in the calculated local line contributions in the 2500 - 2900 cm^{-1} region, and noting that the magnitude of these corrections is 30-40% of the H_2O continuum absorption values in this region, then an estimate of the uncertainties in the comparisons shown in Figures 17(a) and 17(b) due to uncertainties in local line absorption coefficients would be ± 8%.

The uncertainties in the CC/FCD ratios due to corrections for aerosol attenuation are difficult to estimate. The measured Nd-YAG transmittance values can be characterized by a ±3% uncertainty, just as the measured DF laser transmittances. However, the uncertainty associated

with the extrapolation of aerosol extinction values measured at 1.06 μm to 3.8 μm is difficult to ascertain in a quantitative manner. If one assumes that on the average this extrapolation has associated with it a ±25% uncertainty, then the Nd-YAG transmittance-derived aerosol extinction corrections at 3.8 μm would have an uncertainty of ±20%.

Combining the three categories of contributing uncertainties, the measured (and appropriately corrected) data used in the comparisons shown in Figures 17(a) and 17(b) would have associated with them an overall uncertainty of ±55%. This value easily includes the FASCODE-derived H_2O continuum absorption prediction in the 2500 - 2900 cm^{-1} region. The large deviation due to N_2 continuum absorption near 2400 cm^{-1} must be viewed independently from the H_2O continuum comparisons as previously discussed.

3.2 WATER VAPOR LINE ABSORPTION ANALYSIS

3.2.1 SURVEY COMPARISONS BETWEEN MEASUREMENTS AND CALCULATIONS

This section presents a comparison between two of the measured spectra and FASCODE calculations over the full spectral range of the measurements from 1900 cm^{-1} to 3200 cm^{-1}. The two spectra chosen were selected to be representative of low and high water vapor amounts and to have high signal to noise and visibility: spectrum ASL06 corresponds to 2.9 gm cm^{-2} of water vapor along the path with 100 km visibility and spectrum CC159 corresponds to 10.3 gm cm^{-2} of water vapor with 35 km visibility. The calculated spectra were produced using FASCOD1C and the 1982 version of the AFGL Line Tape.

Figure 18 shows a low resolution comparison between one of the measured spectra (ASL06) and the FASCODE calcula-

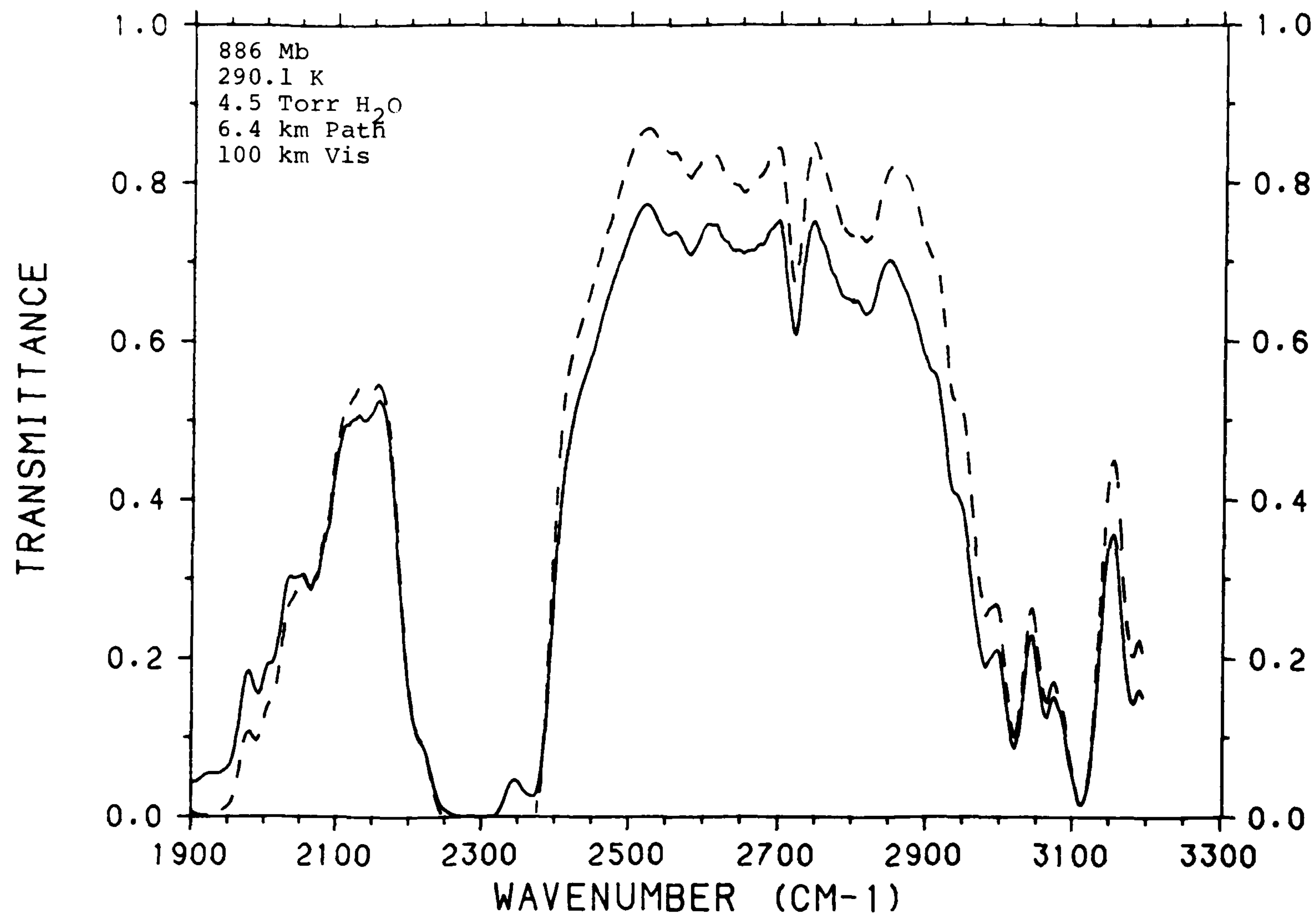

FIGURE 18. SPECTRUM ASL06, 1900-3200 cm^{-1}, DEGRADED WITH A 10 cm^{-1} HWHM TRIANGULAR INSTRUMENT FUNCTION, MEASURED (SOLID) AND FASCODE (DASHED), NO AEROSOL ATTENUATION IS INCLUDED IN THE FASCODE CALCULATION.

tion; both the measured and the calculated spectra have been degraded with a 10 cm^{-1} half-width at half-height triangular instrument function. By degrading the spectra it is possible to survey the whole range from 1900 to 3200 cm^{-1} on a single plot. No aerosol extinction has been included in the FASCODE calculation so that the calculated transmittance in the windows is generally higher than the measured transmittance.

Figures 19 and 20 show the high resolution comparisons for each of the measured spectra in sections of 100 cm^{-1} each. In these comparisons the following points should be noted:

1. No aerosol extinction is included in the calculation.

2. The resolution of the measurement is determined by the instrument function which is a sinc function: $\sin(2\pi\nu L)/(2\pi\nu L)$ where the optical retardation L = 16 cm. The half width at half-height of this function is 0.018 cm^{-1}. The half widths of atmospheric absorption lines are typically 0.08 cm^{-1} but may be as small as 0.009 for some anomalously narrow water lines. Therefore, for most of the absorption lines in this spectra, the absorption at the line center will not be greatly reduced by the limited instrument resolution: for the narrow water lines however, the effect may be large.

3. In the measured spectrum ASL06, zero percent transmittance level in the measurement is displaced by about 0.05 at 1900 cm^{-1} decreasing to a negligible value at 2260 cm^{-1}. There appears to be no displacement at 2390 cm^{-1} and above 2900 cm^{-1}. The non zero transmittance seen between 2330 cm^{-1} and 2390 cm^{-1} is not real but is an artifact of the calibration procedure.

4. There are a number of apparent "mini-windows" in the measured spectrum ASL06 between 1900 cm^{-1} and 2000 cm^{-1} which are not seen in the

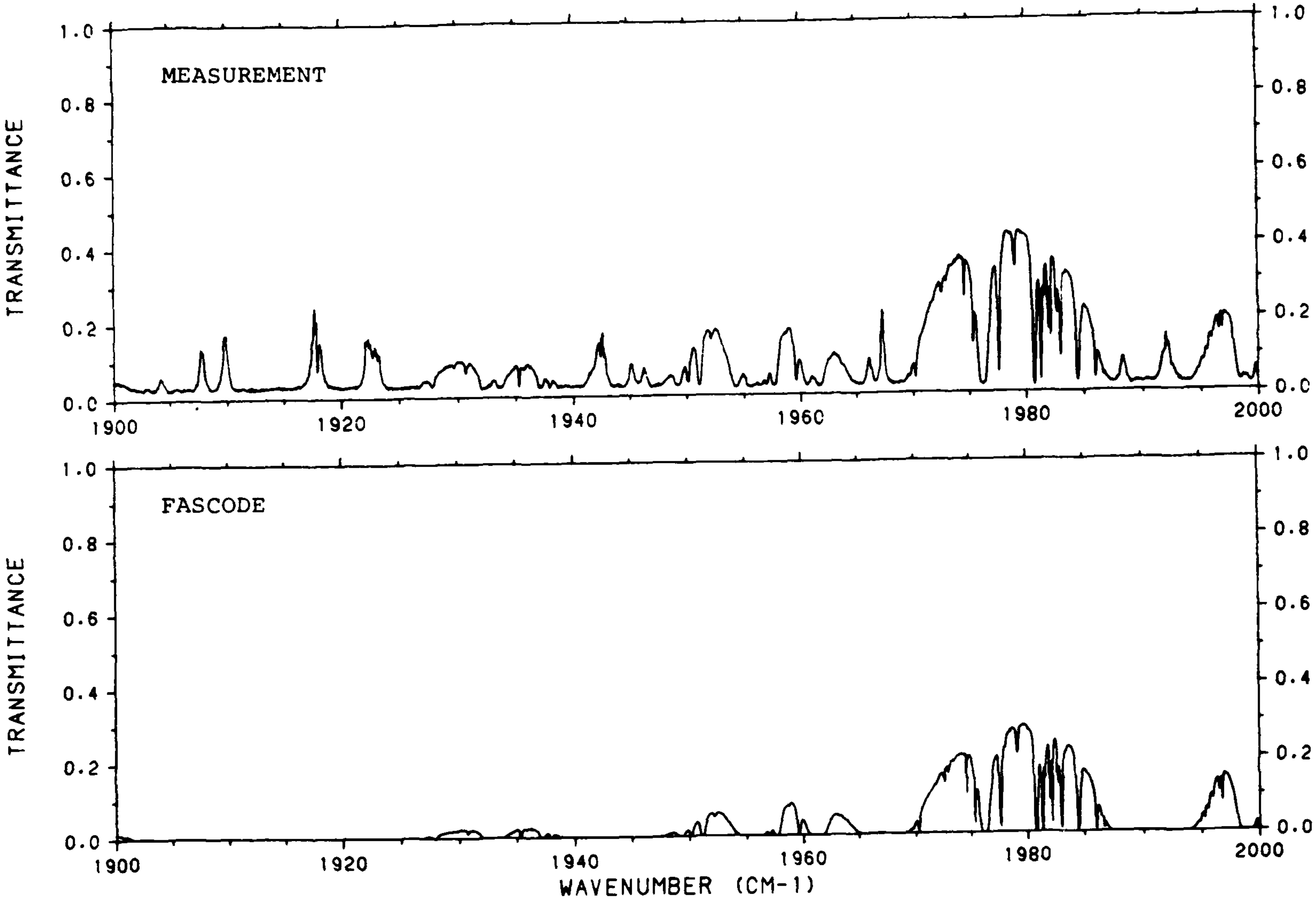

FIGURE 19a. SPECTRUM ASL06, 1900-2000 cm^{-1} : MEASURED (TOP) AND CALCULATED (BOTTOM): 886 Mb, 290.1 K, 4.5 TORR WATER VAPOR, 6.4 KM PATH, 100 KM VIS, NO AEROSOL IN CALCULATION.

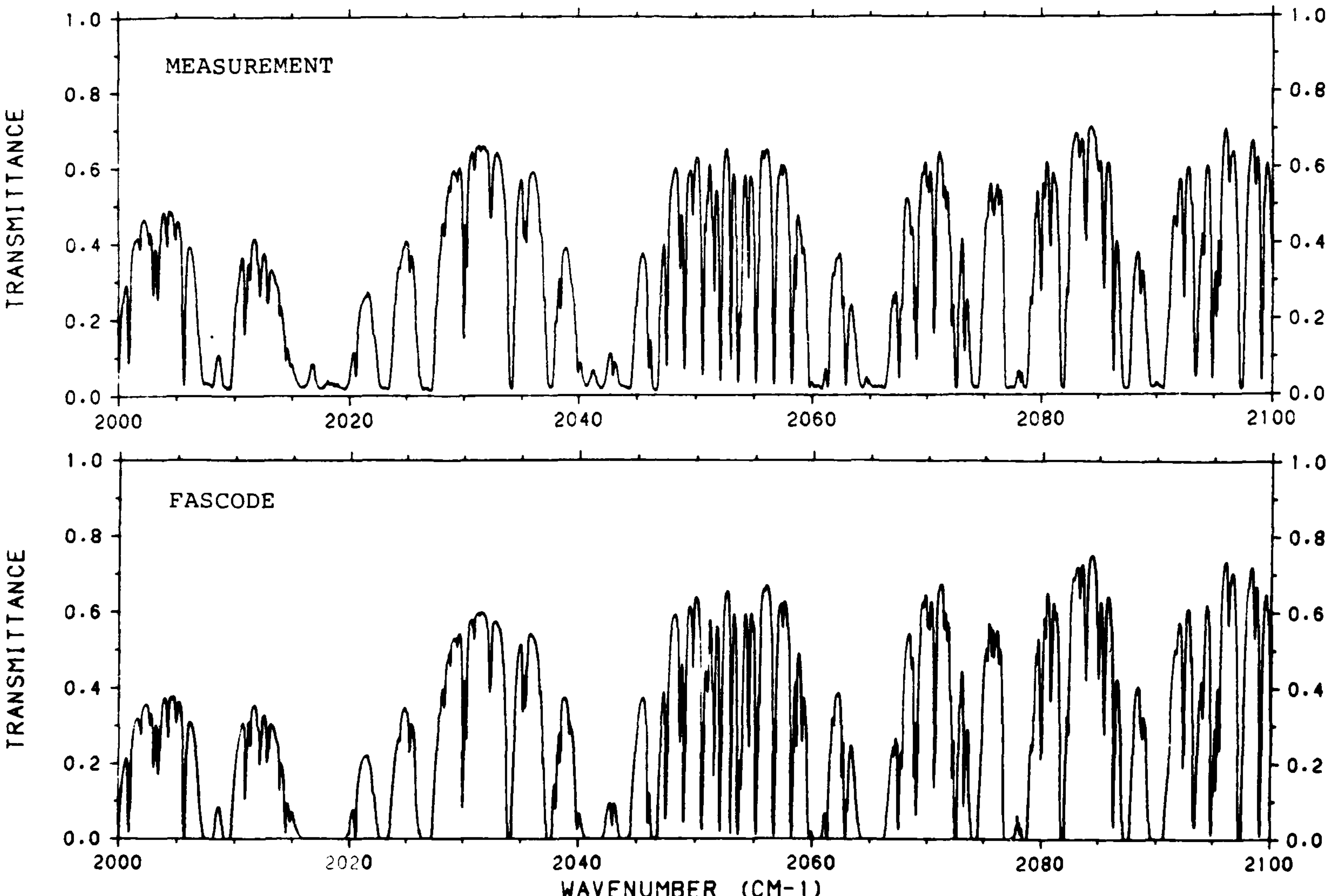

FIGURE 19b. SPECTRUM ASL06, 2000-2100 cm^{-1}: MEASURED (TOP) AND CALCULATED (BOTTOM).

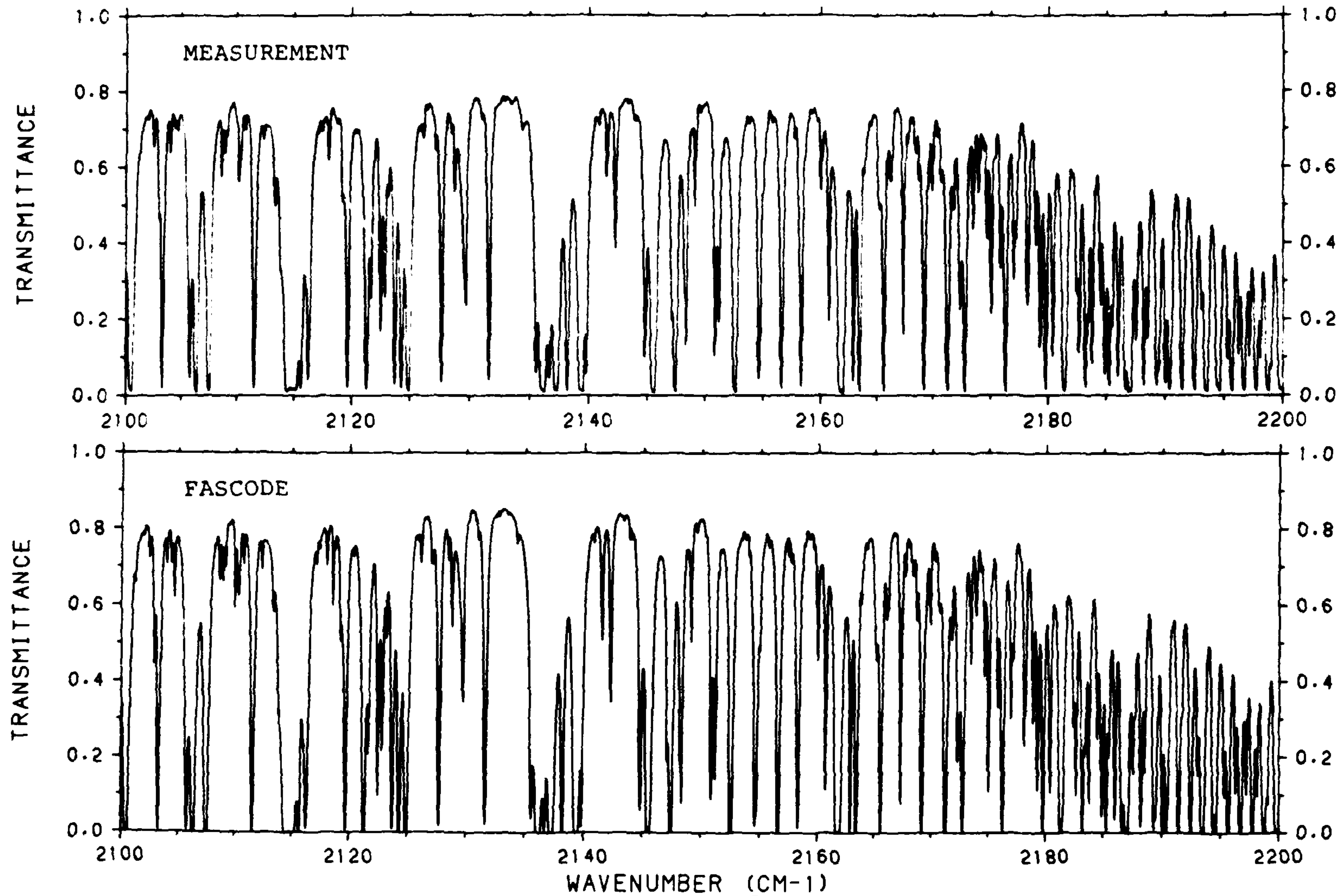

FIGURE 19c. SPECTRUM ASL06, 2100-2200 cm^{-1}: MEASURED (TOP) AND CALCULATED (BOTTOM).

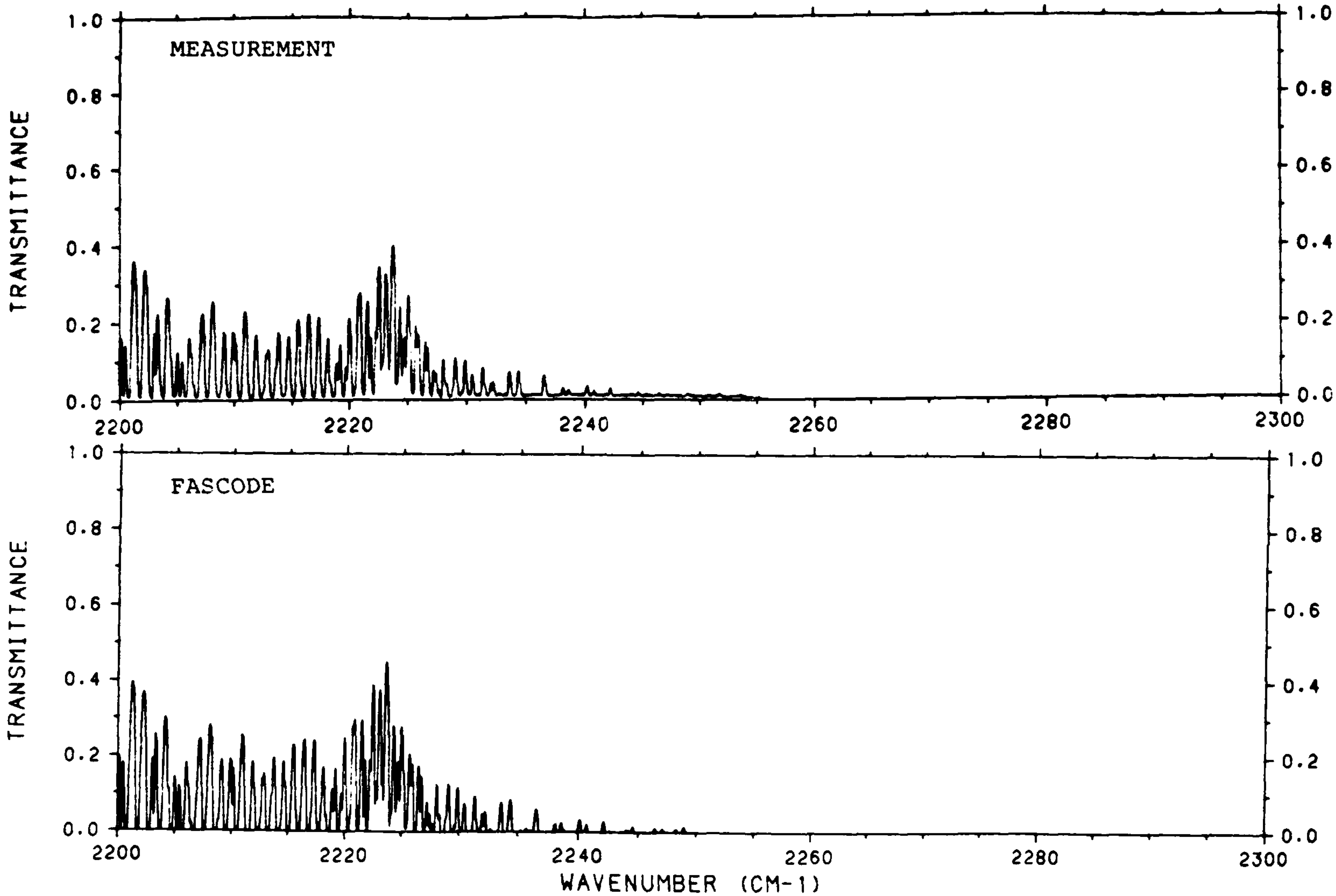

FIGURE 19d. SPECTRUM ASL06, 2200-2300 cm^{-1}: MEASURED (TOP) AND CALCULATED (BOTTOM).

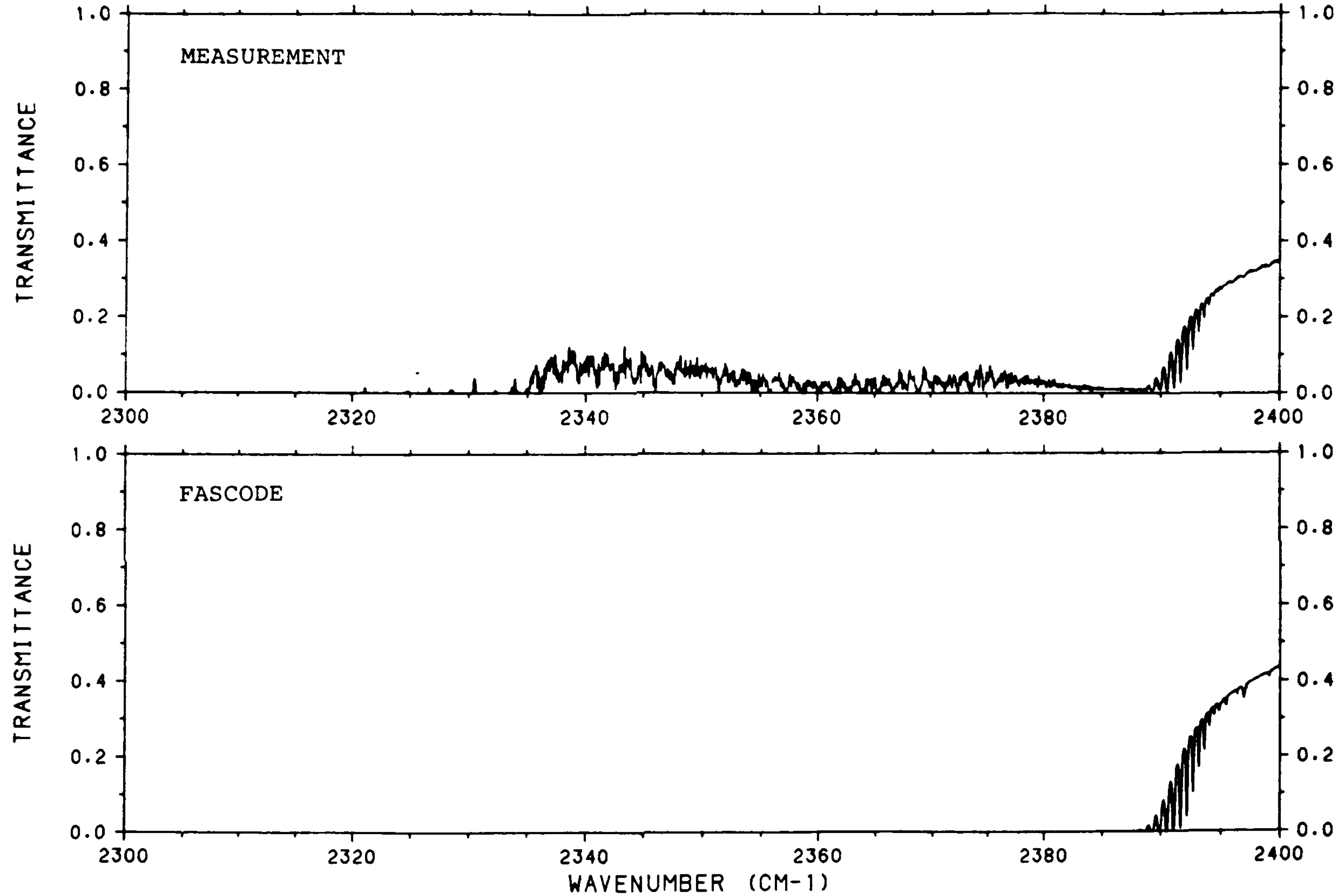

FIGURE 19e. SPECTRUM ASL06, 2300-2400 cm^{-1}: MEASURED (TOP) AND CALCULATED (BOTTOM).

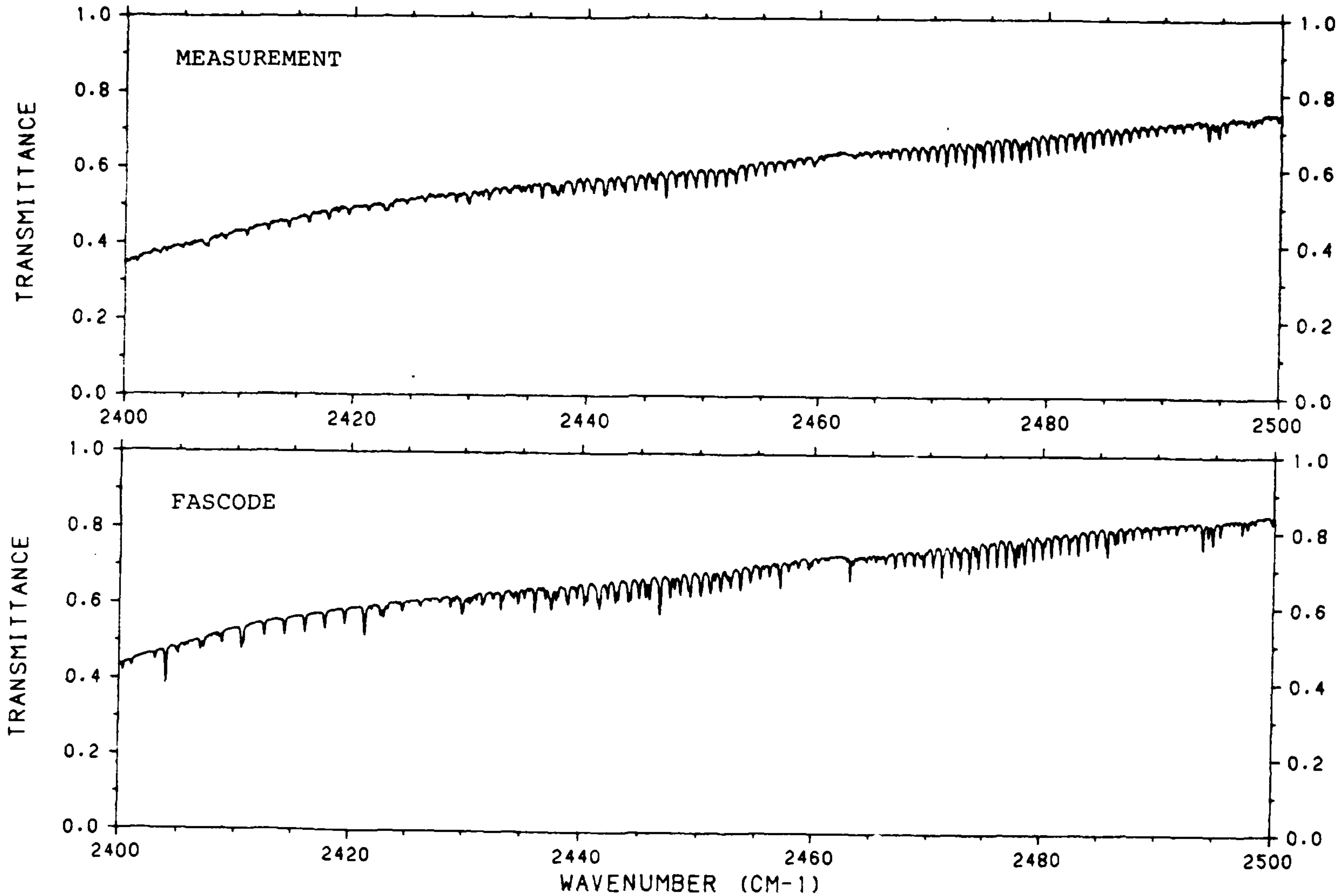

FIGURE 19f. SPECTRUM ASL06, 2400-2500 cm^{-1}: MEASURED (TOP) AND CALCULATED (BOTTOM).

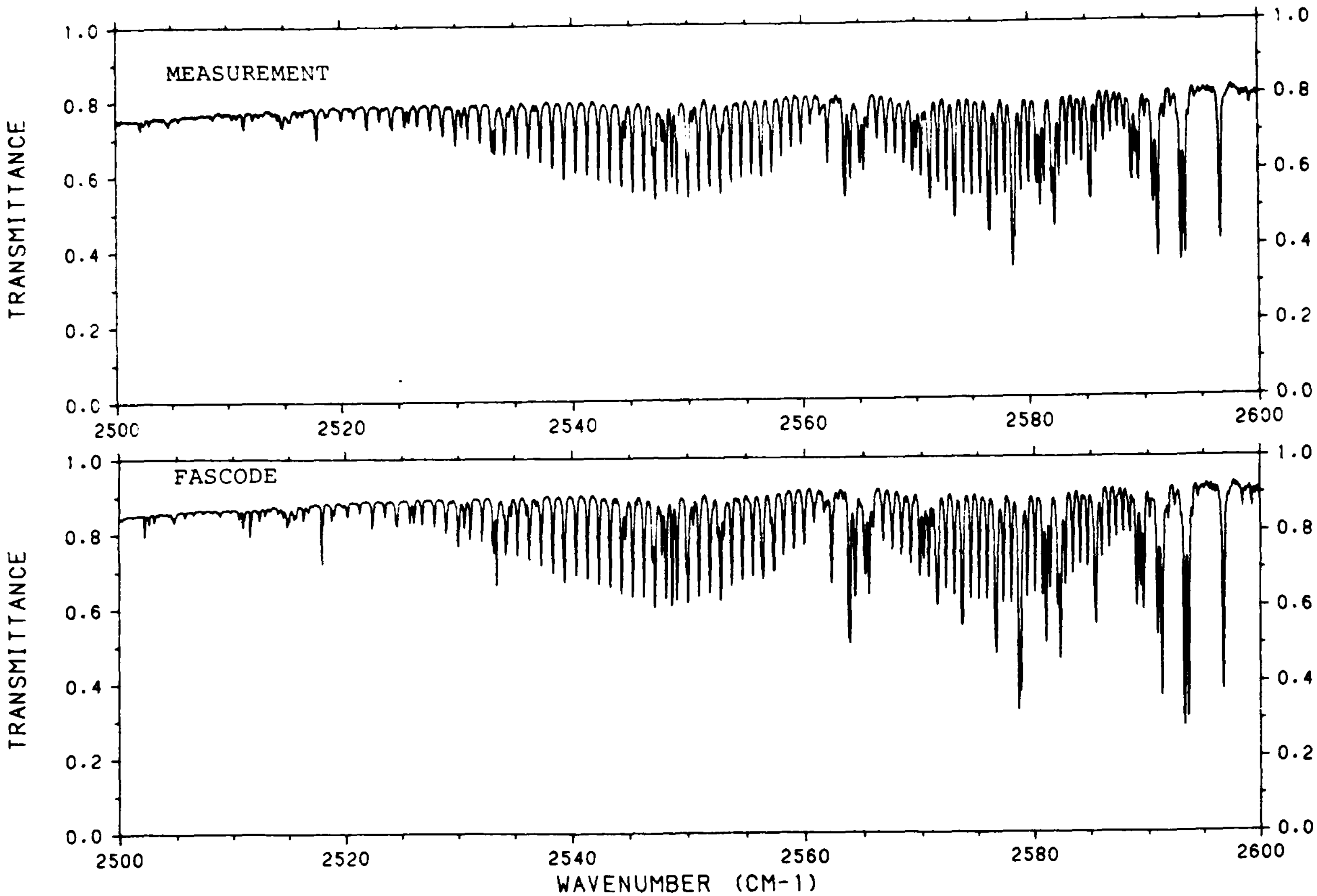

FIGURE 19g. SPECTRUM ASL06, 2500-2600 cm^{-1}: MEASURED (TOP) AND CALCULATED (BOTTOM).

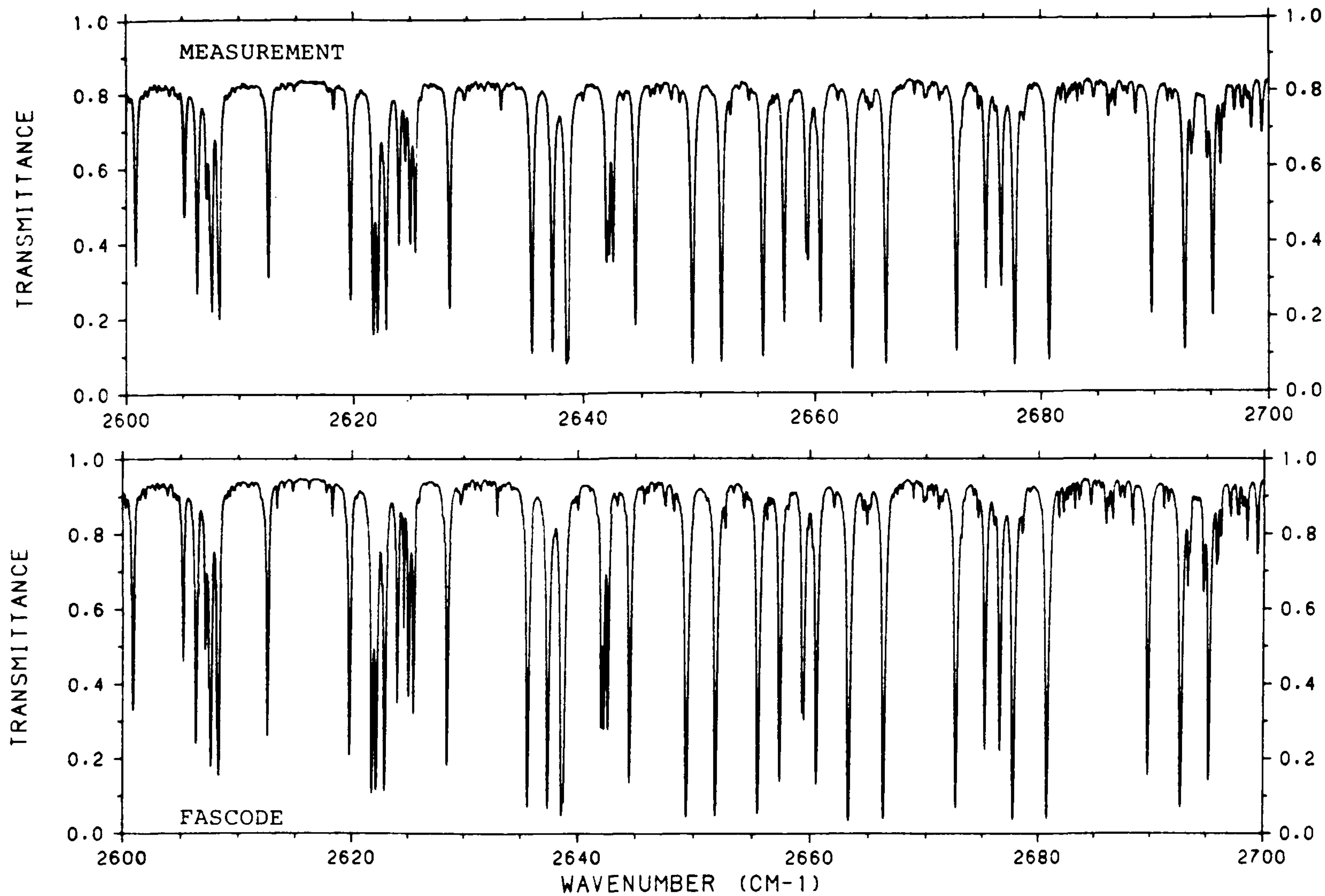

FIGURE 19h. SPECTRUM ASL06, 2600-2700 cm^{-1}: MEASURED (TOP) AND CALCULATED (BOTTOM).

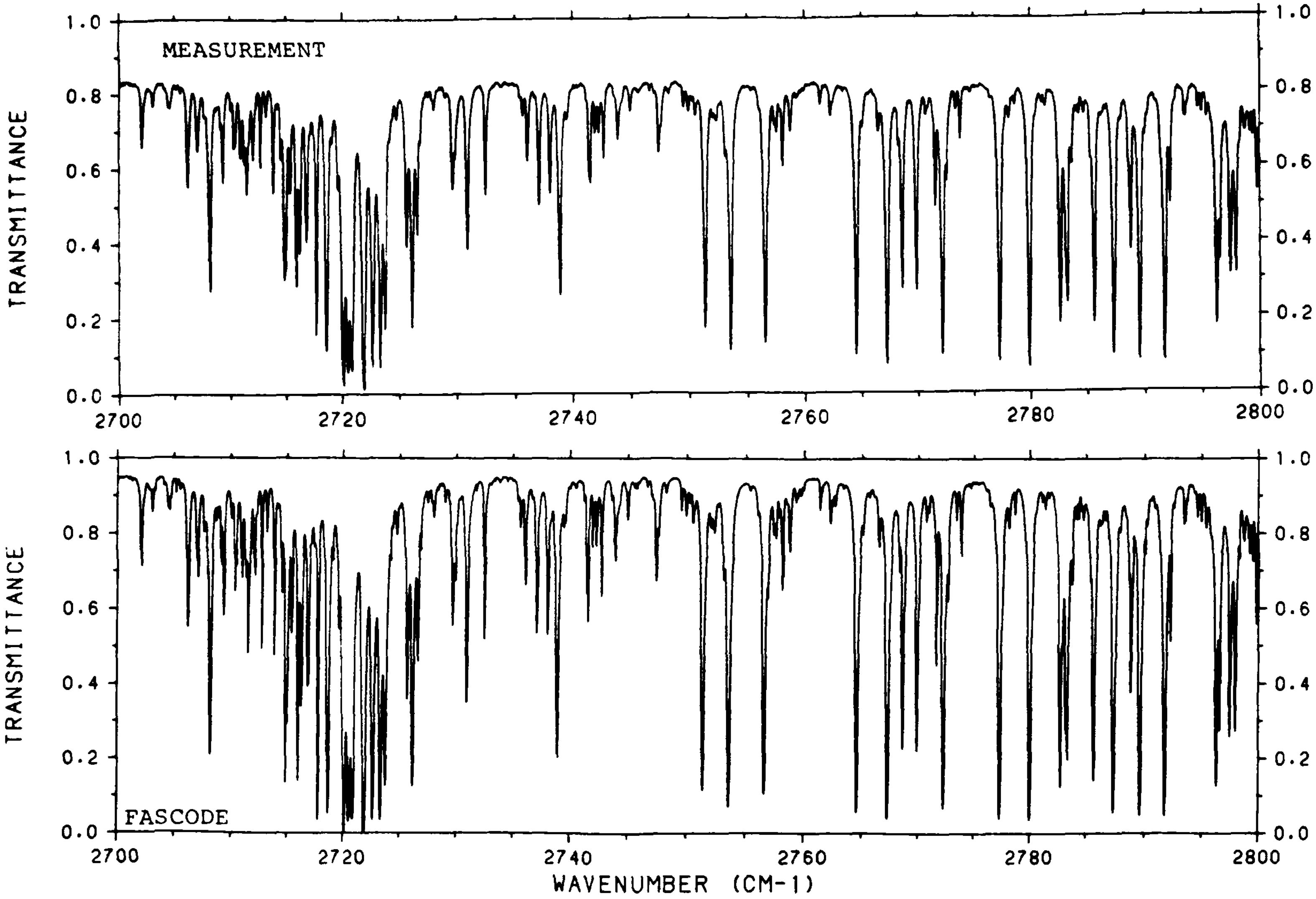

FIGURE 19i. SPECTRUM ASL06, 2700-2800 cm^{-1}: MEASURED (TOP) AND CALCULATED (BOTTOM).

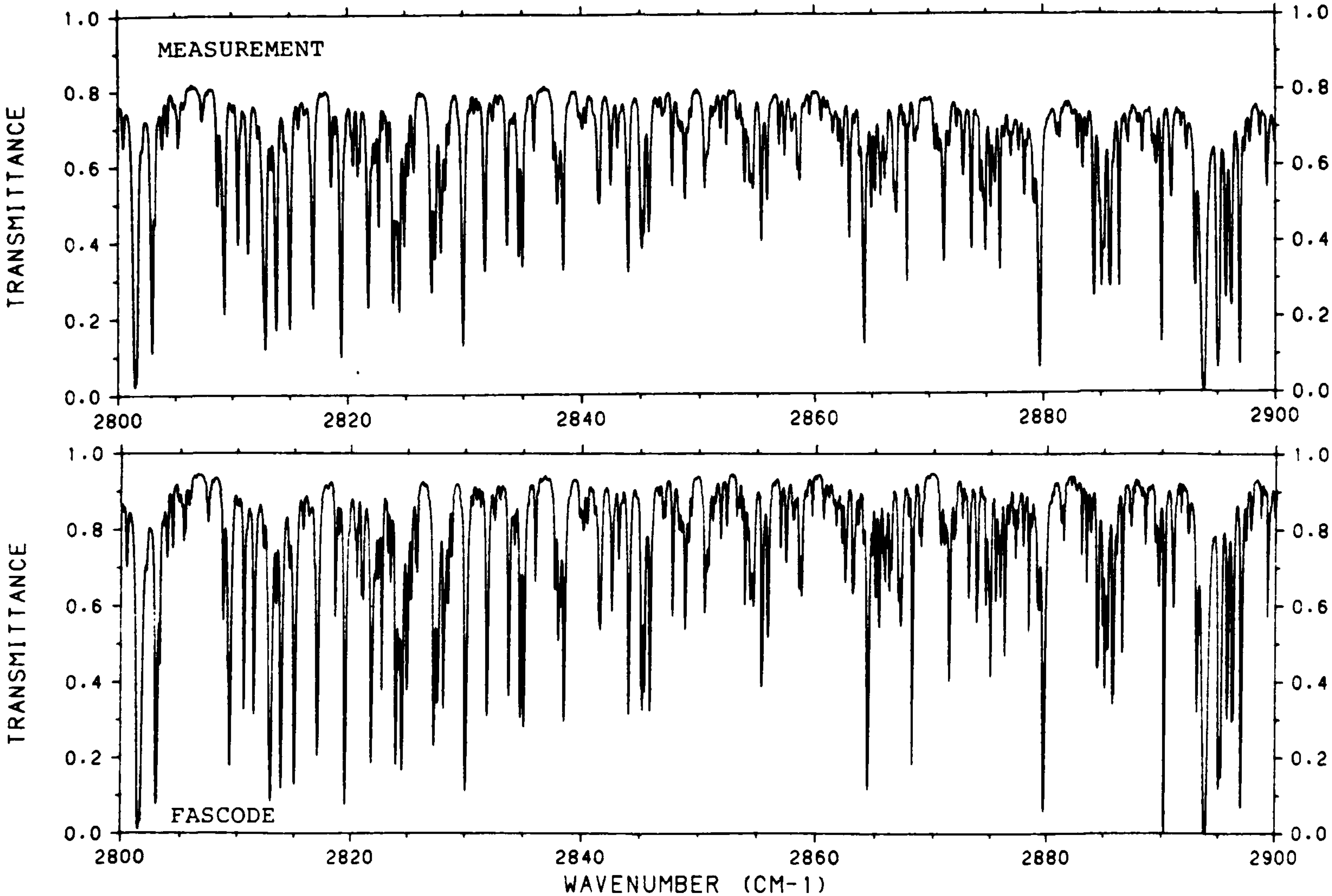

FIGURE 19j. SPECTRUM ASL06, 2800-2900 cm^{-1}: MEASURED (TOP) AND CALCULATED (BOTTOM).

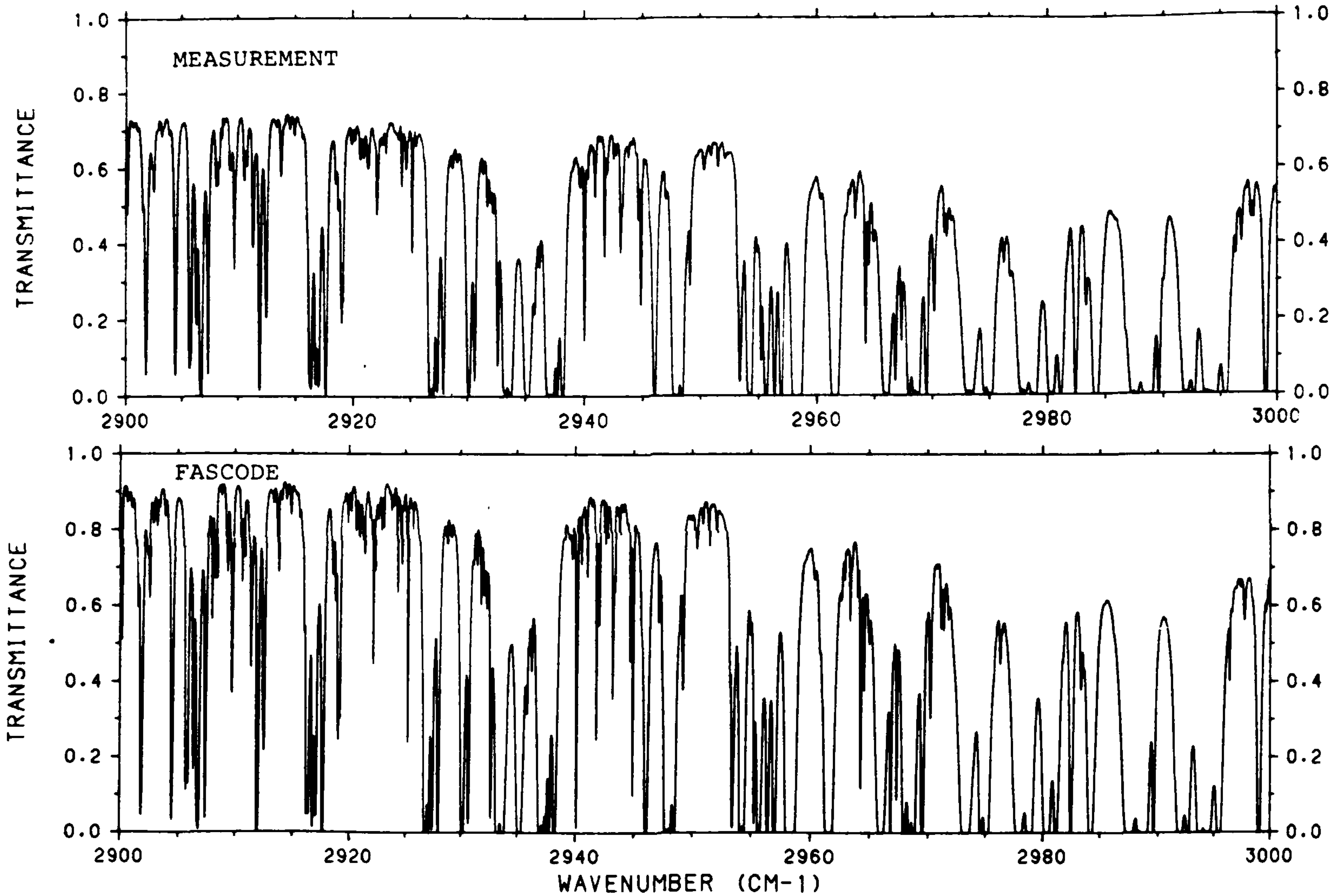

FIGURE 19k. SPECTRUM ASL06, 2900-3000 cm^{-1}: MEASURED (TOP) AND CALCULATED (BOTTOM).

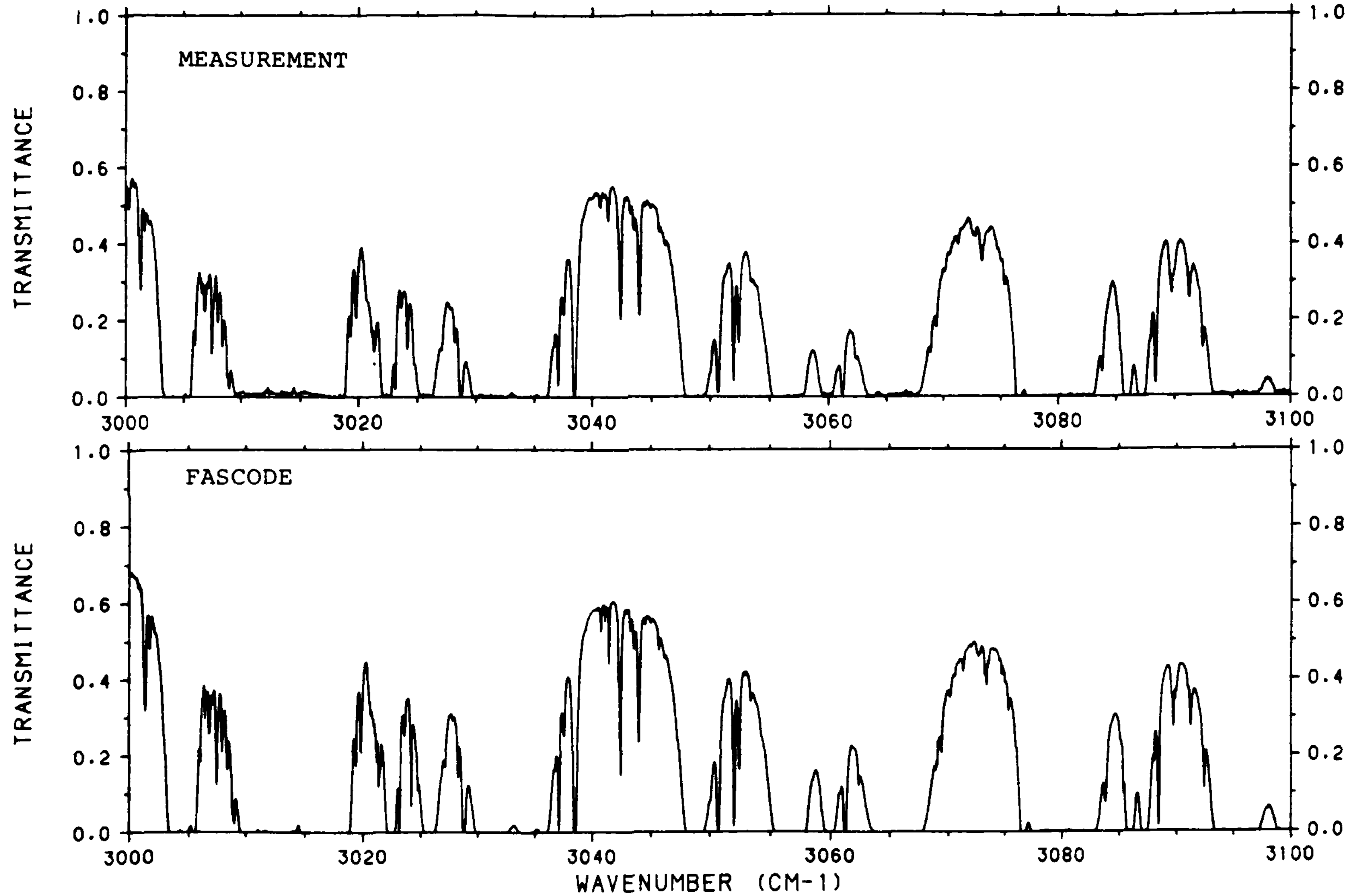

FIGURE 191. SPECTRUM ASL06, 3000-3100 cm^{-1}: MEASURED (TOP) AND CALCULATED (BOTTOM).

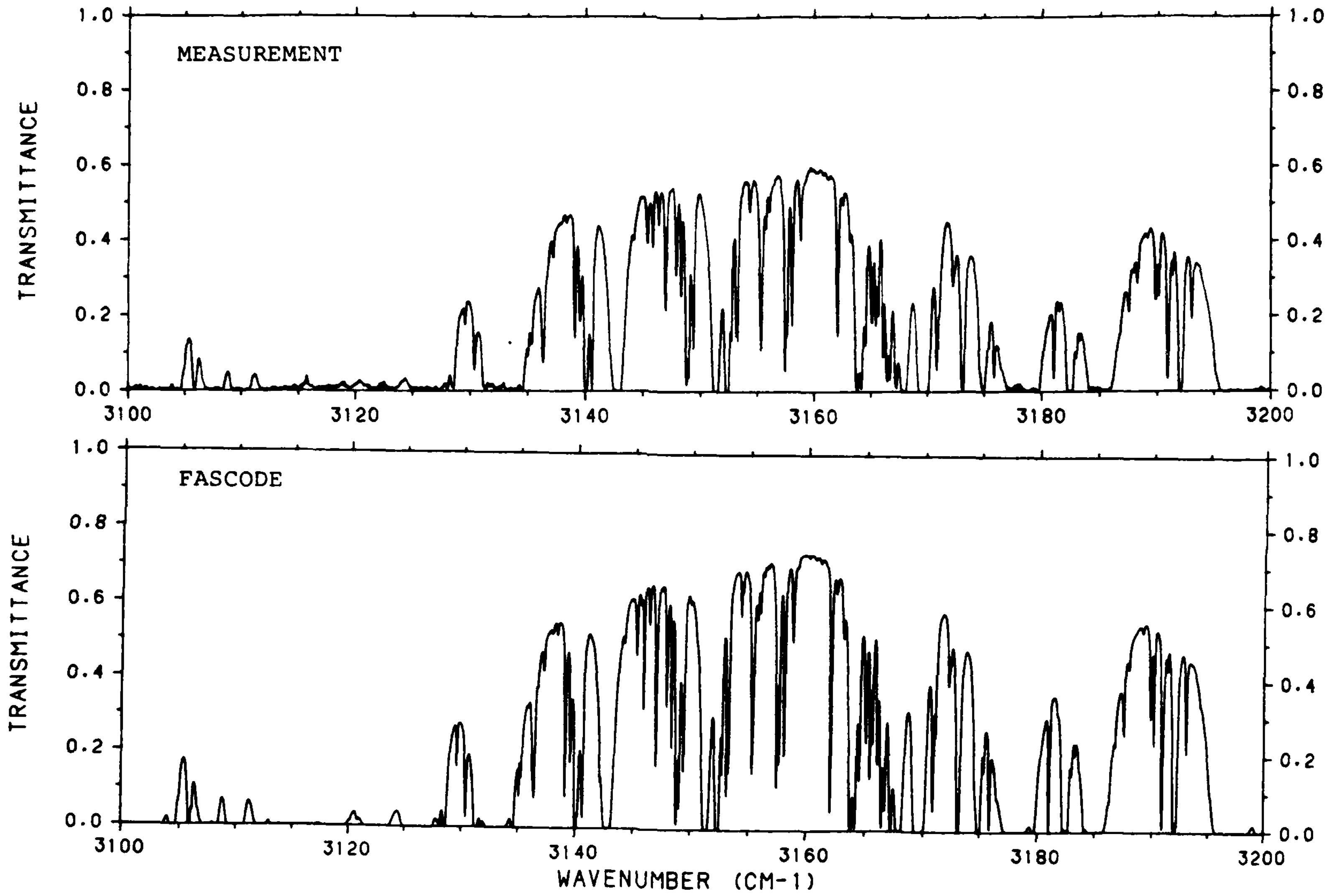

FIGURE 19m. SPECTRUM ASL06, 3100-3200 cm^{-1}: MEASURED (TOP) AND CALCULATED (BOTTOM).

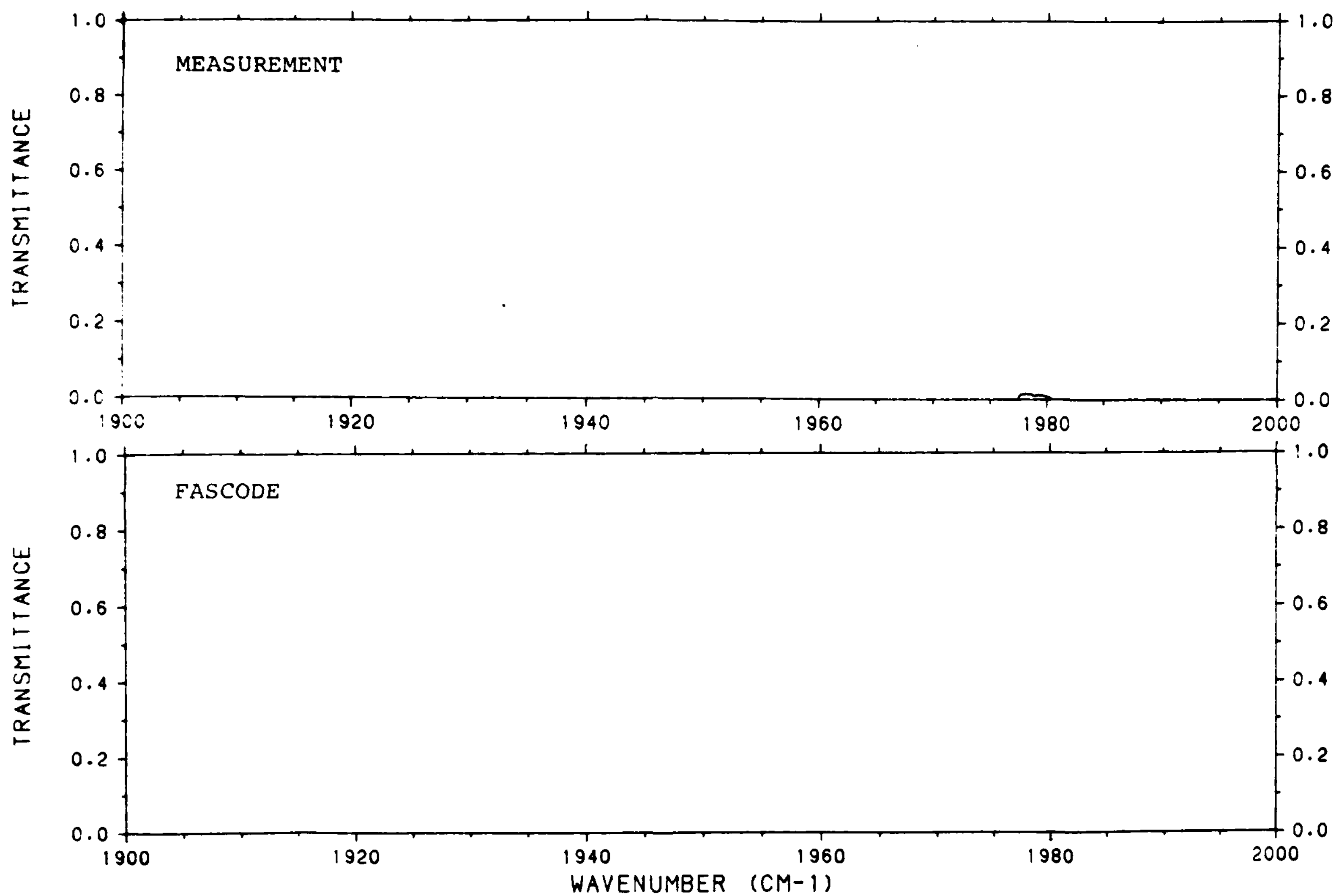

FIGURE 20a. SPECTRUM CC159, 1900-2000 cm^{-1}: MEASURED (TOP) AND CALCULATED (BOTTOM): 1016 Mb, 229.9 K, 21 TORR WATER VAPOR, 5.08 KM PATH, 35 KM VIS (NO AEROSOL IN CALCULATION).

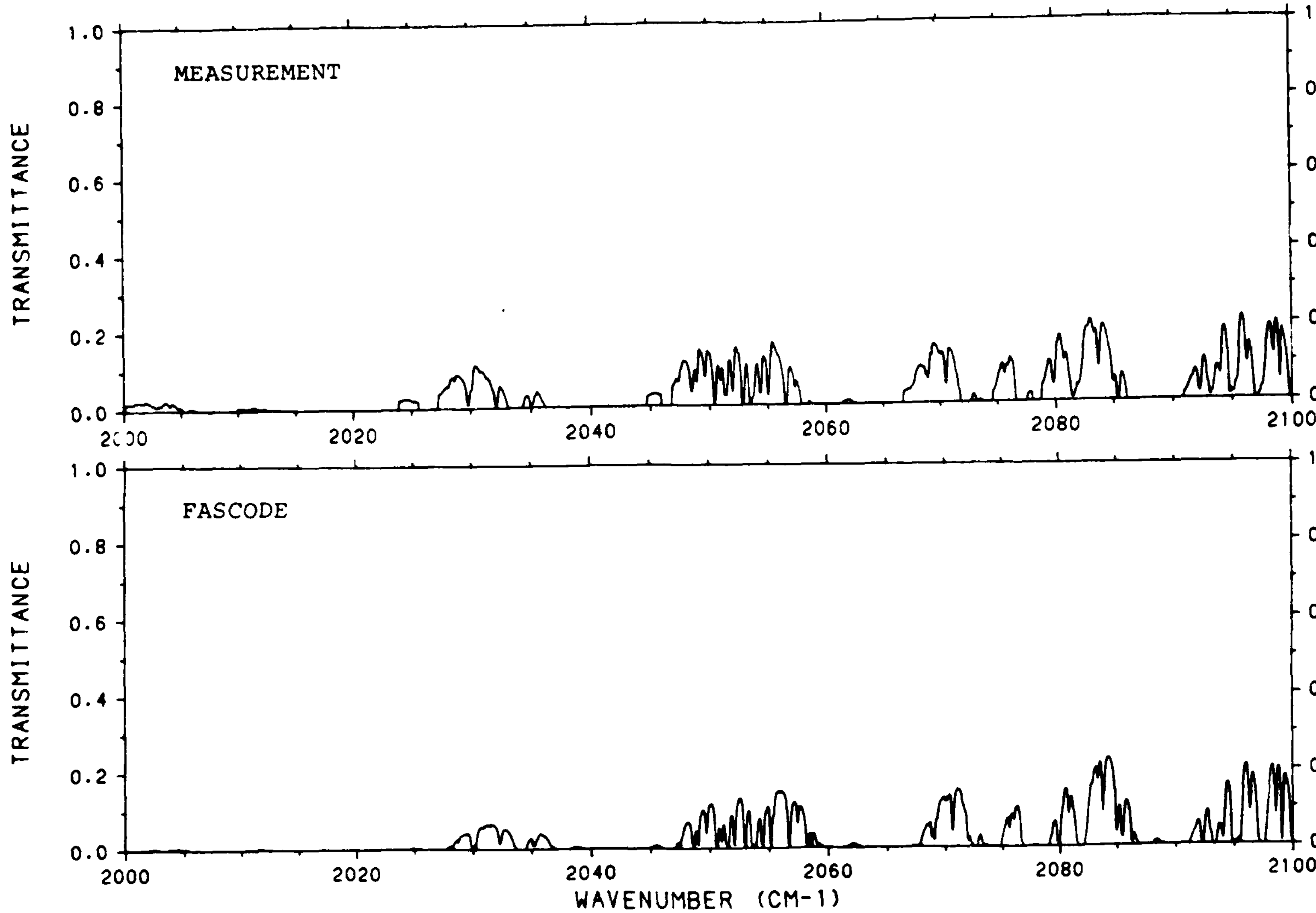

FIGURE 20b. SPECTRUM CC159, 2000-2100 cm^{-1}: MEASURED (TOP) AND CALCULATED (BOTTOM).

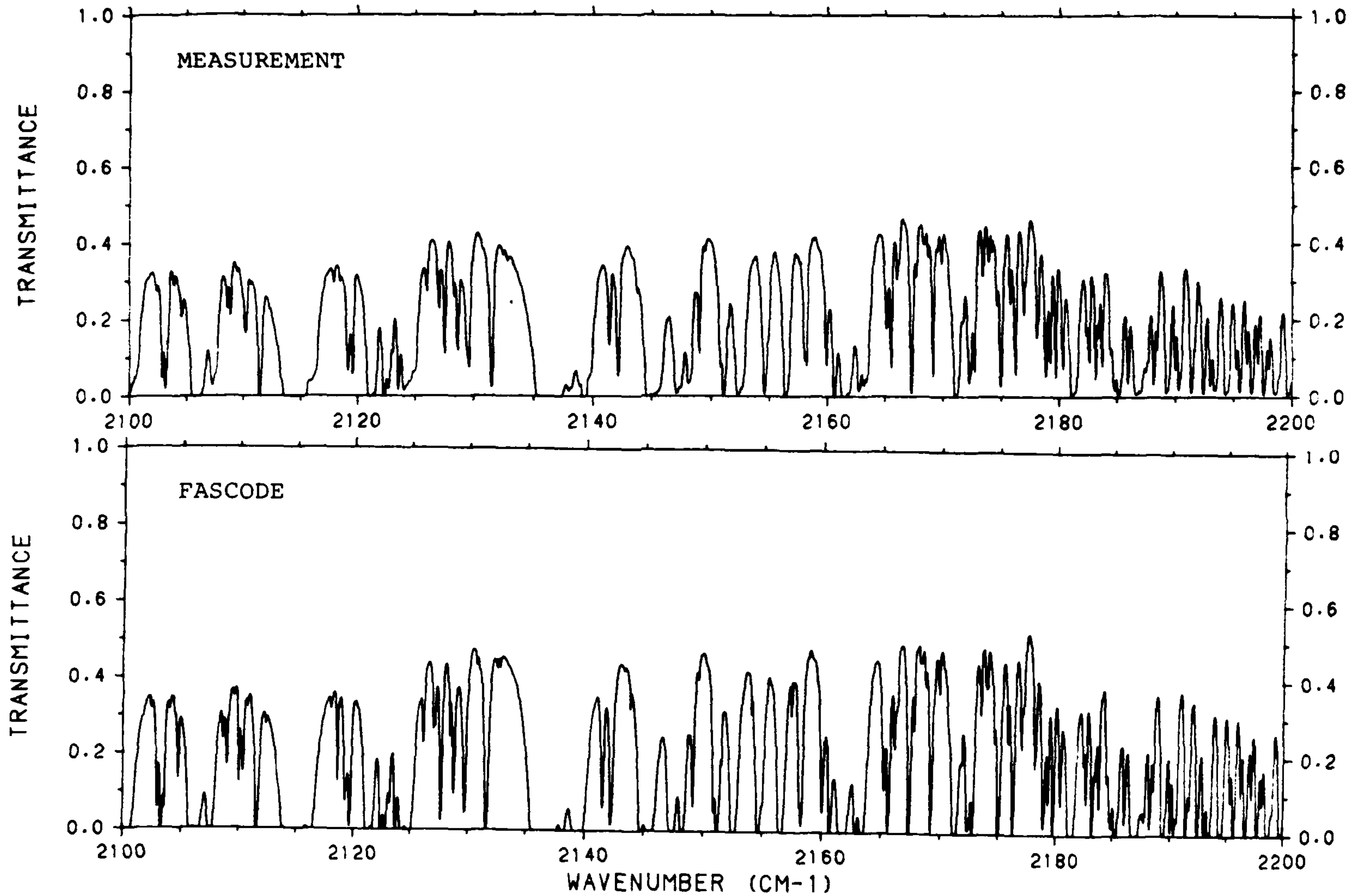

FIGURE 20c. SPECTRUM CC159, 2100-2200 cm^{-1}: MEASURED (TOP) AND CALCULATED (BOTTOM).

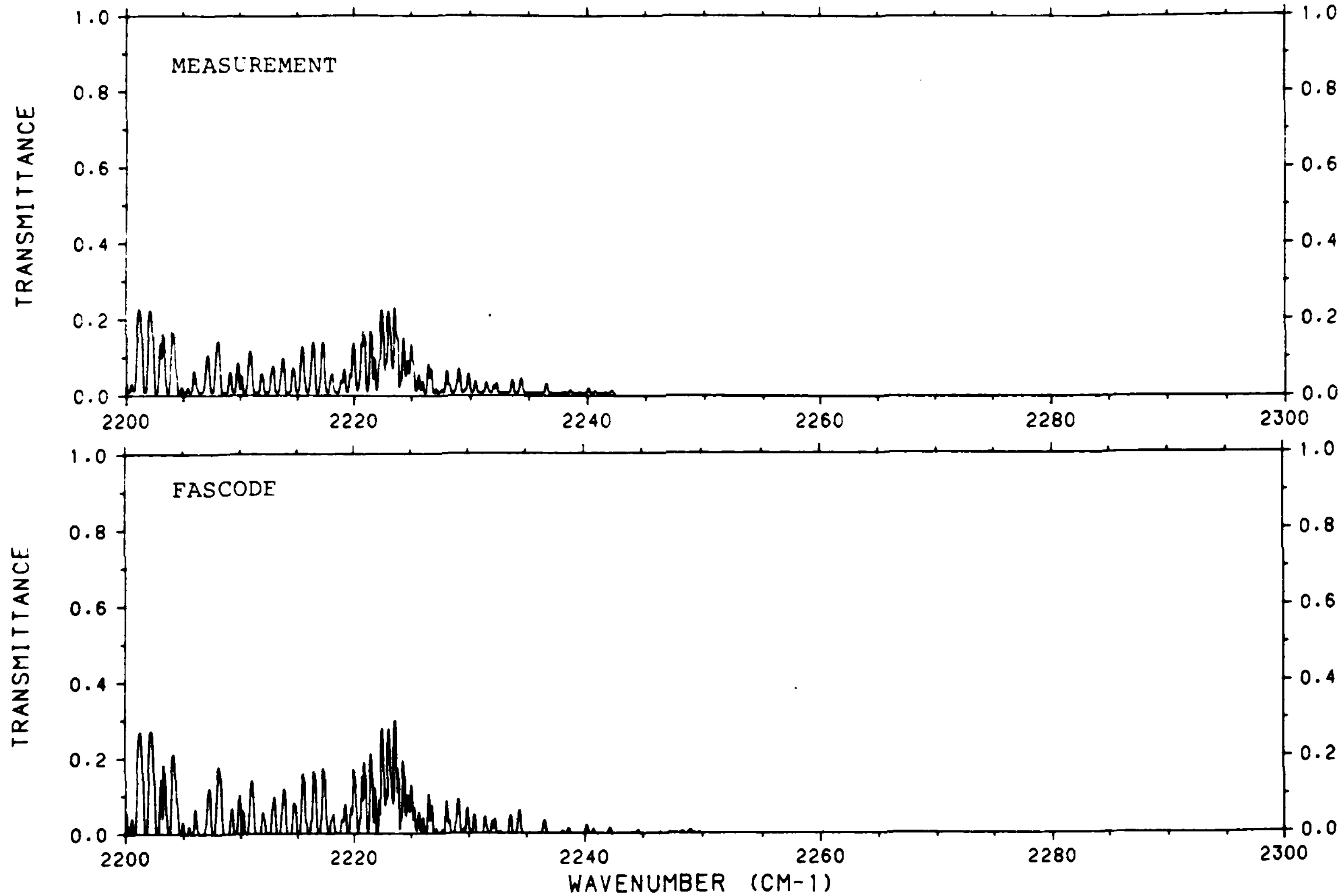

FIGURE 20d. SPECTRUM CC159, 2200-2300 cm^{-1}: MEASURED (TOP) AND CALCULATED (BOTTOM).

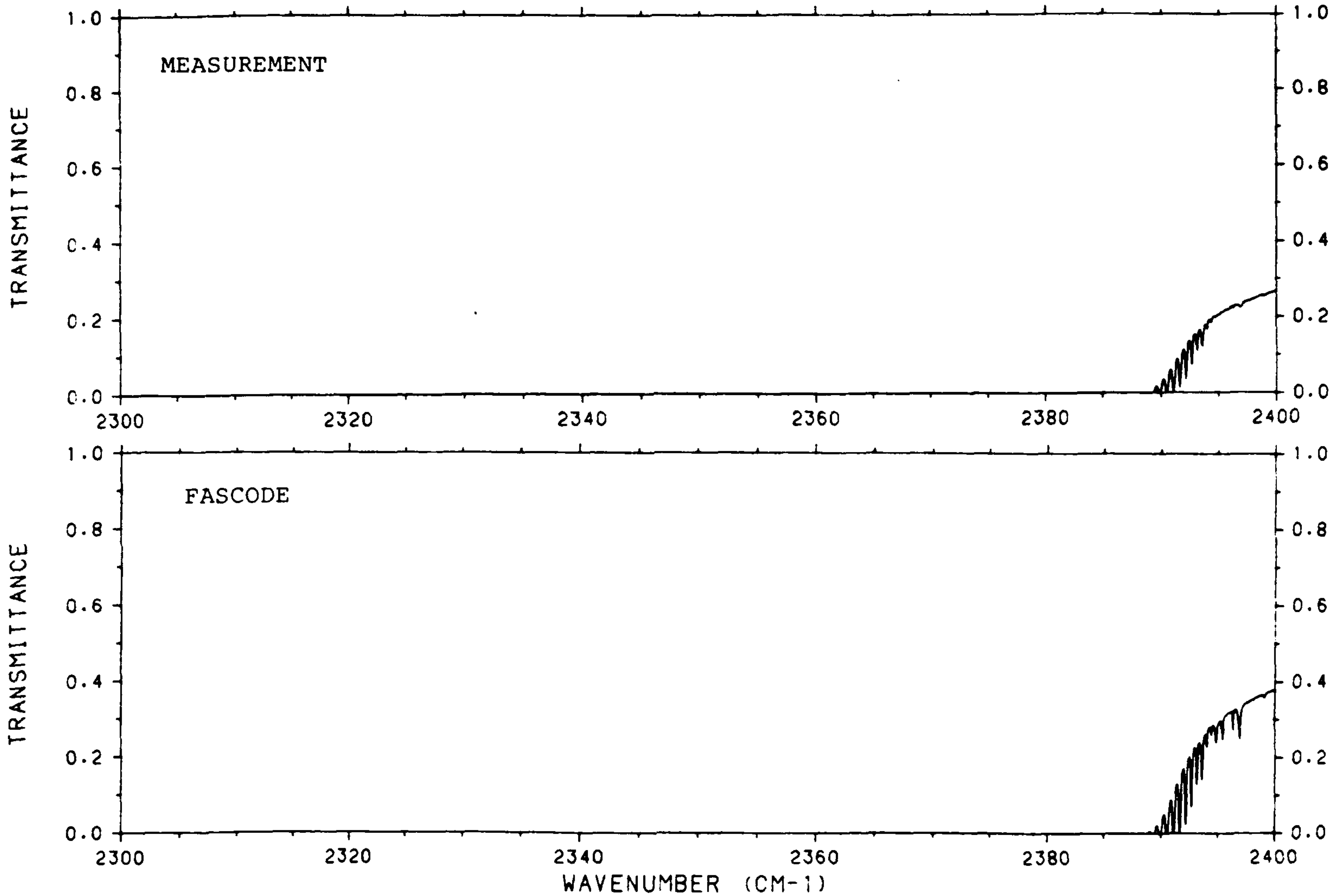

FIGURE 20e. SPECTRUM CC159, 2300-2400 cm^{-1}: MEASURED (TOP) AND CALCULATED (BOTTOM)

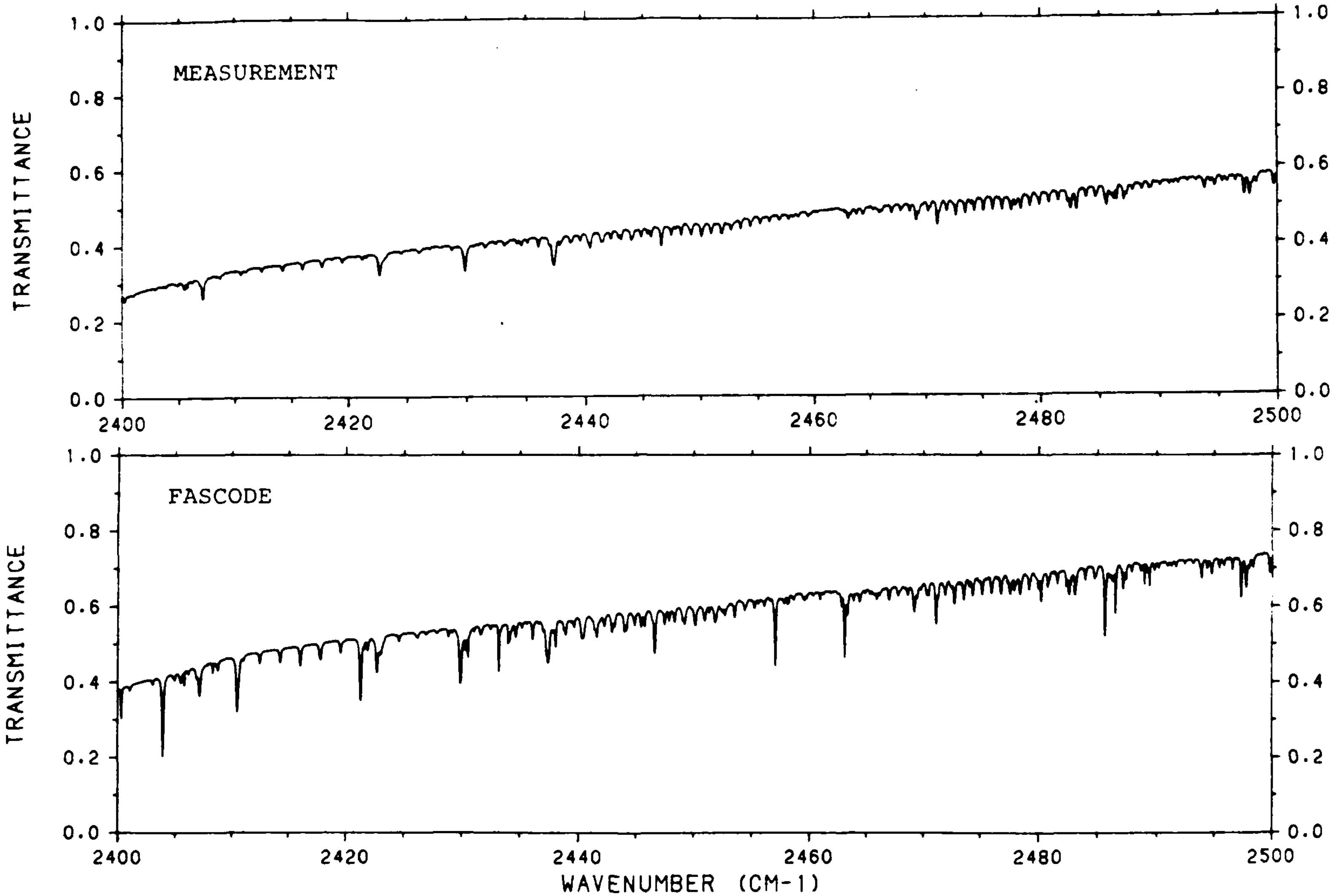

FIGURE 20f. SPECTRUM CC159, 2400-2500 cm^{-1}: MEASURED (TOP) AND CALCULATED (BOTTOM).

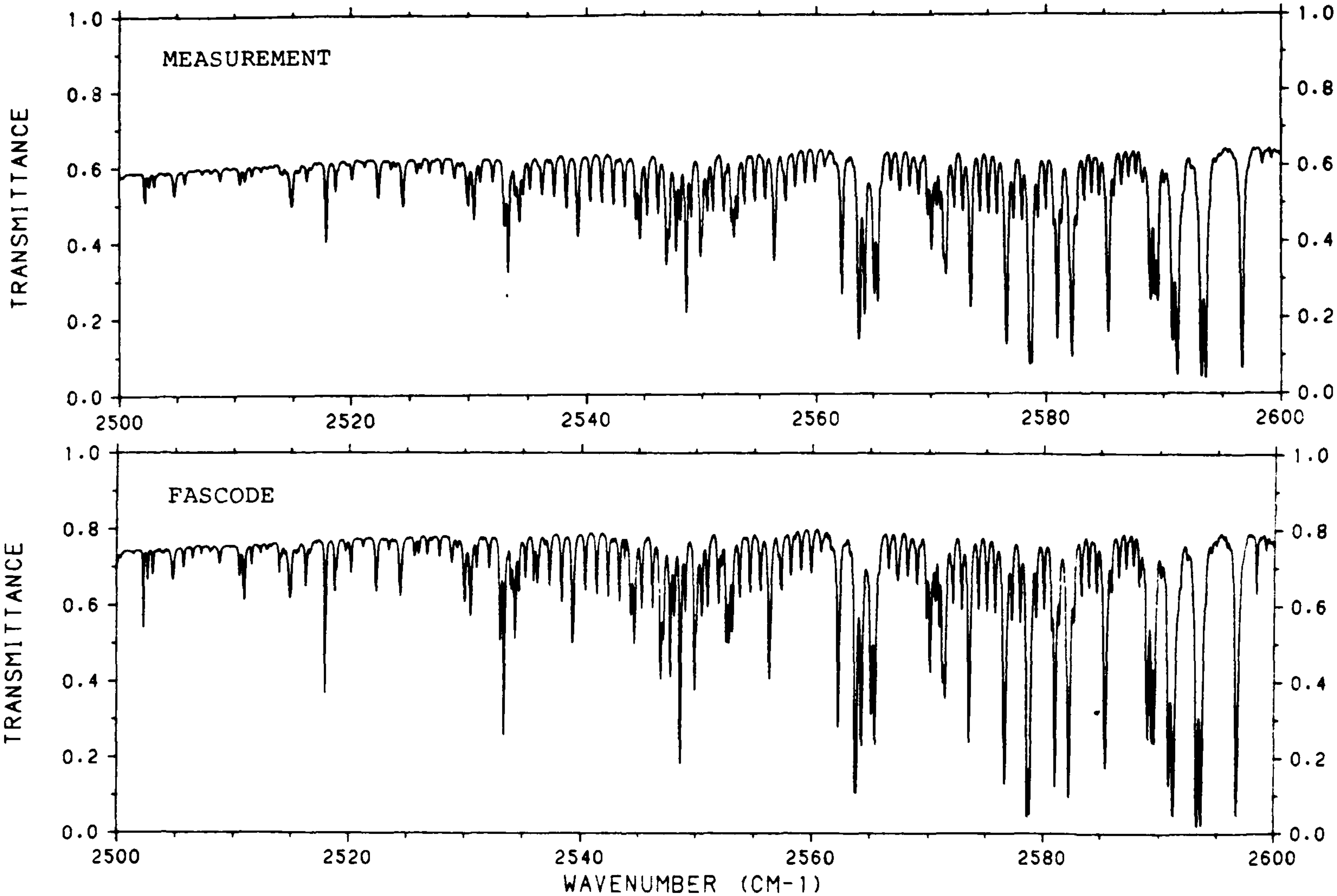

FIGURE 20g. SPECTRUM CC159, 2500-2600 cm^{-1}: MEASURED (TOP) AND CALCULATED (BOTTOM).

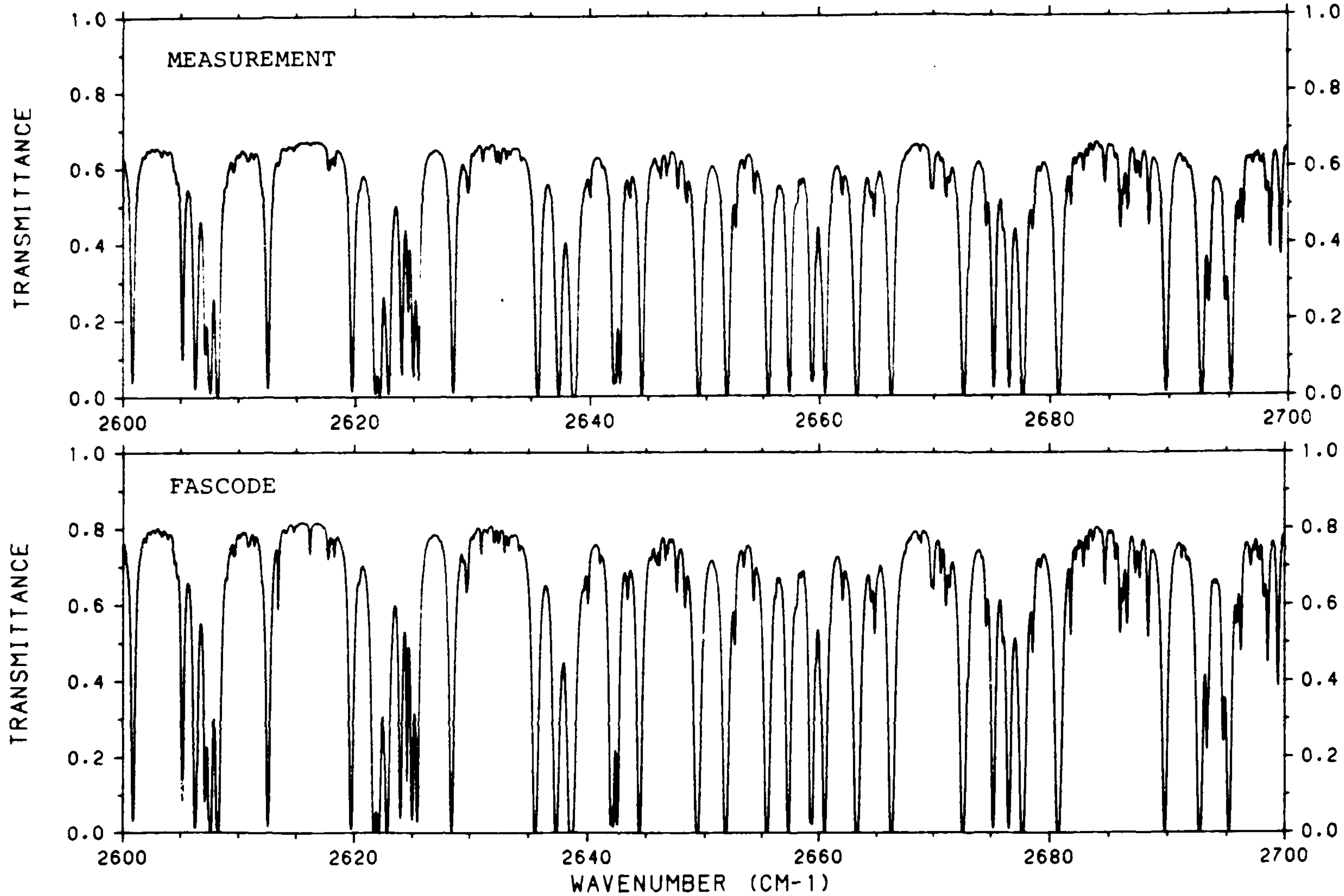

FIGURE 20h. SPECTRUM CC159, 2600-2700 cm^{-1}: MEASURED (TOP) AND CALCULATED (BOTTOM).

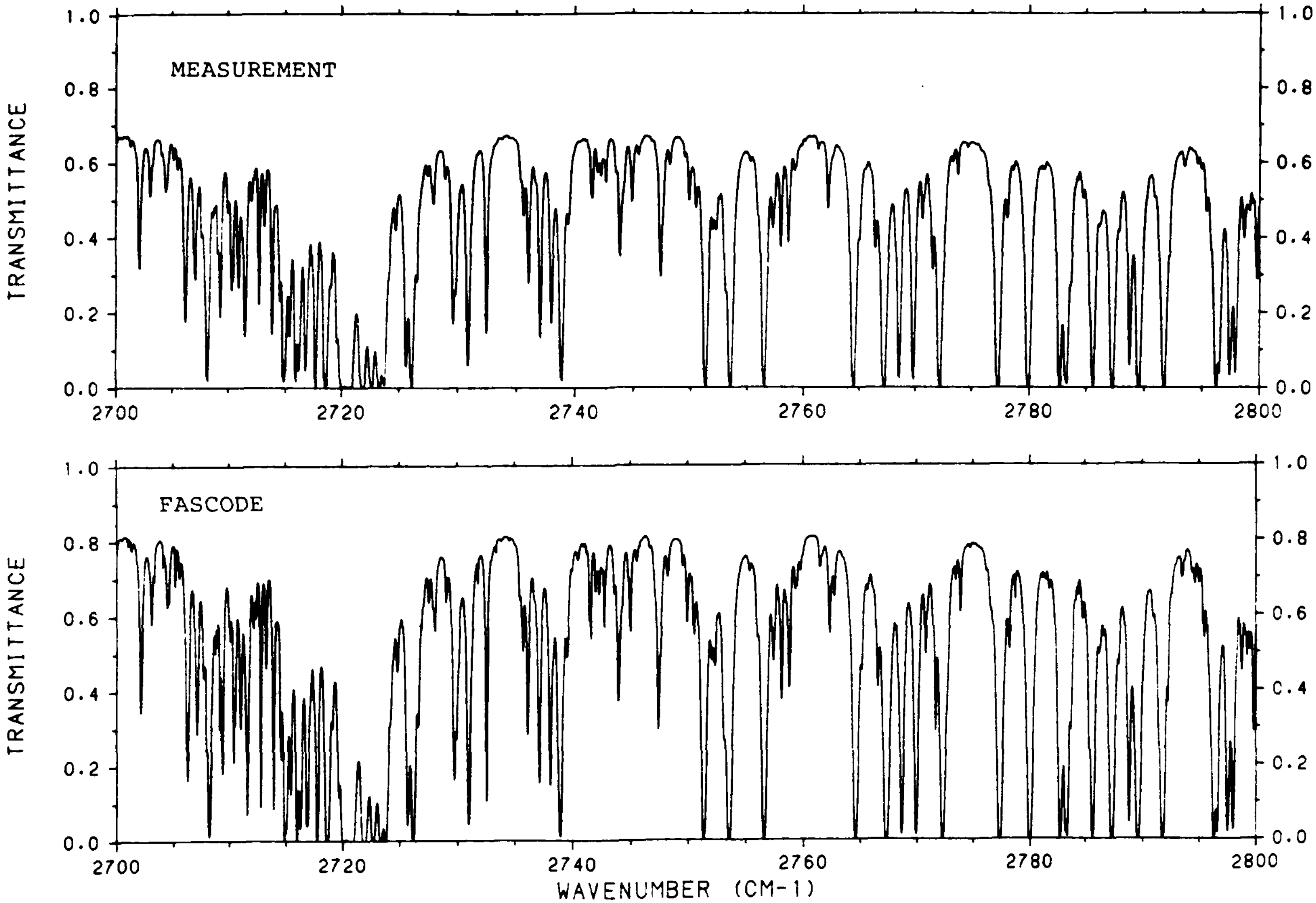

FIGURE 20i. SPECTRUM CC159, 2700-2800 cm^{-1}: MEASURED (TOP) AND CALCULATED (BOTTOM).

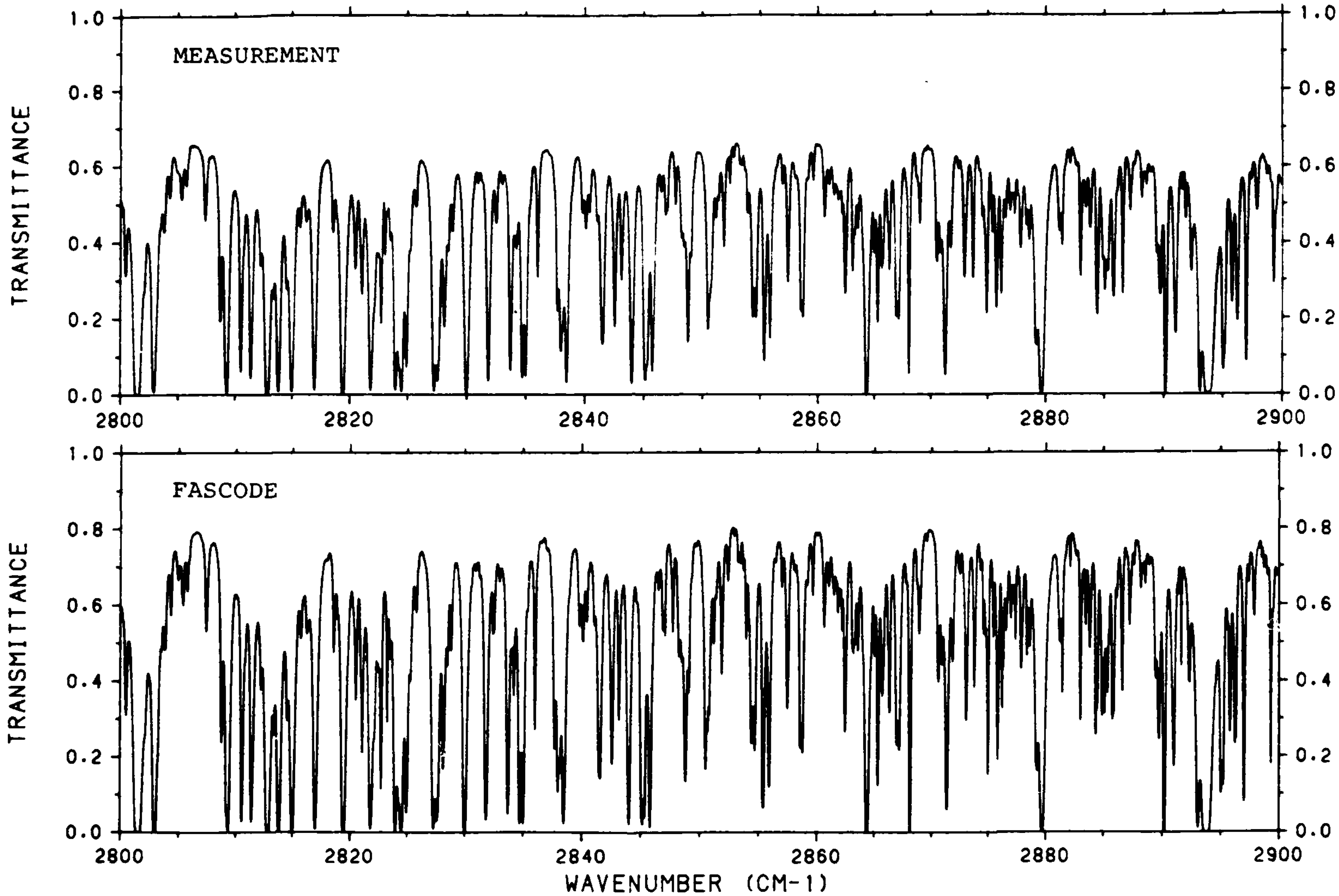

FIGURE 20j. SPECTRUM CC159, 2800-2900 cm^{-1}: MEASURED (TOP) AND CALCULATED (BOTTOM).

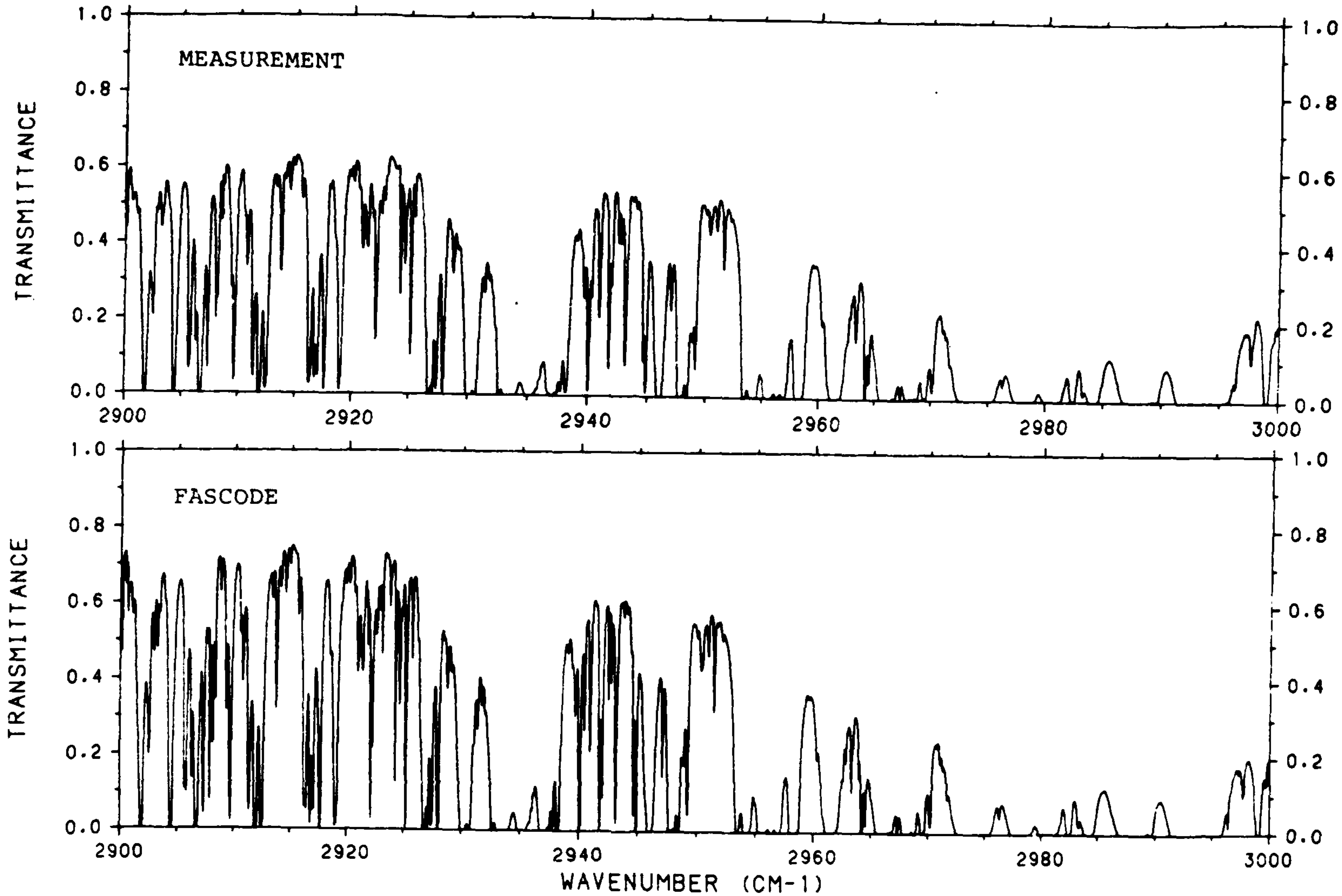

FIGURE 20k. SPECTRUM CC159, 2900-3000 cm^{-1}: MEASURED (TOP) AND CALCULATED (BOTTOM).

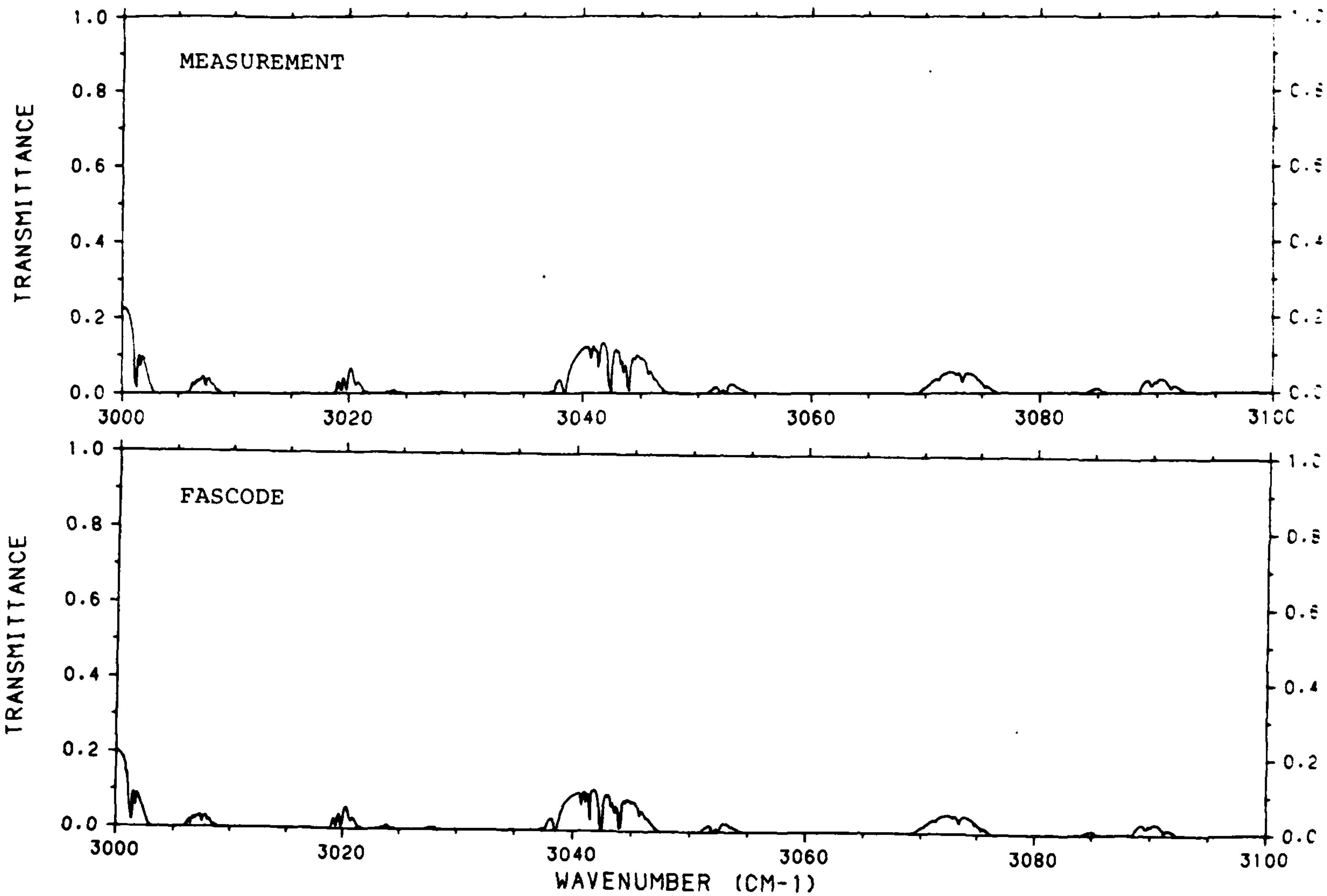

FIGURE 201. SPECTRUM CC159, 3000-3100 cm^{-1}: MEASURED (TOP) AND CALCULATED BOTTOM).

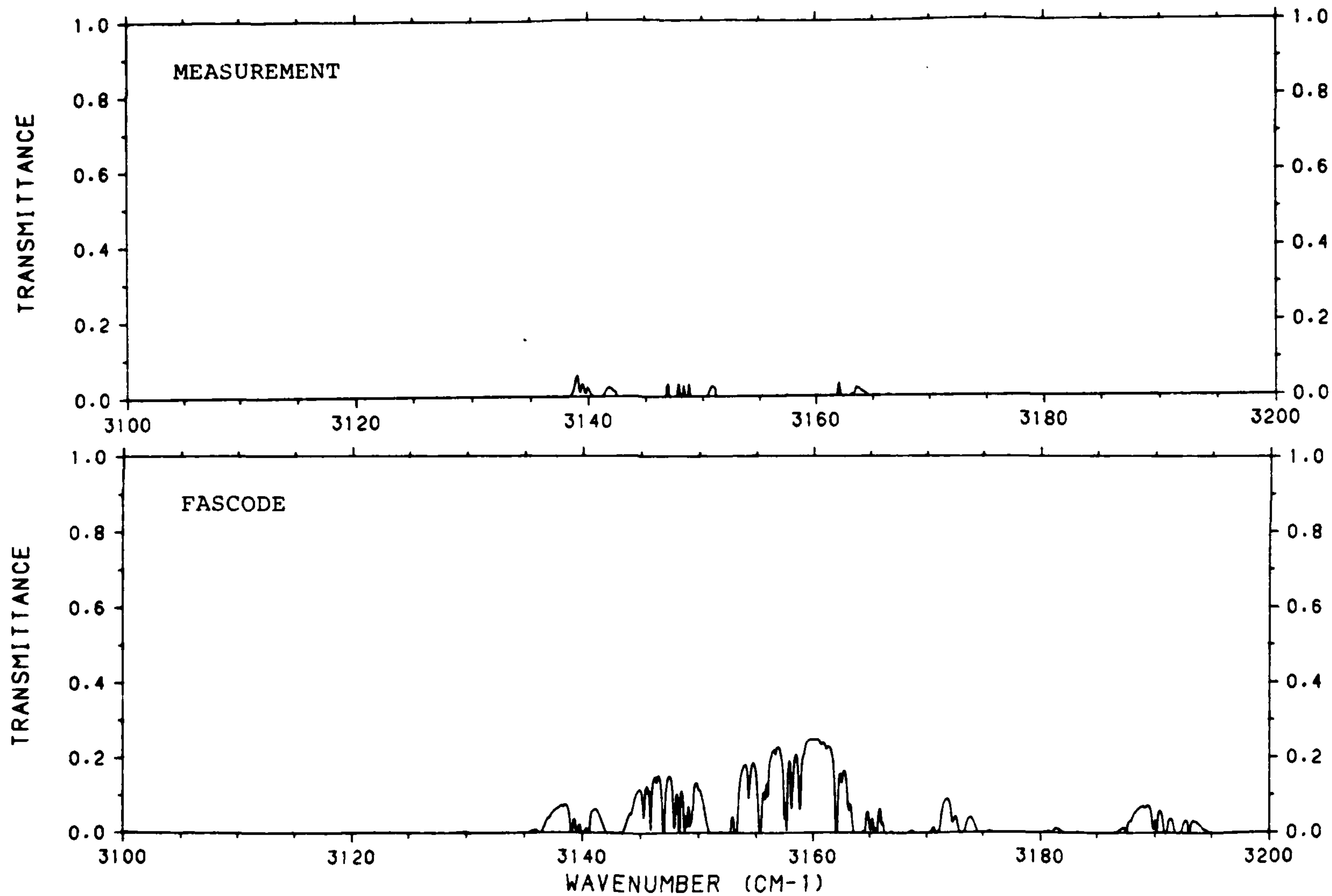

FIGURE 20m. SPECTRUM CC159, 3100-3200 cm^{-1}: MEASURED (TOP) AND CALCULATED (BOTTOM).

calculation, for example, at 1917 cm^{-1} and 1942 cm^{-1}. These features are apparently not real : they are not seen in other high resolution atmospheric spectra under similar conditions, for example, Figure 21, shows a spectrum which was taken at Kitt Peak [18]. This measurement was made at a resolution of about 0.02 cm^{-1} and contains about the same amount of total air in the path as spectrum ASL06 (about 1 air mass) but much less water vapor. These artifacts are also not seen in the measured spectra CC154.

The exact cause of the artifacts is not known. However the positions of these features correspond one-to-one with the positions of strong water vapor lines listed on the AFGL Line Tape. One possible explanation for these features is that they are somehow generated in the calibration procedure when ratioing a long path spectrum to a "zero path" one. Here the source and receiver optical system were separated by about 30 meters. The transmittance measured over this short path is used to normalize the long path transmittance. Strong absorption by these lines over the short path could generate these features in the normalized spectra due to lack of numerical precision in the ratioing of two small numbers which is performed in the normalization procedure.

3.2.2 ESTIMATES OF LINE STRENGTHS FOR WATER VAPOR ABSORPTION LINES IN THE 2390 CM^{-1} TO 2500 CM^{-1} SPECTRAL REGION

There are a number of molecular absorption lines of water vapor between 2390 cm^{-1} to 2500 cm^{-1} whose strengths in the 1982 edition of the AFGL Atmospheric Absorption Line Parameter Compilation [9] are too large. These lines are seen marked by arrows in Figure 22, which is a comparison between the measured spectra CC154 and a FASCODE calculation using the 1982 version of the AFGL Line Compilation. The lines due to water vapor are marked by arrows. Some of these lines stand out clearly in the calculated spectrum but

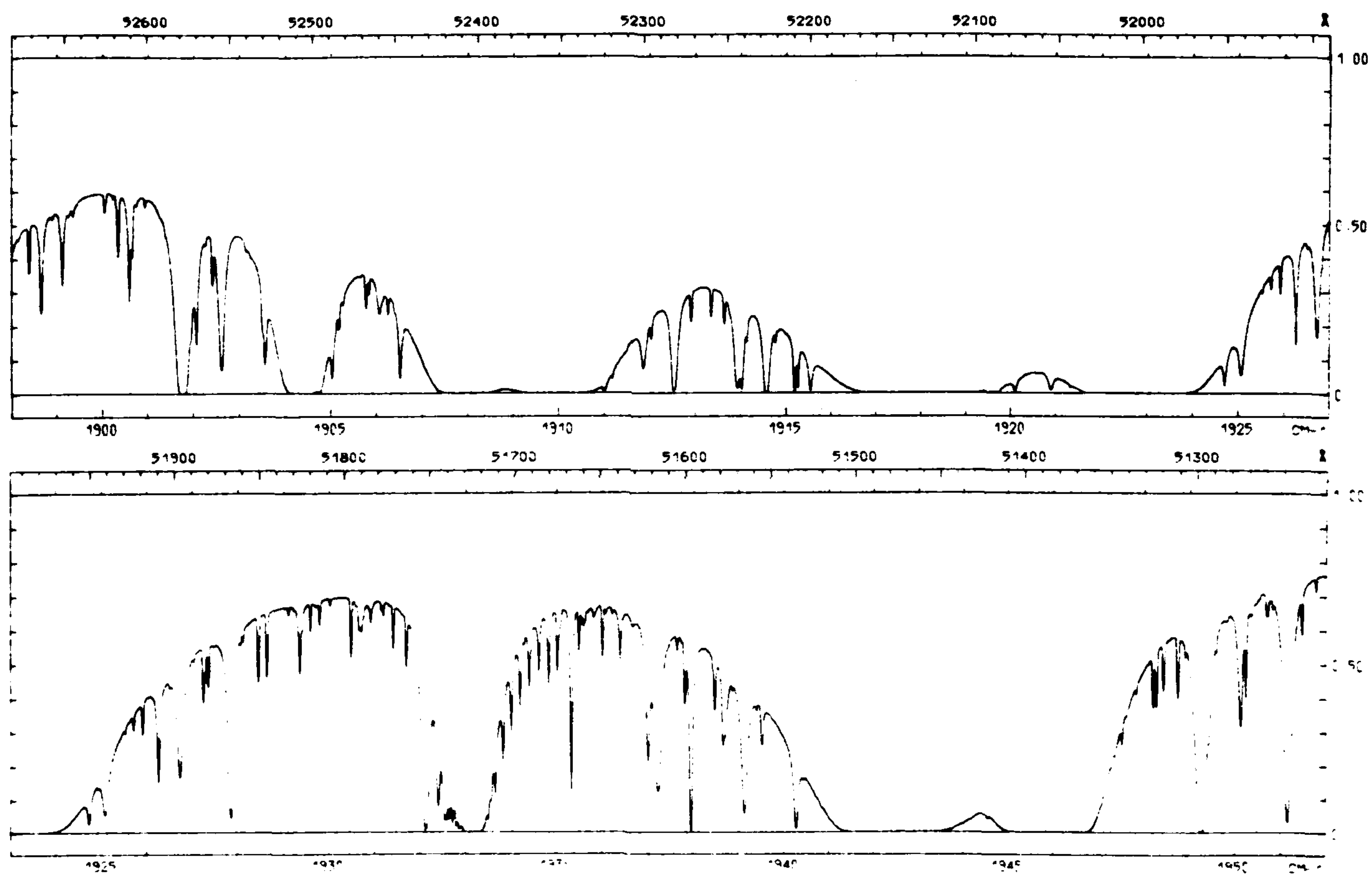

FIGURE 21. ATMOSPHERIC ABSORPTION SPECTRUM FOR 1900-1950 cm^{-1}. MEASURED AT KITT PEAK OBSERVATORY; MEASUREMENT CONDITIONS INCLUDE 0.02 cm^{-1} RESOLUTION, 1.1 AIR-MASS PATH, 0.8 grm cm^{-2} WATER VAPOR ALONG THE PATH; TAKEN FROM [18].

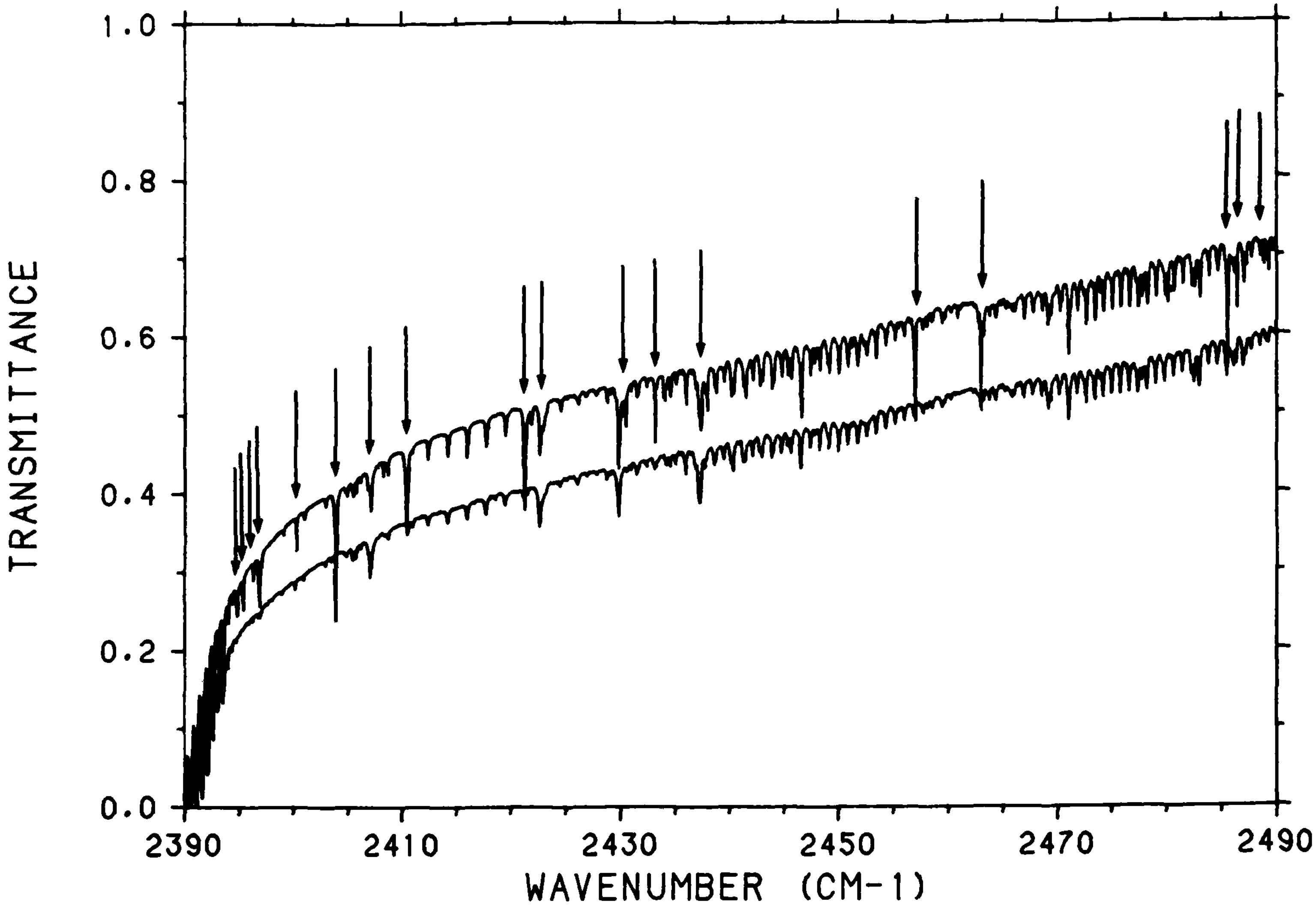

FIGURE 22. MEASURED SPECTRUM CC154 (BOTTOM), AND FASCODE (TOP) CALCULATION. ARROWS POINT TO WATER VAPOR LINES.

are much weaker or completely absent in the measurement. Figure 23 shows separately the 1 cm^{-1} region around each of the marked lines and include the measured spectrum CC154 and FASCODE calculations using both the 1982 version of the AFGL Line Compilation (solid line) and the 1980 version (dashed line). There are several points which can be made concerning these comparisons:

1. The calculations are monochromatic while the measurement includes the effect of a sinc instrument function with a half width at half height of 0.018 cm^{-1}. The widths of some of these water lines are as small as 0.01 cm^{-1} so that these narrow lines are somewhat degraded in the measured spectra.

2. Due to the lack of aerosol extinction in the calculation, the measured lines ride on lower background transmittances than the calculation, so that even if the calculated lines were of the proper strength, the calculated lines would appear deeper (in transmittance) than the measured.

3. The strengths for these lines were revised for the 1980 version of the AFGL Line Compilation. In most cases the strengths were increased. When it was realized that these revised strengths were too large compared to measurements, the earlier line strength values from the 1978 compilation were used again for the 1982 compilation.

4. There is a small systematic error in the wavenumber scale of the measured spectrum as determined by comparison with accurately known N_2O lines around 2450 cm^{-1}. This error has been corrected in the plots as shown in Figure 22.

From the plots in Figure 22 it is possible to estimate the strength of the measured lines relative to the calculated values. This was done by comparing the depths of the absorption line at the line center relative to the local background between the measured and the calculated lines

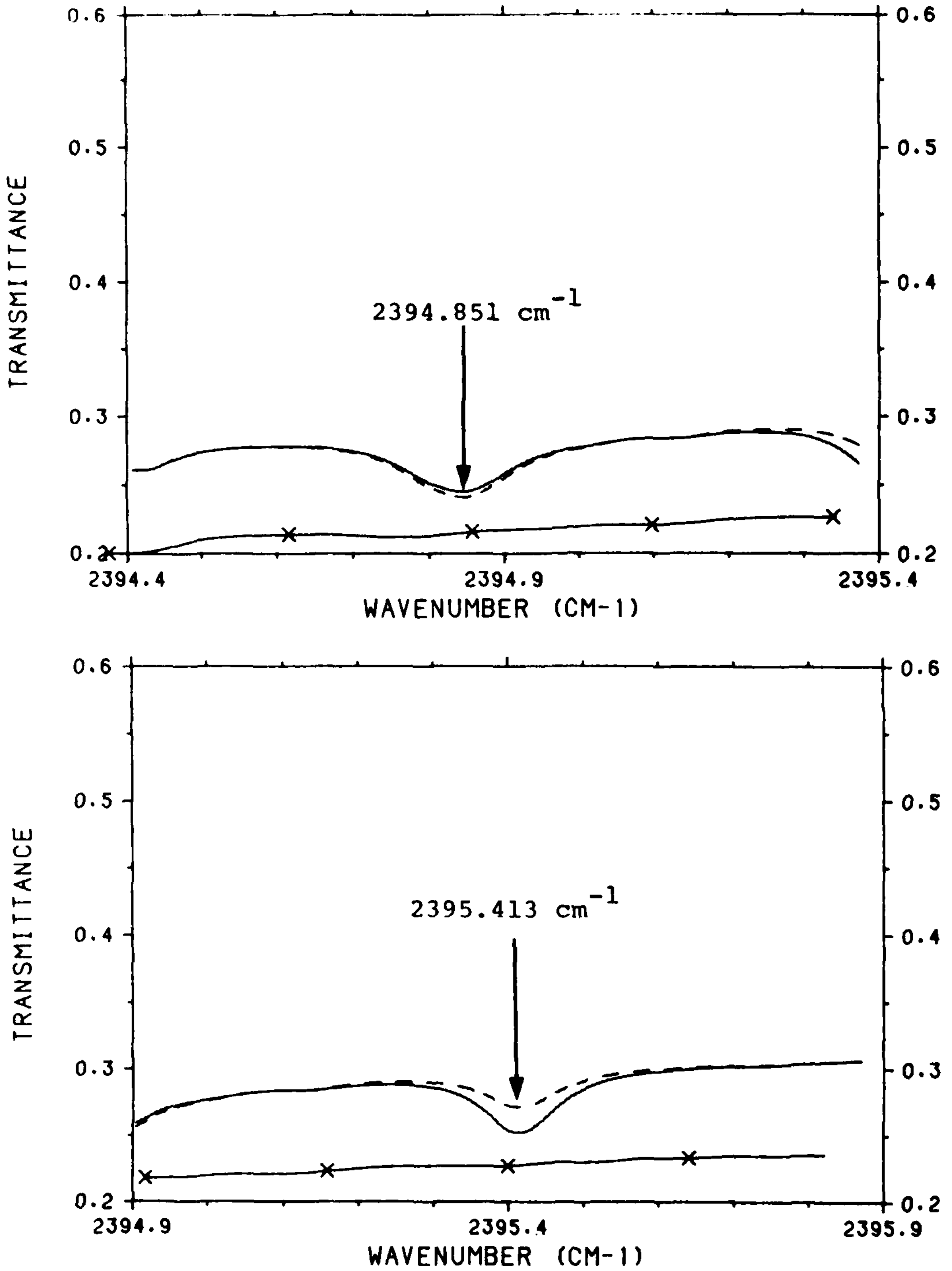

FIGURE 23. MEASURED SPECTRUM CC154 (SYMBOLS) AND FASCODE CALCULATION WITH AFGL LINE TAPE, 1982 VERSION (SOLID LINE) AND 1980 VERSION (DASHED LINE). ARROW POINTS TO CENTER OF WATER VAPOR LINE.

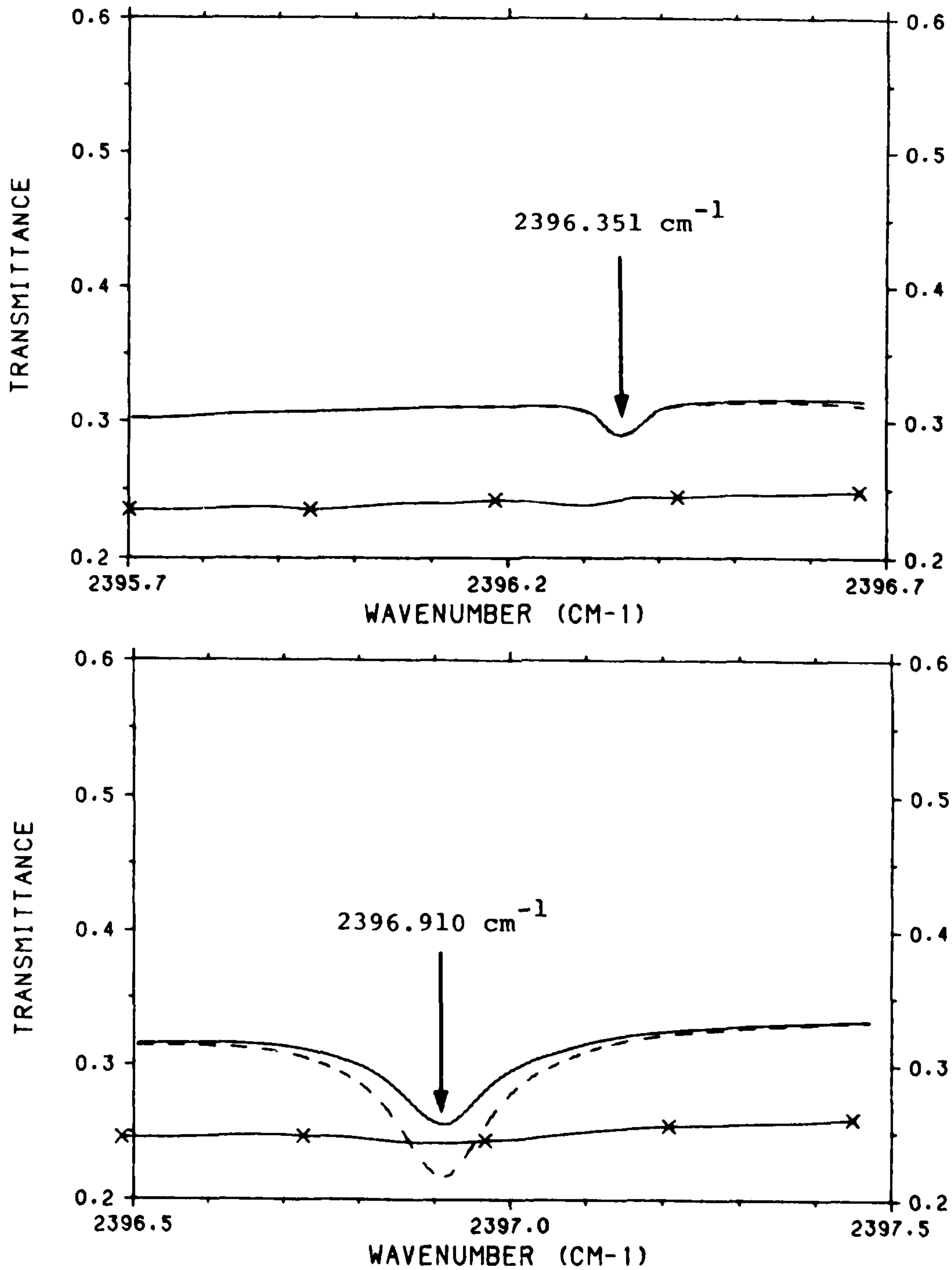

FIGURE 23. (CONTINUED).

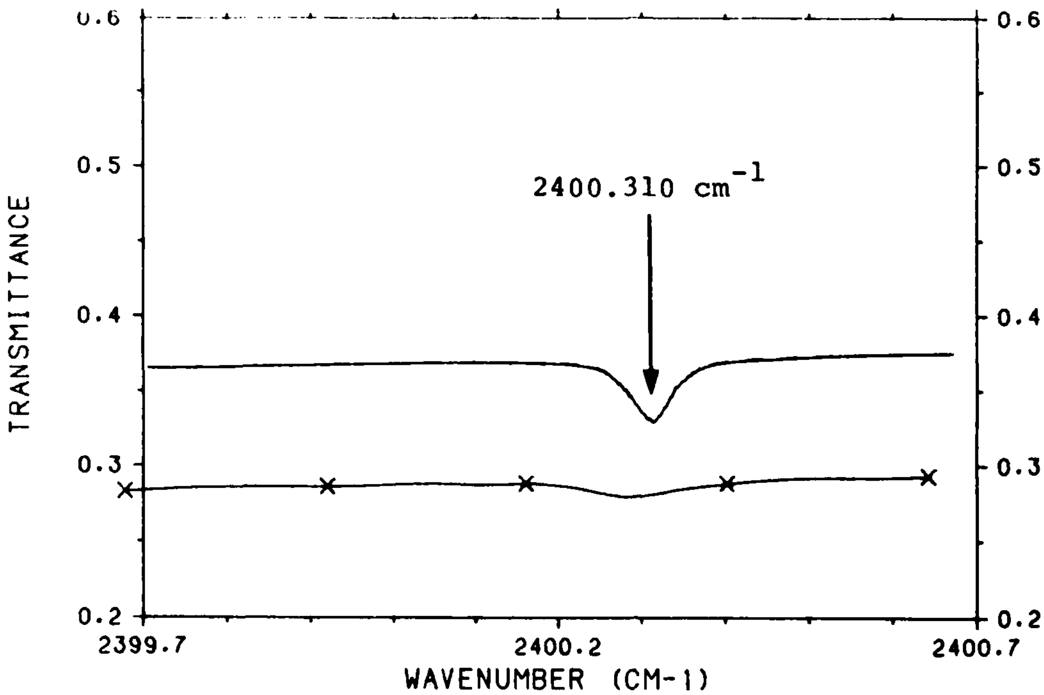

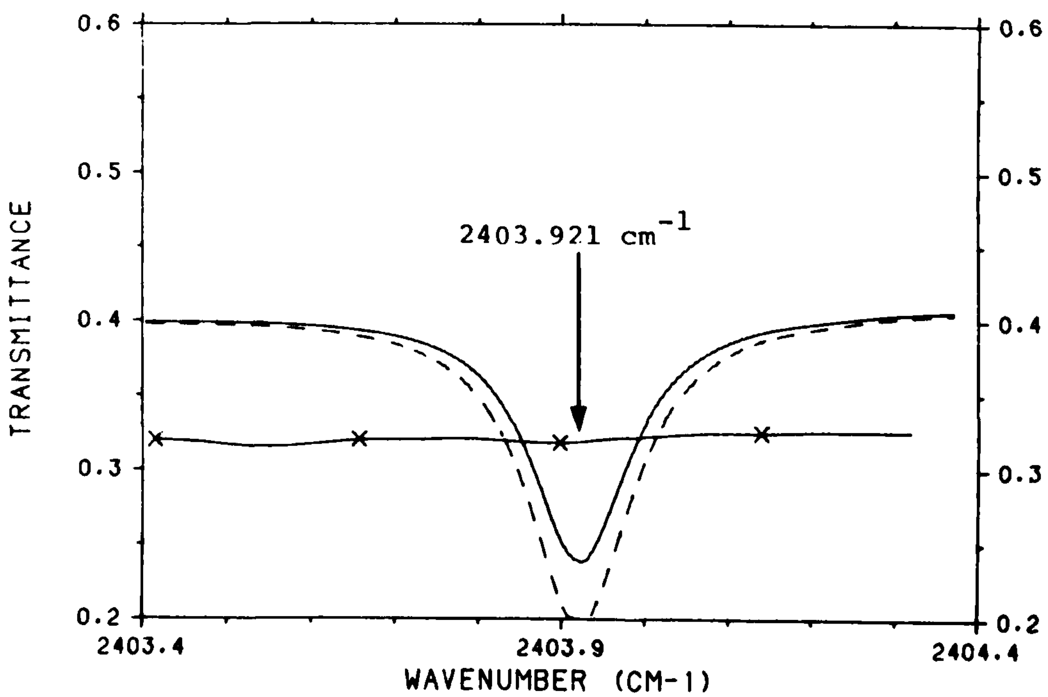

FIGURE 23. (CONTINUED).

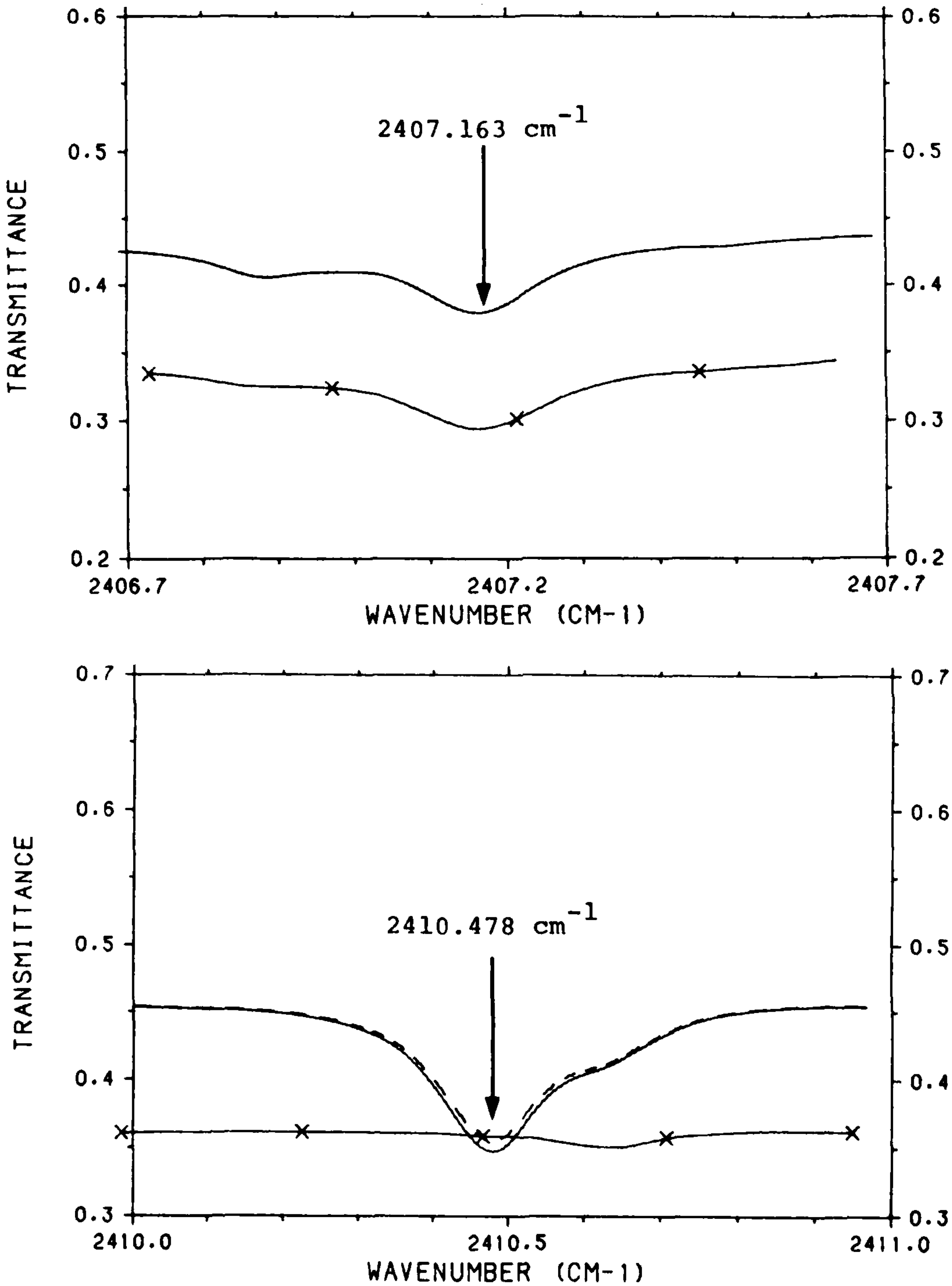

FIGURE 23. (CONTINUED).

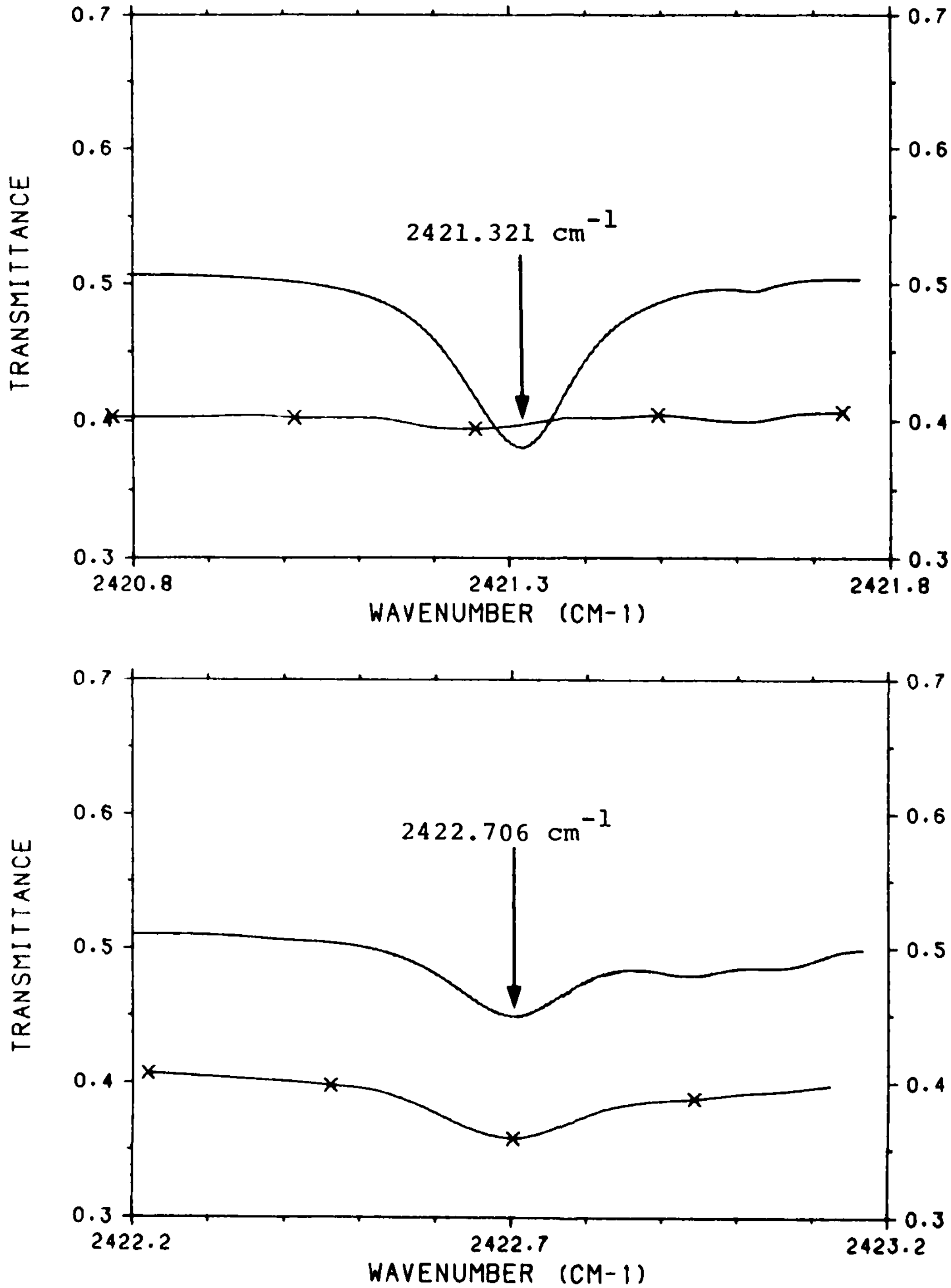

FIGURE 23. (CONTINUED).

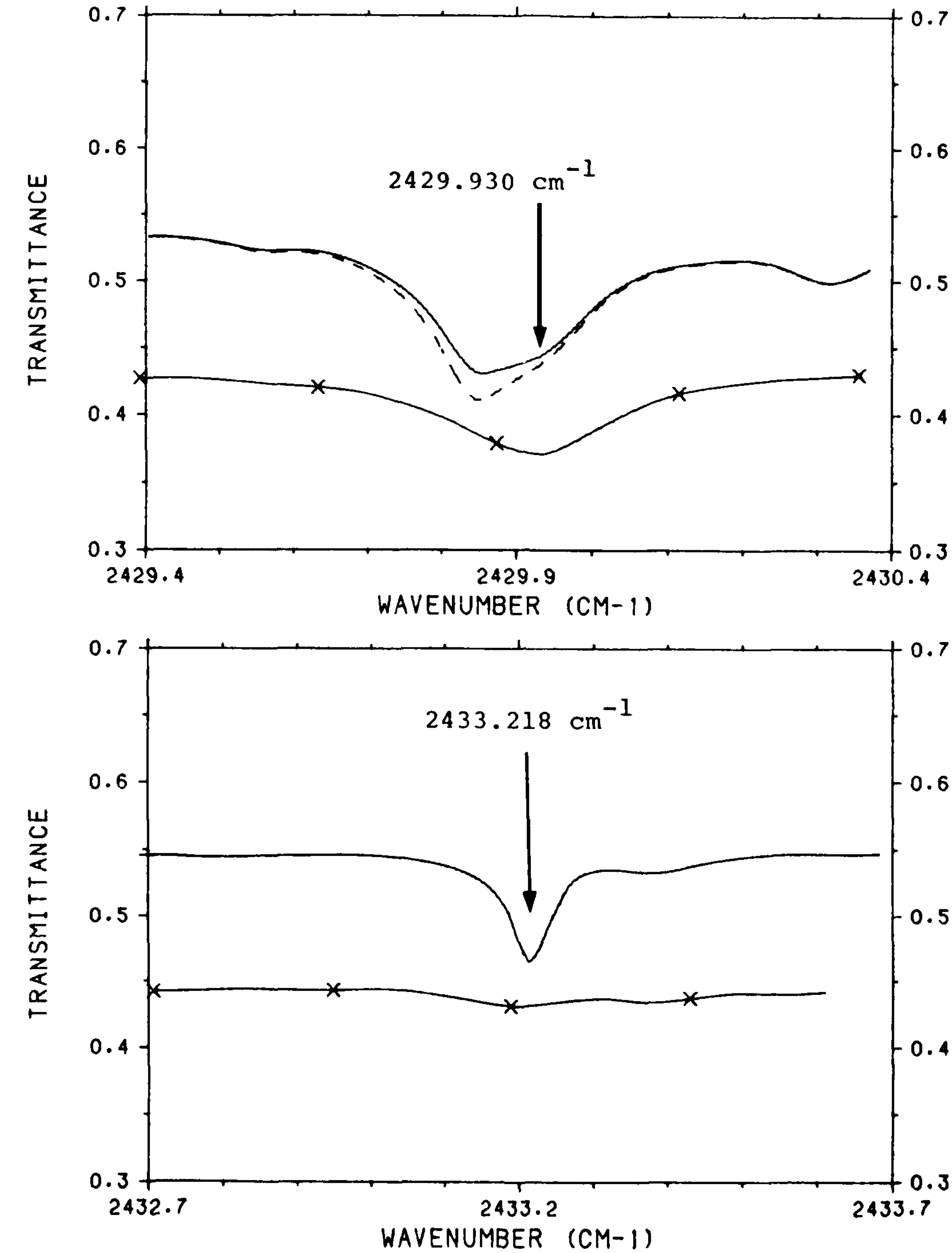

FIGURE 23. (CONTINUED).

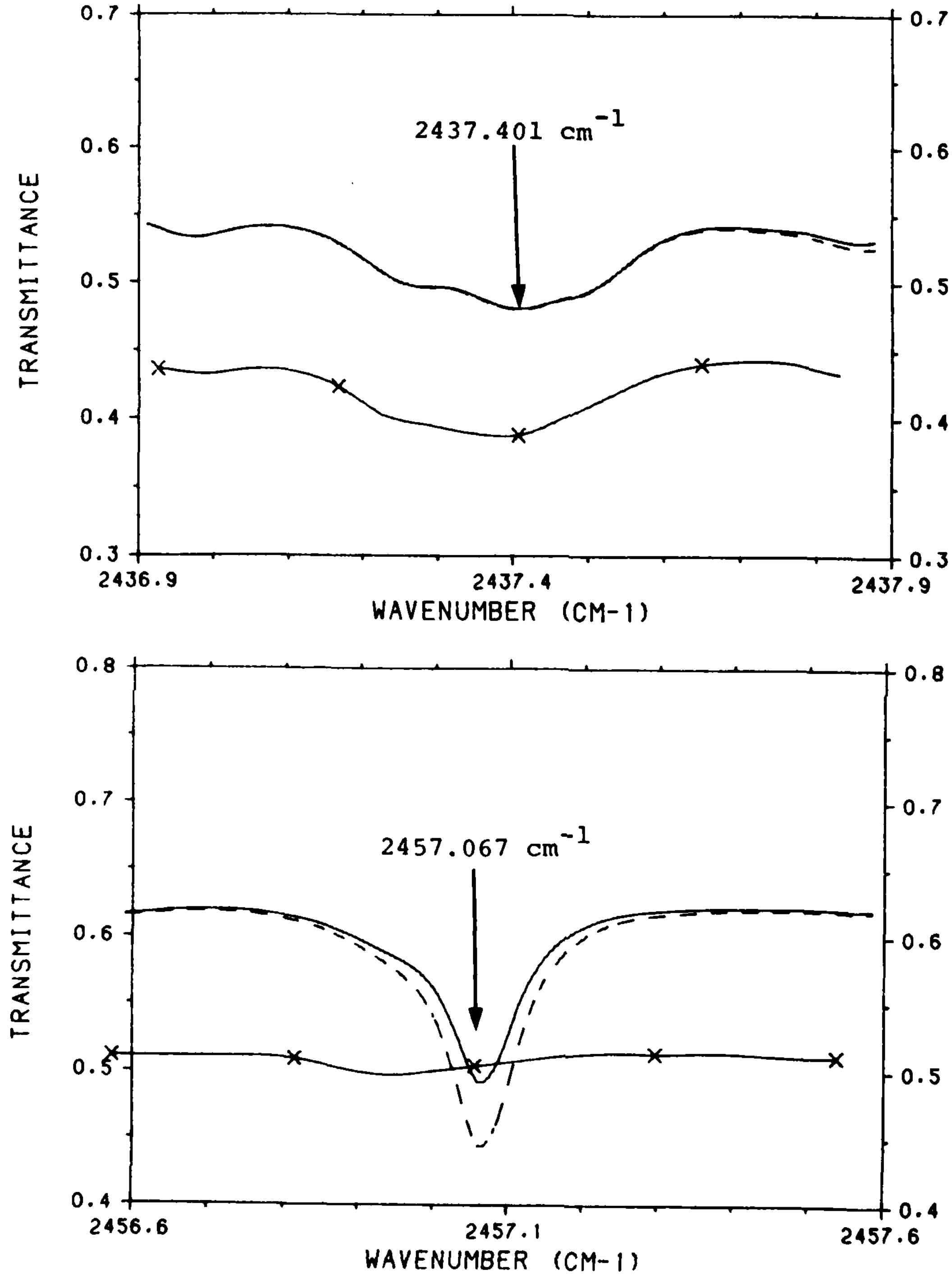

FIGURE 23. (CONTINUED).

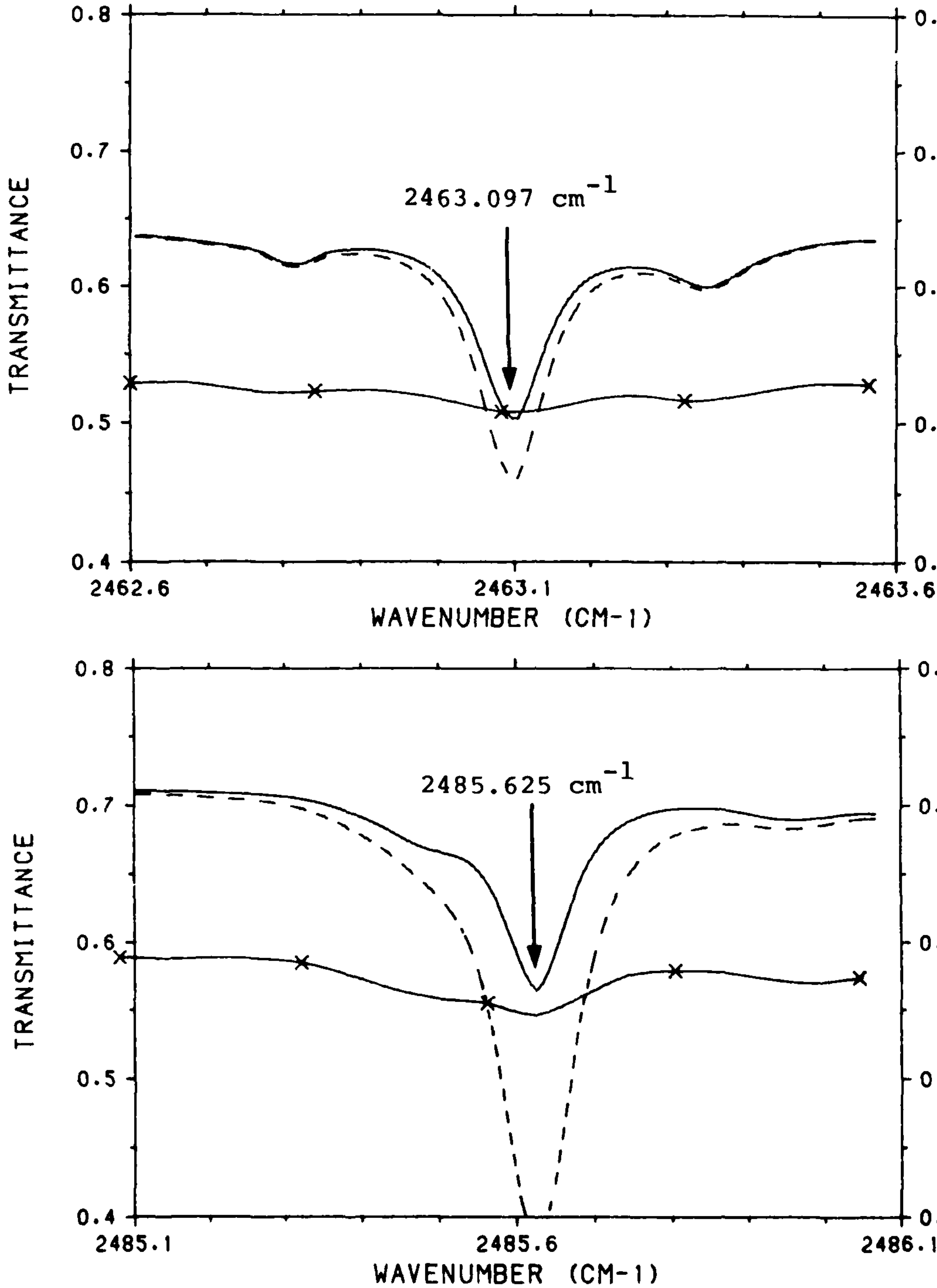

FIGURE 23. (CONTINUED).

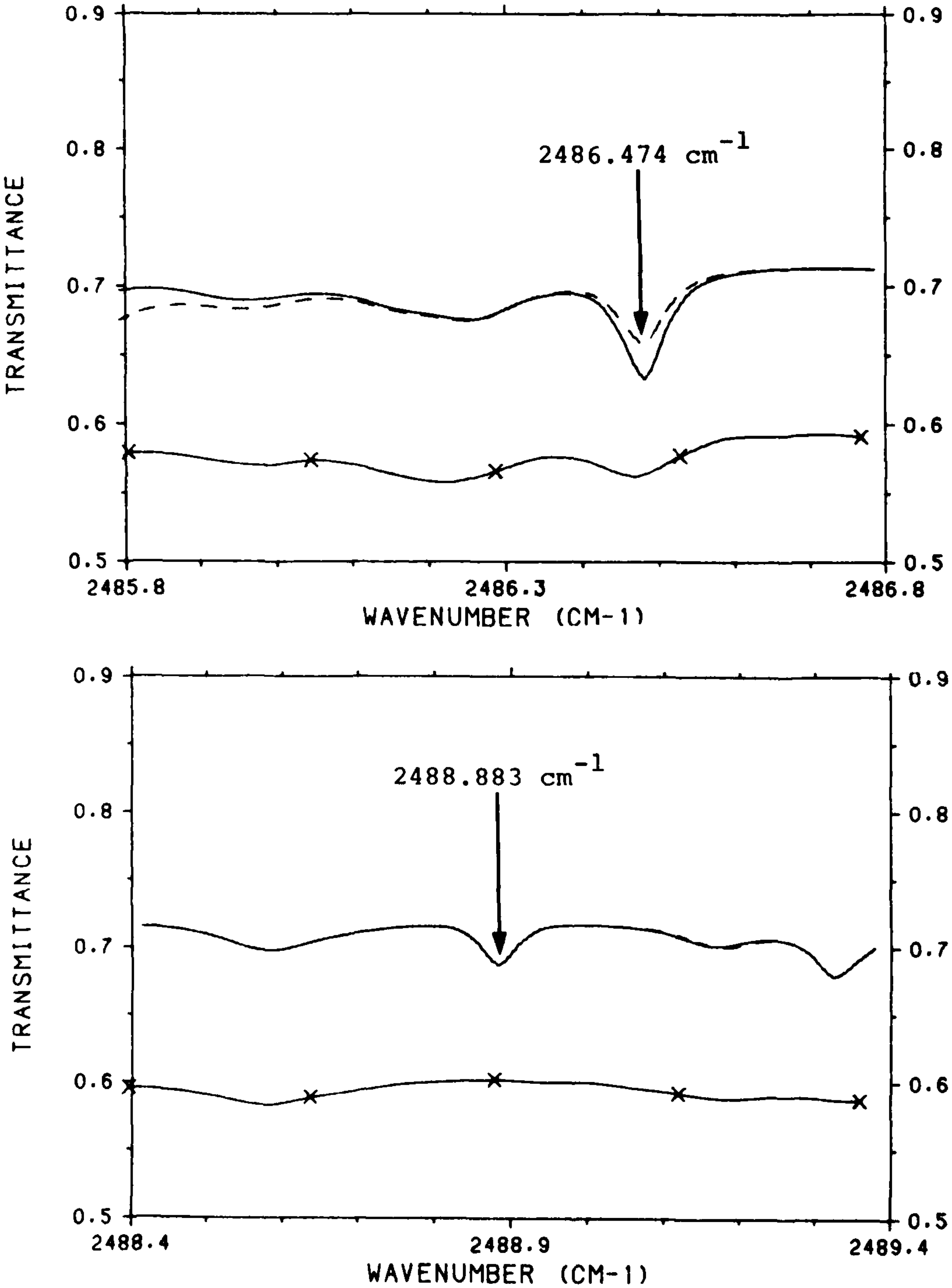

FIGURE 23. (CONTINUED).

using the 1982 version of the AFGL compilation. The effect of the different background transmittance levels was accounted for but the effect of the finite resolution of the measurement was not. In many cases the absorption line is not discernible in the measurement above the noise. In these cases, the depth of the measured line was taken to be equal to the level of the noise, as estimated from the plots (about ±0.01 transmittance) and only an upper limit for the strength of these lines is given.

The results of this analysis are given in Table 12 which lists for each absorption line, the frequency of the line center, the strength, the halfwidth, and the upper and lower vibrational and rotational quantum numbers, all taken from the 1982 version of the AFGL Line Compilation [9]. The last column, labeled R, is the ratio of the measured line strength to the value in the AFGL line compilation. Values of R which represent an upper limit are indicated by <. Estimates of some of the values are uncertain due to interfering lines of other molecules; these values are indicated with an asterisk. Estimates for the remaining values are uncertain by ±10 percent, based on comparisons performed for lines whose strengths are well known.

Note that the lines for which R is significantly different from 1.0 belong to the band (010,000): the measured strengths for the band (001,010) all agree with the AFGL values within the experimental uncertainty. The AFGL strengths were calculated based on observations of strong lines from the (010,000) band. The extrapolation of the calculation to the weaker lines involves large uncertainties, especially for values of ΔK_a = 3 or 5 [19].

TABLE 12. RATIO R OF MEASURED LINE STRENGTH TO AFGL VALUE FOR SELECTED WATER LINES, 2390 CM^{-1} TO 2500 CM^{-1}

	ν (cm^{-1})	S ($mol/cm^2/cm^{-1}$)	α (cm^{-1})	V'	V"	J'	K_a'	K_c"	J"	K_a"	K_c"	R
1	2394.851	1.27 x 10^{25}	0.0686	010	000	9	7	3	8	4	4	< .1
2	2395.413	1.01 x " "	0.0496	010	000	9	5	5	8	0	8	.08
3	2396.351	0.27 x " "	0.0182	010	000	12	12	1	11	11	0	.3
4	2396.910	1.77 x " "	0.0616	010	000	8	6	3	7	1	6	.16
5	2400.310	0.44 x " "	0.0190	010	000	15	3	12	14	2	13	.3
6	2403.921	3.88 x " "	0.0562	010	000	9	7	2	8	4	5	< .02
7	2407.163	1.65 x " "	0.0899	001	010	6	3	3	5	1	4	1.1
8	2410.478	2.52 x " "	0.0725	010	000	10	7	4	9	4	5	<0.06
9	2421.321	2.37 x " "	0.0700	010	000	11	4	7	10	1	10	<0.08
10	2422.706	1.19 x " "	0.0831	001	010	5	3	3	4	1	4	1.0
11	2429.930	1.75 x " "	0.0864	001	010	6	2	4	5	0	5	.74*
12	2433.218	0.50 x " "	0.0110	010	000	15	2	13	14	1	14	.18
13	2437.401	1.23 x " "	0.0861	001	010	6	4	2	5	2	3	1.2*
14	2457.067	1.43 x " "	0.0459	010	000	11	7	4	10	4	7	.12
15	2463.097	1.40 x " "	0.0457	010	000	10	5	6	9	0	9	.17
16	2485.625	1.23 x " "	0.0432	010	000	10	6	5	9	1	8	.3*
17	2486.474	0.22 x " "	0.0400	010	000	12	7	5	11	4	8	.4*
18	2488.883	0.16 x " "	0.009	010	000	16	2	14	15	1	15	< .1

ν = center frequency, S = line strength, α = halfwidth (at half height), V = vibrational quantum number, J, K_a, K_c = rotational quantum numbers, ' = upper state, " = lower state, R = measured strength/s, * = value uncertain due to interfering lines

4
CONCLUSIONS AND RECOMMENDATIONS

4.1 CONCLUSIONS

The conclusions which have been reached as a result of this study can be summarized as follows:

1. The several sets of spectra described in Section 2.2 have been shown to be accurate to $\lesssim \pm 3\%$ in absolute transmission, based on the established accuracy of the DF laser transmittance measurements used to provide the absolute transmittance calibrations for each spectrum. The RMS deviations from the hypothetical, ideal multiplicative scale factor of unity which characterize the accuracy of the absolute transmittance normalization procedure over the range of DF laser measurements used to normalize a particular spectrum has been shown to be within 4% in absolute transmission units in all but a few isolated cases. In most cases the RMS deviations is less than 2%. The normalized spectra typically differs from unity by less than 1%. See Section 2.2 for a discussion of these results which are tabulated in Tables 1, 3, 4, and 5.

2. The CCAFS results have been found to be most useful for the purposes of the present study for two reasons, namely:

   a) these data correspond to a wider range of atmospheric humidity conditions than do the other data and include measurements under higher absolute humidities than do the other data sets. The resolution of questions concerning water vapor continuum absorption (treated in Section 3.1.4) is best addressed using several of the CCAFS spectra measured during high visibility (low aerosol extinction), high water vapor conditions, and

   b) during several of the CCAFS measurements, laser transmittance measurements using a Nd-YAG laser operating at 1.06 μm were performed. The results of these measurements, scaled to 3.7 μm are considered a more reliable measure of aerosol extinction at 3.7 μm than concurrent, land-based (and surf-influenced) aerosol particulate

spectrometer data or than estimates derived from maritime aerosol extinction models. (See Section 3.1.2.2).

3. Determination of the aerosol extinction contributions to the total measured extinction probably represents the largest source of uncertainty in the analysis of the data. Various approaches were evaluated depending upon the amount of independent information available for each data set. Only visibility data (supplied by the NAVCOM, PRNAS) were available for the PRNAS data. Independent Nd-YAG laser transmissometer data were available for some of the CCAFS data and provide the most useful means of determining the value of aerosol extinction at 3.7 μm.

4. Using the semi-empirical procedure of determining the aerosol extinction component at 3.7 μm by subtracting the FASCODE-calculated molecular absorption coefficient from the measured total extinction coefficient (actually optical depth), the shape of the envelope of the measured optical depth as a function of wavenumber (corrected for N_2 and CO_2 continua, and local line effects) was compared with the equivalent FASCODE calculation. In nearly all cases (see Figures 12 through 15) the measured data show a smaller optical depth relative to the calculations for 1979 $cm^{-1} < \nu < 2177$ cm^{-1} and again for $\nu > 2920$ cm^{-1}. For 2400 $cm^{-1} < \nu < 2650$ cm^{-1} the measured optical depths are larger than the calculated values. The former comparisons are interpreted as indicating differences between the predicted and measured H_2O continuum absorption contribution. The latter comparisons (in the 2400-2650 cm^{-1} range) are interpreted as pointing up a discrepancy between the calculated N_2 continuum absorption coefficient and the measured values.

5. The FASCODE-generated water vapor continuum optical depth is seen to agree with the experimental data in the 2600 cm^{-1} to 2800 cm^{-1} range to within the range of

uncertainty of the data, conservatively estimated to be ±55%. See section 3.1.4 for a discussion of the estimated experimental uncertainty.

6. The high-resolution survey comparisons shown in Figures 19 and 20 point-out certain discrepancies between the measured and calculated high resolution spectra in each of the cases compared. In spectrum ASL06, shown in Figure 19(a) through 19(m) certain features appear in the measured data in the region between 1900 cm^{-1} and 2000 cm^{-1}. These features do not appear in the calculation. Since these features do not appear in the CC159 spectrum or in the high resolution Kitt Peak spectrum shown in Figure 21, they therefore must represent artifacts introduced in the measurement and/or data reduction processes. Since their location corresponds to the location of strong water vapor absorption lines, the most likely explanation involves the lack of sufficient dynamic range in the computations used in the numerical ratio of the long path spectrum to its zero-path-counterpart.

It can also be seen that the FASCODE calculation shows generally lower transmission than the measurement in this region (1900-2000 cm^{-1}). Although no aerosol attenuation has been included in the calculation, making a one-to-one comparison of the measured and calculated transmission values invalid, the amount of aerosol extinction that would realistically correspond to the measurement conditions (100 km visibility corresponding to $\sim$ 0.003 km^{-1} aerosol attenuation at 3.8 μm) is quite small and should not substantially alter the comparison shown in Figure 19(a).

7. The line-strengths of several of the weak water vapor absorption lines occurring between 2390 cm^{-1} and 2490 cm^{-1} are seen to be overestimated in the current AFGL atmospheric absorption line compilation. As demonstrated in Section 3.2.2 the 1982 version of the line compilation is in better agreement with experimental observations than are the data

included in the 1980 version. The results of comparisons of the experimental data to calculations performed using the 1982 version of the line compilation are summarized in the Table 12 and show that the measured line strengths vary from 0.02 to 1.2 times the values predicted using the 1982 compilation. On the average the observed values are in the range of about 10 to 30% of the predicted values.

4.2 RECOMMENDATIONS

Certain recommendations can be made as a consequence of the comparisons and analyses performed during the present study. These recommendations include the following:

1. More extensive quantitative comparisons of the high-resolution FTS data treated in this study might be developed if the aerosol extinction component at 3.7 μm in the various spectra can be determined unequivocally. Use of the comparisons shown in Figures 12-15 as a basis to establish a "zero-order" aerosol extinction coefficient, combined with the use of aerosol model predictions in a self-consistent analysis is recommended. The somewhat detailed statistical analysis that would be required was not possible within the scope of the present study. If this recommendation were to be implemented, the water vapor dependence of the 3-5 μm water vapor continuum absorption could be examined in greater detail.

2. A further investigation of the apparent excess N_2 continuum absorption evidenced in the comparisons shown in section 3.1.3.4 should be performed. The suggestion has been made [20] that an unaccounted for temperature dependence of the N_2 continuum absorption may be responsible for the discrepancies between the calculated and measured results shown in Figure 17. This question should be further investigated using the data treated in this study as well as pertinent laboratory data.

3. The line strengths of several of the weak water vapor absorption lines occurring between 2390 cm^{-1} and 2490 cm^{-1} are clearly too large as they appear in the 1982 AFGL atmospheric absorption line compilation. The line strength values for these lines should be modified on future editions of the compilation to reflect the values tabulated in Table 12.

4. The analysis performed in the present study has shown certain of the CCAFS spectra to be the most useful in comparisons of calculated and measured values for the weak, 3-5 μm water vapor absorption coefficient. These are the spectra collected during high humidity, high visibility conditions. Atmospheric conditions corresponding to substantially greater absolute humidities than the 20 torr ppH_2O corresponding to several of the CCAFS spectra are unlikely to occur at any experimental site. The only remaining alternative to increasing the total path-integral amount of water vapor in an experimental configuration is the use of a longer measurement path-length. The use of larger collecting apertures ($\sim$1.2 m) which can provide complete collection of a laser transmissometer beam under conditions of moderate atmospheric turbulence over paths lengths of 10-50 km is currently under study. Data similar to those discussed in the present study but collected over much longer paths (provided that aerosol attentuation remains small and/or usefully characterized) should provide information which can be used to reduce the quantitative uncertainties which persist as a result of the present analysis.

REFERENCES

1. T.H. Cosden, et. al. "Atmospheric Transmission Measurement Program Report for 1 July through 30 September 1976 (TQ 1976)" NRL Report 8104, September 1977.

2. A. Gutman, ed., "Data Compendium for Atmospheric Laser Propagation Studies Conducted at Cape Canaveral, Florida February - May 1977", NRL Memorandum Report 3611, September 1977.

3. J.A. Dowling, "Analysis of 1977 Cape Canaveral Air Force Station Atmospheric Laser Propagation and Fourier Transform Spectroscopic Data Base" NRL Report to be published (1984).

4. J.A. Dowling, et. al., "Laser-Extinction and High-Resolution Atmospheric Transmission Measurements Conducted at White Sands Missile Range, New Mexico, March 1979" NRL Report 8446, November 1980.

5. J.A. Dowling, et. al. "Results of Laser-Calibrated High-Resolution Transmission Measurements and Comparisons with Broadband Transmissometer Data: San Nicolas Island, California, May 1979" NRL Report 8618, September 1982.

6. J.A. Dowling, et. al. "High-Resolution Field Measurement of Atmospheric Transmission" SPIE Proceedings Vol. 142, 25 (1978).

7. K.M. Haught and J.A. Dowling, "Long-Path High Resolution Field Measurements of Absolute Transmission in the 3.5 to 4.0 μm Atmospheric Window", Opt. Ltrs. 1, 121, (1977).

8. S.A. Clough, et. al. "Atmospheric Spectral Transmittance and Radiance: FASCOD1B" SPIE Proceedings Vol. 277, 152, (1981); update to FASCOD1C, documented in AFGL Memorandum: OPI (S.A. Clough), 1 August 1982; available from: National Climatic Center, Environmental Data Service, Federal Building, Asheville, N.C., 28801.

9. L.S. Rothman, et. al. "AFGL Atmospheric Absorption Line Parameters Compilation: 1982", Appl. Opt., 22 2247 (1983).

10. J.A. Dowling, et. al., "Atmospheric Transmission Measurement and Field Test Plan:, NRL Report 8059, November 1977.

11. R.W. Harris, "Electronic Instrumentation for a High-Accuracy Atmospheric Extinction Experiment", (Abstract), J. Opt. Soc. Am. 65, 1201 (1975).

12. J.A. Dowling, et. al., "Atmospheric Extinction Measurements at Nd-YAG and DF Laser Wavelengths Performed in Conjunction with JAN Propagation Tests, June - September 1975", NRL Report 8058, February 1978.

13. P.L. Roney, et. al, Opt. Ltr. 6, 151 (1981).

14. S.G. Gathman, Optical Properties of the Marine Aerosol as predicted by a BASIC Version of the Navy Aerosol Model, NRL Memorandum Report 5157, Naval Research Laboratory, Washington, D.C., September 1983, ADA132411.

15. R.E. Larson, Atmospheric ^{222}Rn Measurements at San Nicolas Island, NRL Memorandum Report 4099, Naval Research Laboratory, Washington, D.C., November 1979, ADA077363.

16. R.E. Larson and R.K. Jeck, Atmospheric ^{222}Rn Measurements at San Nicolas Island during 1980, NRL Memorandum Report 4649, Naval Research Laboratory, Washington, D.C., October 1981, ADA104802.

17. E.P. Shettle and R.W. Fenn, "Models for the Aerosols of the Lower Atmosphere and the Effects of Humidity Variations on Their Optical Properties", AFGL-TR-79-0214, 20 September 1979, ADA085951.

18. L. Delfouille, G. Roland, J. Brault, and L. Testerman, "Photometric Atlas of the Solar Spectrum from 1850 to 10,000 cm^{-1}", Kitt Peak National Observatory (1981).

19. Lawrence Rothman, AFGL, private communication.

20. Darrell Burch, Ford Aerospace Corp., private communication.

APPENDIX A

COMPARISON OF MEASURED EXTINCTION COEFFICIENTS, CORRECTED FOR LOCAL LINE AND FOR N_2 AND CO_2 CONTINUUM ABSORPTION, TO FASCODE WATER-VAPOR-CONTINUUM ABSORPTION CALCULATIONS

WATER VAPOR EXTINCTION COEFFICIENT

WAVENUMBER (CM**-1)	FASCODE CASE 3 (KM**-1)	ASL17 AS/FCD	ASL17 AS-FCD	ASL18 AS/FCD	ASL18 AS-FCD	ASL19 AS/FCD	ASL19 AS-FCD
1930.300	.137	.295	-.097	.359	-.088	.813	-.026
1952.500	.093	.048	-.089	.196	-.075	.727	-.025
1974.100	.061	.058	-.057	.260	-.045	.852	-.009
1979.600	.053	.021	-.052	.199	-.042	.824	-.009
2004.650	.035	-.315	-.046	-.031	-.036	.833	-.006
2031.250	.020	-.722	-.035	-.177	-.024	1.035	.001
2056.050	.013	-1.022	-.026	-.177	-.015	1.613	.008
2084.350	.008	-2.027	-.024	-.553	-.012	1.809	.006
2102.150	.006	-3.403	-.025	-1.437	-.014	1.731	.004
2130.500	.004	-4.171	-.021	-1.559	-.010	2.531	.006
2150.050	.003	-6.145	-.025	-2.644	-.013	1.557	.002
2159.050	.003	-6.380	-.024	-2.472	-.011	1.836	.003
2166.800	.003	-6.334	-.023	-1.528	-.008	2.497	.005
2177.600	.003	-7.591	-.024	-3.304	-.012	1.449	.001
2190.950	.003	-8.578	-.025	-3.387	-.012	1.355	.001
2223.680	.003	2.517	.004	7.543	.016	12.091	.028
2400.000	.002	1.201	.000	3.461	.005	10.430	.019
2420.420	.002	-1.169	-.004	2.253	.003	7.076	.012
2440.850	.002	-4.231	-.011	-1.493	-.005	2.414	.003
2480.330	.002	-4.269	-.011	-1.899	-.006	1.252	.001
2501.000	.002	-3.949	-.010	-1.801	-.006	1.204	.000
2520.650	.002	-3.313	-.009	-1.003	-.004	1.239	.000
2540.830	.002	-2.528	-.007	-1.132	-.004	.964	-.000
2560.420	.002	-1.969	-.006	-.489	-.003	1.461	.001
2580.370	.002	-2.240	-.007	-.858	-.004	.816	-.000
2599.840	.002	-1.220	-.005	-.330	-.003	.779	-.000
2618.640	.002	-.839	-.004	-.013	-.002	1.031	.000
2640.580	.002	-.179	-.003	-.267	-.003	.981	-.000
2661.550	.002	-.103	-.003	.683	-.001	1.138	.000
2679.510	.002	.458	-.001	.584	-.001	.577	-.001
2700.720	.002	1.000	-.000	1.000	-.000	1.000	-.000
2719.280	.002	-.309	-.003	-.769	-.004	-.297	-.003
2740.740	.002	2.431	.003	1.645	.002	.924	-.000
2760.690	.002	3.514	.006	2.068	.003	1.287	.001
2778.950	.002	2.739	.004	1.167	.000	.592	-.001
2800.100	.002	3.548	.006	1.517	.001	.348	-.002
2820.110	.002	3.564	.006	1.940	.002	.711	-.001
2839.400	.002	4.717	.009	2.767	.004	.477	-.001
2860.190	.002	4.928	.009	2.052	.002	.502	-.001
2880.800	.002	6.074	.012	3.872	.007	1.594	.001
2899.720	.003	5.777	.012	3.594	.006	.715	-.001
2920.400	.003	5.348	.013	2.884	.006	.517	-.001
2941.370	.004	4.645	.015	3.118	.009	2.045	.004
2959.870	.006	3.393	.013	1.931	.005	1.215	.001
2979.520	.008	4.949	.031	3.488	.020	3.886	.023
3000.550	.012	2.956	.024	2.028	.013	1.776	.009
3020.260	.015	2.519	.023	1.444	.007	1.368	.006
3040.450	.019	2.496	.029	1.983	.019	1.622	.012
3058.710	.021	1.809	.017	1.615	.013	1.955	.020

WATER VAPOR EXTINCTION COEFFICIENT

WAVENUMBER (CM**-1)	FASCODE CASE 3 (KM**-1)	ASL20 AS/FCD	AS-FCD
1930.300	.137	.821	-.025
1952.500	.093	.695	-.028
1974.100	.061	.737	-.016
1979.600	.053	.686	-.017
2004.650	.035	.628	-.013
2031.250	.020	.556	-.009
2056.050	.013	.824	-.002
2084.350	.008	.389	-.005
2102.150	.006	.080	-.005
2130.500	.004	.063	-.004
2150.050	.003	-1.134	-.007
2159.050	.003	-1.176	-.007
2166.800	.003	-.667	-.005
2177.600	.003	-1.568	-.007
2190.950	.003	-1.901	-.008
2223.680	.003	8.938	.020
2400.000	.002	7.735	.014
2420.420	.002	4.530	.007
2440.850	.002	-.060	-.002
2480.330	.002	-.231	-.003
2501.000	.002	-.515	-.003
2520.650	.002	-.254	-.003
2540.830	.002	-.150	-.002
2560.420	.002	.265	-.001
2580.370	.002	-.299	-.003
2599.840	.002	.374	-.001
2618.640	.002	.192	-.002
2640.580	.002	.594	-.001
2661.550	.002	.613	-.001
2679.510	.002	.582	-.001
2700.720	.002	1.000	-.000
2719.280	.002	.366	-.001
2740.740	.002	1.449	.001
2760.690	.002	1.741	.002
2778.950	.002	.908	-.000
2800.100	.002	1.393	.001
2820.110	.002	1.285	.001
2839.400	.002	1.713	.002
2860.190	.002	1.667	.002
2880.800	.002	2.955	.005
2899.720	.003	2.675	.004
2920.400	.003	1.743	.002
2941.370	.004	2.862	.008
2959.870	.006	1.914	.005
2979.520	.008	4.516	.028
3000.550	.012	2.302	.016
3020.260	.015	1.857	.013
3040.450	.019	1.930	.018
3058.710	.021	2.820	.038

WATER VAPOR EXTINCTION COEFFICIENT

WAVENUMBER (CM**-1)	FASCODE CASE 4 (KM**-1)	ASL23 AS/FCD	ASL23 AS-FCD	ASL21 AS/FCD	ASL21 AS-FCD
1930.300	.223	.206	-.177	.290	-.158
1952.500	.152	.025	-.148	.159	-.128
1974.100	.100	.015	-.098	.246	-.075
1979.600	.086	-.013	-.087	.279	-.062
2004.650	.057	-.291	-.074	.155	-.048
2031.250	.034			.053	-.032
2056.050	.021			.107	-.019
2084.350	.013			-.194	-.016
2102.150	.010			-.330	-.013
2130.500	.007			-.653	-.012
2150.050	.006			-1.288	-.014
2159.050	.006			-1.630	-.015
2166.800	.005			-1.979	-.016
2177.600	.005	-7.638	-.042	-2.521	-.017
2190.950	.005	-8.207	-.042	-2.146	-.014
2223.680	.004	-1.281	-.010	1.413	.002
2400.000	.003	.150	-.003	3.046	.007
2420.420	.003	-1.412	-.008	1.018	.000
2440.850	.003	-3.019	-.014	.125	-.003
2480.330	.003	-3.414	-.015	-.655	-.006
2501.000	.003	-2.840	-.013	-.275	-.004
2520.650	.003	-2.947	-.014	-.210	-.004
2540.830	.003	-2.599	-.012	-.329	-.005
2560.420	.003	-2.206	-.011	.100	-.003
2580.370	.003	-2.540	-.012	-.382	-.005
2599.840	.004	-1.097	-.008	.350	-.002
2618.640	.004	-.981	-.007	.111	-.003
2640.580	.004	-1.289	-.009	.325	-.003
2661.550	.004	-.805	-.007	.380	-.002
2679.510	.004	-.401	-.005	.320	-.003
2700.720	.004	1.000	0.000	1.000	-.000
2719.280	.004	-1.555	-.010	-.562	-.006
2740.740	.004	1.172	.001	1.192	.001
2760.690	.004	1.289	.001	1.384	.001
2778.950	.004	1.185	.001	1.111	.000
2800.100	.004	.810	-.001	.523	-.002
2820.110	.004	1.621	.002	1.145	.001
2839.400	.004	3.023	.008	1.665	.002
2860.190	.004	3.175	.008	1.471	.002
2880.800	.004	3.473	.010	2.146	.004
2899.720	.004	3.212	.009	2.160	.005
2920.400	.005	3.617	.013	2.081	.005
2941.370	.006	2.239	.008	1.459	.003
2959.870	.009	1.674	.006	.463	-.005
2979.520	.013	.604	-.005	-.328	-.017
3000.550	.020	.862	-.003	.737	-.005
3020.260	.025	1.015	.000	.586	-.010
3040.450	.031	1.724	.023	.869	-.004
3058.710	.034	1.837	.028	.840	-.005

WATER VAPOR EXTINCTION COEFFICIENT

WAVENUMBER (CM**-1)	FASCODE CASE 2 (KM**-1)	ASL13 AS/FCD	ASL13 AS-FCD	ASL14 AS/FCD	ASL14 AS-FCD	ASL15 AS/FCD	ASL15 AS-FCD
1930.300	.242	.027	-.235	.008	-.240	-.139	-.275
1952.500	.164	-.185	-.195	-.207	-.198	-.310	-.215
1974.100	.108	-.145	-.124	-.176	-.127	-.199	-.130
1979.600	.093	-.165	-.109	-.189	-.111	-.168	-.109
2004.650	.062	-.528	-.095	-.496	-.093	-.447	-.090
2031.250	.037	-.937	-.072	-.942	-.072	-.707	-.063
2056.050	.023	-1.460	-.057	-1.386	-.055	-1.068	-.048
2084.350	.015					-2.105	-.045
2102.150	.011					-2.795	-.041
2130.500	.008					-3.258	-.033
2150.050	.006					-4.777	-.037
2159.050	.006	-7.160	-.050	-6.519	-.046	-4.473	-.033
2166.800	.006	-7.480	-.049	-7.101	-.047	-4.781	-.033
2177.600	.005	-8.454	-.050	-8.217	-.049	-6.399	-.039
2190.950	.005	104*78	-.057	-9.257	-.051	-7.638	-.043
2223.680	.005	-7.221	-.037	-6.561	-.034	-6.360	-.033
2400.000	.004	-1.531	-.009	-.220	-.005	1.775	.003
2420.420	.004	-3.133	-.015	-2.415	-.012	-1.420	-.009
2440.850	.004	-4.798	-.021	-3.253	-.015	-1.779	-.010
2480.330	.004	-4.561	-.020	-3.491	-.016	-3.190	-.015
2501.000	.004	-3.531	-.016	-2.895	-.014	-2.680	-.013
2520.650	.004	-3.369	-.016	-2.730	-.013	-2.690	-.013
2540.830	.004	-2.990	-.014	-2.698	-.013	-1.135	-.008
2560.420	.004	-2.793	-.014	-2.053	-.011	-1.305	-.009
2580.370	.004	-3.263	-.016	-2.730	-.014	-2.940	-.015
2599.840	.004	-1.342	-.009	-.869	-.007	-1.391	-.009
2618.640	.004	-.790	-.007	-.996	-.008	-1.437	-.010
2640.580	.004	-.929	-.008	-.510	-.006	-.742	-.007
2661.550	.004	-.365	-.006	-.637	-.007	-1.484	-.010
2679.510	.004	-.409	-.006	-.526	-.006	.281	-.003
2700.720	.004	1.000	-.000	1.000	-.000	1.000	-.000
2719.280	.004	-2.199	-.013	-2.506	-.014	-3.390	-.018
2740.740	.004	1.555	.002	1.327	.001	.290	-.003
2760.690	.004	2.237	.005	2.088	.004	1.819	.003
2778.950	.004	1.778	.003	1.339	.001	-.253	-.005
2800.100	.004	.913	-.000	1.179	.001	-.709	-.007
2820.110	.004	2.091	.004	1.638	.003	.832	-.001
2839.400	.004	3.198	.009	3.515	.010	2.209	.005
2860.190	.004	3.993	.012	3.888	.012	1.583	.002
2880.800	.004	4.481	.014	4.339	.014	2.034	.004
2899.720	.004	4.082	.013	3.559	.011	2.061	.005
2920.400	.005	3.999	.016	3.099	.011	2.072	.006
2941.370	.007	3.147	.015	2.468	.010	1.403	.003
2959.870	.010	1.540	.005	.886	-.001	.210	-.008
2979.520	.014	-.898	-.027	-1.159	-.030	-2.380	-.048
3000.550	.021	1.184	.004	1.144	.003	.337	-.014
3020.260	.027	.904	-.003	.697	-.008	.095	-.024
3040.450	.034	1.429	.014	1.246	.008	.814	-.006
3058.710	.037	.338	-.024	.097	-.033	-.949	-.071

WATER VAPOR EXTINCTION COEFFICIENT

WAVENUMBER (CM**-1)	FASCODE CASE 1 (KM**-1)	ASL04 AS/FCD	ASL04 AS-FCD	ASL06 AS/FCD	ASL06 AS-FCD
1930.300	.331	.508	-.163	.531	-.155
1952.500	.225	.462	-.121	.467	-.120
1974.100	.149	.567	-.065	.582	-.062
1979.600	.129	.564	-.056	.607	-.051
2004.650	.086	.561	-.038	.604	-.034
2031.250	.052	.526	-.024	.608	-.020
2056.050	.032	.899	-.003	.915	-.003
2084.350	.021	.838	-.003	.970	-.001
2102.150	.015	.634	-.006	.880	-.002
2130.500	.011	.789	-.002	.982	-.000
2150.050	.009	.461	-.005	.793	-.002
2159.050	.009	.173	-.007	.506	-.004
2166.800	.008	.005	-.008	.282	-.006
2177.600	.008	.055	-.007	.397	-.005
2190.950	.007	.500	-.004	.691	-.002
2223.680	.006	5.445	.028	5.102	.026
2400.000	.005	2.937	.010	4.655	.019
2420.420	.005	2.176	.006	2.837	.009
2440.850	.005	.961	-.000	1.769	.004
2480.330	.005	.864	-.001	1.116	.001
2501.000	.005	.549	-.002	1.115	.001
2520.650	.005	.360	-.003	.961	-.000
2540.830	.005	.889	-.001	1.305	.002
2560.420	.005	.919	-.000	1.244	.001
2580.370	.005	.920	-.000	1.238	.001
2599.840	.005	.980	-.000	1.144	.001
2618.640	.005	.863	-.001	1.058	.000
2640.580	.005	.691	-.002	.969	-.000
2661.550	.005	.659	-.002	.911	-.000
2679.510	.005	.946	-.000	.858	-.001
2700.720	.006	1.000	0.000	1.000	0.000
2719.280	.006	1.278	.002	1.031	.000
2740.740	.006	1.108	.001	1.085	.000
2760.690	.006	1.107	.001	1.225	.001
2778.950	.006	1.080	.000	1.172	.001
2800.100	.006	1.049	.000	1.450	.003
2820.110	.006	1.631	.004	1.812	.005
2839.400	.005	1.362	.002	1.722	.004
2860.190	.005	1.674	.004	2.094	.006
2880.800	.006	2.486	.008	3.313	.013
2899.720	.006	2.372	.008	3.214	.013
2920.400	.007	2.639	.012	3.421	.017
2941.370	.010	2.284	.012	3.006	.019
2959.870	.013	2.110	.015	2.817	.024
2979.520	.019	3.437	.046	3.857	.054
3000.550	.029	1.061	.002	1.405	.012
3020.260	.036	1.245	.009	1.389	.014
3040.450	.046	.932	-.003	1.057	.003
3058.710	.050	1.956	.047	2.075	.053

WATER VAPOR EXTINCTION COEFFICIENT

WAVENUMBER (CM**-1)	FASCODE CASE 15 (KM**-1)	PR037 PR/FCD	PR037 PR-FCD	PR039 PR/FCD	PR039 PR-FCD
2400.000	.005	4.265	.015	4.523	.017
2420.420	.005	1.697	.003	2.341	.006
2440.850	.005	.653	-.002	1.076	.000
2480.330	.005	.152	-.004	-.296	-.006
2501.000	.005	-.652	-.008	-1.248	-.011
2520.650	.005	-.150	-.005	-.968	-.009
2540.830	.005	.540	-.002	.274	-.003
2560.420	.005	.366	-.003	.109	-.004
2580.370	.005	.956	-.000	.324	-.003
2599.840	.005	.398	-.003	.579	-.002
2618.640	.005	-.095	-.005	.359	-.003
2640.580	.005	.476	-.003	.121	-.004
2661.550	.005	.157	-.004	.288	-.004
2679.510	.005	.479	-.003	.790	-.001
2700.720	.005	1.000	-.000	1.000	-.000
2719.280	.005	-.662	-.008	-.901	-.010
2740.740	.005	1.124	.001	1.081	.000
2760.690	.005	1.398	.002	.926	-.000
2778.950	.005	.949	-.000	.558	-.002
2800.100	.005	-.329	-.007	.893	-.001
2820.110	.005	1.964	.005	2.286	.007
2839.400	.005	1.104	.001	2.301	.007
2860.190	.005	2.105	.006	3.038	.010
2880.800	.005	1.725	.004	3.843	.015
2899.720	.006	2.315	.007	3.144	.012
2920.400	.007	3.016	.013	3.049	.014
2941.370	.009	2.063	.009	2.755	.015
2959.870	.012	.800	-.002	1.182	.002
2979.520	.017	-.901	-.033	-.466	-.025
3000.550	.026	.532	-.012	.971	-.001
3020.260	.033	.457	-.018	.435	-.019
3040.450	.042	.332	-.028	.629	-.016
3058.710	.045	-.611	-.073	-.096	-.050

WATER VAPOR EXTINCTION COEFFICIENT

WAVENUMBER	FASCODE CASE 16	PR040		PR042		PR054	
(CM**-1)	(KM**-1)	PR/FCD	PR-FCD	PR/FCD	PR-FCD	PR/FCD	PR-FCD
2400.000	.005	5.003	.020	4.167	.015	1.820	.004
2420.420	.005	2.637	.008	1.998	.005	-.408	-.007
2440.850	.005	2.390	.007	1.859	.004	-1.409	-.012
2480.330	.005	.476	-.002	.048	-.004	-1.290	-.011
2501.000	.005	-.575	-.007	-.363	-.006	-1.475	-.012
2520.650	.005	.524	-.002	.637	-.002	-.308	-.006
2540.830	.005	1.023	.000	.049	-.004	-.447	-.007
2560.420	.005	.732	-.001	.147	-.004	-.799	-.009
2580.370	.005	.747	-.001	-.290	-.006	.311	-.003
2599.840	.005	1.127	.001	.610	-.002	.326	-.003
2618.640	.005	.419	-.003	-.065	-.005	-.391	-.007
2640.580	.005	.496	-.003	.871	-.001	-.208	-.006
2661.550	.005	.832	-.001	1.426	.002	.395	-.003
2679.510	.005	.541	-.002	-.049	-.006	.927	-.000
2700.720	.005	1.000	-.000	1.000	-.000	1.000	-.000
2719.280	.005	-.297	-.007	-1.025	-.011	-.883	-.010
2740.740	.005	1.605	.003	.665	-.002	.774	-.001
2760.690	.005	1.102	.001	1.232	.001	1.661	.003
2778.950	.005	1.336	.002	.545	-.002	1.533	.003
2800.100	.005	1.569	.003	1.064	.000	1.269	.001
2820.110	.005	2.053	.006	.814	-.001	2.016	.005
2839.400	.005	1.816	.004	.486	-.003	3.078	.011
2860.190	.005	3.605	.014	2.038	.005	4.147	.017
2880.800	.005	5.131	.022	2.951	.010	4.433	.018
2899.720	.006	4.624	.021	2.653	.009	4.698	.021
2920.400	.007	4.536	.024	1.747	.005	3.885	.020
2941.370	.009	3.630	.024	2.074	.010	3.982	.027
2959.870	.013	2.850	.023	1.381	.005	2.112	.014
2979.520	.018	.948	-.001	.569	-.008	.750	-.004
3000.550	.027	.863	-.004	.455	-.015	1.484	.013
3020.260	.034	.591	-.014	-.138	-.039	.598	-.014
3040.450	.043	.721	-.012	.480	-.022	.963	-.002
3058.710	.047	.304	-.033	.499	-.023	1.147	.007

WATER VAPOR EXTINCTION COEFFICIENT

WAVENUMBER (CM**-1)	FASCODE CASE 17 (KM**-1)	PR049 PR/FCD	PR049 PR-FCD	PR050 PR/FCD	PR050 PR-FCD
2400.000	.007	4.278	.024	4.172	.024
2420.420	.007	2.786	.013	2.412	.010
2440.850	.007	1.400	.003	1.220	.002
2480.330	.007	1.106	.001	1.042	.000
2501.000	.007	1.200	.001	.612	-.003
2520.650	.007	1.479	.003	.566	-.003
2540.830	.007	.523	-.003	1.584	.004
2560.420	.007	1.072	.001	.149	-.006
2580.370	.007	1.375	.003	-.584	-.012
2599.840	.008	.980	-.000	1.366	.003
2618.640	.008	.712	-.002	1.015	.000
2640.580	.008	1.031	.000	.815	-.001
2661.550	.008	.838	-.001	.427	-.004
2679.510	.008	.606	-.003	-.483	-.012
2700.720	.008	1.000	-.000	1.000	-.000
2719.280	.008	.091	-.007	1.891	.007
2740.740	.008	1.590	.005	.195	-.006
2760.690	.008	1.588	.005	1.186	.001
2778.950	.008	.675	-.003	1.449	.004
2800.100	.008	1.045	.000	.687	-.003
2820.110	.008	2.186	.009	2.408	.011
2839.400	.008	1.443	.003	.740	-.002
2860.190	.008	2.486	.012	1.995	.008
2880.800	.008	2.301	.010	4.387	.027
2899.720	.009	2.684	.014	2.961	.017
2920.400	.010	2.413	.014	4.195	.032
2941.370	.013	1.966	.013	1.557	.008
2959.870	.019	1.361	.007	2.754	.033
2979.520	.027	1.854	.023	3.456	.066
3000.550	.041	.650	-.014	1.148	.006
3020.260	.052	.238	-.039	.943	-.003
3040.450	.065	.573	-.028	.943	-.004
3058.710	.070	.540	-.032	2.965	.138

WATER VAPOR EXTINCTION COEFFICIENT

WAVENUMBER (CM**-1)	FASCODE CASE 18 (KM**-1)	PR055 PR/FCD	PR055 PR-FCD	PR056 PR/FCD	PR056 PR-FCD
2400.000	.008	1.726	.006	1.755	.006
2420.420	.008	1.507	.004	1.595	.005
2440.850	.008	.951	-.000	1.059	.000
2480.330	.008	.883	-.001	.953	-.000
2501.000	.008	.797	-.00[illegible]	.492	-.004
2520.650	.008	1.086	.001	.816	-.002
2540.830	.008	.915	-.001	.927	-.001
2560.420	.008	.913	-.001	.923	-.001
2580.370	.008	.901	-.001	.667	-.003
2599.840	.009	1.128	.001	1.048	.000
2618.640	.009	1.088	.001	.896	-.001
2640.580	.009	.637	-.003	.612	-.003
2661.550	.009	.881	-.001	.858	-.001
2679.510	.009	.957	-.000	.738	-.002
2700.720	.009	1.000	-.000	1.000	-.000
2719.280	.009	.041	-.009	-.378	-.012
2740.740	.009	1.042	.000	1.042	.000
2760.690	.009	1.207	.002	.904	-.001
2778.950	.009	.690	-.003	.663	-.003
2800.100	.009	1.184	.002	.106	-.008
2820.110	.009	1.358	.003	1.666	.006
2839.400	.009	1.163	.001	1.333	.003
2860.190	.009	1.661	.006	1.486	.004
2880.800	.009	2.380	.013	1.944	.009
2899.720	.010	2.035	.010	2.764	.017
2920.400	.012	2.376	.016	2.212	.014
2941.370	.015	1.961	.015	2.006	.016
2959.870	.021	1.639	.014	1.171	.004
2979.520	.031	1.119	.004	1.057	.002
3000.550	.046	.711	-.013	.695	-.014
3020.260	.059	.583	-.025	.539	-.027
3040.450	.074	.621	-.028	.606	-.029
3058.710	.080	1.183	.015	1.169	.014

WATER VAPOR EXTINCTION COEFFICIENT

WAVENUMBER (CM**-1)	FASCODE CASE 19 (KM**-1)	PR024 PR/FCD	PR-FCD
2400.000	.019	1.438	.008
2420.420	.019	1.105	.002
2440.850	.019	.775	-.004
2480.330	.018	.459	-.010
2501.000	.018	.526	-.009
2520.650	.018	.575	-.008
2540.830	.018	.718	-.005
2560.420	.018	.658	-.006
2580.370	.018	.737	-.005
2599.840	.018	.787	-.004
2618.640	.019	.736	-.005
2640.580	.019	.755	-.005
2661.550	.019	.882	-.002
2679.510	.019	.905	-.002
2700.720	.019	1.000	0.000
2719.280	.019	.980	-.000
2740.740	.019	1.127	.002
2760.690	.019	1.280	.005
2778.950	.020	1.383	.007
2800.100	.020	1.520	.010
2820.110	.019	1.910	.018
2839.400	.019	1.785	.015
2860.190	.019	2.271	.024
2880.800	.020	2.867	.036
2899.720	.021	2.697	.036
2920.400	.025	2.677	.042
2941.370	.033	2.302	.043
2959.870	.046	1.865	.040
2979.520	.067	2.136	.076
3000.550	.100	.963	-.004
3020.260	.126	.979	-.003
3040.450	.158	.913	-.014
3058.710	.172	1.766	.132

WATER VAPOR EXTINCTION COEFFICIENT

WAVENUMBER (CM**-1)	FASCODE CASE 5 (KM**-1)	SNI24 SN/FCD	SNI24 SN-FCD	SNI17 SN/FCD	SNI17 SN-FCD
1930.300	.861	.699	-.259	.454	-.470
1952.500	.591	.575	-.251	.375	-.369
1974.100	.395	.621	-.150	.429	-.225
1979.600	.343	.680	-.110	.483	-.178
2004.650	.232	.680	-.074	.476	-.122
2031.250	.142	.676	-.046	.411	-.084
2056.050	.092	.864	-.012	.532	-.043
2084.350	.060	.935	-.004	.456	-.033
2102.150	.046	.929	-.003	.367	-.029
2130.500	.033	.893	-.004	.346	-.022
2150.050	.029	.860	-.004	.237	-.022
2159.050	.027	.674	-.009	.074	-.025
2166.800	.026	.699	-.008	.037	-.025
2177.600	.024	.820	-.004	.120	-.021
2190.950	.022	.980	-.000	.315	-.015
2223.680	.019	2.774	.034	.025	-.019
2400.000	.014	2.991	.028	1.896	.013
2420.420	.014	2.209	.017	1.489	.007
2440.850	.014	1.928	.013	1.137	.002
2480.330	.013	1.364	.005	.785	-.003
2501.000	.013	1.145	.002	.753	-.003
2520.650	.013	1.059	.001	.667	-.004
2540.830	.013	1.361	.005	1.062	.001
2560.420	.013	1.201	.003	.828	-.002
2580.370	.013	1.318	.004	1.000	.000
2599.840	.014	1.174	.002	.952	-.001
2618.640	.014	1.230	.003	1.031	.000
2640.580	.014	1.036	.001	.724	-.004
2661.550	.014	.987	-.000	.833	-.002
2679.510	.014	.981	-.000	.840	-.002
2700.720	.014	1.000	-.000	1.000	-.000
2719.280	.014	1.113	.002	.248	-.011
2740.740	.014	.960	-.001	.977	-.000
2760.690	.014	1.103	.001	1.224	.003
2778.950	.014	.874	-.002	.888	-.002
2800.100	.014	.622	-.005	.401	-.009
2820.110	.014	1.086	.001	.914	-.001
2839.400	.014	.657	-.005	.901	-.001
2860.190	.014	.643	-.005	.924	-.001
2880.800	.014	.997	-.000	1.169	.002
2899.720	.015	1.038	.001	1.434	.007
2920.400	.018	1.141	.003	1.142	.003
2941.370	.024	.866	-.003	1.091	.002
2959.870	.034	.988	-.000	.857	-.005
2979.520	.049	1.943	.046	1.478	.023
3000.550	.073	.898	-.007	.875	-.009
3020.260	.092	1.040	.004	.937	-.006
3040.450	.116	.963	-.004	.804	-.023
3058.710	.126	2.152	.145	1.458	.058

WATER VAPOR EXTINCTION COEFFICIENT

WAVENUMBER (CM**-1)	FASCODE CASE 5 (KM**-1)	SNI05 SN/FCD	SNI05 SN-FCD	SNI04 SN/FCD	SNI04 SN-FCD	SNI12 SN/FCD	SNI12 SN-FCD
1930.300	.861	114*95	998*61	.778	-.192	.572	-.368
1952.500	.591	.784	-.128	.914	-.051	.512	-.288
1974.100	.395	.813	-.074	.882	-.047	.548	-.179
1979.600	.343	.955	-.015	1.017	.006	.587	-.142
2004.650	.232	1.146	.034	1.364	.084	.547	-.105
2031.250	.142	1.106	.015	1.165	.023	.464	-.076
2056.050	.092	1.827	.076	1.845	.077	.605	-.036
2084.350	.060	1.848	.051	1.816	.049	.527	-.028
2102.150	.046	1.903	.042	1.935	.043	.318	-.032
2130.500	.033	2.073	.036	2.018	.034	.163	-.028
2150.050	.029	2.351	.038	2.147	.033	-.063	-.030
2159.050	.027	2.020	.028	1.927	.025	-.423	-.038
2166.800	.026	1.932	.024	1.924	.024	-.295	-.033
2177.600	.024	1.886	.021	1.654	.015	-.395	-.033
2190.950	.022	1.560	.012	1.250	.005	-.294	-.028
2223.680	.019	1.828	.016	1.093	.002	-.239	-.024
2400.000	.014	3.631	.037	3.588	.036	2.235	.017
2420.420	.014	3.510	.035	3.126	.029	1.660	.009
2440.850	.014	2.396	.019	2.494	.021	1.063	.001
2480.330	.013	1.900	.012	2.130	.015	.679	-.004
2501.000	.013	1.707	.009	1.658	.009	.653	-.005
2520.650	.013	1.369	.005	1.690	.009	.534	-.006
2540.830	.013	1.455	.006	1.571	.008	.804	-.003
2560.420	.013	1.506	.007	1.343	.005	.722	-.004
2580.370	.013	1.018	.000	1.059	.001	.899	-.001
2599.840	.014	1.250	.003	1.253	.003	.966	-.000
2618.640	.014	1.046	.001	1.100	.001	1.031	.000
2640.580	.014	.948	-.001	.933	-.001	.591	-.006
2661.550	.014	.698	-.004	.976	-.000	.635	-.005
2679.510	.014	.785	-.003	.957	-.001	1.008	.000
2700.720	.014	1.000	.000	1.000	-.000	1.000	-.000
2719.280	.014	.481	-.007	.376	-.009	.993	-.000
2740.740	.014	.871	-.002	.886	-.002	1.053	.001
2760.690	.014	.760	-.003	.947	-.001	1.219	.003
2778.950	.014	.289	-.010	.674	-.005	1.209	.003
2800.100	.014	.110	-.013	.192	-.012	.778	-.003
2820.110	.014	.469	-.008	.861	-.002	1.474	.007
2839.400	.014	.509	-.007	.819	-.003	1.370	.005
2860.190	.014	.589	-.006	.899	-.001	1.467	.007
2880.800	.014	.816	-.003	1.251	.004	1.563	.008
2899.720	.015	.588	-.006	1.057	.001	1.679	.011
2920.400	.018	.741	-.005	1.255	.005	1.871	.016
2941.370	.024	.698	-.007	1.138	.003	1.373	.009
2959.870	.034	.606	-.013	.938	-.002	1.091	.003
2979.520	.049	1.560	.027	1.829	.040	1.793	.039
3000.550	.073	.752	-.018	.875	-.009	.958	-.003
3020.260	.092	.896	-.010	.998	-.000	1.163	.015
3040.450	.116	.925	-.009	.990	-.001	.955	-.005
3058.710	.126	2.699	.214	1.848	.107	2.278	.161

WATER VAPOR EXTINCTION COEFFICIENT

WAVENUMBER (CM**-1)	FASCODE CASE 6 (KM**-1)	SNI02 SN/FCD	SNI02 SN-FCD	SNI06 SN/FCD	SNI06 SN-FCD
1930.300	.923	107*27	999*23	107*27	999*23
1952.500	.633	1.269	.170	.819	-.114
1974.100	.424	1.142	.060	.953	-.020
1979.600	.369	1.343	.126	1.127	.047
2004.650	.250	2.146	.286	1.331	.083
2031.250	.153	2.043	.160	1.379	.058
2056.050	.099	3.527	.251	1.925	.092
2084.350	.065	3.719	.177	2.074	.070
2102.150	.050	3.665	.134	2.371	.069
2130.500	.036	3.881	.105	2.727	.063
2150.050	.031	4.279	.102	2.862	.058
2159.050	.029	3.798	.082	2.778	.052
2166.800	.028	3.979	.083	2.882	.052
2177.600	.026	3.591	.067	2.700	.044
2190.950	.024	2.901	.045	2.888	.045
2223.680	.021	2.347	.028	4.518	.074
2400.000	.015	5.297	.065	4.459	.053
2420.420	.015	4.449	.052	3.545	.038
2440.850	.015	3.374	.035	2.851	.027
2480.330	.014	2.561	.022	2.134	.016
2501.000	.014	2.354	.019	1.906	.013
2520.650	.014	2.097	.016	1.662	.009
2540.830	.014	1.890	.013	1.884	.013
2560.420	.014	1.616	.009	1.502	.007
2580.370	.014	1.237	.003	1.310	.004
2599.840	.014	1.556	.008	1.489	.007
2618.640	.015	1.482	.007	1.181	.003
2640.580	.015	1.046	.001	.992	-.000
2661.550	.015	.611	-.006	.762	-.004
2679.510	.015	.597	-.006	.747	-.004
2700.720	.015	1.000	-.000	1.000	-.000
2719.280	.015	.034	-.015	.661	-.005
2740.740	.015	.652	-.005	.852	-.002
2760.690	.015	.551	-.007	.993	-.000
2778.950	.015	.226	-.012	.533	-.007
2800.100	.015	-.234	-.019	.402	-.009
2820.110	.015	-.027	-.016	.857	-.002
2839.400	.015	-.059	-.016	.559	-.007
2860.190	.015	.023	-.015	.653	-.005
2880.800	.015	.054	-.015	.994	-.000
2899.720	.017	.213	-.013	1.406	.007
2920.400	.020	.294	-.014	1.029	.001
2941.370	.026	.345	-.017	1.105	.003
2959.870	.036	.317	-.025	.933	-.002
2979.520	.052	1.239	.012	1.915	.048
3000.550	.078	.678	-.025	.773	-.018
3020.260	.099	.723	-.027	.937	-.006
3040.450	.124	.896	-.013	.961	-.005
3058.710	.135	1.748	.101	1.778	.105

WATER VAPOR EXTINCTION COEFFICIENT

WAVENUMBER (CM**-1)	FASCODE CASE 7 (KM**-1)	SNI01 SN/FCD	SNI01 SN-FCD	SNI10 SN/FCD	SNI10 SN-FCD	SNI09 SN/FCD	SNI09 SN-FCD
1930.300	.985	.645	-.349	.722	-.274	.562	-.431
1952.500	.676	.701	-.202	.504	-.335	.500	-.338
1974.100	.453	.721	-.127	.379	-.281	.639	-.163
1979.600	.394	.856	-.057	.400	-.237	.640	-.142
2004.650	.267	.933	-.018	.282	-.192	.745	-.068
2031.250	.165	.888	-.018	.100	-.148	.793	-.034
2056.050	.107	1.150	.016	-.051	-.112	.981	-.002
2084.350	.070	1.240	.017	-.322	-.093	1.257	.018
2102.150	.054	1.312	.017	-.692	-.092	1.397	.022
2130.500	.040	1.396	.016	-1.197	-.087	1.414	.016
2150.050	.034	1.378	.013	-1.642	-.089	1.611	.021
2159.050	.032	1.220	.007	-1.926	-.093	1.678	.021
2166.800	.030	1.328	.010	-2.055	-.092	1.347	.010
2177.600	.028	1.180	.005	-2.1[illegible]	-.088	1.585	.016
2190.950	.026	.839	-.004	-2.110	-.081	2.290	.034
2223.680	.023	1.769	.018	-1.604	-.059	6.462	.125
2400.000	.016	2.675	.027	.131	-.014	2.804	.029
2420.420	.016	2.071	.017	-.242	-.020	2.570	.025
2440.850	.016	1.433	.007	-.908	-.030	2.110	.017
2480.330	.015	.982	-.000	-.994	-.030	1.472	.007
2501.000	.015	.887	-.002	-.726	-.026	1.149	.002
2520.650	.015	.711	-.004	-1.069	-.032	1.070	.001
2540.830	.015	.855	-.002	-.715	-.026	1.465	.007
2560.420	.015	.650	-.005	-.417	-.022	1.267	.004
2580.370	.015	.765	-.004	-.244	-.019	1.413	.006
2599.840	.015	.850	-.002	-.355	-.021	1.155	.002
2618.640	.016	.870	-.002	-.570	-.025	1.109	.002
2640.580	.016	.617	-.006	.150	-.014	1.012	.000
2661.550	.016	.678	-.005	.189	-.013	.996	-.000
2679.510	.016	.620	-.006	.341	-.011	.850	-.002
2700.720	.016	1.000	-.000	1.000	-.000	1.000	-.000
2719.280	.016	.821	-.003	.438	-.009	1.444	.007
2740.740	.016	1.078	.001	.887	-.002	.883	-.002
2760.690	.016	.929	-.001	.911	-.001	.685	-.005
2778.950	.016	.798	-.003	1.061	.001	.725	-.005
2800.100	.016	.799	-.003	1.218	.004	.798	-.003
2820.110	.016	1.328	.005	1.838	.014	1.084	.001
2839.400	.016	1.289	.005	1.895	.014	.796	-.003
2860.190	.016	1.444	.007	1.950	.015	.472	-.008
2880.800	.016	1.805	.013	1.990	.016	1.473	.008
2899.720	.018	1.695	.012	1.948	.017	1.319	.006
2920.400	.021	1.637	.013	2.292	.027	1.152	.003
2941.370	.028	1.600	.017	1.718	.020	1.008	.000
2959.870	.038	1.208	.008	1.592	.023	.802	-.008
2979.520	.055	2.024	.057	2.174	.065	2.077	.060
3000.550	.083	1.019	.002	1.194	.016	.879	-.010
3020.260	.105	1.151	.016	1.216	.023	1.038	.004
3040.450	.132	1.130	.017	1.118	.016	.887	-.015
3058.710	.143	1.912	.131	2.570	.225	2.350	.193

AD-A150 682 ANALYSIS OF ATMOSPHERIC INTERFEROMETER DATA(U) 3/3
OPTIMETRICS INC LAS CRUCES NM J A DOWLING ET AL.
JUL 84 OMI-102 AFGL-TR-84-0177 F19628-83-C-0040

UNCLASSIFIED F/G 20/14 NL

END
FILMED
DTIC

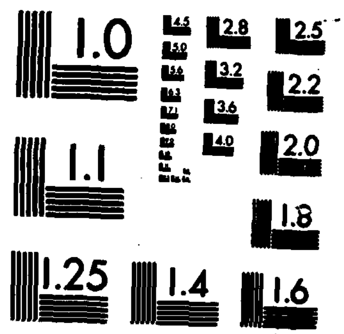

MICROCOPY RESOLUTION TEST CHART
NATIONAL BUREAU OF STANDARDS-1963-A

WATER VAPOR EXTINCTION COEFFICIENT

WAVENUMBER (CM**-1)	PASCODE CASE 7 (KM**-1)	SNI16 SN/PCD	SNI16 SN-PCD	SNI14 SN/PCD	SNI14 SN-PCD	SNI11 SN/PCD	SNI11 SN-PCD
1930.300	.985	.495	-.497	.627	-.367	.388	-.602
1952.500	.676	.453	-.370	.510	-.331	.387	-.415
1974.100	.453	.523	-.216	.561	-.199	.386	-.278
1979.600	.394	.564	-.172	.632	-.145	.366	-.250
2004.650	.267	.574	-.114	.647	-.094	.295	-.189
2031.250	.165	.566	-.071	.627	-.061	.089	-.150
2056.050	.107	.701	-.032	.745	-.027	.051	-.101
2084.350	.070	.685	-.022	.794	-.014	-.286	-.090
2102.150	.054	.715	-.015	.773	-.012	-.622	-.088
2130.500	.040	.704	-.012	.773	-.009	-1.046	-.081
2150.050	.034	.615	-.013	.692	-.010	-1.427	-.082
2159.050	.032	.441	-.018	.419	-.018	-1.677	-.085
2166.800	.030	.325	-.020	.423	-.017	-1.829	-.085
2177.600	.028	.385	-.017	.611	-.011	-1.827	-.079
2190.950	.026	.611	-.010	.652	-.009	-1.704	-.070
2223.680	.023	1.146	.003	1.387	.009	-1.645	-.060
2400.000	.016	2.191	.019	2.182	.019	.452	-.009
2420.420	.016	1.744	.012	1.881	.014	-.435	-.023
2440.850	.016	1.158	.002	1.257	.004	-.724	-.027
2480.330	.015	.885	-.002	.952	-.001	-.732	-.026
2501.000	.015	.881	-.002	.761	-.004	-.654	-.025
2520.650	.015	.766	-.004	.734	-.004	-.783	-.027
2540.830	.015	.857	-.002	.996	-.000	-.207	-.018
2560.420	.015	.777	-.003	.841	-.002	-.155	-.018
2580.370	.015	.791	-.003	.910	-.001	-.011	-.015
2599.840	.015	.698	-.005	.711	-.004	.085	-.014
2618.640	.016	.812	-.003	.723	-.004	-.087	-.017
2640.580	.016	.796	-.003	.973	-.000	.336	-.011
2661.550	.016	.942	-.001	.853	-.002	.546	-.007
2679.510	.016	.808	-.003	.969	-.001	.609	-.006
2700.720	.016	1.000	-.000	1.000	-.000	1.000	-.000
2719.280	.016	.456	-.009	.948	-.001	.759	-.004
2740.740	.016	.995	-.000	1.008	.000	1.058	.001
2760.690	.016	1.144	.002	1.164	.003	1.256	.004
2778.950	.016	.905	-.002	.783	-.004	1.254	.004
2800.100	.016	.736	-.004	.650	-.006	.938	-.001
2820.110	.016	1.154	.002	1.149	.002	2.012	.016
2839.400	.016	1.155	.002	1.388	.006	2.043	.017
2860.190	.016	1.120	.002	1.159	.003	2.334	.021
2880.800	.016	1.561	.009	1.530	.009	2.785	.029
2899.720	.018	1.105	.002	1.264	.005	2.384	.024
2920.400	.021	1.192	.004	1.308	.006	2.606	.034
2941.370	.028	1.045	.001	1.110	.003	2.030	.028
2959.870	.038	.930	-.003	.941	-.002	1.760	.029
2979.520	.055	1.658	.036	2.010	.056	2.358	.075
3000.550	.083	.798	-.017	.957	-.004	1.099	.008
3020.260	.105	.875	-.013	1.053	.006	1.219	.023
3040.450	.132	.866	-.018	.994	-.001	1.114	.015
3058.710	.143	1.461	.066	2.205	.173	2.016	.146

WATER VAPOR EXTINCTION COEFFICIENT

WAVENUMBER (CM**-1)	FASCODE CASE 8 (KM**-1)	CC083 CC/FCD	CC-FCD
1979.600	.597	.580	-.251
2004.650	.407	.481	-.211
2031.250	.254	.565	-.110
2056.050	.166	.753	-.041
2084.350	.111	.585	-.046
2102.150	.086	.534	-.040
2130.500	.063	.401	-.038
2150.050	.054	.700	-.016
2159.050	.050	.522	-.024
2166.800	.048	.066	-.044
2177.600	.044	.377	-.027
2190.950	.041	.105	-.036
2223.680	.036	.514	-.017
2400.000	.024	2.279	.031
2420.420	.023	1.821	.019
2440.850	.023	1.189	.004
2480.330	.022	1.608	.014
2501.000	.022	1.163	.004
2520.650	.022	.825	-.004
2540.830	.022	.465	-.012
2560.420	.022	.607	-.009
2580.370	.022	.197	-.018
2599.840	.022	.625	-.008
2618.640	.023	.140	-.020
2640.580	.023	.751	-.006
2661.550	.023	1.475	.011
2679.510	.023	.691	-.007
2700.720	.024	1.000	-.000
2719.280	.023	-.173	-.027
2740.740	.023	.672	-.008
2760.690	.023	1.321	.008
2778.950	.024	.833	-.004
2800.100	.024	1.036	.001
2820.110	.023	.508	-.012
2839.400	.023	.967	-.001
2860.190	.023	.862	-.003
2880.800	.024	.322	-.016
2899.720	.026	.614	-.010
2920.400	.030	.685	-.010
2941.370	.040	.526	-.019
2959.870	.056	.557	-.025
2979.520	.081	1.817	.066
3000.550	.121	.741	-.031
3020.260	.153	.568	-.066
3040.450	.192	.587	-.079

WATER VAPOR EXTINCTION COEFFICIENT

WAVENUMBER (CM**-1)	FASCODE CASE 9 (KM**-1)	CC144 CC/FCD	CC144 CC-FCD	CC145 CC/FCD	CC145 CC-FCD
1979.600	.622	.582	-.260	.588	-.256
2004.650	.424	.629	-.157	.636	-.154
2031.250	.263	.672	-.086	.679	-.084
2056.050	.172	.924	-.013	.933	-.012
2084.350	.114	1.059	.007	1.069	.008
2102.150	.088	.970	-.003	.985	-.001
2130.500	.064	1.146	.009	1.163	.010
2150.050	.054	1.197	.011	1.209	.011
2159.050	.051	1.063	.003	1.093	.005
2166.800	.048	1.144	.007	1.158	.008
2177.600	.045	1.209	.009	1.223	.010
2190.950	.041	1.167	.007	1.161	.007
2223.680	.036	2.849	.067	2.841	.066
2400.000	.024	2.623	.040	2.645	.040
2420.420	.024	2.380	.033	2.368	.033
2440.850	.023	2.042	.024	2.051	.025
2480.330	.023	1.618	.014	1.623	.014
2501.000	.023	1.631	.014	1.634	.014
2520.650	.022	1.513	.012	1.483	.011
2540.830	.022	1.513	.011	1.515	.011
2560.420	.022	1.442	.010	1.412	.009
2580.370	.023	1.411	.009	1.364	.008
2599.840	.023	1.218	.005	1.220	.005
2618.640	.023	1.138	.003	1.124	.003
2640.580	.024	1.083	.002	1.040	.001
2661.550	.024	1.054	.001	1.040	.001
2679.510	.024	.993	-.000	.994	-.000
2700.720	.024	1.000	-.000	1.000	0.000
2719.280	.024	.447	-.013	.497	-.012
2740.740	.024	.893	-.003	.851	-.004
2760.690	.024	.913	-.002	.885	-.003
2778.950	.024	.869	-.003	.870	-.003
2800.100	.024	.882	-.003	.920	-.002
2820.110	.024	.862	-.003	.847	-.004
2839.400	.024	.783	-.005	.798	-.005
2860.190	.024	.798	-.005	.769	-.005
2880.800	.024	.854	-.004	.855	-.004
2899.720	.026	.704	-.008	.662	-.009
2920.400	.031	.685	-.010	.674	-.010
2941.370	.042	.597	-.017	.561	-.018
2959.870	.058	.468	-.031	.452	-.032
2979.520	.084	.914	-.007	.910	-.008
3000.550	.126	.499	-.063	.496	-.064
3020.260	.159	.630	-.059	.638	-.058
3040.450	.200	.650	-.070	.638	-.072

WATER VAPOR EXTINCTION COEFFICIENT

WAVENUMBER	FASCODE CASE 10	CC147		CC148	
(CM**-1)	(KM**-1)	CC/FCD	CC-FCD	CC/FCD	CC-FCD
1979.600	.708	.522	-.338	.560	-.311
2004.650	.483	.565	-.210	.645	-.172
2031.250	.302	.630	-.112	.698	-.091
2056.050	.198	.856	-.029	1.011	.002
2084.350	.132	.946	-.007	1.148	.020
2102.150	.103	.806	-.020	.900	-.010
2130.500	.075	.957	-.003	1.030	.002
2150.050	.063	.962	-.002	1.102	.006
2159.050	.059	.852	-.009	.979	-.001
2166.800	.056	.900	-.006	1.045	.003
2177.600	.052	.926	-.004	1.051	.003
2190.950	.048	.761	-.011	.867	-.006
2223.680	.042	2.534	.064	2.761	.074
2400.000	.028	2.170	.032	2.188	.033
2420.420	.027	2.000	.027	2.036	.028
2440.850	.027	1.709	.019	1.760	.020
2480.330	.026	1.357	.009	1.390	.010
2501.000	.025	1.403	.010	1.435	.011
2520.650	.025	1.295	.007	1.339	.009
2540.830	.025	1.296	.007	1.340	.009
2560.420	.025	1.226	.006	1.258	.007
2580.370	.025	1.147	.004	1.203	.005
2599.840	.026	1.123	.003	1.110	.003
2618.640	.026	1.008	.000	.985	-.000
2640.580	.027	.903	-.003	.945	-.001
2661.550	.027	.924	-.002	.922	-.002
2679.510	.027	.919	-.002	.917	-.002
2700.720	.027	1.000	0.000	1.000	0.000
2719.280	.027	.231	-.021	.300	-.019
2740.740	.027	.857	-.004	.878	-.003
2760.690	.027	.935	-.002	.966	-.001
2778.950	.027	.890	-.003	.945	-.001
2800.100	.027	1.037	.001	1.018	.000
2820.110	.027	.847	-.004	.893	-.003
2839.400	.027	.890	-.003	.901	-.003
2860.190	.027	.992	-.000	1.025	.001
2880.800	.027	1.063	.002	1.017	.000
2899.720	.030	.825	-.005	.887	-.003
2920.400	.035	.864	-.005	.847	-.005
2941.370	.047	.697	-.014	.724	-.013
2959.870	.066	.556	-.029	.565	-.028
2979.520	.094	.998	-.000	1.052	.005
3000.550	.142	.574	-.060	.606	-.056
3020.260	.179	.685	-.056	.679	-.058
3040.450	.224	.706	-.066	.704	-.066

WATER VAPOR EXTINCTION COEFFICIENT

WAVENUMBER (CM**-1)	FASCODE CASE 11 (KM**-1)	CC153 CC/FCD	CC153 CC-FCD	CC154 CC/FCD	CC154 CC-FCD
1979.600	.760	.544	-.346	.551	-.341
2004.650	.519	.601	-.207	.625	-.195
2031.250	.325	.679	-.104	.702	-.097
2056.050	.214	.952	-.010	.981	-.004
2084.350	.143	1.067	.010	1.098	.014
2102.150	.111	.889	-.012	.913	-.010
2130.500	.081	1.020	.002	1.041	.003
2150.050	.069	1.072	.005	1.099	.007
2159.050	.065	.988	-.001	1.004	.000
2166.800	.061	1.037	.002	1.059	.004
2177.600	.056	1.081	.005	1.083	.005
2190.950	.052	.973	-.001	.992	-.000
2223.680	.045	2.662	.075	2.693	.076
2400.000	.030	2.264	.037	2.286	.038
2420.420	.029	2.058	.031	2.101	.032
2440.850	.028	1.790	.022	1.824	.023
2480.330	.028	1.410	.011	1.433	.012
2501.000	.027	1.484	.013	1.503	.014
2520.650	.027	1.370	.010	1.386	.010
2540.830	.027	1.389	.010	1.404	.011
2560.420	.027	1.317	.008	1.321	.009
2580.370	.027	1.277	.008	1.293	.008
2599.840	.028	1.136	.004	1.138	.004
2618.640	.028	1.073	.002	1.076	.002
2640.580	.028	.994	-.000	.996	-.000
2661.550	.029	.985	-.000	1.008	.000
2679.510	.029	.962	-.001	.985	-.000
2700.720	.029	1.000	-.000	1.000	0.000
2719.280	.029	.313	-.020	.362	-.018
2740.740	.029	.841	-.005	.860	-.004
2760.690	.029	.945	-.002	.935	-.002
2778.950	.029	.874	-.004	.876	-.004
2800.100	.029	.870	-.004	.902	-.003
2820.110	.029	.828	-.005	.844	-.004
2839.400	.028	.809	-.005	.799	-.006
2860.190	.028	.878	-.003	.877	-.003
2880.800	.029	.962	-.001	.943	-.002
2899.720	.032	.750	-.008	.722	-.009
2920.400	.038	.782	-.008	.751	-.009
2941.370	.050	.688	-.016	.664	-.017
2959.870	.070	.584	-.029	.552	-.031
2979.520	.101	.899	-.010	.988	-.001
3000.550	.151	.537	-.070	.553	-.067
3020.260	.191	.636	-.069	.678	-.061
3040.450	.239	.663	-.081	.680	-.077

WATER VAPOR EXTINCTION COEFFICIENT

WAVENUMBER (CM**-1)	FASCODE CASE 12 (KM**-1)	CC119 CC/FCD	CC119 CC-FCD	CC120 CC/FCD	CC120 CC-FCD	CC121 CC/FCD	CC121 CC-FCD
1979.600	.807	.522	-.385	.594	-.328	.525	-.383
2004.650	.553	.543	-.253	.632	-.203	.551	-.248
2031.250	.347	.633	-.127	.719	-.097	.628	-.129
2056.050	.230	.795	-.047	.902	-.022	.802	-.045
2084.350	.154	.894	-.016	1.031	.005	.879	-.019
2102.150	.120	.891	-.013	1.008	.001	.849	-.018
2130.500	.088	1.046	.004	1.174	.015	.965	-.003
2150.050	.074	1.040	.003	1.194	.014	.953	-.003
2159.050	.070	.962	-.003	1.096	.007	.874	-.009
2166.800	.066	1.019	.001	1.137	.009	.873	-.008
2177.600	.061	1.062	.004	1.181	.011	.890	-.007
2190.950	.056	.994	-.000	1.123	.007	.782	-.012
2223.680	.049	2.574	.077	2.694	.083	1.989	.048
2400.000	.032	2.217	.039	2.331	.042	2.192	.038
2420.420	.031	1.994	.031	2.108	.034	1.876	.027
2440.850	.030	1.724	.022	1.846	.026	1.597	.018
2480.330	.029	1.410	.012	1.482	.014	1.238	.007
2501.000	.029	1.453	.013	1.512	.015	1.310	.009
2520.650	.029	1.383	.011	1.455	.013	1.276	.008
2540.830	.029	1.400	.011	1.438	.013	1.261	.007
2560.420	.029	1.290	.008	1.328	.009	1.157	.004
2580.370	.029	1.236	.007	1.286	.008	1.083	.002
2599.840	.029	1.196	.006	1.234	.007	1.071	.002
2618.640	.030	1.089	.003	1.106	.003	1.020	.001
2640.580	.030	.992	-.000	1.030	.001	.941	-.002
2661.550	.030	.989	-.000	1.048	.001	.947	-.002
2679.510	.030	.971	-.001	.998	-.000	.904	-.003
2700.720	.031	1.000	-.000	1.000	-.000	1.000	0.000
2719.280	.030	.294	-.021	.525	-.014	.312	-.021
2740.740	.030	.918	-.002	.889	-.003	.917	-.003
2760.690	.030	.954	-.001	.925	-.002	1.046	.001
2778.950	.031	.897	-.003	.926	-.002	.969	-.001
2800.100	.031	1.022	.001	1.086	.003	1.043	.001
2820.110	.030	.857	-.004	.884	-.004	.913	-.003
2839.400	.030	.893	-.003	.891	-.003	1.006	.000
2860.190	.030	1.029	.001	.947	-.002	1.143	.004
2880.800	.031	1.173	.005	1.104	.003	1.312	.010
2899.720	.033	.886	-.004	.861	-.005	1.113	.004
2920.400	.040	.993	-.000	.915	-.003	1.123	.005
2941.370	.053	.834	-.009	.801	-.011	.959	-.002
2959.870	.074	.671	-.024	.686	-.023	.784	-.016
2979.520	.106	.904	-.010	1.292	.031	1.140	.015
3000.550	.159	.536	-.074	.599	-.064	.640	-.057
3020.260	.201	.628	-.075	.734	-.053	.723	-.056
3040.450	.252	.665	-.085	.734	-.067	.774	-.057

WATER VAPOR EXTINCTION COEFFICIENT

WAVENUMBER	FASCODE CASE 13	CC157		CC158		CC159	
(CM**-1)	(KM**-1)	CC/FCD	CC-FCD	CC/FCD	CC-FCD	CC/FCD	CC-FCD
1979.600	.907	.629	-.336	.570	-.390	.670	-.299
2004.650	.622	.778	-.138	.701	-.186	.830	-.106
2031.250	.392	.833	-.065	.771	-.090	.886	-.045
2056.050	.260	1.156	.041	1.033	.009	1.173	.045
2084.350	.175	1.272	.048	1.120	.021	1.258	.045
2102.150	.137	.987	-.002	.873	-.017	.964	-.005
2130.500	.100	1.083	.008	.952	-.005	1.042	.004
2150.050	.085	1.149	.013	1.005	.000	1.096	.008
2159.050	.080	1.091	.007	.922	-.006	1.018	.001
2166.800	.075	1.107	.008	.954	-.003	1.037	.003
2177.600	.069	1.119	.008	.979	-.001	1.038	.003
2190.950	.064	.986	-.001	.861	-.009	.896	-.007
2223.680	.055	2.645	.091	2.440	.079	2.707	.094
2400.000	.035	2.118	.039	1.993	.035	2.005	.035
2420.420	.034	1.948	.033	1.814	.028	1.846	.029
2440.850	.034	1.716	.024	1.564	.019	1.620	.021
2480.330	.032	1.358	.012	1.245	.008	1.286	.009
2501.000	.032	1.423	.014	1.304	.010	1.352	.011
2520.650	.032	1.330	.010	1.213	.007	1.262	.008
2540.830	.031	1.337	.011	1.261	.008	1.274	.009
2560.420	.031	1.279	.009	1.183	.006	1.222	.007
2580.370	.032	1.238	.008	1.182	.006	1.191	.006
2599.840	.032	1.101	.003	1.045	.001	1.084	.003
2618.640	.033	1.041	.001	.996	-.000	1.028	.001
2640.580	.033	1.025	.001	.990	-.000	.980	-.001
2661.550	.033	1.024	.001	1.010	.000	1.012	.000
2679.510	.033	1.004	.000	.989	-.000	.985	-.000
2700.720	.034	1.000	-.000	1.000	-.000	1.000	0.000
2719.280	.033	.625	-.012	.630	-.012	.645	-.012
2740.740	.033	.868	-.004	.877	-.004	.859	-.005
2760.690	.033	.953	-.002	.971	-.001	.947	-.002
2778.950	.034	.964	-.001	1.000	.000	.976	-.001
2800.100	.034	1.062	.002	1.104	.004	1.136	.005
2820.110	.033	.945	-.002	.991	-.000	.962	-.001
2839.400	.033	.882	-.004	.943	-.002	.896	-.003
2860.190	.033	.937	-.002	1.003	.000	.941	-.002
2880.800	.034	.943	-.002	1.036	.001	.992	-.000
2899.720	.037	.811	-.007	.883	-.004	.844	-.006
2920.400	.044	.789	-.009	.890	-.005	.816	-.008
2941.370	.059	.719	-.017	.775	-.013	.753	-.014
2959.870	.082	.620	-.031	.658	-.028	.674	-.027
2979.520	.118	1.152	.018	1.223	.026	1.290	.034
3000.550	.177	.618	-.067	.640	-.064	.658	-.060
3020.260	.223	.768	-.052	.774	-.050	.824	-.039
3040.450	.280	.740	-.073	.751	-.070	.796	-.057

WATER VAPOR EXTINCTION COEFFICIENT

WAVENUMBER (CM**-1)	FASCODE CASE 14 (KM**-1)	CC160 CC/FCD	CC160 CC-FCD	CC161 CC/FCD	CC161 CC-FCD
1979.600	.921	.396	-.557	.577	-.390
2004.650	.632	.439	-.354	.763	-.150
2031.250	.398	.627	-.149	.896	-.041
2056.050	.264	.832	-.044	1.231	.061
2084.350	.177	.936	-.011	1.356	.063
2102.150	.138	.836	-.023	1.096	.013
2130.500	.101	.962	-.004	1.210	.021
2150.050	.086	1.000	.000	1.313	.027
2159.050	.081	.900	-.008	1.203	.016
2166.800	.076	.957	-.003	1.241	.018
2177.600	.070	.991	-.001	1.268	.019
2190.950	.065	.846	-.010	1.124	.008
2223.680	.056	2.301	.072	3.036	.113
2400.000	.036	2.058	.038	2.356	.048
2420.420	.035	1.847	.029	2.131	.039
2440.850	.034	1.625	.021	1.874	.030
2480.330	.033	1.269	.009	1.482	.016
2501.000	.032	1.359	.012	1.543	.018
2520.650	.032	1.271	.009	1.432	.014
2540.830	.032	1.276	.009	1.437	.014
2560.420	.032	1.210	.007	1.360	.011
2580.370	.032	1.186	.006	1.350	.011
2599.840	.032	1.087	.003	1.199	.006
2618.640	.033	1.011	.000	1.121	.004
2640.580	.034	.955	-.002	1.083	.003
2661.550	.034	.944	-.002	1.074	.002
2679.510	.033	.933	-.002	1.055	.002
2700.720	.034	1.000	0.000	1.000	0.000
2719.280	.034	.460	-.018	.703	-.010
2740.740	.034	.861	-.005	.853	-.005
2760.690	.034	.951	-.002	.919	-.003
2778.950	.034	.940	-.002	.950	-.002
2800.100	.034	1.029	.001	1.150	.005
2820.110	.034	.931	-.002	.901	-.003
2839.400	.033	.901	-.003	.807	-.006
2860.190	.033	1.057	.002	.890	-.004
2880.800	.034	1.186	.006	.972	-.001
2899.720	.037	.966	-.001	.805	-.007
2920.400	.045	1.004	.000	.801	-.009
2941.370	.059	.893	-.006	.722	-.017
2959.870	.083	.742	-.021	.688	-.026
2979.520	.120	1.187	.022	1.213	.025
3000.550	.179	.581	-.075	.603	-.071
3020.260	.226	.696	-.069	.785	-.049
3040.450	.283	.705	-.084	.742	-.073

WATER VAPOR EXTINCTION COEFFICIENT

WAVENUMBER (CM**-1)	FASCODE CASE 9 (KM**-1)	CC144 CC/FCD	CC144 CC-FCD	CC145 CC/FCD	CC145 CC-FCD
1979.600	.622	.643	-.222	.650	-.218
2004.650	.424	.720	-.118	.728	-.115
2031.250	.263	.823	-.047	.830	-.045
2056.050	.172	1.158	.027	1.168	.029
2084.350	.114	1.419	.048	1.431	.049
2102.150	.088	1.441	.039	1.459	.040
2130.500	.064	1.805	.052	1.826	.053
2150.050	.054	1.985	.054	2.002	.054
2159.050	.051	1.905	.046	1.941	.048
2166.800	.048	2.042	.050	2.061	.051
2177.600	.045	2.185	.053	2.205	.054
2190.950	.041	2.236	.051	2.236	.051
2223.680	.036	4.094	.111	4.094	.111
2400.000	.024	4.659	.089	4.693	.090
2420.420	.024	4.490	.083	4.490	.083
2440.850	.023	4.211	.075	4.233	.076
2480.330	.023	3.890	.066	3.909	.066
2501.000	.023	3.948	.067	3.965	.067
2520.650	.022	3.875	.065	3.859	.064
2540.830	.022	3.921	.065	3.937	.065
2560.420	.022	3.852	.064	3.837	.064
2580.370	.023	3.824	.064	3.792	.063
2599.840	.023	3.613	.060	3.629	.061
2618.640	.023	3.514	.059	3.514	.059
2640.580	.024	3.446	.058	3.416	.058
2661.550	.024	3.421	.058	3.421	.058
2679.510	.024	3.400	.057	3.415	.058
2700.720	.024	3.392	.058	3.406	.058
2719.280	.024	2.879	.045	2.944	.047
2740.740	.024	3.330	.056	3.302	.056
2760.690	.024	3.393	.057	3.379	.057
2778.950	.024	3.349	.057	3.364	.057
2800.100	.024	3.365	.058	3.417	.059
2820.110	.024	3.408	.058	3.408	.058
2839.400	.024	3.395	.057	3.425	.057
2860.190	.024	3.433	.057	3.419	.057
2880.800	.024	3.428	.059	3.443	.060
2899.720	.026	3.105	.056	3.076	.055
2920.400	.031	2.714	.054	2.714	.054
2941.370	.042	2.135	.048	2.107	.046
2959.870	.058	1.583	.034	1.574	.033
2979.520	.084	1.693	.058	1.693	.058
3000.550	.126	1.023	.003	1.023	.003
3020.260	.159	1.048	.008	1.059	.009
3040.450	.200	.987	-.003	.976	-.005

WATER VAPOR EXTINCTION COEFFICIENT

WAVENUMBER (CM**-1)	FASCODE CASE 10 (KM**-1)	CC147 CC/FCD	CC147 CC-FCD	CC148 CC/FCD	CC148 CC-FCD
1979.600	.708	.521	-.339	.555	-.315
2004.650	.483	.563	-.211	.639	-.175
2031.250	.302	.629	-.112	.689	-.094
2056.050	.198	.856	-.028	.999	-.000
2084.350	.132	.949	-.007	1.133	.018
2102.150	.103	.812	-.019	.882	-.012
2130.500	.075	.970	-.002	1.010	.001
2150.050	.063	.981	-.001	1.083	.005
2159.050	.059	.874	-.007	.960	-.002
2166.800	.056	.926	-.004	1.027	.002
2177.600	.052	.956	-.002	1.035	.002
2190.950	.048	.797	-.010	.853	-.007
2223.680	.042	2.586	.066	2.754	.073
2400.000	.028	2.330	.037	2.257	.035
2420.420	.027	2.172	.032	2.117	.030
2440.850	.027	1.894	.024	1.851	.023
2480.330	.026	1.567	.015	1.503	.013
2501.000	.025	1.627	.016	1.560	.014
2520.650	.025	1.530	.013	1.475	.012
2540.830	.025	1.542	.014	1.486	.012
2560.420	.025	1.482	.012	1.414	.010
2580.370	.025	1.410	.010	1.367	.009
2599.840	.026	1.392	.010	1.281	.007
2618.640	.026	1.280	.007	1.161	.004
2640.580	.027	1.181	.005	1.128	.003
2661.550	.027	1.212	.006	1.115	.003
2679.510	.027	1.215	.006	1.119	.003
2700.720	.027	1.302	.008	1.208	.006
2719.280	.027	.544	-.012	.518	-.013
2740.740	.027	1.178	.005	1.104	.003
2760.690	.027	1.268	.007	1.204	.006
2778.950	.027	1.229	.006	1.189	.005
2800.100	.027	1.383	.010	1.270	.007
2820.110	.027	1.208	.006	1.158	.004
2839.400	.027	1.265	.007	1.179	.005
2860.190	.027	1.377	.010	1.313	.008
2880.800	.027	1.446	.012	1.306	.008
2899.720	.030	1.186	.006	1.161	.005
2920.400	.035	1.176	.006	1.085	.003
2941.370	.047	.936	-.003	.907	-.004
2959.870	.066	.731	-.018	.701	-.020
2979.520	.094	1.122	.011	1.148	.014
3000.550	.142	.659	-.048	.673	-.046
3020.260	.179	.753	-.044	.732	-.048
3040.450	.224	.762	-.053	.748	-.056

WATER VAPOR EXTINCTION COEFFICIENT

WAVENUMBER (CM**-1)	FASCODE CASE 11 (KM**-1)	CC153 CC/FCD	CC153 CC-FCD	CC154 CC/FCD	CC154 CC-FCD
1979.600	.760	.551	-.341	.553	-.339
2004.650	.519	.611	-.202	.629	-.193
2031.250	.325	.695	-.099	.708	-.095
2056.050	.214	.977	-.005	.991	-.002
2084.350	.143	1.105	.015	1.114	.016
2102.150	.111	.938	-.007	.933	-.007
2130.500	.081	1.088	.007	1.069	.006
2150.050	.069	1.154	.011	1.131	.009
2159.050	.065	1.076	.005	1.039	.002
2166.800	.061	1.130	.008	1.096	.006
2177.600	.056	1.181	.010	1.123	.007
2190.950	.052	1.083	.004	1.036	.002
2223.680	.045	2.791	.081	2.745	.079
2400.000	.030	2.475	.044	2.370	.040
2420.420	.029	2.276	.037	2.188	.034
2440.850	.028	2.014	.029	1.914	.026
2480.330	.028	1.644	.018	1.526	.015
2501.000	.027	1.723	.020	1.598	.016
2520.650	.027	1.613	.017	1.483	.013
2540.830	.027	1.636	.017	1.503	.013
2560.420	.027	1.566	.015	1.420	.011
2580.370	.027	1.524	.014	1.391	.011
2599.840	.028	1.380	.010	1.237	.007
2618.640	.028	1.317	.009	1.173	.005
2640.580	.028	1.235	.007	1.093	.003
2661.550	.029	1.226	.006	1.105	.003
2679.510	.029	1.206	.006	1.083	.002
2700.720	.029	1.244	.007	1.098	.003
2719.280	.029	.560	-.013	.461	-.015
2740.740	.029	1.088	.003	.959	-.001
2760.690	.029	1.196	.006	1.036	.001
2778.950	.029	1.123	.004	.975	-.001
2800.100	.029	1.120	.003	1.002	.000
2820.110	.029	1.082	.002	.946	-.002
2839.400	.028	1.070	.002	.904	-.003
2860.190	.028	1.141	.004	.982	-.000
2880.800	.029	1.218	.006	1.046	.001
2899.720	.032	.986	-.000	.817	-.006
2920.400	.038	.982	-.001	.831	-.006
2941.370	.050	.839	-.008	.725	-.014
2959.870	.070	.694	-.021	.596	-.028
2979.520	.101	.975	-.002	1.019	.002
3000.550	.151	.588	-.062	.573	-.064
3020.260	.191	.677	-.062	.694	-.058
3040.450	.239	.696	-.073	.693	-.073

WATER VAPOR EXTINCTION COEFFICIENT

WAVENUMBER (CM**-1)	FASCODE CASE 13 (KM**-1)	CC157 CC/FCD	CC157 CC-FCD	CC158 CC/FCD	CC158 CC-FCD	CC159 CC/FCD	CC159 CC-FCD
1979.600	.907	.643	-.324	.584	-.377	.678	-.292
2004.650	.622	.798	-.126	.722	-.173	.841	-.099
2031.250	.392	.866	-.053	.805	-.077	.904	-.038
2056.050	.260	1.206	.054	1.084	.022	1.200	.052
2084.350	.175	1.347	.061	1.197	.034	1.298	.052
2102.150	.137	1.083	.011	.973	-.004	1.016	.002
2130.500	.100	1.217	.022	1.090	.009	1.114	.011
2150.050	.085	1.308	.026	1.169	.014	1.182	.015
2159.050	.080	1.261	.021	1.097	.008	1.111	.009
2166.800	.075	1.287	.022	1.140	.011	1.136	.010
2177.600	.069	1.316	.022	1.181	.013	1.145	.010
2190.950	.064	1.200	.013	1.082	.005	1.013	.001
2223.680	.055	2.898	.105	2.700	.094	2.844	.102
2400.000	.035	2.543	.054	2.431	.050	2.236	.044
2420.420	.034	2.387	.048	2.266	.044	2.085	.037
2440.850	.034	2.169	.039	2.031	.035	1.867	.029
2480.330	.032	1.835	.027	1.736	.024	1.545	.018
2501.000	.032	1.909	.029	1.805	.026	1.617	.020
2520.650	.032	1.826	.026	1.725	.023	1.533	.017
2540.830	.031	1.840	.026	1.779	.025	1.548	.017
2560.420	.031	1.786	.025	1.706	.022	1.498	.016
2580.370	.032	1.746	.024	1.705	.022	1.468	.015
2599.840	.032	1.602	.019	1.563	.018	1.357	.012
2618.640	.033	1.540	.018	1.510	.017	1.300	.010
2640.580	.033	1.519	.017	1.500	.017	1.249	.008
2661.550	.033	1.523	.017	1.523	.017	1.283	.009
2679.510	.033	1.506	.017	1.506	.017	1.258	.009
2700.720	.034	1.499	.017	1.515	.017	1.272	.009
2719.280	.033	1.133	.004	1.154	.005	.923	-.003
2740.740	.033	1.377	.013	1.402	.013	1.137	.005
2760.690	.033	1.469	.016	1.503	.017	1.228	.008
2778.950	.034	1.478	.016	1.529	.018	1.256	.009
2800.100	.034	1.576	.020	1.634	.021	1.416	.014
2820.110	.033	1.469	.016	1.531	.018	1.247	.008
2839.400	.033	1.418	.014	1.496	.016	1.189	.006
2860.190	.033	1.477	.016	1.560	.018	1.235	.008
2880.800	.034	1.468	.016	1.577	.020	1.279	.009
2899.720	.037	1.298	.011	1.384	.014	1.109	.004
2920.400	.044	1.201	.009	1.314	.014	1.040	.002
2941.370	.059	1.030	.002	1.096	.006	.923	-.005
2959.870	.082	.845	-.013	.889	-.009	.797	-.017
2979.520	.118	1.309	.036	1.385	.045	1.376	.044
3000.550	.177	.723	-.049	.748	-.044	.716	-.050
3020.260	.223	.852	-.033	.861	-.031	.870	-.029
3040.450	.280	.807	-.054	.820	-.050	.833	-.047

WATER VAPOR EXTINCTION COEFFICIENT

WAVENUMBER (CM**-1)	FASCODE CASE 14 (KM**-1)	CC160 CC/FCD	CC160 CC-FCD	CC161 CC/FCD	CC161 CC-FCD
1979.600	.921	.406	-.547	.584	-.383
2004.650	.632	.454	-.345	.774	-.143
2031.250	.398	.651	-.139	.913	-.035
2056.050	.264	.869	-.034	1.258	.068
2084.350	.177	.993	-.001	1.396	.070
2102.150	.138	.909	-.013	1.148	.020
2130.500	.101	1.063	.006	1.281	.028
2150.050	.086	1.120	.010	1.397	.034
2159.050	.081	1.029	.002	1.293	.024
2166.800	.076	1.094	.007	1.337	.026
2177.600	.070	1.139	.010	1.372	.026
2190.950	.065	1.008	.001	1.238	.015
2223.680	.056	2.492	.083	3.170	.121
2400.000	.036	2.379	.049	2.581	.056
2420.420	.035	2.180	.041	2.365	.047
2440.850	.034	1.969	.033	2.115	.038
2480.330	.033	1.628	.021	1.734	.024
2501.000	.032	1.728	.024	1.802	.026
2520.650	.032	1.645	.021	1.694	.022
2540.830	.032	1.655	.021	1.703	.022
2560.420	.032	1.592	.019	1.628	.020
2580.370	.032	1.569	.018	1.618	.020
2599.840	.032	1.468	.015	1.466	.015
2618.640	.033	1.387	.013	1.385	.013
2640.580	.034	1.328	.011	1.345	.012
2661.550	.034	1.319	.011	1.337	.011
2679.510	.033	1.314	.010	1.321	.011
2700.720	.034	1.377	.013	1.264	.009
2719.280	.034	.844	-.005	.972	-.001
2740.740	.034	1.246	.008	1.123	.004
2760.690	.034	1.341	.011	1.192	.006
2778.950	.034	1.328	.011	1.222	.008
2800.100	.034	1.417	.014	1.422	.014
2820.110	.034	1.327	.011	1.178	.006
2839.400	.033	1.306	.010	1.091	.003
2860.190	.033	1.464	.015	1.176	.006
2880.800	.034	1.583	.020	1.250	.009
2899.720	.037	1.334	.012	1.063	.002
2920.400	.045	1.314	.014	1.018	.001
2941.370	.059	1.127	.008	.886	-.007
2959.870	.083	.911	-.007	.807	-.016
2979.520	.120	1.305	.036	1.296	.035
3000.550	.179	.660	-.061	.659	-.061
3020.260	.226	.760	-.054	.829	-.039
3040.450	.283	.756	-.069	.778	-.063

APPENDIX B

CALCULATED LOCAL LINE CONTRIBUTIONS TO THE OPTICAL DEPTH

(cm^{-1})	FASCODE CASE 1	2	3	4	5	6	7
1930.300	1.127	.860	.486	.755	1.725	1.842	1.954
1952.500	.974	.746	.425	.657	1.446	1.537	1.639
1974.100	.374	.286	.161	.250	.586	.624	.665
1979.600	.251	.194	.109	.168	.364	.388	.411
2004.650	.301	.236	.132	.200	.425	.454	.481
2031.250	.120	.095	.056	.082	.166	.176	.187
2056.050	.147	.127	.101	.119	.172	.179	.187
2084.350	.121	.104	.075	.093	.144	.151	.158
2102.150	.091	.079	.063	.074	.106	.111	.115
2130.500	.056	.051	.042	.047	.058	.060	.062
2150.050	.072	.064	.050	.057	.077	.081	.084
2159.050	.109	.101	.088	.095	.103	.106	.108
2166.800	.089	.086	.075	.079	.079	.081	.083
2177.600	.120	.119	.114	.114	.099	.100	.101
2190.950	.404	.394	.384	.389	.338	.340	.343
2223.680	.612	.610	.594	.589	.490	.492	.493
2400.000	.016	.017	.016	.016	.013	.013	.013
2420.420	.003	.003	.002	.002	.002	.002	.002
2440.850	.011	.011	.011	.011	.009	.009	.010
2480.330	.020	.019	.016	.017	.018	.019	.019
2501.000	.001	.001	.001	.001	.001	.001	.001
2520.650	.004	.003	.003	.003	.003	.003	.003
2540.830	.017	.016	.017	.017	.015	.015	.015
2560.420	.018	.017	.017	.018	.016	.016	.016
2580.370	.059	.056	.054	.057	.053	.054	.055
2599.840	.036	.034	.030	.033	.034	.035	.035
2618.640	.019	.016	.012	.015	.024	.025	.026
2640.580	.023	.018	.012	.016	.032	.034	.036
2661.550	.028	.021	.012	.019	.044	.047	.050
2679.510	.029	.022	.014	.020	.043	.046	.048
2700.720	.005	.004	.003	.004	.008	.008	.009
2719.280	.160	.121	.069	.109	.231	.246	.261
2740.740	.017	.014	.011	.014	.022	.023	.024
2760.690	.010	.008	.006	.008	.012	.013	.014
2778.950	.038	.029	.019	.027	.055	.058	.062
2800.100	.104	.086	.064	.083	.133	.140	.147
2820.110	.084	.072	.057	.069	.098	.102	.107
2839.400	.028	.023	.015	.021	.039	.041	.043
2860.190	.016	.013	.009	.012	.021	.022	.023
2880.800	.038	.032	.025	.030	.046	.048	.050
2899.720	.057	.049	.038	.046	.067	.070	.073
2920.400	.040	.037	.033	.035	.039	.040	.041
2941.370	.053	.046	.034	.041	.057	.060	.063
2959.870	.185	.161	.129	.151	.210	.220	.228
2979.520	.914	.780	.603	.739	1.061	1.112	1.158
3000.550	.175	.142	.098	.130	.234	.247	.261
3020.260	.493	.414	.325	.400	.612	.644	.672
3040.450	.173	.135	.086	.124	.248	.263	.278
3058.710	1.322	1.032	.684	.974	1.889	2.003	2.120

(cm^{-1})	8	9	10	11	12	13	14
	FASCODE CASE						
1930.300	3.795	4.215	4.733	5.047	5.230	5.880	6.057
1952.500	3.148	3.515	3.945	4.204	4.331	4.880	5.027
1974.100	1.292	1.441	1.615	1.725	1.789	2.016	2.077
1979.600	.809	.913	1.025	1.094	1.127	1.271	1.314
2004.650	.971	1.122	1.260	1.346	1.379	1.566	1.627
2031.250	.372	.427	.478	.511	.525	.594	.616
2056.050	.328	.365	.402	.424	.434	.482	.497
2084.350	.302	.351	.390	.415	.422	.477	.497
2102.150	.209	.236	.259	.273	.281	.313	.322
2130.500	.110	.127	.139	.148	.149	.167	.174
2150.050	.157	.185	.204	.216	.218	.247	.257
2159.050	.182	.209	.225	.236	.236	.262	.272
2166.800	.141	.165	.178	.187	.186	.206	.215
2177.600	.144	.155	.159	.163	.162	.170	.174
2190.950	.466	.487	.502	.510	.509	.530	.540
2223.680	.666	.707	.718	.726	.718	.743	.753
2400.000	.018	.020	.020	.020	.020	.021	.021
2420.420	.004	.005	.005	.005	.005	.005	.006
2440.850	.013	.014	.015	.015	.015	.016	.016
2480.330	.035	.042	.045	.048	.047	.053	.056
2501.000	.002	.002	.002	.002	.002	.003	.003
2520.650	.005	.006	.006	.006	.006	.007	.007
2540.830	.019	.019	.019	.019	.019	.019	.019
2560.420	.021	.020	.021	.021	.021	.022	.022
2580.370	.075	.076	.079	.081	.083	.087	.088
2599.840	.054	.057	.061	.063	.065	.069	.070
2618.640	.045	.048	.053	.056	.058	.064	.066
2640.580	.064	.069	.076	.081	.085	.094	.096
2661.550	.090	.095	.106	.112	.118	.131	.133
2679.510	.086	.091	.100	.107	.113	.124	.127
2700.720	.016	.017	.019	.020	.021	.023	.023
2719.280	.481	.516	.577	.614	.639	.709	.723
2740.740	.041	.042	.047	.049	.051	.057	.057
2760.690	.023	.024	.026	.028	.029	.032	.032
2778.950	.108	.111	.124	.131	.138	.151	.153
2800.100	.249	.257	.285	.300	.312	.342	.347
2820.110	.188	.202	.225	.237	.246	.270	.277
2839.400	.077	.081	.091	.096	.100	.111	.113
2860.190	.040	.043	.048	.051	.053	.058	.059
2880.800	.088	.096	.105	.112	.115	.127	.130
2899.720	.125	.135	.149	.157	.161	.178	.182
2920.400	.067	.074	.080	.084	.085	.093	.097
2941.370	.119	.141	.155	.165	.166	.187	.196
2959.870	.398	.437	.482	.506	.516	.576	.594
2979.520	2.027	2.222	2.448	2.583	2.665	2.966	3.047
3000.550	.481	.526	.583	.621	.642	.716	.732
3020.260	1.135	1.206	1.324	1.403	1.451	1.589	1.620
3040.450	.506	.542	.604	.641	.669	.744	.759
3058.710	3.744	3.973	4.411	4.687	4.872	5.386	5.487

FASCODE CASE

(cm^{-1})	15	16	17	18	19
1930.300	.712	.771	1.169	1.462	3.149
1952.500	.607	.657	.989	1.233	2.640
1974.100	.228	.247	.376	.470	1.017
1979.600	.153	.168	.256	.328	.704
2004.650	.169	.188	.289	.382	.826
2031.250	.070	.077	.116	.150	.319
2056.050	.119	.123	.148	.168	.279
2084.350	.086	.091	.116	.143	.263
2102.150	.068	.072	.089	.105	.182
2130.500	.046	.047	.055	.064	.102
2150.050	.050	.053	.065	.080	.138
2159.050	.099	.102	.113	.128	.180
2166.800	.069	.072	.080	.094	.132
2177.600	.108	.112	.116	.125	.140
2190.950	.399	.401	.409	.421	.458
2223.680	.644	.660	.674	.715	.747
2400.000	.014	.014	.015	.017	.018
2420.420	.002	.002	.003	.003	.004
2440.850	.010	.010	.011	.011	.012
2480.330	.016	.017	.020	.025	.040
2501.000	.001	.001	.001	.001	.002
2520.650	.003	.003	.004	.004	.005
2540.830	.019	.018	.018	.018	.018
2560.420	.021	.021	.021	.020	.022
2580.370	.062	.061	.062	.062	.072
2599.840	.031	.032	.035	.037	.050
2618.640	.015	.015	.020	.022	.039
2640.580	.016	.017	.024	.027	.054
2661.550	.020	.021	.031	.036	.075
2679.510	.021	.022	.031	.036	.073
2700.720	.004	.004	.006	.007	.014
2719.280	.103	.109	.163	.194	.405
2740.740	.015	.015	.019	.020	.036
2760.690	.008	.008	.010	.011	.020
2778.950	.030	.030	.042	.047	.092
2800.100	.084	.085	.109	.118	.211
2820.110	.067	.069	.085	.096	.167
2839.400	.021	.021	.029	.034	.065
2860.190	.012	.012	.016	.018	.034
2880.800	.029	.030	.038	.043	.077
2899.720	.046	.047	.059	.066	.112
2920.400	.034	.035	.039	.042	.060
2941.370	.039	.041	.052	.064	.114
2959.870	.173	.177	.210	.236	.380
2979.520	.785	.799	.978	1.098	1.868
3000.550	.131	.138	.187	.225	.429
3020.260	.444	.450	.552	.603	1.023
3040.450	.126	.131	.185	.215	.428
3058.710	1.048	1.068	1.460	1.631	3.178

APPENDIX C

CALCULATED CO_2 AND N_2 CONTINUUM CONTRIBUTIONS TO THE OPTICAL DEPTH

	FASCODE CASE						
(cm^{-1})	1	2	3	4	5	6	7
1930.300	0.000	0.000	0.000	0.000	0.000	0.000	0.000
1952.500	0.000	0.000	0.000	0.000	0.000	0.000	0.000
1974.100	0.000	0.000	.001	0.000	0.000	0.000	0.000
1979.600	0.000	0.000	0.000	0.000	0.000	0.000	0.000
2004.650	0.000	0.000	0.000	0.000	0.000	0.000	0.000
2031.250	0.000	0.000	.001	0.000	0.000	0.000	0.000
2056.050	0.000	.001	0.000	0.000	0.000	0.000	.001
2084.350	.002	.002	.002	.001	.001	.002	.002
2102.150	.004	.004	.004	.004	.004	.004	.004
2130.500	.014	.013	.014	.014	.013	.013	.013
2150.050	.037	.035	.036	.037	.032	.032	.033
2159.050	.054	.051	.052	.054	.047	.048	.048
2166.800	.072	.069	.070	.072	.063	.063	.064
2177.600	.092	.088	.090	.093	.081	.080	.080
2190.950	.121	.116	.118	.121	.106	.106	.105
2223.680	.206	.196	.199	.205	.180	.180	.180
2400.000	.773	.739	.752	.773	.676	.676	.676
2420.420	.483	.463	.470	.483	.423	.422	.423
2440.850	.368	.352	.358	.367	.321	.321	.322
2480.330	.184	.176	.179	.184	.161	.162	.162
2501.000	.123	.118	.120	.122	.107	.107	.107
2520.650	.079	.076	.077	.079	.069	.069	.069
2540.830	.048	.046	.047	.048	.042	.042	.042
2560.420	.033	.030	.032	.032	.028	.028	.028
2580.370	.022	.021	.021	.023	.020	.020	.020
2599.840	.014	.013	.014	.014	.013	.013	.013
2618.640	.009	.008	.009	.009	.007	.008	.008
2640.580	.006	.006	.006	.006	.005	.005	.005
2661.550	.006	.006	.006	.006	.005	.005	.005
2679.510	.004	.004	.004	.004	.003	.003	.003
2700.720	.002	.002	.002	.002	.001	.001	.001
2719.280	.001	.001	.001	.001	.001	.001	.001
2740.740	0.000	.001	.001	0.000	0.000	0.000	0.000
2760.690	0.000	0.000	0.000	0.000	0.000	0.000	0.000
2778.950	0.000	0.000	0.000	0.000	0.000	0.000	0.000
2800.100	0.000	0.000	0.000	0.000	0.000	0.000	0.000
2820.110	0.000	0.000	0.000	.001	0.000	0.000	0.000
2839.400	0.000	0.000	0.000	0.000	0.000	0.000	0.000
2860.190	0.000	0.000	0.000	0.000	0.000	0.000	0.000
2880.800	0.000	0.000	0.000	0.000	0.000	0.000	0.000
2899.720	0.000	0.000	0.000	0.000	0.000	0.000	0.000
2920.400	0.000	0.000	0.000	0.000	0.000	0.000	0.000
2941.370	0.000	0.000	0.000	0.000	0.000	0.000	0.000
2959.870	0.000	0.000	0.000	0.000	0.000	0.000	0.000
2979.520	0.000	0.000	0.000	0.000	0.000	0.000	0.000
3000.550	0.000	0.000	0.000	0.000	0.000	0.000	0.000
3020.260	0.000	0.000	0.000	0.000	0.000	0.000	0.000
3040.450	0.000	0.000	0.000	0.000	0.000	0.000	0.000
3058.710	0.000	0.000	0.000	0.000	0.000	0.000	0.000

(cm^{-1})	FASCODE CASE 8	9	10	11	12	13	14
1930.300	0.000	0.000	0.000	0.000	0.000	0.000	0.000
1952.500	0.000	0.000	0.000	0.000	0.000	0.000	0.000
1974.100	0.000	0.000	0.000	0.000	0.000	0.000	0.000
1979.600	0.000	0.000	0.000	0.000	0.000	0.000	0.000
2004.650	0.000	0.000	0.000	.001	0.000	0.000	0.000
2031.250	0.000	.001	0.000	.001	0.000	0.000	0.000
2056.050	.001	0.000	0.000	0.000	0.000	0.000	0.000
2084.350	.002	.002	.001	.002	.002	.002	.001
2102.150	.005	.005	.004	.004	.005	.004	.005
2130.500	.015	.014	.014	.014	.014	.014	.014
2150.050	.038	.036	.036	.036	.037	.036	.036
2159.050	.056	.053	.053	.053	.053	.053	.052
2166.800	.074	.071	.071	.071	.071	.070	.070
2177.600	.095	.090	.090	.090	.092	.090	.089
2190.950	.125	.119	.119	.118	.120	.118	.117
2223.680	.212	.201	.201	.201	.203	.201	.198
2400.000	.797	.759	.758	.756	.764	.755	.747
2420.420	.499	.475	.474	.473	.478	.472	.467
2440.850	.379	.361	.360	.360	.364	.359	.356
2480.330	.190	.181	.180	.180	.182	.180	.178
2501.000	.126	.120	.121	.120	.121	.120	.119
2520.650	.081	.077	.078	.077	.079	.077	.076
2540.830	.050	.048	.047	.047	.047	.047	.046
2560.420	.034	.031	.032	.032	.032	.032	.031
2580.370	.023	.022	.022	.021	.022	.022	.021
2599.840	.015	.014	.014	.014	.014	.014	.014
2618.640	.009	.008	.008	.008	.009	.009	.008
2640.580	.006	.006	.006	.007	.006	.006	.006
2661.550	.007	.005	.006	.006	.006	.006	.006
2679.510	.004	.004	.004	.003	.004	.003	.004
2700.720	.001	.002	.001	.002	.001	.001	.001
2719.280	.001	.001	.001	.001	0.000	.001	.001
2740.740	.001	0.000	0.000	.001	.001	.001	.001
2760.690	0.000	0.000	0.000	0.000	0.000	0.000	0.000
2778.950	0.000	0.000	0.000	0.000	0.000	0.000	0.000
2800.100	0.000	0.000	0.000	.001	0.000	0.000	0.000
2820.110	0.000	0.000	0.000	0.000	0.000	0.000	0.000
2839.400	0.000	0.000	0.000	.001	0.000	0.000	0.000
2860.190	0.000	0.000	0.000	0.000	0.000	0.000	0.000
2880.800	.001	0.000	0.000	0.000	0.000	0.000	0.000
2899.720	0.000	0.000	0.000	0.000	0.000	0.000	0.000
2920.400	0.000	0.000	0.000	0.000	0.000	0.000	0.000
2941.370	0.000	0.000	0.000	0.000	0.000	0.000	0.000
2959.870	0.000	0.000	0.000	0.000	0.000	0.000	0.000
2979.520	0.000	0.000	0.000	0.000	0.000	0.000	0.000
3000.550	0.000	0.000	0.000	0.000	0.000	0.000	0.000
3020.260	0.000	0.000	0.000	0.000	0.000	0.000	0.000
3040.450	0.000	0.000	0.000	0.000	0.000	0.000	0.000
3058.710	0.000	0.000	0.000	0.000	0.000	0.000	0.000

	FASCODE CASE				
(cm^{-1})	15	16	17	18.	19
1930.300	0.000	0.000	0.000	0.000	0.000
1952.500	0.000	0.000	0.000	0.000	0.000
1974.100	0.000	0.000	0.000	0.000	0.000
1979.600	0.000	0.000	0.000	.001	0.000
2004.650	0.000	.001	0.000	0.000	0.000
2031.250	0.000	0.000	.001	0.000	0.000
2056.050	0.000	0.000	.001	0.000	.001
2084.350	.002	.002	.002	.002	.002
2102.150	.005	.005	.005	.004	.005
2130.500	.017	.017	.016	.015	.014
2150.050	.044	.042	.042	.039	.039
2159.050	.064	.062	.060	.057	.056
2166.800	.086	.083	.081	.076	.074
2177.600	.110	.106	.103	.097	.095
2190.950	.144	.139	.136	.127	.125
2223.680	.244	.235	.231	.216	.212
2400.000	.919	.885	.870	.812	.798
2420.420	.574	.553	.544	.508	.499
2440.850	.437	.421	.413	.387	.380
2480.330	.219	.211	.207	.193	.190
2501.000	.146	.141	.138	.129	.127
2520.650	.094	.091	.089	.083	.081
2540.830	.057	.056	.054	.050	.050
2560.420	.038	.037	.036	.034	.033
2580.370	.027	.026	.025	.023	.023
2599.840	.017	.016	.016	.015	.015
2618.640	.011	.010	.010	.009	.009
2640.580	.007	.007	.007	.006	.006
2661.550	.007	.007	.007	.006	.006
2679.510	.005	.004	.005	.004	.004
2700.720	.002	.002	.002	.001	.002
2719.280	.001	.001	.001	.001	.001
2740.740	0.000	.001	0.000	0.000	.001
2760.690	0.000	0.000	0.000	0.000	0.000
2778.950	0.000	0.000	0.000	0.000	0.000
2800.100	0.000	0.000	0.000	0.000	0.000
2820.110	0.000	0.000	0.000	0.000	0.000
2839.400	0.000	0.000	0.000	0.000	0.000
2860.190	0.000	0.000	0.000	0.000	0.000
2880.800	0.000	0.000	0.000	0.000	0.000
2899.720	0.000	0.000	0.000	0.000	0.000
2920.400	0.000	0.000	0.000	0.000	0.000
2941.370	0.000	0.000	0.000	0.000	0.000
2959.870	0.000	0.000	0.000	0.000	0.000
2979.520	0.000	0.000	0.000	0.000	0.000
3000.550	0.000	0.000	0.000	0.000	0.000
3020.260	0.000	0.000	0.000	0.000	0.000
3040.450	0.000	0.000	0.000	0.000	0.000
3058.710	0.000	0.000	0.000	0.000	0.000

END

FILMED

3-85

DTIC